

METHODOLOGIES IN ORGANIC CHEMISTRY AND
THEIR APPLICATIONS TO THE SYNTHESIS OF BIO-
ACTIVE SMALL MOLECULES

Jonathan Hudon

Department of Chemistry

McGill University

Montreal, Quebec, Canada

August 2009

A thesis submitted to McGill University in partial fulfillment of the requirements
of the degree of Doctor of Philosophy

© Jonathan Hudon 2009 All rights reserved.

Abstract

This thesis is separated into two parts. In part A, a novel 5-alkyl-2-silyloxy cyclopentadiene is presented. Racemic and enantioselective syntheses of the new cyclopentadiene have been developed. This new cyclopentadiene is significantly more stable towards 1,5-H shifts than most cyclopentadienes. Through the use of computational modeling, it was determined that the added stability comes from the electron donation of the 2-silyloxy group into the LUMO of the diene. The novel diene was used for Diels-Alder cycloadditions at room temperature with a variety of dienophiles. An europium Lewis acid was found to be compatible with the diene while activating dienophiles for cycloaddition. It was also determined that an enantioenriched diene will generate a cycloaddition product with no erosion in enantiomeric excess. Stabilization by a silyloxy group was also used to generate a stable 1-alkyl-3-silyloxy cyclopentadiene that underwent smooth Diels-Alder reaction. The 5-alkyl-2-silyloxy cyclopentadiene was used as a cycloaddition partner in the synthesis of part of the natural product palau'amine. Through a Diels-Alder/oxidative cleavage sequence, the E-ring stereoarray of the originally proposed structure of Palau'amine was obtained.

In part B, the synthesis and purification of a novel multi-action drug, triciferol, are presented. Triciferol was designed to combine a vitamin D₃ framework and a metal binding group with histone deacetylase inhibition properties. The secosteroidal core of triciferol is obtained from degradation of vitamin D₂. The vitamin D A-ring is obtained from (-)-quinic acid and is appended to the core by a Horner reaction. The unsaturated side chain is built by sequential Wittig reactions and terminated by a metal-binding hydroxamic acid. This conjugated hydroxamic acid group was found to be susceptible to exposition to trace metals. The final purification of triciferol could only be accomplished using reverse phase silica chromatography. Triciferol was found to be an effective bifunctional agent, acting both as an agonist of the vitamin D receptor and an inhibitor of histone deacetylase. Moreover, it proved to be a potent anti-cancer drug *in vitro*.

Résumé

Cette thèse comprend deux parties. Dans la partie A, un nouveau 5-alkyl-2-silyloxy cyclopentadiène est présenté. Deux synthèses de ce nouveau cyclopentadiène ont été développées : l'une racémique et l'autre énantiosélective. Le nouveau cyclopentadiène est significativement plus stable vis-à-vis de la migration 1,5 d'hydrogène que la plupart des cyclopentadiènes connus. À l'aide de la modélisation par ordinateur, la stabilité du nouveau cyclopentadiène a été attribuée à une donation électronique du groupe 2-silyloxy au LUMO du diène. Le nouveau cyclopentadiène a été utilisé lors de cycloadditions Diels-Alder à température ambiante avec une sélection de diénophiles. Un acide de Lewis à base d'euprium, permettant d'activer les diénophiles sans décomposer le diène, a été trouvé. Il fut aussi déterminé qu'une version énantioenrichie du cyclopentadiène génère un produit de cycloaddition sans aucune détérioration de l'excès énantiomérique initial. La stabilisation par un groupe silyloxy a aussi été appliquée avec succès à un cyclopentadiène 1-alkyle-3-silyloxy, lui permettant d'encourir un Diels-Alder sans problème. Le 5-alkyle-2-silyloxy cyclopentadiène a été utilisé lors d'une cycloaddition menant à la synthèse d'une partie de la palau'amine, un produit naturel. La stéréochimie de l'anneau E de la structure originale de la palau'amine a été atteinte grâce à une séquence de Diels-Alder / clivage oxydatif.

Dans la partie B, la synthèse et la purification d'un nouveau médicament bi-fonctionnel, le triciferol, sont présentées. Le triciferol a été conçu afin de combiner la structure de la vitamine D₃ à un groupe chélateur de métaux, ayant la capacité d'inhiber les HDAC. Le centre sécostéroïde du triciferol est obtenu par dégradation de la vitamine D₂. L'anneau A est synthétisé à partir d'acide quinique et est attaché au centre sécostéroïde grâce à une réaction de Horner. La chaîne insaturée est construite par réactions de Wittig et est terminée par un acide hydroxamique chélateur. Cet acide hydroxamique insaturé se décompose facilement en présence de métaux ; la purification finale du triciferol doit être

effectuée par une chromatographie en phase inverse. Le triciférol a les capacité d'un médicament bi-fonctionnel : c'est un agoniste du récepteur de la vitamine D et un inhibiteur des enzymes HDAC.

Dedication

I dedicate this thesis to my family, because of their continued support. To my mother, Michèle, for giving me the inner strength to overcome all the obstacles I encounter in life. To my father, Robert, for giving me the energy and motivation to accomplish my goals. Finally, to my brother, Jean-Philippe, for being such a great guy that I am encouraged to work hard and try to make the world better.

Acknowledgements

First, I would like to thank my supervisor, James Gleason, for years of support and dedication. Jim has an amazing ability to teach that I could feel and experience every day. With him, I learned a lot about chemistry and even more about science, research and communication. Coming out of the Gleason laboratory, I am confident in my skills and knowledge. I owe this to a great supervisor who is always available for his students. I am also indebted to Jim for the many hours of revision work he invested in reading and re-reading this thesis and giving very detailed comments and suggestions.

The Gleason laboratory itself was a wonderful place to learn. In my first years, I was mentored by great students such as Dr Jeffrey Manthorpe, Dr Alain Ajamian, Dr James Ashenhurst and Dr Timothy Cernak. I also enjoyed very much having intelligent and joyful coworkers to discuss with, to give me perspective on my projects, from whom I could learn useful chemistry techniques and who made the lab so alive. In this regard, I would like to thank Christian Drouin, David Soriano del Amo, Azélie Arpin, Neenah Navasero, Erica Tiong, Rodrigo Mendoza Sanchez, Lise Feldborg, Joe Carrigan, Dr. Tan Quach, Bin Zhao, Daniel Rivalti, Dr. Marc Lamblin, Melanie Burger, Jeff St. Denis, Laurie Lim and Jean-François Lacroix. I also developed a passion for teaching and supervision by working with great undergraduate students. I will especially thank the first of such students to closely work with me, Boran Xu, for trusting me and giving me the passion to teach. I also got much help in many other laboratories for the use of instruments. Naming everybody would be impossible, but I would like to mention two women who ran their respective labs with an iron fist in a velvet glove and helped me a lot with HPLC work: Janice Lawandi from the Moitessier lab and Dr Patricia MacLeod from the Li lab.

The department of chemistry at Mc Gill University is an amazing place to be. The ambiance, open-minded attitude and helpfulness of professors and staff is remarkable. I would like to thank all the professors of the department for teaching

me and answering my never-ending questions. In that regard, I would like to thank especially professor Bruce Lennox, professor Massad Dahma, professor Nicolas Moitessier and the late professor George Just. I also got an amazing amount of administrative help from Chantal Marotte and Sandra Aerssen. In the NMR center, I spent a lot of time learning from Dr Fred Morin and Dr Paul Xia. For MS and HRMS, I gratefully thank Dr Alain Lesimple and Nadim Saade.

All of the work in this thesis could not have been possible without the important direct involvement of other people. First, I would like to re-iterate my gratitude to my supervisor for giving me the opportunity to work on wonderful projects where he had an extremely important intellectual input. I also have more specific acknowledgements to make.

For the diene project, I thank Dr James Ashenhurst and Dr Tim Cernak for initiating the project. James developed the synthesis of the racemic diene, which I later refined. James and Tim did preliminary Diels-Alder and tropone cycloaddition studies. Jim Gleason did most of the computational simulations, with Tim and I completing his work. I would like to thank professor Mark Snapper for trying his catalyst for the resolution of our enone alcohol. Also for trying his own catalyst, I would like to thank professor Scott Miller and his students Chad Lewis and Aaron Coffin. Tim Cernak worked extensively on the Palau'amine total synthesis during his Ph.D. He developed the initial route to the E-ring of palau'amine using chloromethyloxazolone, which I later refined.

For the triciferol project, I thank Dr Tan Quach for developing the original synthetic route to triciferol, which I later refined. I am also indebted to Christian Drouin for optimizing the A-ring deoxygenation step. The triciferol project would never have started without the pioneering work of professor John White and his team on vitamin D and trichostatin A. The biological studies done on triciferol were performed in the White lab by Dr Luz Tavera-Mendoza, Basel Dabbas and Ana Palijan.

Table of Contents

Abstract.....	i
Dedication.....	iv
Acknowledgements.....	v
Table of Contents.....	vii
List of Figures.....	ix
List of Tables.....	xii
Abbreviations.....	xiii
1 General Introduction.....	1
1.1 Part A : Development of substituted cyclopentadienes and their uses in cycloadditions.....	3
1.1.1 Physical-Organic studies of 5-substituted cyclopentadienes.....	8
1.1.2 Uses of 5-substituted cyclopentadienes in the Diels-Alder reaction	10
1.1.2.1 Corey's initial approach: low temperature handling.....	10
1.1.2.2 Corey's second approach : delete the problematic hydrogen ...	10
1.1.2.3 The exception : 5-trimethylsilyl cyclopentadiene with bulky fumarates	12
1.1.2.4 The leash and the trap : intramolecular Diels-Alder reactions .	13
1.1.2.5 Working with the thermodynamic mixture: the Yamamoto approach	14
1.1.3 Our need for a 5-substituted cyclopentadiene.....	15
1.2 Part B : Synthesis of the multiple ligand drug triciferol, agonist of the nuclear vitamin D receptor and inhibitor of histone deacetylases.....	17
1.2.1 Vitamin D ₃	17
1.2.2 Histone Deacetylase Inhibitors (HDACi).....	18
1.2.3 Synergistic effects of vitamin D ₃ and HDACi.....	19
1.2.4 Multiple ligand drugs.....	20
1.3 Reference.....	23
2 Substituted Cyclopentadienes and Their Uses in Cycloadditions.....	29
2.1 Development of a new 5-substituted cyclopentadiene.....	29
2.1.1 Synthesis of a 5-alkyl-2-silyloxy cyclopentadiene.....	31
2.1.2 Experimental studies of the diene's stability towards 1,5-H shift	33
2.1.3 Computational studies of the diene isomerization.....	34
2.1.4 Theoretical explanation of the diene's stability.....	38
2.2 Use of the new diene in Diels-Alder cycloadditions.....	39
2.2.1 Optimization of the Diels-Alder reaction conditions.....	39
2.2.2 Optimization of the isolation protocol.....	40
2.2.3 Survey of dienophiles.....	42
2.2.4 Compatibility of the diene with Lewis acids.....	46
2.3 Synthesis and use of an enantioenriched 5-alkyl-2-silyloxy cyclopentadiene.....	49
2.3.1 Ab Initio calculations to determine the enantiostability of the diene	49

2.3.2	Enantioselective synthesis of the diene's precursor.....	50
2.3.3	Synthesis and use of the enantioenriched diene.....	52
2.4	2-silyloxy-4-alkyl cyclopentadiene.....	53
2.5	Conclusion.....	53
2.6	References.....	54
3	Efforts towards the total synthesis of the natural product palau'amine.....	56
3.1	Introduction.....	56
3.2	Retrosynthetic analysis of the palau'amine original structure.....	57
3.3	Synthesis of the original palau'amine E ring structure.....	60
3.4	Exploration of synthesis avenues for the E ring of the corrected structure of palau'amine.....	64
3.4.1	Carbon C6 installation.....	66
3.5	Conclusion.....	67
3.6	References.....	67
4	Synthesis of the multiple ligand drug triciferol, agonist of the nuclear vitamin D receptor and inhibitor of histone deacetylases.....	70
4.1	Rational design of triciferol.....	70
4.2	Synthesis of triciferol.....	74
4.2.1	Isolation of triciferol.....	77
4.2.2	Synthesis of C-20 <i>epi</i> -triciferol precursor.....	78
4.3	Biological results with triciferol.....	80
4.4	Conclusion.....	82
4.5	References.....	83
5	Contributions to knowledge.....	84
6	Appendix 1 Experimental section.....	85
6.1	References.....	119
7	Appendix 2 Publications.....	121
9	Appendix 3 Selected NMR spectra.....	134
10	Appendix 4 : Conversion of the calculated Activation Energies (E _a) for the 1,5-H shift of 2-substituted cyclopentadienes into a value suitable to perform a Hammett plot.....	170
10.1	References:.....	173

List of Figures

Figure 1-1 General Diels-Alder reaction	3
Figure 1-2 Frontier molecular orbital interactions of Diels-Alder reactions.....	5
Figure 1-3 Regioselectivity of the Diels-Alder.....	5
Figure 1-4 Secondary orbital interactions in the Diels-Alder reaction	6
Figure 1-5 Diene conformation affecting the reactivity in Diels-Alder reactions ..	7
Figure 1-6 The range of possibilities for linking two pharmacophores in a multiple ligand drug	21
Figure 2-1 Kinetics of the decomposition of the 5-alkyl-2-silyoxycyclopentadiene through 1,5-H shift at room temperature	33
Figure 2-2 Calculated transition state for the 1,5-H shift in 2-hydroxy-5-methylcyclopentadiene	35
Figure 2-3 Increase in the calculated activation energy for 1,5-H shift in 2-oxo-cyclopentadiene	36
Figure 2-4 Correlation between the 1,5-H activation energy of 2-substituted cyclopentadienes and the substituent's electronic properties	36
Figure 2-5 Correlation between the 1,5-H activation energy of 2-substituted cyclopentadienes and the substituent's Sigma p- constant.....	37
Figure 2-6 Correlation between the predicted 1,5-H activation energy and the predicted LUMO energy of 2-substituted cyclopentadienes.....	38
Figure 2-7 Frontier molecular orbital influence on the 1,5 sigmatropic shift	39
Figure 2-8 Calculated relative enthalpies of different substituted cyclopentadienes and the transition states between them	50
Figure 2-9 Enantioselective synthesis of the diene's precursor.....	52
Figure 3-1 Palau'amine, originally proposed structure.....	56
Figure 3-2 Palau'amine, revised structure.....	57
Figure 4-1 HDAC inhibitors and their structural similarities	71
Figure 4-2 Vitamin D receptor analogs: agonists and antagonist	72
Figure 4-3 Triciferol: Vitamin D agonist and	72
Scheme 1-1 The total synthesis of reserpine by Woodward.....	4
Scheme 1-2 Retrosynthetic analysis of the Corey approach to the prostaglandins	8
Scheme 1-3 Summary of the McLean and Haynes physical-organic study of substituted cyclopentadienes	9
Scheme 1-4 Corey's initial approach to the Prostaglandins using a 5-substituted cyclopentadiene	10
Scheme 1-5 Corey's development of a thermally stable 5-substituted cyclopentadiene	11
Scheme 1-6 Fujisawa's use of fulvenes in the total synthesis of protaglandins....	12
Scheme 1-7 Achiwa's use of steric bulk to promote only one cycloadduct isomer	13
Scheme 1-8 Diels-Alder trapping of one cyclopentadiene isomer through intramolecular tethering of the dienophile	14

Scheme 1-9 Yamamoto's sequential reactions of substituted cyclopentadiene isomers	15
Scheme 1-10 Succinct representation of the Gleason's retrosynthetic analysis of palau'amine and phomoidride A	16
Scheme 1-11 Example of linked pharmacophores.....	21
Scheme 1-12 An example of joined pharmacophores.....	22
Scheme 1-13 An example of overlapped pharmacophores	22
Scheme 1-14 An example of fully merged pharmacophores.....	23
Scheme 2-1 Using a cyclopentenone as a cyclopentadiene precursor	30
Scheme 2-2 Retrosynthesis of the new 5-substituted cyclopentadiene.....	31
Scheme 2-3 Synthesis of the new 5-substituted cyclopentadiene.....	32
Scheme 2-4 Identification of the isomerized diene product	34
Scheme 2-5 Isolation of the silyl enol ether Diels-Alder products	41
Scheme 2-6 Rearomatization of the quinone Diels-Alder adduct.....	41
Scheme 2-7 Comparison of a two step versus a three step isolation protocol for the Diels-Alder adducts	42
Scheme 2-8 Addition of the new diene to azo dicarbonyl compounds.....	43
Scheme 2-9 Diels-Alder competition experiment between cyclopentadiene and the 5-alkyl-2-silyloxy diene	46
Scheme 2-10 Influence of the 2-silyl group on the endo/exo ratio of the Diels-Alder	46
Scheme 2-11 Successful use of a Lewis Acid to accelerated the Diels-Alder reaction of 2-silyloxycyclopentadienes	48
Scheme 2-12 Catalytic kinetic resolution by the Miller catalyst	51
Scheme 2-13 Diels-Alder reaction of the enantioenriched diene	52
Scheme 2-14 Formation and Diels-Alder reaction of a 1,3-disubstituted cyclopentadiene	53
Scheme 3-1 Retrosynthetic analysis of Palau'amine, originally proposed structure	59
Scheme 3-2 Use of 5-alkyl-2-silyloxycyclopentadiene in the retrosynthetic analysis of Palau'amine, originally proposed structure	59
Scheme 3-3 Synthesis attempts at obtaining the complex E-ring stereoarray of Palau'amine	61
Scheme 3-4 Use of the Diels-Alder reaction en route to the complex E-ring stereoarray of Palau'amine	62
Scheme 3-5 Synthesis of the E-ring stereoarray of Palau'amine, originally reported structure.....	63
Scheme 3-6 Retrosynthetic analysis of Palau'amine, revised structure.....	64
Scheme 3-7 Retrosynthetic analysis leading to an intramolecular Diels-Alder ...	65
Scheme 3-8 First attempts at an intramolecular Diels-Alder.....	65
Scheme 3-9 Second attempt at an intramolecular Diels-Alder.....	66
Scheme 3-10 Planned synthesis route for the early introduction of the C6 carbon of Palau'amine	67
Scheme 4-1 Retrosynthetic planning for the synthesis of triciferol.....	73
Scheme 4-2 Synthesis of the A-ring analog of triciferol.....	75
Scheme 4-3 Synthesis of triciferol	77

Scheme 4-4 Epimerization of C-20 of triciferol	79
Scheme 4-5 Synthesis and separation of the C-20 epimers of triciferol	80

List of Tables

Table 2-1 Diels-Alder cycloaddition with the new diene.....	44
Table 2-2 Screening of Lewis Acids to accelerate the Diels-Alder reaction of the 2-silyloxydiene	47

Abbreviations

Ac	acetyl
Aq	aqueous
BOC	<i>tert</i> -butoxycarbonyl
Bz	benzoyl
d	doublet
D.A.	Diels-Alder reaction
DABCO	1,4-diazabicyclo[2.2.2]octane
DCM	dichloromethane
dd	doublet of doublets
ddd	doublet of doublet of doublets
DEAD	diethyl azo dicarboxylate
DFT	density functional theory
DIBAL-H	diisobutylaluminum hydride
DIPEA	<i>N,N</i> -diisopropylethylamine
DMAD	dimethylacetylenedicarboxylate
DMAP	4-(dimethylamino)pyridine
DMDO	dimethyldioxirane
DMF	<i>N,N</i> -dimethylformamide
DMSO	dimethylsulfoxide
DNA	deoxyribonucleic acid
ee	enantiomeric excess
EWG	electron-withdrawing group
eq.	equivalents
ESI	electrospray ionization
Et	ethyl
EtOAc	ethyl acetate
Et ₂ O	diethyl ether
fod	6,6,7,7,8,8,8-heptafluoro-2,2-dimethyl-3,5-octanedionato

FMO	frontier molecular orbital
g	gram(s)
h	hour(s)
HAT	histone acetyl transferase
HDAC	histone deacetylase
HDACi	histone deacetylase inhibitor(s)
hfc	3-(heptafluoropropylhydroxymethylene)-(-)-camphorato
HOMO	highest occupied molecular orbital
HPLC	high performance liquid chromatography
HRMS	high resolution mass spectrometry
Hz	hertz
<i>J</i>	coupling constant
L	litre
L.A.	Lewis acid
LDA	lithium diisopropyl amine
LUMO	lowest unoccupied molecular orbital
m	multiplet
M	moles per litre
MCPBA	<i>meta</i> -chloroperbenzoic acid
Me	methyl
MeOH	methanol
mL	millilitre
mmol	millimole
mol	mole
MS	mass spectrometry
MW	molecular weight
<i>m/z</i>	mass to charge ratio
ND	not determined

NMR	nuclear magnetic resonance spectroscopy
P.G.	protecting group
pH	$-\log[\text{H}^+]$
Ph	phenyl
Pr	propyl
PTAD	4-Phenyl-1,2,4-triazoline-3,5-dione
PTSA	<i>para</i> -toluene sulfonic acid
RNA	ribonucleic acid
RT	room temperature
s	singlet
SAHA	suberoyl anilide hydroxamic acid
SM	starting material
<i>t</i>	tertiary
t	triplet
TBAF	tetrabutylammonium fluoride
TBS	<i>tert</i> -butyl dimethyl silyl
TBSOTf	<i>tert</i> -butyldimethylsilyl trifluoromethanesulfonate
TCDI	1,1'-thiocarbonyl diimidazole
TEA	triethylamine
TES	triethylsilyl
<i>tert</i>	tertiary
TFA	trifluoroacetic acid
THF	tetrahydrofuran
TLC	thin layer chromatography
TMS	trimethylsilyl
Tos	tosyl, <i>para</i> -toluene sulfonate
TSA	trichostatin A
$t_{1/2}$	half-life
UV	ultraviolet light

VDR	vitamin D receptor
Z	benzyloxycarbonyl
1,25D ₃	1 α ,25-dihydroxyvitamin D ₃
μ g	microgram
μ M	micromolar
~	approximately
$^{\circ}$ C	degree Celsius

1 General Introduction

Chemical synthesis deals with the transformation of matter to create new or already known molecules. This happens through the breaking and formation of chemical bonds in predictable ways. The patterns that are used for controlling such changes are called chemical reactions.

Therefore, chemical synthesis has two facets. It can be seen as a means to obtain an end result: a desired molecule, or it can be envisioned as an art that deserves improvement. Improving chemical synthesis means obtaining a greater understanding of a reaction so that its power can be harnessed in more productive ways (less side products leading to higher yields, diminished reaction time, broader substrate scope, etc.). More controlled chemical reactions will lead to an increased accessibility of desired molecules. These molecules have an infinity of potential applications, from plastics, to dyes, to drugs, etc.

A very important subset of chemical synthesis is organic synthesis. This field deals with the transformation of carbon-based chemical bonds. Because of its close relationship with living systems (life being primarily based on carbon), organic synthesis has had a huge impact on medicine during the past century.

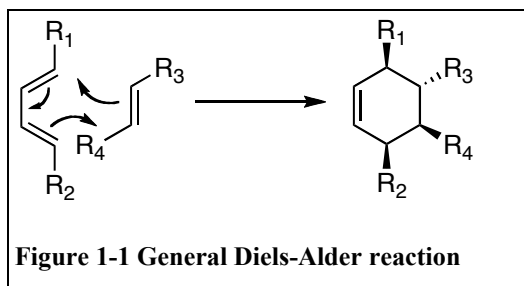
This thesis touches on both aspects of organic synthesis. First, the improvement of the field by obtaining a better understanding of a chemical process, followed by the development of a new method based on the acquired knowledge. Second, the use of organic synthesis to obtain target molecules. In this particular case, the target molecules are bio-active compounds.

This thesis is divided into two main projects. The first one involves the development of a new synthetic method based on substituted cyclopentadienes. This method is then used as a means to obtain a complex and highly interesting natural product, palau'amine. However, natural product total synthesis projects often span many Ph.D.s when the targets are highly challenging. Palau'amine is one such project and has not been completed yet. Concurrently, another different project was undertaken. Its goal was the synthesis of a new potential anti-cancer drug in the context of medicinal chemistry. While this second project involved the

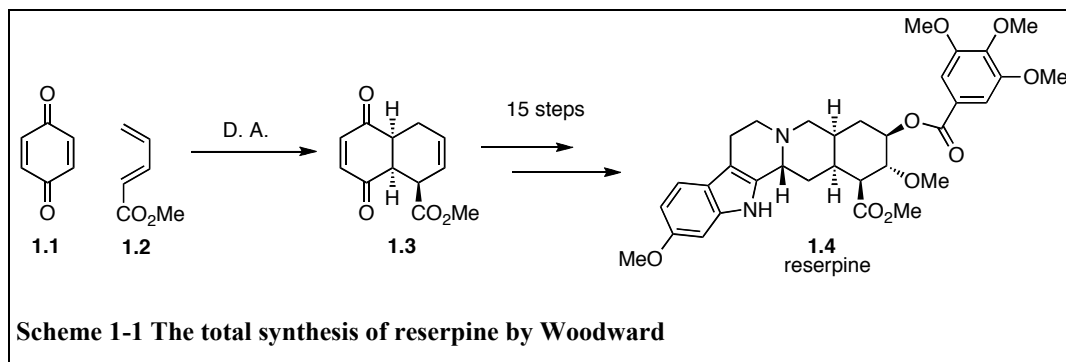
need to understand chemical processes and optimize them, its main goal was to obtain the desired final molecule, so that biological testing by our collaborators could be done. Thus, both aspects of chemical synthesis have been explored in this thesis : improving the possibilities of chemical transformations by gathering new knowledge on a chemical reaction, and using the toolbox of chemical knowledge to obtain target molecules of high value.

1.1 Part A : Development of substituted cyclopentadienes and their uses in cycloadditions

One of the most powerful and versatile reactions in organic synthesis is the Diels-Alder reaction.¹ It brings together two cycloaddition partners, a diene and a dienophile. The Diels-Alder reaction is a concerted $[4\pi+2\pi]$ thermally allowed pericyclic reaction in which three π -bonds are converted into two σ -bonds and one π -bond. This reaction has seen extensive use in synthesis because of its convergency and also because it can create up to four new stereocenters in a single step. Another significant advantage of this reaction is that the new stereocenters are set with predictable and potentially good regio and stereocontrol.² Diastereoselective Diels-Alder reactions are achievable, for example if a chiral auxiliary is linked with the dienophile. As well, enantioselective Diels-Alder reactions can be performed in the presence of chiral additives, such as Lewis acid catalysts.

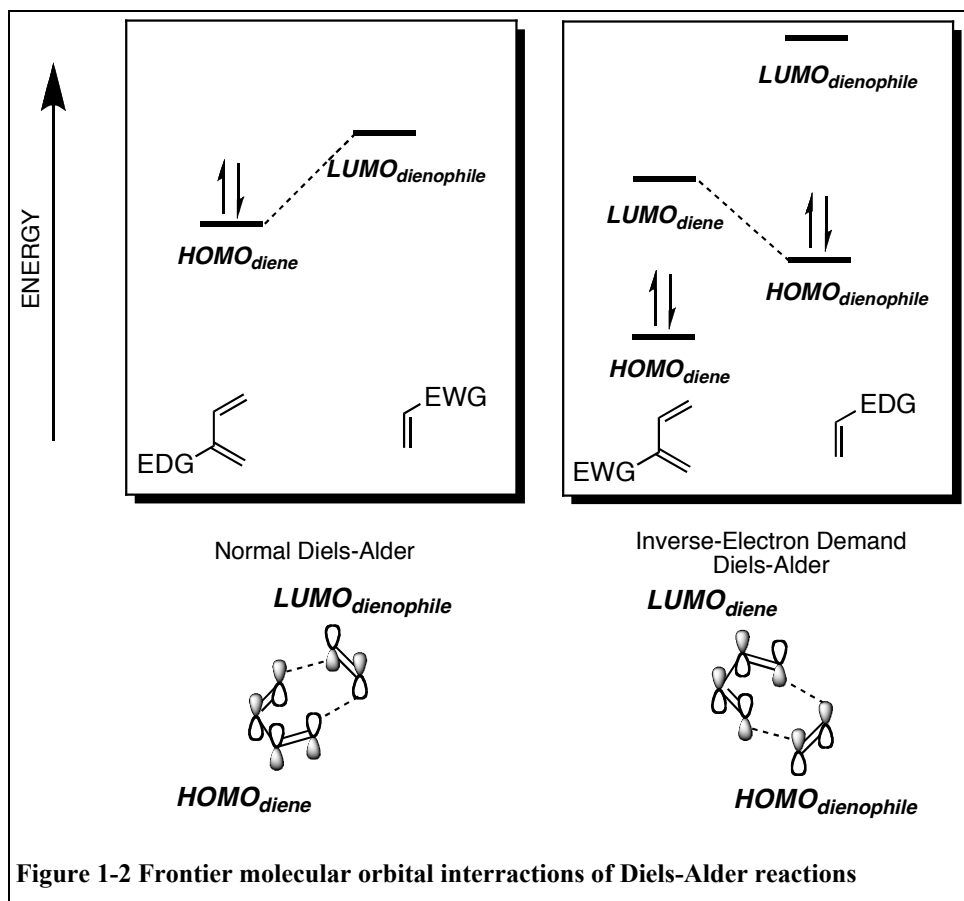


A classical demonstration of the use of the Diels-Alder is the total synthesis of reserpine by Woodward *et al.* in 1956.³ In this magnificent example, the Diels-Alder was used to set the first three of the six stereocenters of the molecule in one powerful step. After this first step, the rest of the molecule was elaborated in fifteen more chemical steps, showing the usefulness of the Diels-Alder reaction in obtaining products of high complexity.

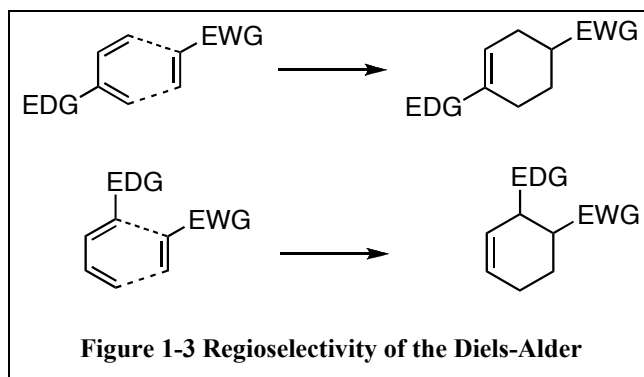


Much of the reactivity and selectivity of the Diels-Alder reaction can be explained using frontier molecular orbital (FMO) theory.^{4,5} According to this theory, a normal electron-demand Diels-Alder reaction involves interaction of the HOMO of the diene with the LUMO of the dienophile, both interacting in a suprafacial way. Substituents on the diene that increase the energy of the HOMO, such as electron-donating groups, will increase the orbital overlap in the Diels-Alder and thus accelerate the reaction. The situation is reversed for the dienophile: substituents that lower the LUMO energy, such as electron withdrawing groups, will accelerate the rate of reaction. Furthermore, many reactions can be accelerated by the addition of a Lewis acid which lowers the LUMO of the dienophile and therefore increases the reaction rate. The same effect can be achieved by the formation of an iminium on the carbonyl of the dienophile.

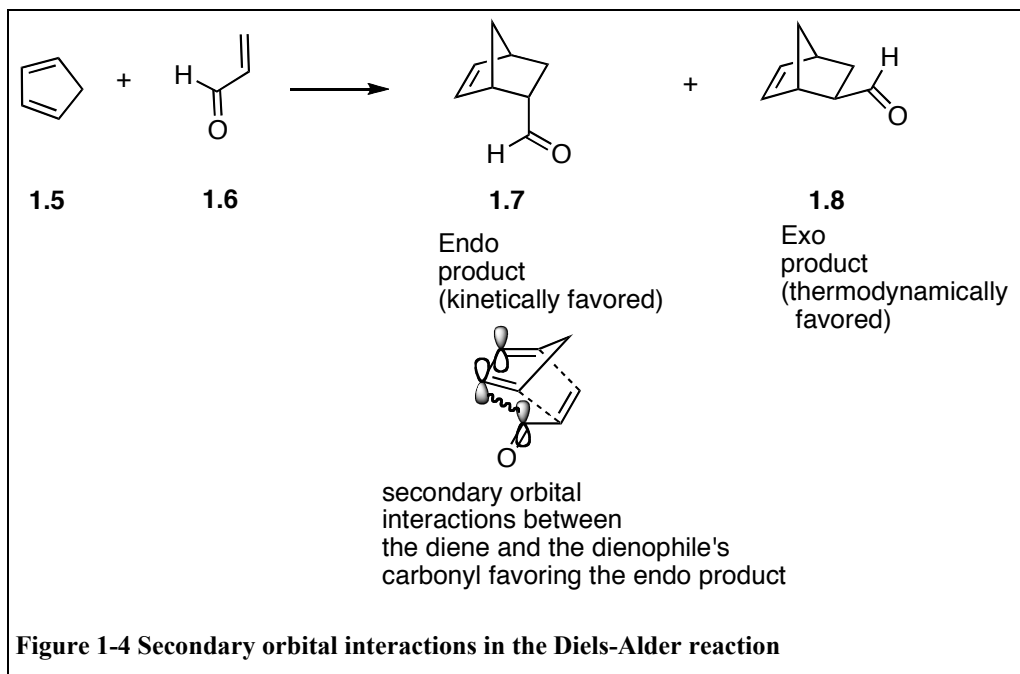
The influence of FMO in Diels-Alder reactions is such that it is possible to completely reverse the importance of reacting orbitals. Inverse electron demand Diels-Alder are reactions where the diene's LUMO interacts with the dienophile's HOMO. This happens when the diene's LUMO is lowered in energy by electron-withdrawing groups while the dienophile's HOMO is raised by electron-donating groups.



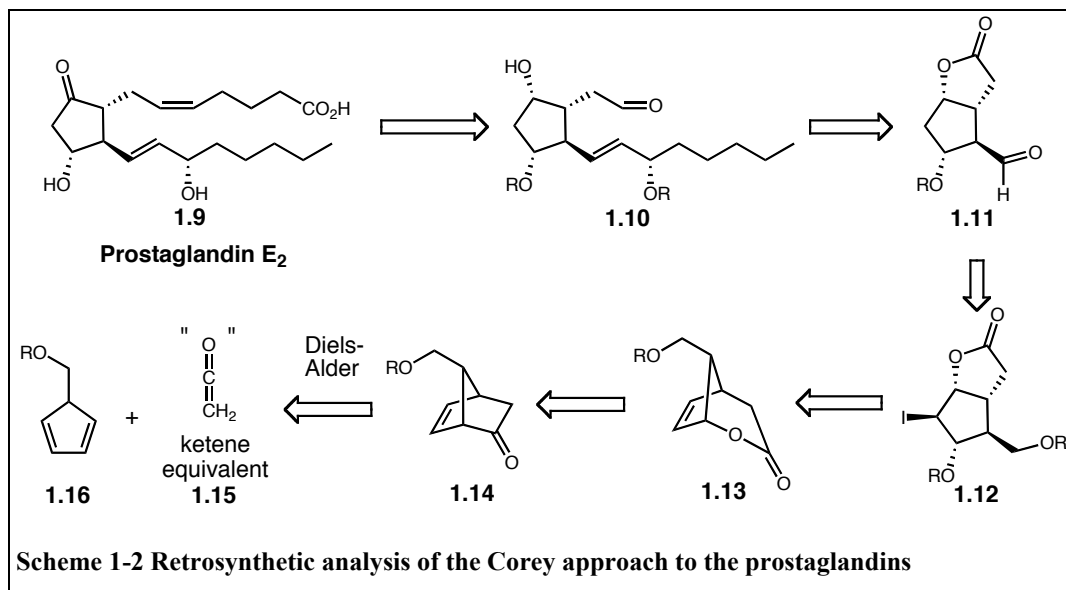
The Diels-Alder's regioselectivity is also controlled by orbital overlap: the end of the diene with the largest coefficient of the reacting HOMO will react with the end of the dienophile with the largest coefficient of the reacting LUMO. As can be seen from examples in Figure 1-3, the regioselectivity of Diels-Alder reactions often leads to 1,2 or 1,4 substituted products.



The Diels-Alder reaction is often stereoselective: the endo product (where the diene's electron-withdrawing group is oriented towards the newly formed π -bond in the transition state) generally being kinetically favored due to secondary orbital interactions occurring between the dienophile's electron-withdrawing substituent and the diene.⁶ The exo product is often thermodynamically favored due to decreased steric strain.

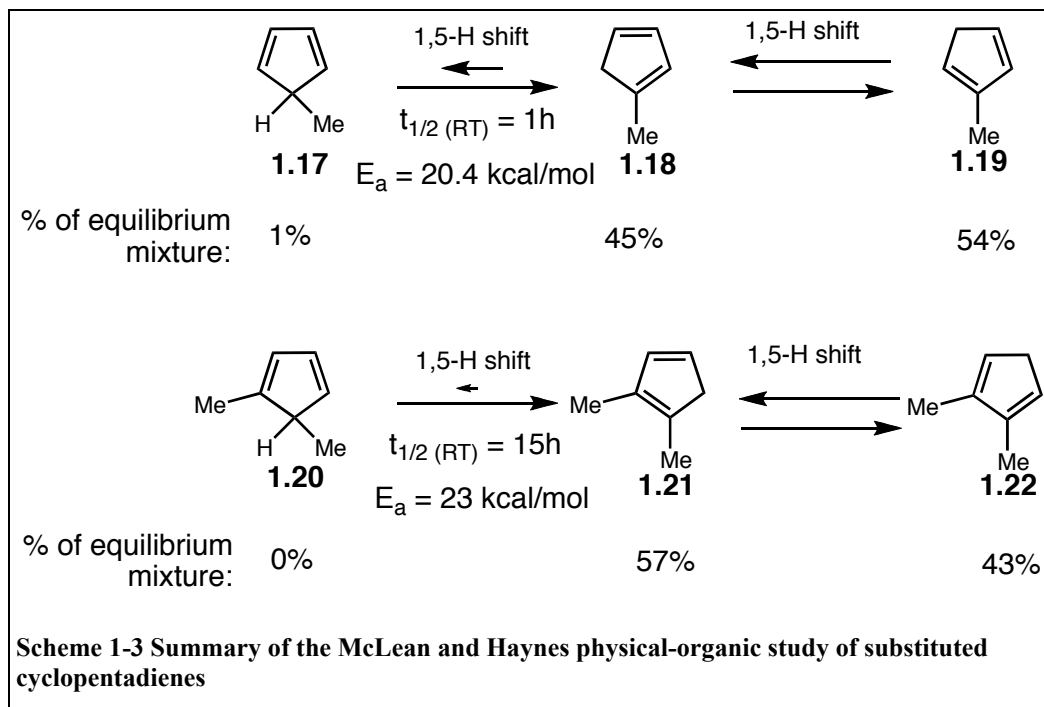


An important factor in the Diels-Alder reaction is the conformation of the diene. For the dienophile to be able to interact simultaneously with the orbitals on both ends of the diene, the diene must adopt a “s-cis” conformation. A diene locked in the “s-trans” conformation will not undergo a Diels-Alder reaction. In many open dienes, such as for 1,3-butadiene, the “s-trans” conformation dominates and the Diels-Alder reaction is a slow process. Therefore, dienes locked in the “s-cis” conformation are much more reactive. Cyclopentadiene is a prime example of a locked “s-cis” diene and is correspondingly a very reactive diene for the Diels-Alder reaction.



1.1.1 Physical-Organic studies of 5-substituted cyclopentadienes

Cyclopentadiene undergoes a rapid 1,5-hydrogen shift at room temperature. In 1963, Mironov showed clearly through deuteration studies that this process occurs through a suprafacial sigmatropic rearrangement.¹⁰ Mironov also investigated the equilibrium point of this process for differently substituted cyclopentadienes and found that at thermodynamic equilibrium many positional isomers are present in solution. Subsequently, during extensive kinetic studies of the 1,5-H shift rearrangements of methyl cyclopentadiene, McLean and Haynes found that the 2-isomer was favored, followed by the 1-isomer, with little 5-isomer present.¹¹ Similar results were obtained with the 1,2-dimethylcyclopentadiene. These results are summarized in Scheme 1-3.



McLean and Haynes found that the half-life for the conversion of 5-methyl cyclopentadiene to 1-methyl cyclopentadiene was only one hour at room temperature. They did not measure exactly the rate of conversion of the 1-methyl to the 2-methyl isomer, but reported it to be a much slower process. These investigators found similar results for 1,5-dimethyl cyclopentadiene transforming to its daughter isomers, with the marked difference that it was much more stable towards the 1,5-H shift than the 5-methyl cyclopentadiene, having a half-life at room temperature of about 15 hours.

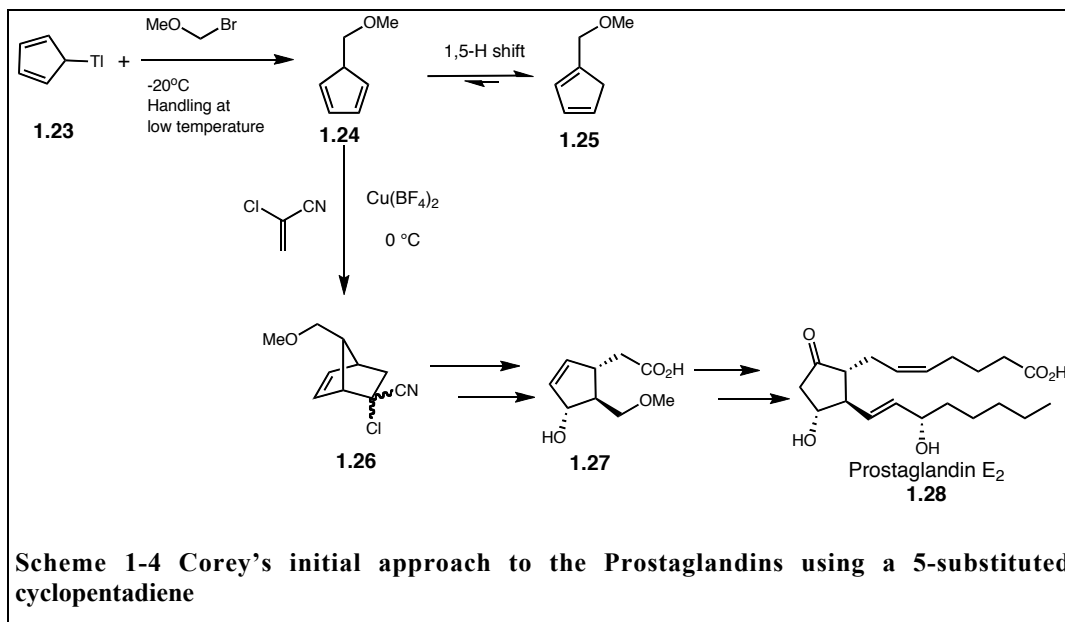
In a similar short study, Breslow *et al.* investigated the isomerization of halogen-substituted cyclopentadienes.¹² They synthesized 5-chloro, 5-bromo and 5-iodo cyclopentadienes. It was found that halogen substituents at the 5-position of cyclopentadiene reduce the rate of sigmatropic hydrogen shifts, but no theoretical rationale was put forward to explain this phenomenon.

From these studies, it can be understood that working with 5-alkyl-substituted cyclopentadienes near room temperature will be a challenge due to their inherent instability. Significant isomerization is expected to happen within minutes at room temperature and be complete within hours.

1.1.2 Uses of 5-substituted cyclopentadienes in the Diels-Alder reaction

1.1.2.1 Corey's initial approach: low temperature handling

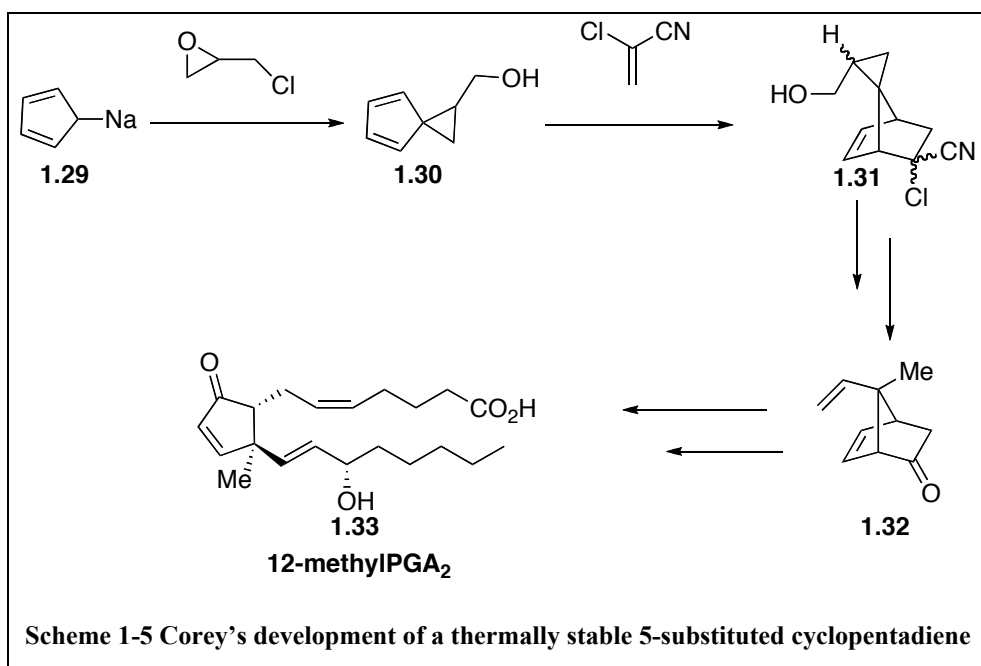
As previously mentioned (*vide supra*), Corey used 5-substituted cyclopentadienes in a key Diels-Alder step for his original synthesis of the prostaglandins.⁷ The 5-substituted cyclopentadienes were obtained from the low temperature alkylation of thallous cyclopentadienide (see Scheme 1-4).¹³ Workup of the resulting products was done at temperatures below 0 °C to prevent the undesirable 1,5-H shift, followed by a low temperature Diels-Alder reaction with a strong dienophile further activated by a Lewis acid. While this approach has the advantage of yielding the products of interest, the manipulations are tedious and the Diels-Alder method is limited to very reactive dienophiles or those that can be activated by strong Lewis acids.



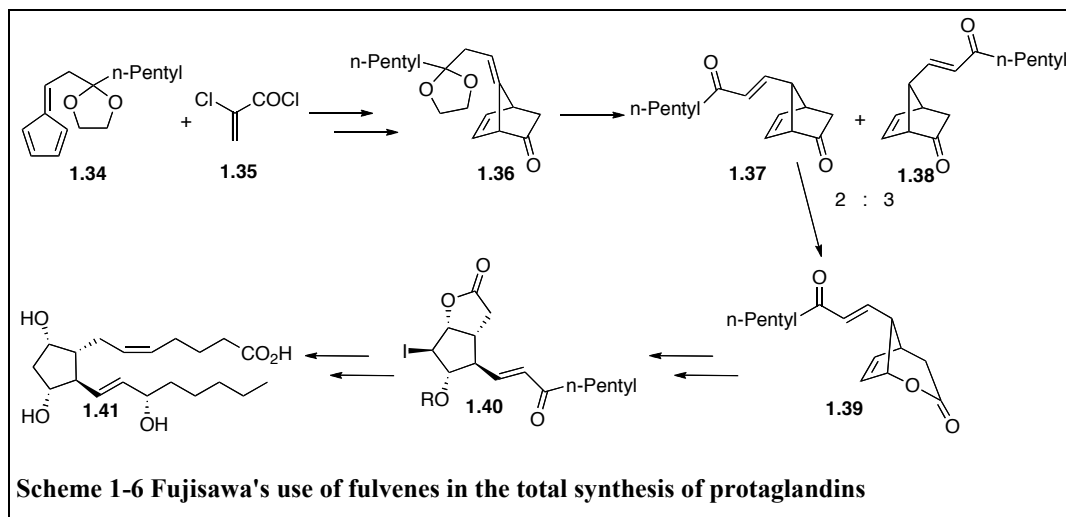
1.1.2.2 Corey's second approach : delete the problematic hydrogen

A few years after his initial work with 5-substituted cyclopentadienes, Corey circumvented the 1,5-H shift problem by eliminating the problematic hydrogen.¹⁴ In the context of the synthesis of 12-methyl PGA₂, Corey prepared

the spiro diene **1.30** which lacked the offending 5-hydrogen and therefore was thermally stable (see Scheme 1-5). This method was used for the synthesis of prostaglandin analogs. A few decades later, the same principle was adopted by Carreira in his synthesis of the core of the Axinellamines.¹⁵ This method has definitive merit because it eliminates the 1,5-H shift problem. However, it is limited to substrates in which a quaternary carbon is desired.



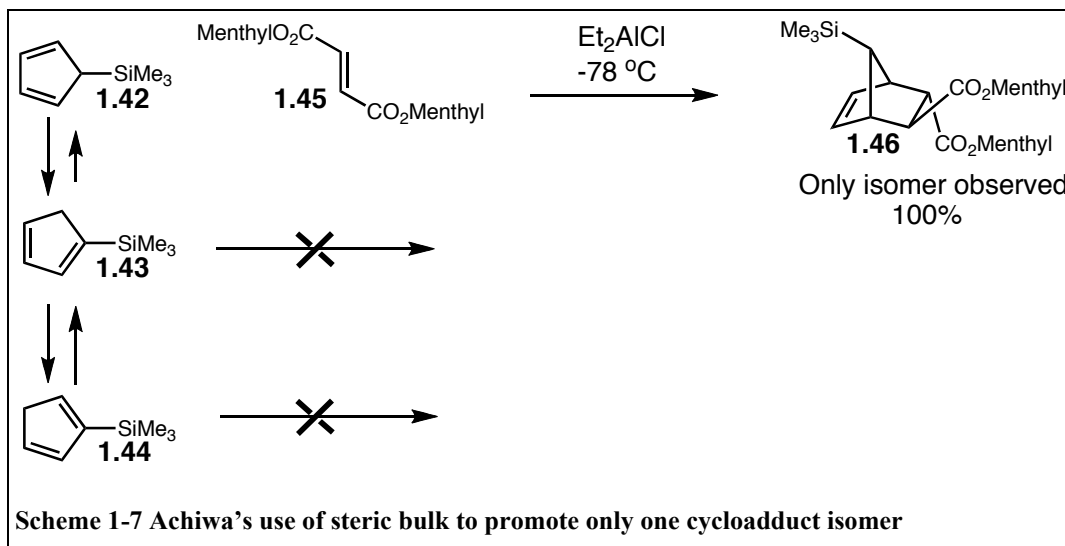
Another variant of this concept is the use of fulvenes which also lack a hydrogen at the 5 position. An example of this approach is the synthesis of prostaglandins by Fujisawa (see Scheme 1-6).¹⁶ Fulvene **1.34** underwent clean 4+2 cycloaddition with a ketene equivalent to yield, after a few steps, the cycloadduct **1.36**. The ketal of this cycloadduct was hydrolyzed and yielded a mixture of syn and anti norbornenes **1.37** and **1.38**. Product **1.37** could be converted to the prostaglandin **1.41**. While fulvenes have potential as useful reaction partners, they react with poor endo/exo selectivity, are unstable and difficult to handle.



1.1.2.3 The exception : 5-trimethylsilyl cyclopentadiene with bulky fumarates

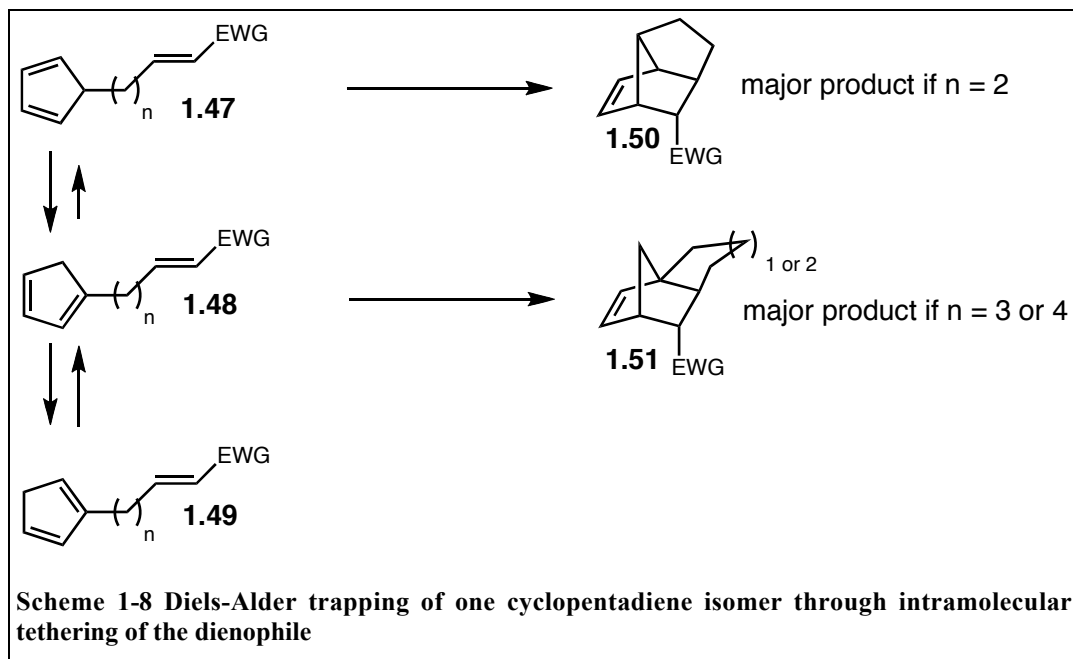
Under specific circumstances, a single isomer of a substituted cyclopentadiene may react preferentially to other isomers. For instance, 5-trimethylsilyl cyclopentadiene can be exquisitely selective for cycloadditions. The use of 5-trimethylsilyl cyclopentadienes in Diels-Alder reactions dates back from the work of Kraihanzel and Losee in 1968.¹⁷ This cyclopentadiene was observed to react similarly to other 5-substituted cyclopentadienes and gave multiple cycloadduct isomers corresponding to the parent cyclopentadiene isomers. However, even though all three possible positional isomers were observed in solution, only the 5- and the 2- isomers would undergo cycloaddition with a dienophile. In 1993, Achiwa further improved this selective reactivity by showing that bulky fumaric esters would only react with the 5-trimethylsilyl isomer to give one cycloadduct isomer.¹⁸ Since the unreactive 1- and 2- substituted cyclopentadiene isomers would isomerize in solution to the 5-substituted isomer, an excellent yield of the desired cycloadduct could be obtained. This selectivity was recently utilized by Carreira in his synthesis of the Massadine cyclopentane core.¹⁹ No study has been done to fully explore the scope of this selectivity, but from the early results of Kraihanzel and Losee, it is to be expected that this

exquisite selectivity is only attainable when bulky 1,2-disubstituted dienophiles are reacted with cyclopentadienes having a bulky side chain.



1.1.2.4 The leash and the trap : intramolecular Diels-Alder reactions

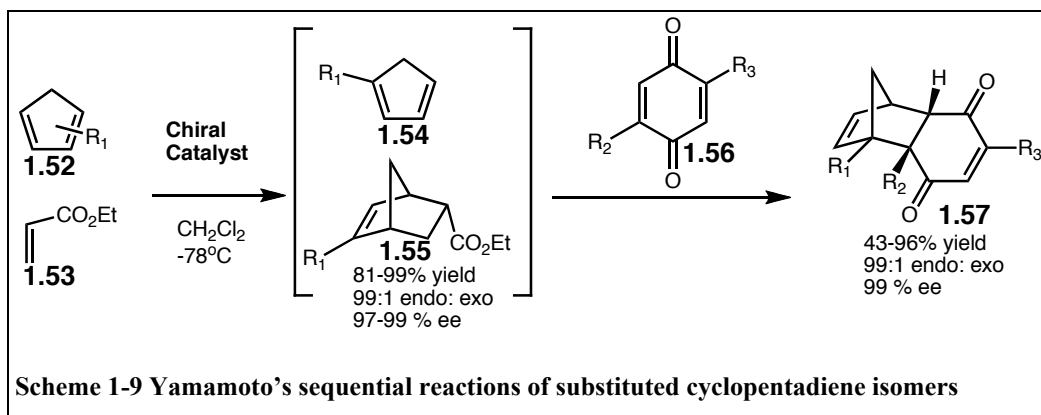
Many studies have shown that intramolecular reactions between cyclopentadiene and a tethered dienophile will give mainly one cycloaddition isomer.²⁰ The nature of this isomer being dependant on the length of the tether; while the cyclopentadiene isomerization takes place, one of the cyclopentadiene isomers will be more prone to Diels-Alder reaction and will thus be trapped, leading to the formation of one main product through LeChatelier's principle. As can be seen from Scheme 1-8, with tethers constituted of two carbon atoms, mainly the 5-substituted isomer reacts and gives products of type **1.50**. With tethers of three to four carbon atoms, mainly the 1-substituted isomer reacts, yielding product of type **1.51**. While this approach works very well for certain substrates, it lacks the generality of the intermolecular Diels-Alder reaction.



1.1.2.5 Working with the thermodynamic mixture: the Yamamoto approach

Recently, Yamamoto suggested an interesting way of dealing with the 1,5-shift problem : simply accepting it and getting the most out of the available thermodynamic mixture of isomers.²¹ From an equilibrated mixture of mono-substituted cyclopentadienes, it was observed that, because of lower steric hindrance in the transition state, the 2 substituted isomer is much more reactive towards cycloadditions than the 1-substituted isomer. Therefore, Yamamoto *et al.* cooled a thermodynamic mixture of substituted cyclopentadiene isomers to -78°C to stop the isomerization process. The more reactive 2-substituted isomer was then allowed to react with one equivalent of a dienophile **1.53** in the presence of a chiral Lewis acid catalyst (see Scheme 1-9) . Under these conditions, only the 2-substituted isomer reacted to give high yields of one major cycloaddition isomer **1.55** in excellent enantiomeric excesses. Upon completion of this first Diels-Alder reaction, a second dienophile **1.56** was added to react with the remaining 1-substituted isomer **1.54**, again yielding one major cycloaddition isomer **1.57** in high enantiomeric excess. The whole process gives two products of complex

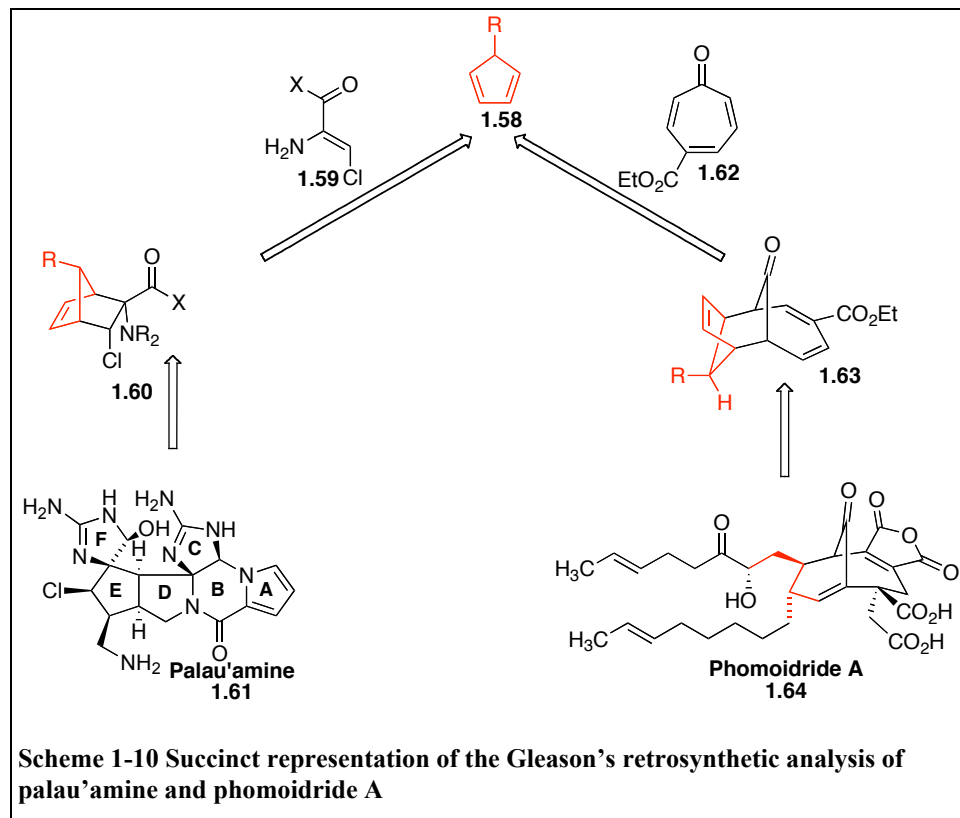
nature. If only the product of the 1-substituted isomer were desired, then the first dienophile would be a sacrificial one to deplete the amount of 2-substituted cyclopentadiene in solution. The limitation of this method is that the maximum yield of each cycloadduct is proportional to the relative amount of its parent cyclopentadiene isomer in the thermodynamic mixture. Also, since the 5-substituted cyclopentadiene isomer comprises only 1 % or less of the equilibrated thermodynamic mixture, this method is not suitable to access this particular isomer.



1.1.3 Our need for a 5-substituted cyclopentadiene

The Gleason laboratory is pursuing the total syntheses of the natural products phomoidride A²² and palau'amine²³. Their respective retrosynthetic approaches are succinctly presented in Scheme 1-10. A common theme in the synthetic approaches to these molecules is the use of a 5-substituted cyclopentadiene to construct a central ring system of the target structure with maximum convergency. In the former case, the [4.3.1] bicycle would be formed via a 6+4 cycloaddition while in the latter case the hexasubstituted cyclopentane would be obtained using a Diels-Alder [4+2] cycloaddition. However, these syntheses share a common synthetic problem: the inherent instability of 5-substituted cyclopentadienes. The current approaches to the synthetic uses of 5-substituted cyclopentadienes were not found to be suitable to our needs. We therefore sought to develop a new methodology for the synthesis and handling of 5-substituted cyclopentadienes. Chapter 2 of this thesis will discuss the

development of a stable 5-substituted cyclopentadiene. In Chapter 3, the application of this stable cyclopentadiene to the synthesis of the E-ring of palau'amine will be detailed.



1.2 Part B : Synthesis of the multiple ligand drug triciferol, agonist of the nuclear vitamin D receptor and inhibitor of histone deacetylases

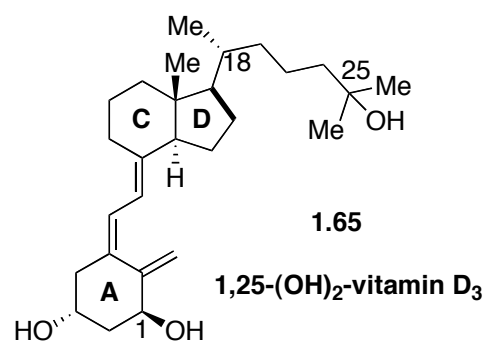
For decades, chemists have been trying to fight cancer by developing new drugs for chemotherapy. Many of the first generation drugs were DNA alkylating agents or DNA intercalators.²⁴ These drugs indiscriminately interfere with cellular DNA in the hope that rapidly dividing cancer cells would die faster than the rest of the patient. Obviously, such an aggressive approach was associated with significant side effects, amongst them the genesis of new cancers due to DNA disruption. More specific and less toxic approaches for treating cancer are therefore needed.

There are many cellular housekeeping mechanisms that prevent normal cells from becoming cancerous. Using those mechanisms already present in the body would be a more specific way of fighting the disease than simply killing dividing cells.²⁵ One such way is through the innate control of cell proliferation. There are many nuclear receptors associated with cell cycle regulation and proliferation. Cancerous cells often down-regulate cellular mechanisms associated with cancer prevention. For example, in acute promyelocytic leukemia, a fusion protein alters the function of the retinoic acid receptor, allowing cancer progression.²⁶ Treatment of this cancer has been very successful with high doses of retinoic acid to compensate for the loss of receptor sensitivity. In other cases, restoring or enhancing the function of cellular housekeeping mechanisms could trigger the selective apoptosis of cancer cells.²⁷ These different approaches are not mutually exclusive and using a combination therapy might prove more effective, for example in preventing the onset of resistance.

1.2.1 Vitamin D₃

The biologically active metabolite of vitamin D₃, 1 α ,25-dihydroxyvitamin D₃ (1,25D₃), is well known for its effects on calcium homeostasis but is also implicated in cell cycle regulation and cell differentiation.^{28,29} The binding of

1,25D₃ to the nuclear vitamin D receptor leads to cofactor recruitment and



eventually to the transcription of target genes associated with reduced cell proliferation. Indeed, 1,25D₃ and some of its analogs are currently being used or investigated for the treatment of hyperproliferative disorders, such as psoriasis and cancer.^{30,31} However, two

main obstacles prevent 1,25D₃ from becoming an effective anti-cancer drug: its effect on calcium homeostasis and the development of resistance to 1,25D₃ in cancer therapy. The undesirable effects of 1,25D₃ on the level of calcium in the body are reduced or eliminated in some artificial analogs of vitamin D₃. However, it was found that the development of resistance to vitamin D in cancer is not linked to the binding of the hormone to its nuclear receptor, but rather a consequence of epigenetic factors affecting the availability of the DNA sequence of the vitamin D response elements to be transcribed. As a consequence, no subtle chemical change in the analogs of vitamin D will prevent the onset of cancer resistance to this hormone. Fortunately, work by our collaborators showed that co-administration of vitamin D with a second type of molecule, a histone deacetylase inhibitor, could reverse cancer resistance and allow for effective suppression of cancer cell growth *in vitro*.

1.2.2 Histone Deacetylase Inhibitors (HDACi)

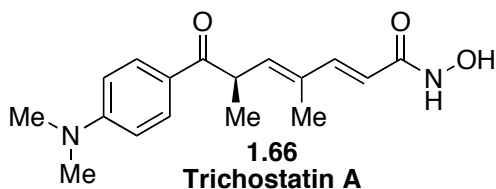
Histone deacetylases (HDAC) are enzymes known to regulate gene expression and participate in cell division.³² An important part of their biological role is to work in tandem with histone acetyl transferases (HAT) and regulate the acetylation of histones, in the chromatin. HAT are involved in the acetylation of the side chains of the lysine amino acids of histones while HDAC do the inverse and remove these acetyl groups. The action of HDAC liberates a primary amine, which is protonated under physiological pH. The resulting positive charge on histones attracts the negatively charged DNA backbone and causes a tighter

interaction between the two, resulting in a more compact chromatin. A compacted chromatin hinders the access of transcriptions factors to the DNA, hence preventing gene activation.³³ Histone deacetylase inhibitors (HDACi) prevent the action of HDAC and therefore promote gene expression. More recently, HDACs have also been linked to the deacetylation of non-histone proteins such as tubulin and heat shock protein 90.^{34,35}

Many HDACi are currently being used or investigated as anti-cancer agents.³⁶ For example, suberoyl anilide hydroxamic acid (SAHA, or Zolinza®) is currently on the market for cutaneous T-cell lymphoma while many other HDACi are in clinical trials.^{37,38} HDACi promote cell differentiation and apoptosis of cancer cells.³⁹ These effects are believed to originate from the activation of anti-cancer genes resulting from chromatin expansion; cancer represses certain genes, allowing itself to thrive, and reactivation of those genes stops the cancer. This reactivation of silenced genes by HDACi could also be used to counter some forms of cancer resistance to chemotherapies.

1.2.3 Synergistic effects of vitamin D₃ and HDACi

Even though some cancers can become resistant to the antiproliferative effects of 1,25D₃, it was shown that an HDACi could reverse this condition. Two independent groups, including our collaborator professor John White, found that



coadministration of trichostatin A (TSA), a hydroxamic acid-based HDACi, and 1,25D₃ was significantly more potent at inhibiting the growth of vitamin D-resistant cancer cells than either 1,25D₃

or TSA alone.⁴⁰ More importantly, synergistic effects between the two molecules were noted; even though 1,25D₃ and TSA independently can inhibit cancer growth, the combination of the two molecules has a higher potency than the sum of the effects of the two individual components.⁴¹ This synergistic effect may result from the gene activation properties of TSA as an HDACi, causing a higher

activation of vitamin D-related genes and therefore enhanced cell cycle regulation of 1,25D₃.⁴²

1.2.4 Multiple ligand drugs

It has been known for many decades that treating a disease with multiple drugs is often more successful than using a single drug. A well-known example is the combination therapy of a protease inhibitor and a reverse transcriptase inhibitor in the treatment of HIV infections. Advantages of combination therapies include the delay of resistance development to the drugs and the limitations of side effects caused by a high concentration of a toxic drug. However, combination therapies also have their disadvantages: the drugs have to be matched in terms of pharmacokinetic profiles and dose/toxicity relationships, which complicates clinical trials and drug intake during treatment. Considering that clinical trials account for 55% of a drug's development costs, any reduction in the complexity of this step is bound to reduce significantly the cost of the overall process.⁴³ From a synthetic chemist's point of view, the solution is fairly straightforward: to move from two different drug molecules to a single entity. This approach of having one molecule interacting with multiple biological targets has gained significant popularity in the past decade and many new drug candidates are now "multiple ligand drugs" (also referred to as "chimera drugs", "hybrid molecule drugs", "non-specific ligands drugs", "dual action drugs" or "promiscuous drugs").^{44,45} An occasional advantage of some of these drugs is the potential to localize two effects based on the properties of one constituent of the multiple ligands molecules. For example, one structure might be specifically delivered to a certain organ or cellular organelle, aiding in the co-localization of the second pharmacophore of the drug. Multiple ligand drugs share common positive features with combination therapies and also have significant additional advantages.

Multiple ligand drugs can be designed in many ways along a continuum of structural possibilities (see Figure 1-6). At one end of the spectrum, two separate agents can be linked *via* a tether. Such a design leads to a drug molecule significantly larger than both original molecules. This approach works well only if the binding sites of both individual molecules are accessible from the protein surface. An example of tethered pharmacophores is molecule **1.69**, which is a combination of adenosine receptor A₃ agonist **1.67** attached to adenosine receptor A₁

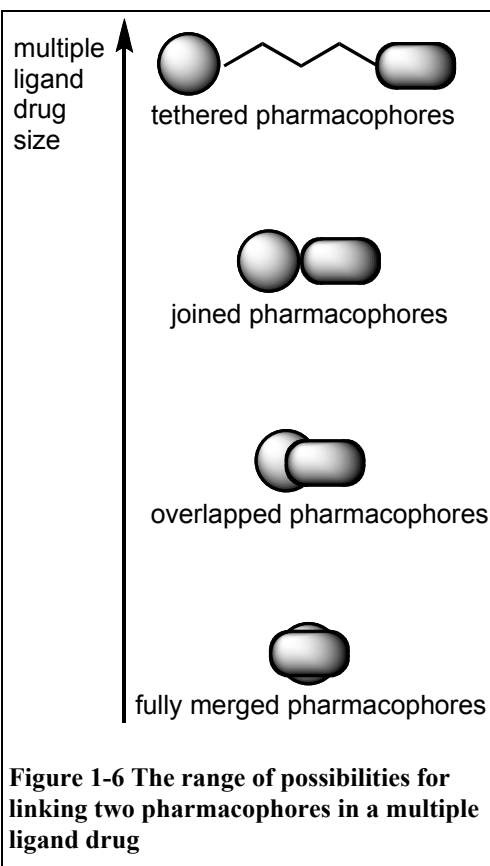
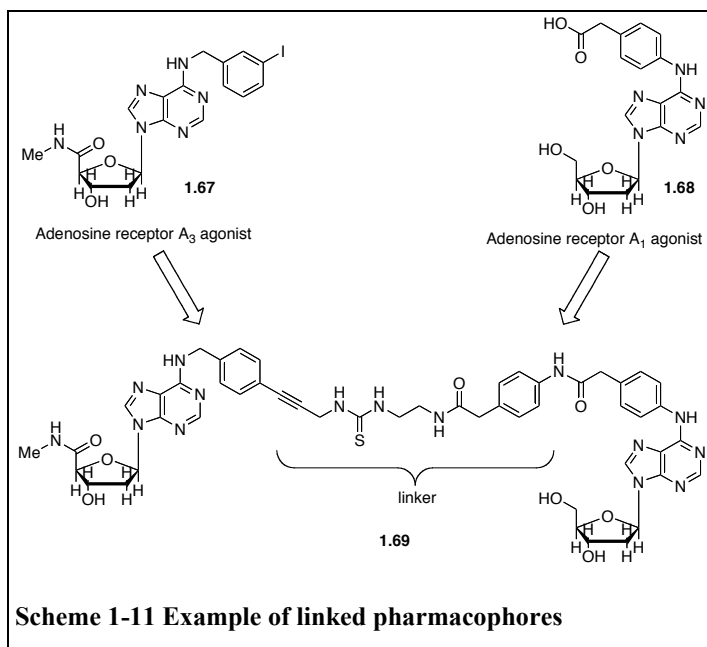


Figure 1-6 The range of possibilities for linking two pharmacophores in a multiple ligand drug

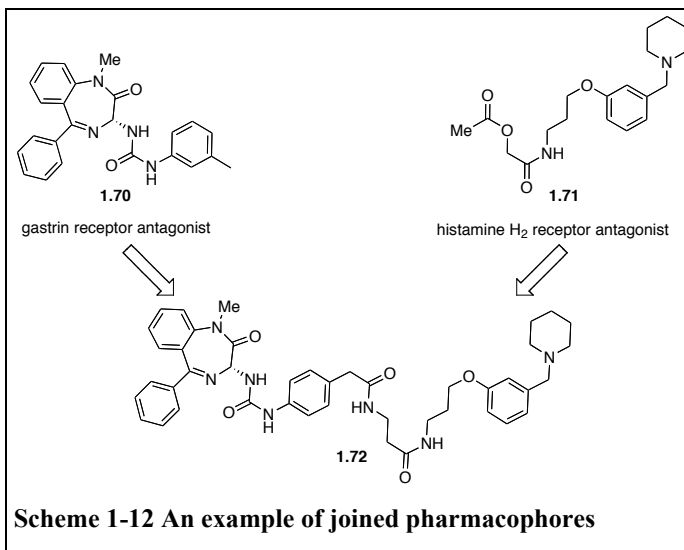
agonist **1.68**.⁴⁶ Partially down the multiple ligand spectrum, the drugs can also simply be joined together with no tether and with minimal change to both original structures. For example, molecule **1.72** arises from the fusion of gastrin receptor



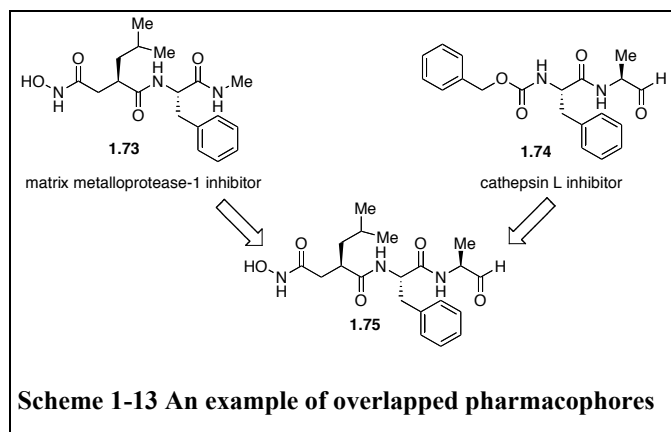
Scheme 1-11 Example of linked pharmacophores

antagonist molecule **1.70** and histamine H₂ receptor antagonist **1.71**.⁴⁷ Alternatively, if both pharmacophores share a common motif, an overlapped structure can be created. As an example, both pharmacophores of the matrix metalloprotease-1 inhibitor **1.73** and

cathepsin-L inhibitor **1.74** share a terminal phenylalanine and thus both structures have been overlapped to create the dual inhibitor **1.75**, which is larger than either molecule but smaller than both molecules together.⁴⁸ Finally, the other extreme of the



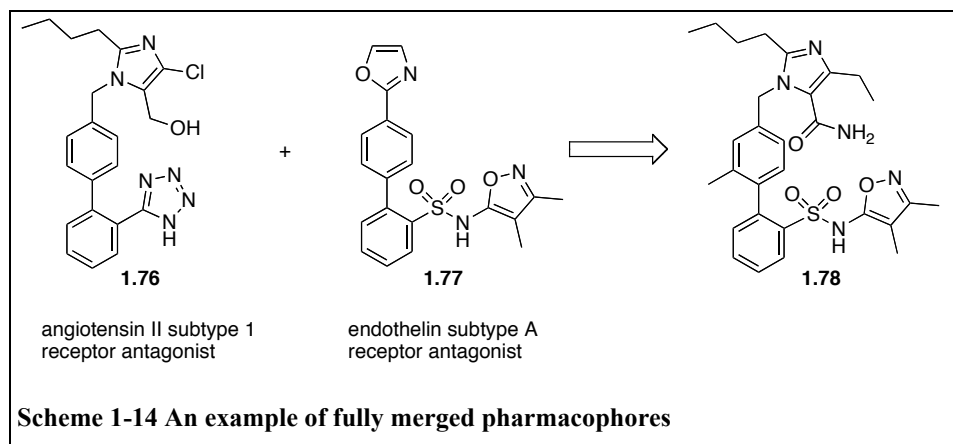
multiple ligand drug spectrum is reached when the dual ligand is no bigger than the largest of the two original structures. This “fully merged” scenario is



exemplified by the combination of angiotensin II subtype 1 receptor antagonist **1.76** and endothelin subtype A receptor antagonist **1.77**, where the resulting multiple ligand **1.78** is only slightly larger than either of

the original molecules.⁴⁹ The design of multiple ligands drugs can thus vary widely depending on the structures of the individual ligands and the requirements for target binding.

The synergy between 1,25D₃ and TSA in inhibiting the growth of cancer cells *in vitro* inspired us to create a multiple ligand drug based on the structures of Vitamin D₃ and TSA, with the goal that such a molecule might be an effective anti-cancer drug. The new single molecule would be capable of binding either target proteins and would have the advantages of multiple ligand drugs, such as the potential to co-localize both of its effects in the cell’s nucleus and also a



simplified pharmacokinetic profile. Chapter 4 of this thesis will describe the design, synthesis and characterization of triciferol, a fully bifunctional hybrid molecule which combines agonism for the vitamin D receptor and inhibition of histone deacetylase and which possesses improved cytostatic and cytotoxic properties relative to 1,25D₃.

1.3 Reference

¹ Otto Diels; Kurt Alder, *Justus Liebig's Annalen der Chemie* **1928**, 460 (1), 98-122.

² Nicolaou, K.C.; Snyder, S.A.; Montagnon, T.; Vassilikogiannakis, G., *Angewandte Chemie International Edition* **2002**, 41 (10), 1668-1698.

³ Woodward, R. B.; Bader, F. E.; Bickel, H.; Frey, A. J.; Kierstead, R. W., *Journal of the American Chemical Society* **1956**, 78 (9), 2023-2025.

⁴ Fukui, K.; Yonezawa, T.; Shingu, H., *The Journal of Chemical Physics* **1952**, 20 (4), 722-725.

⁵ Fleming, I., *Frontier orbitals and organic chemical reactions*. Wiley: London ; New York, 1977; 249 pages

⁶ Hoffmann, R.; Woodward, R. B., *Journal of the American Chemical Society* **2002**, 87 (19), 4388-4389.

-
- ⁷ A) Corey, E. J.; Weinschenker, N. M.; Schaaf, T. K.; Huber, W., *Journal of the American Chemical Society* **1969**, *91* (20), 5675-5677. B) Corey, E. J.; Noyori, R.; Schaaf, T. K., *Journal of the American Chemical Society* **1970**, *92* (8), 2586-2587. C) Corey, E. J.; Koelliker, U.; Neuffer, J., *Journal of the American Chemical Society* **1970**, *93* (6), 1489-1490.
- ⁸ Corey, E. J.; Ensley, H. E., *Journal of the American Chemical Society* **1975**, *97* (23), 6908-6909.
- ⁹ Corey, E. J.; Loh, T. P., *Journal of the American Chemical Society* **1991**, *113* (23), 8966-8967.
- ¹⁰ Mironov, V. A.; Sobolev, E. V.; Elizarova, A. N., *Tetrahedron* **1963**, *19* (12), 1939-1958.
- ¹¹ A) McLean, S.; Haynes, P., *Tetrahedron Letters* **1964**, *5* (34), 2385-2390. B) McLean, S.; Haynes, P., *Tetrahedron* **1965**, *21* (9), 2329-2342.
- ¹² Breslow, R.; Hoffman, J. M.; Perchonock, C., *Tetrahedron Letters* **1973**, *14* (38), 3723-3726.
- ¹³ Corey, E. J.; Koelliker, U.; Neuffer, J., *Journal of the American Chemical Society* **1971**, *93* (6), 1489-1490.
- ¹⁴ Corey, E. J.; Shiner, C. S.; Volante, R. P.; Cyr, C. R., *Tetrahedron Letters* **1975**, *16* (13), 1161-1164.
- ¹⁵ A) Ledford, B. E.; Carreira, E. M., *Journal of the American Chemical Society* **1995**, *117* (47), 11811-11812. B) Starr, J. T.; Baudat, A.; Carreira, E. M., *Tetrahedron Letters* **1998**, *39* (32), 5675-5678. C) Starr, J. T.; Koch, G.; Carreira, E. M., *Journal of the American Chemical Society* **2000**, *122* (36), 8793-8794.
- ¹⁶ Sakai, K.; Kobori, T.; Fujisawa, T., *Tetrahedron Letters* **1981**, *22* (2), 115-118.
- ¹⁷ Kraihanzel, C. S.; Losee, M. L., *Journal of the American Chemical Society* **1968**, *90* (17), 4701-4705.
- ¹⁸ Yamazaki, A.; Morimoto, T.; Achiwa, K., *Tetrahedron: Asymmetry* **1993**, *4* (11), 2287-2290.
- ¹⁹ Breder, A.; Chinigo, G. M.; Waltman, A. W.; Carreira, E. M., *Angewandte Chemie International Edition* **2008**, *47* (44), 8514-8517.

-
- ²⁰ A) Brieger, G., *Journal of the American Chemical Society* **1963**, 85 (23), 3783-3784. B) Corey, E. J.; Glass, R. S., *Journal of the American Chemical Society* **1967**, 89 (11), 2600-2610. C) Breitholle, E. G.; Fallis, A. G., *Journal of Organic Chemistry* **1978**, 43 (10), 1964-1968. D) Snowden, R. L., *Tetrahedron Letters* **1981**, 22 (2), 97-100. E) Sternbach, D. D.; Hughes, J. W.; Burdi, D. F.; Forstot, R. M., *Tetrahedron Letters* **1983**, 24 (32), 3295-3298. F) Stille, J. R.; Grubbs, R. H., *Journal of Organic Chemistry* **1989**, 54 (2), 434-444.
- ²¹ Payette, J. N.; Yamamoto, H., *Journal of the American Chemical Society* **2007**, 129 (31), 9536-9537.
- ²² Dabrah, T. T.; Kaneko, T.; Masefski, W.; Whipple, E. B., *Journal of the American Chemical Society* **1997**, 119 (7), 1594-1598.
- ²³ Kinnel, R. B.; Gehrken, H. P.; Scheuer, P. J., *Journal of the American Chemical Society* **1993**, 115 (8), 3376-3377.
- ²⁴ Gabriel, J. (editor); *The biology of cancer* [electronic resource] ; John Wiley & Sons, Chichester, England, 2007.
- ²⁵ Ruddon, Raymond W., *Cancer biology*, Oxford University Press, Oxford, New York, 2007, 540 p
- ²⁶ Tallman, M. S.; Altman, J. K., *Hematology* **2008**, 2008 (1), 391-399.
- ²⁷ Cotter, T. G., *Nature Reviews Cancer* **2009**, 9 (7), 501-507.
- ²⁸ Lin, R.; White, J. H., *BioEssays* **2004**, 26 (1), 21-28.
- ²⁹ Deeb, K. K.; Trump, D. L.; Johnson, C. S., *Nature Reviews Cancer* **2007**, 7 (9), 684-700.
- ³⁰ Bury, Y.; Ruf, D.; Hansen, C. M.; Kissmeyer, A.-M.; Binderup, L.; Carlberg, C., *Journal of Investigational Dermatology* **2001**, 116 (5), 785-792.
- ³¹ Masuda, S.; Jones, G., *Molecular Cancer Therapeutics* **2006**, 5 (4), 797-808.
- ³² de Ruijter, A. J. M.; van Gennip, A. H.; Caron, H. N.; Kemp, S.; van Kuilenburg, A. B. P., *Biochemistry Journal* **2003**, 370 (3), 737-749.
- ³³ Bhaumik, S. R.; Smith, E.; Shilatifard, A., *Nature Structural & Molecular Biology* **2007**, 14 (11), 1008-1016.
- ³⁴ Zhang, Y.; Kwon, S.; Yamaguchi, T.; Cubizolles, F.; Tousseaux, S.; Kneissel, M.; Cao, C.; Li, N.; Cheng, H.-L.; Chua, K.; Lombard, D.; Mizeracki, A.;

Matthias, G.; Alt, F.W.; Khochbin, S.; Matthias, P., *Molecular and Cellular Biology* **2008**, *28* (5), 1688-1701.

³⁵ Bali, P.; Pranpat, M.; Bradner, J.; Balasis, M.; Fiskus, W.; Guo, F.; Rocha, K.; Kumaraswamy, S.; Boyapalle, S.; Atadja, P.; Seto, E.; Bhalla, K., *Journal of Biological Chemistry* **2005**, *280* (29), 26729-26734.

³⁶ Acharya, M. R.; Sparreboom, A.; Venitz, J.; Figg, W. D., *Molecular Pharmacology* **2005**, *68* (4), 917-932.

³⁷ Marks, P. A.; Breslow, R., *Nature Biotechnology* **2007**, *25* (1), 84-90.

³⁸ Xu, W. S.; Parmigiani, R. B.; Marks, P. A., *Oncogene* *26* (37), 5541-5552.

³⁹ Donald, R. W.; Xiang-Jiao, Y., *Current Oncology; Vol 15, No 5 (2008)* **2008**.

⁴⁰ A) Khanim, F. L.; Gommersall, L. M.; Wood, V. H. J.; Smith, K. L.; Montalvo, L.; O'Neill, L. P.; Xu, Y.; Peehl, D. M.; Stewart, P. M.; Turner, B. M.; Campbell, M. J., *Oncogene* **2004**, *23* (40), 6712-6725. B) Tavera-Mendoza, L.E.; Dabbas, B.; White, J.H.; *unpublished results*

⁴¹ For another significant example of synergistic effects in anti-cancer drugs, see: Adachi, M.; Zhang, Y.; Zhao, X.; Minami, T.; Kawamura, R.; Hinoda, Y.; Imai, K., *Clinical Cancer Research* **2004**, *10* (11), 3853-3862.

⁴² Carlberg, C.; Seuter, S.; *Anticancer Research* **2009**, *29* (9), 3485-3493.

⁴³ Meunier, B., *Accounts of Chemical Research* **2007**, *41* (1), 69-77.

⁴⁴ Morphy, R.; Rankovic, Z., *Drug Discovery Today* **2007**, *12* (3-4), 156-160.

⁴⁵ Morphy, R.; Rankovic, Z., *Journal of Medicinal Chemistry* **2005**, *48* (21), 6523-6543.

⁴⁶ Jacobson, K. A.; Xie, R.; Young, L.; Chang, L.; Liang, B. T. ; *Journal of Biological Chemistry*. **2000**, *275*, 30272-30279

⁴⁷ Kawanishi, Y.; Ishihara, S.; Tsushima, T.; Seno, K.; Miyagoshi, M.; Hagishita, S.; Ishikawa, M.; Shima, N.; Shimamura, M.; Ishihara, Y., *Bioorganic & Medicinal Chemistry Letters* **1996**, *6* (13), 1427-1430.

⁴⁸ Yamamoto, M.; Ikeda, S.; Kondo, H.; Inoue, S. *Bioorganic & Medicinal Chemistry Letters* **2002**, *12*, 375-378

⁴⁹ Tellew, J. E.; Baska, R. A.; Beyer, S. M.; Carlson, K. E.; Cornelius, L. A.; Fadnis, L.; Gu, Z.; Kunst, B. L.; Kowala, M. C.; Monshiza-degan, H.; Murugesan,

N.; Ryan, C. S.; Valentine, M. T.; Yang, Y.; Macor, J. E. *Bioorganic & Medicinal Chemistry Letters* **2003**, *13*, 1093-1096

Part A

2 Substituted Cyclopentadienes and Their Uses in Cycloadditions

Cycloadditions are important in chemical synthesis because they allow for the rapid built-up of complexity. Of all cycloadditions, the Diels-Alder reaction is one of the most studied and used. In this reaction, cyclic dienes allow for the controlled construction of complex bridged bicyclic molecules. Amongst cyclic dienes, cyclopentadiene is one of the most used dienes. In sharp contrast, substituted cyclopentadienes are seldom used in synthesis because of their innate tendency to isomerize easily by 1,5-H shift. The Gleason group is very interested in the use of cycloadditions in total synthesis. This interest led us to the challenge of using substituted cyclopentadienes to rapidly and efficiently build complexity in our synthetic efforts.

2.1 Development of a new 5-substituted cyclopentadiene

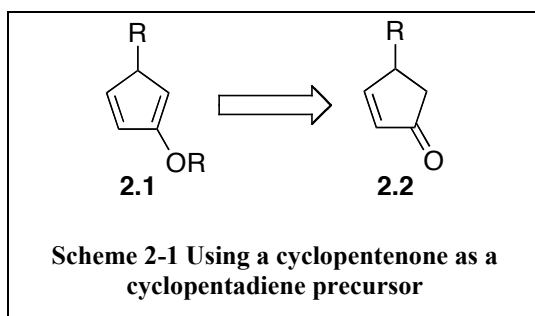
Even though all of the previously published methods for handling substituted cyclopentadienes had some advantages, none was versatile enough to accommodate our specific total synthesis needs. We therefore sought to create a new methodology based on the current knowledge of the different systems available.

To meet our total synthesis goals, we needed a methodology that allowed us to install an appropriate substituent on the 5 position of the cyclopentadiene, depending on the exact retrosynthetic scheme we wanted to use. It was thus evident that the alkylation of thallos cyclopentadienide, as proposed by Corey, had limitations since only very reactive alkylating agents could be used. Nevertheless, isolating an unstable cyclopentadiene at low temperature was considered a possible (even though less than ideal) option. We therefore decided to reverse the general order of reaction that Corey used; Corey had the cyclopentadiene pre-formed and installed the side chain in the last step before cycloaddition. We decided to first attach a side chain of our choice to a cyclopentadiene precursor and then form the cyclopentadiene as the last step. For

this, we needed to utilize an efficient and fast reaction that could form the cyclopentadiene at low temperature.

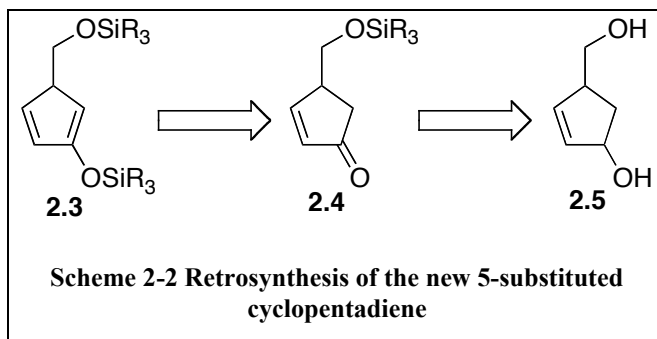
We also had the goal, if possible, to generate a cyclopentadiene that would be more stable than a simple 5-substituted cyclopentadiene (half-life at room temperature of 1 hour) in order to make it easier to handle. From the work of McLean and Haynes (see Scheme 1-3), it can be observed that adding substituents on a cyclopentadiene makes it less susceptible to the undesirable hydride shift. However, adding an extra alkyl group, such as the 2-methyl group used by McLean and Haynes, limits the generality of the method; it introduces an undesirable carbon-carbon bond that would be difficult to delete later during the synthesis.

Taking all of those considerations together, for several reasons it emerged that the ideal reaction to generate a cyclopentadiene would be the enolate trapping of a cyclopentenone precursor (see Scheme 2-1). First, enolates can be quickly formed and trapped at low temperatures, therefore limiting the potential for the rapid thermal 1,5-H shift. Second, as with other electron donating groups, the oxygen substituent on the 2-position might stabilize the diene towards 1,5-H shift as was empirically observed before (vide supra section 1.1.1). In fact, it was observed by our group and others that 2-silyloxy cyclopentadiene is easier to handle and seems to isomerize slower than other substituted cyclopentadienes.⁵⁰ Third, during the Diels-Alder reaction, the strong electron-donating nature of the diene's oxygen would control the regioselectivity of the cycloaddition (FMO control). Finally, the extra oxygen substituent could be used as a synthetic handle for further functionalization of the product after cycloaddition and would easily differentiate the norbornene's two alkenic carbons for selective transformation.



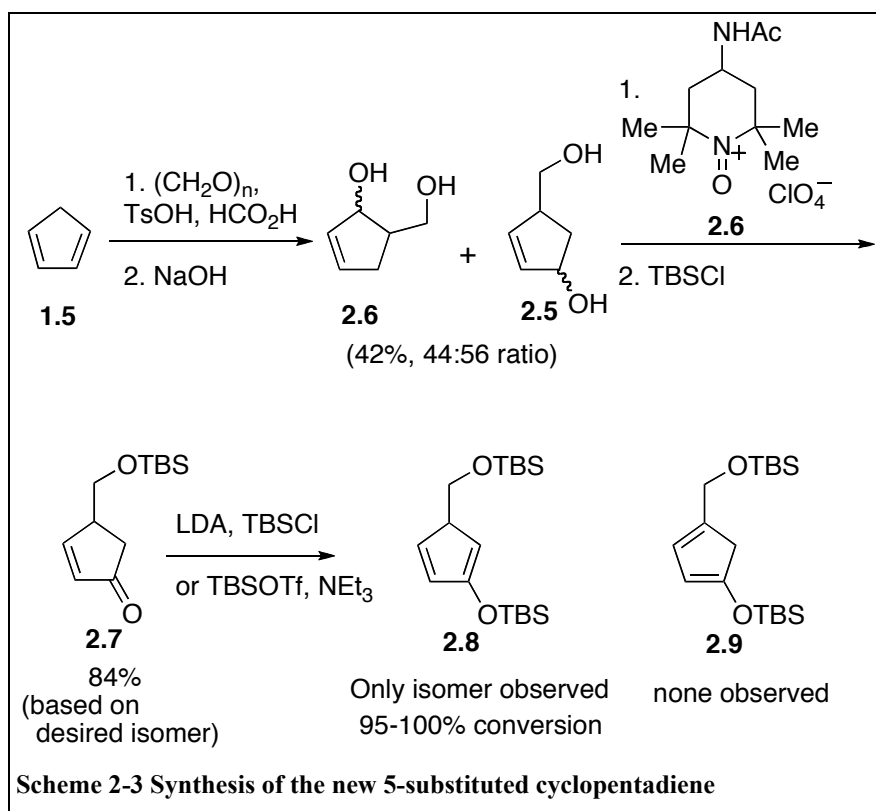
2.1.1 Synthesis of a 5-alkyl-2-silyloxy cyclopentadiene

To trap the enolate of a cyclopentenone and generate a cyclopentadiene, the use of a silyl group emerged as the option of choice.⁵¹ Due to the strong interaction between silicon and oxygen, silyl enol ethers are easy to generate either by trapping of a pre-formed enolate (hard enolization) or by using the silicon as a Lewis acid in combination with a mild base (soft enolization). Also, silyl groups are easily deprotected under a variety of conditions.⁵² As a cyclopentenone substituent, we desired an alkyl group that could be further functionalized according to a variety of synthetic needs. A silyloxy methane group thus appeared to be ideal for this purpose. We therefore thought a diol such as **2.5** would be a suitable synthetic starting point for our desired 5-substituted cyclopentadiene.



The synthesis of our desired diene started with a Prins reaction of cyclopentadiene and formaldehyde following a modification of a published procedure by Saville-Stones *et al.*⁵³ Conducting the reaction in formic acid resulted in the formation of a mixture of formate esters which could be hydrolyzed with sodium hydroxide to give an inseparable mixture of four diol isomers in a combined 42 % yield (see Scheme 2-3). The low overall yield of the desired isomers is compensated by an easily scaled up procedure and inexpensive reagents. Next, it was imperative to differentiate the secondary allylic alcohol and the primary alcohol of the diols, either through selective oxidation of the former or protection of the latter. Selective protection of the primary alcohol could not be efficiently achieved, even with a bulky trityl group. Standard oxidizing agents

normally associated with exclusive or preferential oxidation of an allylic alcohol also showed poor selectivity. However, the Bobbitt's oxidant **2.6** (4-acetamido-2,2,6,6-tetramethyl-1-oxopiperidinium perchlorate) proved extremely useful for the desired transformation. It selectively, cleanly and quickly oxidized the secondary allylic alcohol of the substrate in the presence of the primary alcohol. After oxidation of the mixture of four diol isomers, a mixture of two enones is obtained. This mixture can be separated but was conveniently carried forward by silylation of the primary alcohol, followed by chromatographic separation of the isomers, yielding the desired enone **2.7** in 84% yield based on the desired isomer **2.5** in the diol mixture.

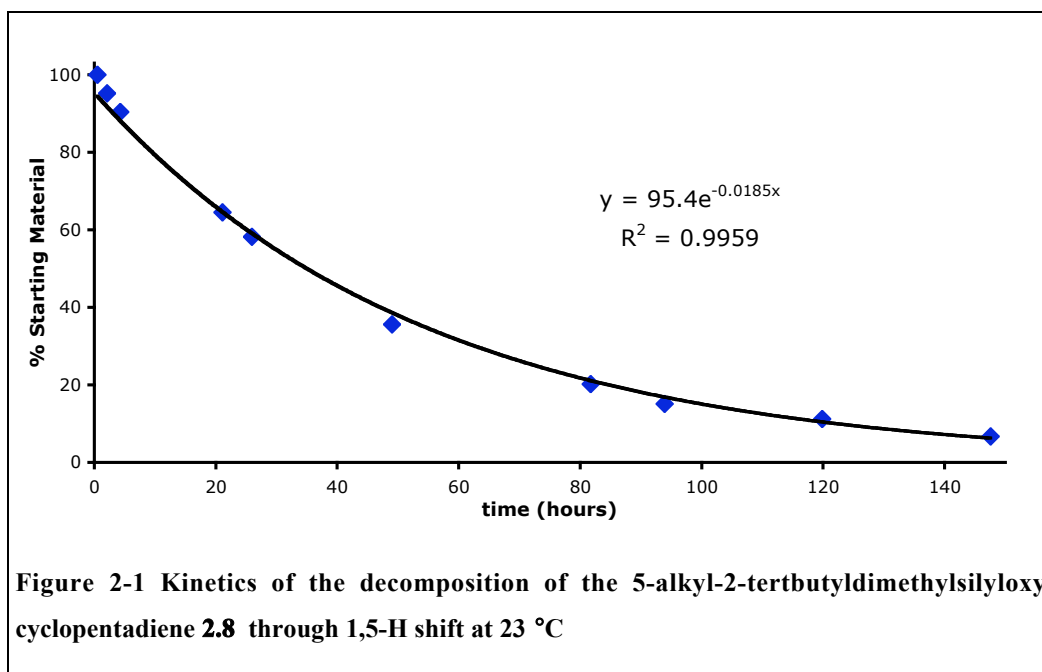


With the enone precursor **2.7** in hand, the generation of the desired cyclopentadiene through enol silylation was investigated. The desired cyclopentadiene could be obtained from hard enolization (deprotonation with LDA at -78°C) and then trapping of the resultant enolate with a silylating agent (R_3SiCl). As well, a soft enolization/trapping procedure (R_3SiOTf , TEA, -10°C)

was found to be equally effective. In both cases, a mild work-up procedure had to be performed to obtain the product in high yield and purity. After enolsilylation of 4-alkyl-2-cyclopentenone, only the cross-conjugate enol ether was obtained. The TMS, TES and TBS silyl enol ethers could be synthesized, with the later being the species of choice due to increased hydrolytic stability. From the stable enone precursor **2.7**, the 5-alkyl-2-silyloxy diene **2.8** could be obtained in two hours, never being exposed to temperatures above 0 °C until NMR analysis.

2.1.2 Experimental studies of the diene's stability towards 1,5-H shift

With the desired 5-alkyl-2-silyloxy diene **2.8** readily available, its stability was investigated both experimentally and *in silico*. The decomposition of the diene through 1,5-H shift was followed by ¹H NMR. A sample of the diene was diluted in deuterated benzene at 23 °C and analyzed periodically by ¹H NMR. The disappearance of the diene's NMR signal over time, as compared to an internal standard, was fitted to a first order exponential decay.

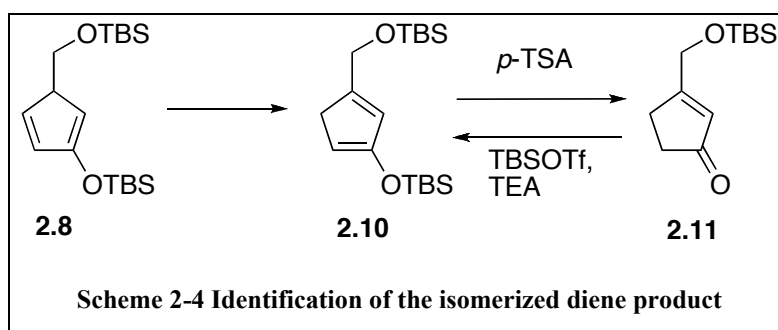


The half life ($t_{1/2}$) of this process can be calculated using the formula:

$$t_{1/2} = \ln(2) / k \quad (2.1)$$

where k is the exponential factor of the regression curve in Figure 2-1. Such an analysis yields a half-life of 37 h (± 15 %) at 23 °C for the isomerization of the diene **2.8**. The new diene was therefore observed to be much more stable than 5-methylcyclopentadiene ($t_{1/2}$ of ~ 1 h at RT) and even more stable than 2,5-dimethylcyclopentadiene ($t_{1/2}$ of ~ 15 h at RT). Practically, this means that the diene can be handled at room temperature for short periods of time without any significant isomerization (less than 2 % isomerized after 1 h). The workup procedure of the diene, involving an aqueous workup and solvent evaporation, can thus be performed at room temperature, avoiding laborious handling protocols at low temperature. The diene displayed a half-life of 10-15 days at -4 °C and could even be stored for a month at -20 °C with little (< 5 % by ^1H NMR) isomerization.

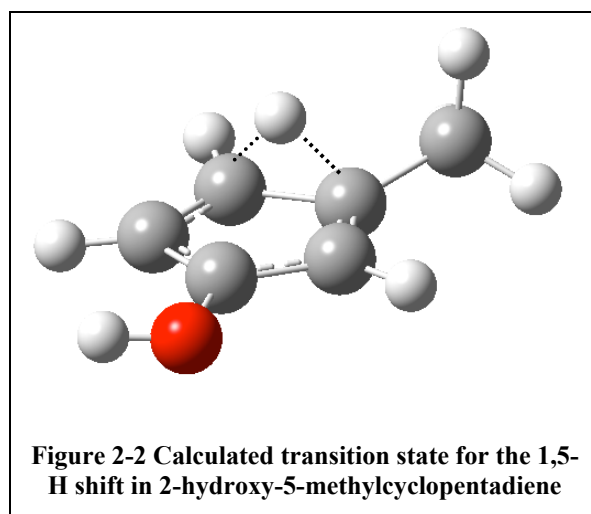
The isomerization of diene **2.8** afforded one predominant product after a few days. However, both **2.8** and the new product could not be isolated by silica gel chromatography due to decomposition. The isomerized product could therefore not easily be unambiguously identified through direct methods. However, quenching the isomerized product with acid afforded the new enone **2.11**. This enone could be resubmitted to the standard enolsilylation conditions and was found to regenerate the major isomerization product **2.10** cleanly, therefore confirming the nature of the isomerization product.



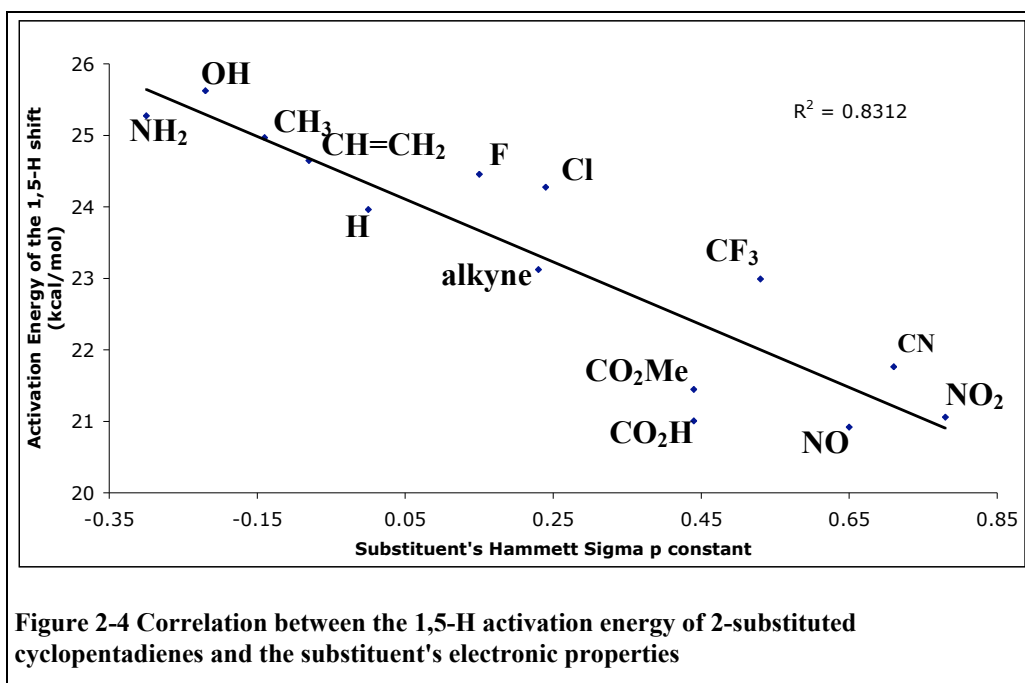
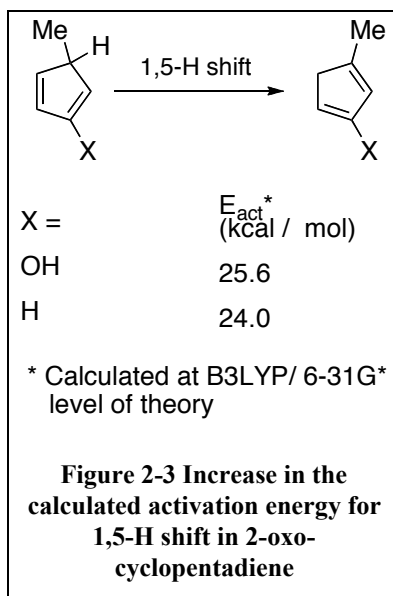
2.1.3 Computational studies of the diene isomerization

With encouraging data in hand about the new diene's thermal stability towards 1,5-H shift, we were interested in better understanding the cause of this increased stability as compared to cyclopentadiene. We therefore used density

functional theory (DFT) simulations at the B3LYP-6/31G* level to calculate the activation enthalpy of many 2-substituted cyclopentadienes undergoing 1,5-H shifts.⁵⁴ We were hoping to observe a stability trend that would give us more insight into this system. To limit the amount of computation needed, the system was simplified to a 5-methylcyclopentadiene and the 2-substituents had a minimum number of atoms. For example, the 2-silyloxy substituent was approximated by a 2-hydroxy group. It is important to point out that DFT calculations do not estimate the absolute energy of a transition state well. However, these types of calculations can be used to compare similar transition states.⁵⁵



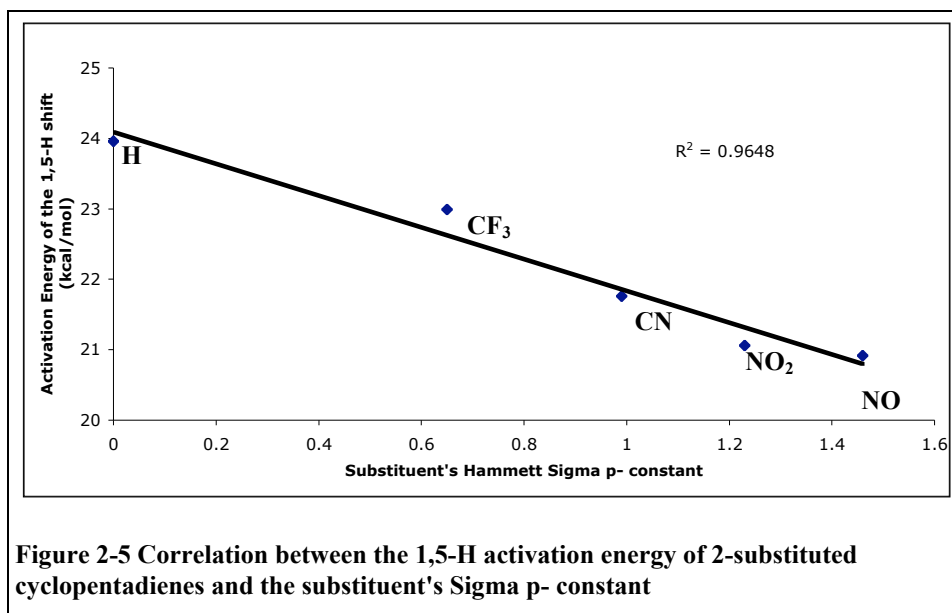
The computations predicted that the activation energy for the 1,5-H shift of a 2-hydroxy-5-methyl cyclopentadiene (see Figure 2-2) would be 25.6 kcal/mol, as compared to 24.0 kcal/mol for 5-methyl cyclopentadiene. This increase in stability of 1.6 kcal/mol with a 2-oxo substituent agrees well with the experimentally observed increase in stability of the new diene versus cyclopentadiene. It was found that substituents having electron-withdrawing power (as compared to hydrogen, ex: CF₃, CN, NO₂) lower the activation energy of the 1,5-H shift whereas substituents having electron-donating ability (ex: OH, NH₂) increased it (see Figure 2-4).



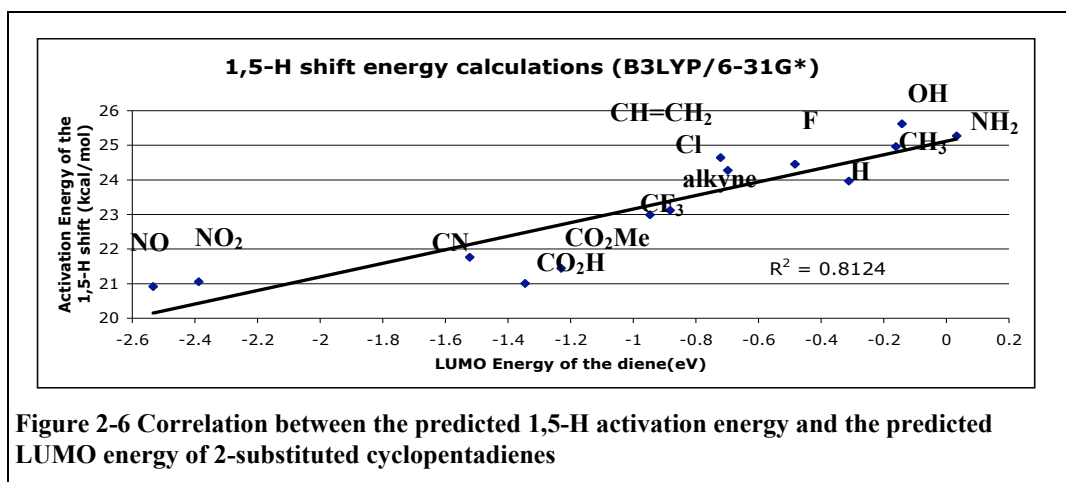
Plotting the computed activation energy for the hydride shift versus the Hammett sigma *p* value⁵⁶ of the cyclopentadiene substituent showed a modest trend (See Figure 2-4). Instead, using the Hammett sigma *p*- value gave a better fit (see Figure 2-5), even though fewer data points were used since the sigma *p*- values are only available for a limited range of substituents. As compared to the normal Hammett sigma *p* value, the Hammett sigma *p*- more accurately takes into

account the resonance effect of the substituent with a developing negative charge during the reaction. The better fit observed could be indicative of a buildup of negative charge on the cyclopentadiene ring during the transition state of the sigmatropic rearrangement. Thus, in this particular case, a 1,5-H shift on cyclopentadiene could be envisioned as a cationic proton migration on an aromatic cyclopentadienide anion. However, this is only an analogy as 1,5-H shifts are also known to proceed on acyclic dienes. In fact, Okamura *et al.* described the acceleration of an acyclic 1,5-H shift by an electron-withdrawing sulfoxide group, an observation in accord with the trends found in our computational studies.⁵⁷ However, no explanation was proposed by Okamura *et al.* for their experimental results.

Performing a Hammett plot using the computed activation energies for the 1,5-H shift yielded a reaction constant ρ of 3.23, meaning that this reaction is very sensitive to electronic effects (see Appendix 4 for a more detailed discussion).

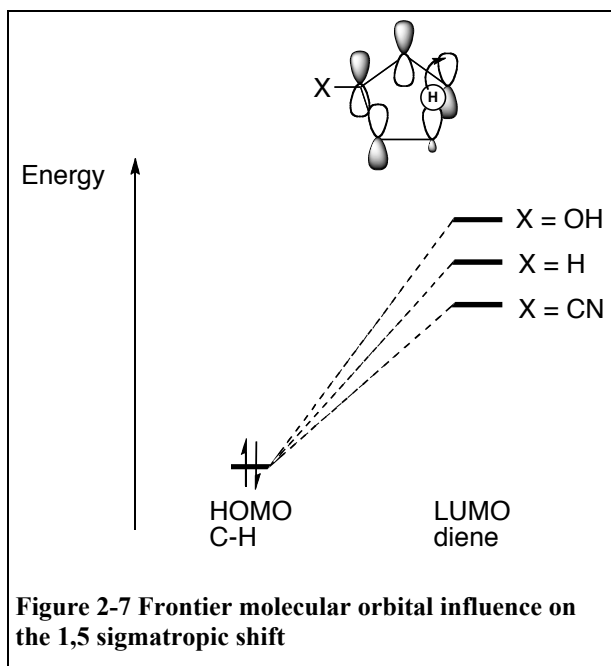


Plotting the computed activation energy for the hydride shift versus the computed LUMO energy of the diene also afforded a modest correlation, again emphasizing the fact that electron-withdrawing substituents accelerate the 1,5-H shift while electron-donating substituents retard it (see Figure 2.6).



2.1.4 Theoretical explanation of the diene's stability

A good theoretical explanation of the 1,5-sigmatropic shift process is proposed in FMO theory: interaction of the HOMO of the breaking C-H bond with the LUMO of the diene. Starting from the FMO description of a 1,5-sigmatropic rearrangement, it can be understood that a 1,5-H shift will be very favorable if there is good overlap between the diene's LUMO and the HOMO of the breaking C-H bond. Thus, electron-withdrawing substituents on the diene will lower its LUMO and create a more favorable interaction with the C-H HOMO, resulting in a lower transition state for the sigmatropic shift. On the other hand, electron-donating substituents on the diene will increase its LUMO, therefore reducing the orbital overlap with the C-H HOMO resulting in a slowing down of the 1,5-H shift (see Figure 2-7). The 2-silyloxy group of the new diene is more electron-donating than a 2-methyl group, making diene **2.8** significantly more stable towards 1,5-H shift than 2-methyl cyclopentadiene. This explanation is further supported by the trend observed in Figure 2-6, where higher LUMO energy generally lead to higher activation energy for the 1,5-H shift. This theory can be used to explain the Okamura results on the acceleration of acyclic 1,5H shift by a sulfoxide group.⁵⁷



This rationale can also explain the results from Breslow *et al.*¹² They found that a halogen at the 5-position of a cyclopentadiene was slowing down the 1,5-H shift. This is probably because the halogen decreases the energy of the adjacent C-H HOMO and thus decreases the orbital overlap with the diene's LUMO. Since an electron-withdrawing substituent (the halogen) on the 5-position of cyclopentadiene will decrease the 1,5-H shift, it can be extrapolated that an electron-donating substituent should increase the 1,5-H shift, by increasing the energy of the C-H HOMO. Since in the new diene **2.8** the 5-substituent is an alkyl group (CH₂OTBS), this substituent is predicted to slightly accelerate the 1,5-H shift. Therefore, according to FMO theory, the observed increased stability of the new diene, as compared cyclopentadiene, is due to the 2-oxo substituent only.

2.2 Use of the new diene in Diels-Alder cycloadditions

2.2.1 Optimization of the Diels-Alder reaction conditions

Our main interest for diene **2.8** was its behavior in cycloadditions. We thus set out to examine its effectiveness in Diels-Alder additions with a variety of dienophiles. For each reaction, the diene was independently synthesized and

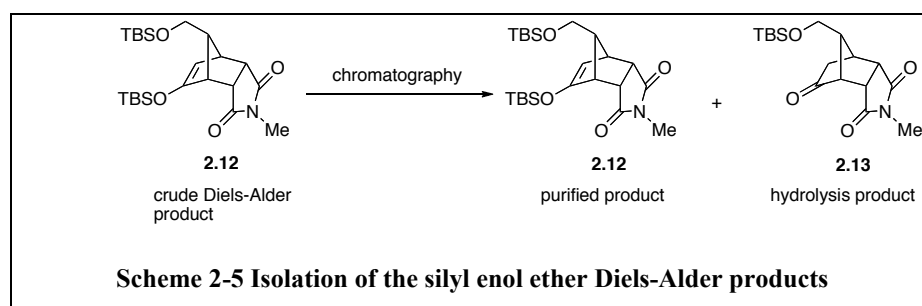
submitted to the Diels-Alder conditions. The reactions were first followed by ^1H NMR (aliquots) to determine the required reaction times and then run again for yield determination. Diels-Alder reactions were performed at $-4\text{ }^\circ\text{C}$ and $23\text{ }^\circ\text{C}$. For example, methyl acrylate was reacted at $-4\text{ }^\circ\text{C}$ for 7 days giving a 66 % yield of product or reacted at $23\text{ }^\circ\text{C}$ for 24 hours to yield 65 % of product. The latter temperature was preferred since any loss in diene stability by running the reaction at higher temperature was almost completely compensated by a significant gain in shorter reaction time, resulting in less time available for the diene to isomerize.

A moderate excess (3 eq.) of dienophile over diene was used in order to obtain favorable reaction times and to push the reactions to completion before the diene would isomerize to any significant degree. This was found to be superior to using an excess of diene over dienophile, as it was observed that the rearranged diene undergoes faster Diels-Alder than the original diene, leading to increased side products (i.e.: if 1 eq. of dienophile and 3 eq. of diene were to be used over a reaction time long enough for 10 % of the diene to isomerize, then 30% of the dienophile would be consumed by the rearranged diene).

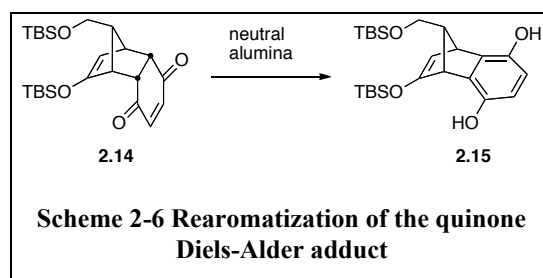
2.2.2 Optimization of the isolation protocol

The products were isolated as norbornene silyl enol ethers of moderate stability. Due to the ring strain associated with the norbornene scaffold, the silyl enol ethers are more labile than usual. Standard silica gel chromatography of the products leads to about 10-20 % hydrolysis of the silyl enol ethers in most cases (Scheme 2-5). This was attributed to the acidic nature of the silica gel. However, neutralization of the silica gel with TEA only led to more decomposition. Similar results were found with Florisil stationary phase. Aluminum oxide, however, is a chromatography medium that can be purchased in an acidic, basic or neutral form, depending on the washing protocols applied to it. It is sold in anhydrous form or "Brockman type I". The Brockman scale goes from I to V, depending on the degree of hydration of the alumina: the more hydrated the alumina, the less its retentive power but the milder it is on the compounds being separated. We optimized the isolation of our compounds on the maleimide cycloaddition

product. A known amount of the pure product was re-submitted to chromatography on neutral alumina of different grades. Brockman type 1 neutral alumina decomposed significantly the cycloaddition product, leading to a low 50 % recovery. Adding water to the alumina led to less decomposition: the Brockman type III (6 % water by weight) led to 75% recovery of the product and the Brockman type IV (10 % water by weight) neutral alumina was able to separate the products with minimal decomposition (99 % recovery). This was thus the medium of choice for the purification of the sensitive silylenoether products.

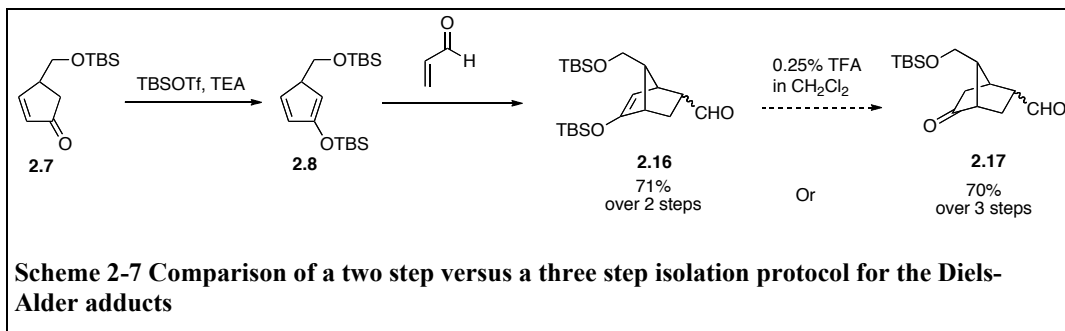


Only the Diels-Alder product of the quinone dienophile needed to be purified by standard silica gel (Scheme 2-6). It seems that the acidic conditions of the silica gel prevented rearomatization of the product, whereas neutral alumina promoted the enolization of the two ketones, resulting in hydroquinone formation and loss of two potentially valuable chiral centers.



The products could also be isolated after a mild hydrolysis of the silylenoether, with little erosion in overall yield. For example, the acrolein cycloadduct could be isolated as its silylenoether in 71% yield over two steps, or as a ketone in 70% yield over three steps after hydrolysis with dilute TFA (see Scheme 2-7). However, no general condition could be found for the hydrolysis

step and every cycloadduct required a specific optimization of the reaction time and acid concentration. Therefore, it was more convenient to isolate all the products as their silylenoethers.



2.2.3 Survey of dienophiles

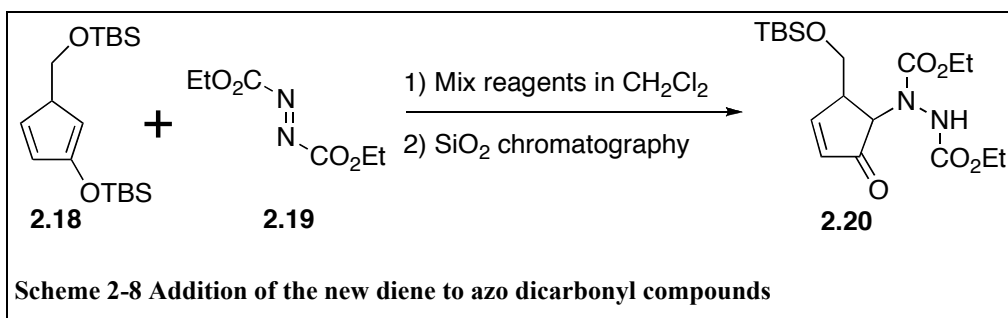
With our optimized reaction conditions in hand, we surveyed the ability of the new diene to undergo Diels-Alder reaction with a variety of dienophiles (see Table 2-1). Reactive dienophiles bearing 2 electron-withdrawing groups underwent cycloaddition very quickly with the new silyloxy diene. Quinone reacted fully in 10 minutes to give exclusively the endo cycloaddition product in 66 % isolated yield. N-Methyl maleimide reacted in 30 minutes to give 79% of isolated endo product. The acetylenic dienophile DMAD reacted in 45 minutes to give 79% of isolated product.

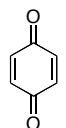
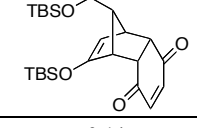
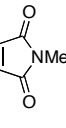
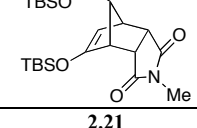
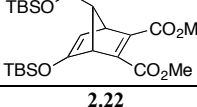
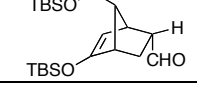
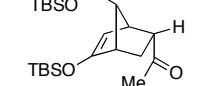
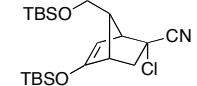
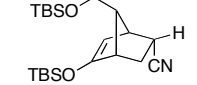
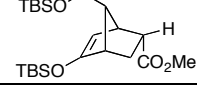
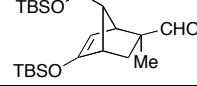
The diene reacted within a few hours with moderately activated dienophiles. Acrolein reacted in 2 hours to give 71 % isolated yield of a 1,4-cyclohexene regioisomer in a 1.6:1 mixture of endo to exo stereoisomers. Methylvinylketone also gave the same regioisomer in 4 hours with a combined isolated yield of 67 % for a 2:1 mixture of endo : exo stereoisomers. Similarly, 2-chloroacrylonitrile reacted in 3.5 hours, yielding 73 % of a 1:3.2 stereoisomer mixture favoring the exo over the endo isomer.

The diene was sufficiently stable that reactions which were complete within 24 hours could be carried out efficiently. Thus, less active dienophiles such as acrylonitrine and methylacrylate could be isolated in 68% yield and 1.2:1 endo : exo mixture for the former and 65% yield of a 2.3:1 endo:exo mixture for the later.

For the hindered dienophile methacrolein, after 43 hours only 35 % isolated yield of the desired cycloadduct could be obtained in a 1:5 endo/exo ratio. This is due to the poor reactivity of the dienophile, leading to much 1,5-H shift isomerization of the diene.

When extremely active azo dicarbonyl dienophiles such as DEAD and PTAD were used, an unexpected product was isolated (see Scheme 2-8). The product was formally the addition product of the enone's silyl enol ether to the azo group. It is uncertain from the NMR of the crude mixture if the product forms initially as the Diels-Alder adduct and then fragments on silical gel during chromatography or if mono addition of the silyl enol ether to the azo group occurs directly.



Dienophile	Product	<i>t</i> (h)	Isolated yield (%)	endo:exo
	 2.14	0.15	66	>95:5
	 2.21	0.5	79	>95:5
	 2.22	0.75	79	--
	 2.16	2	71	1.6:1
	 2.23	4	67	2:1
	 2.24	3.5	73	1:3.2
	 2.25	20	68	1.2:1
	 2.26	24	65	2.3:1
	 2.27	43	35	1:5

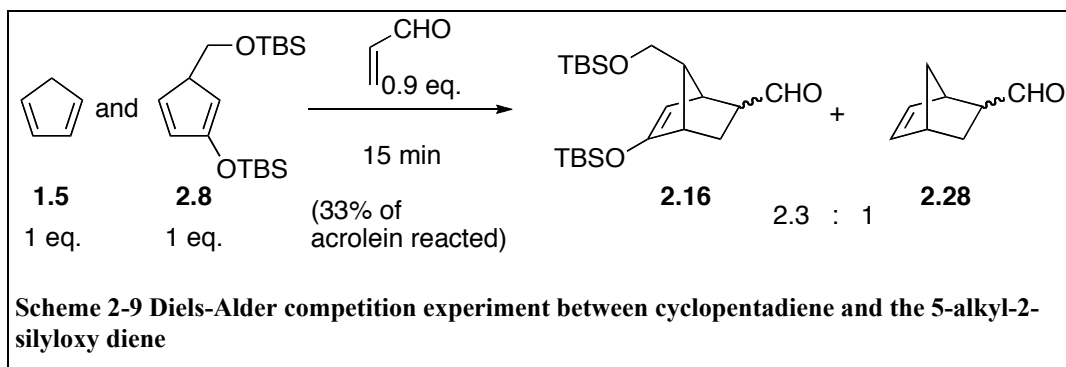
Reactions carried out with excess dienophile (3 eq.) in dichloromethane at room temperature at a diene concentration of 1.0 M. Reported yield is for the two steps of diene formation and Diels-Alder cycloaddition and is based on the starting enone.

Table 2-1 Diels-Alder cycloaddition with the new diene

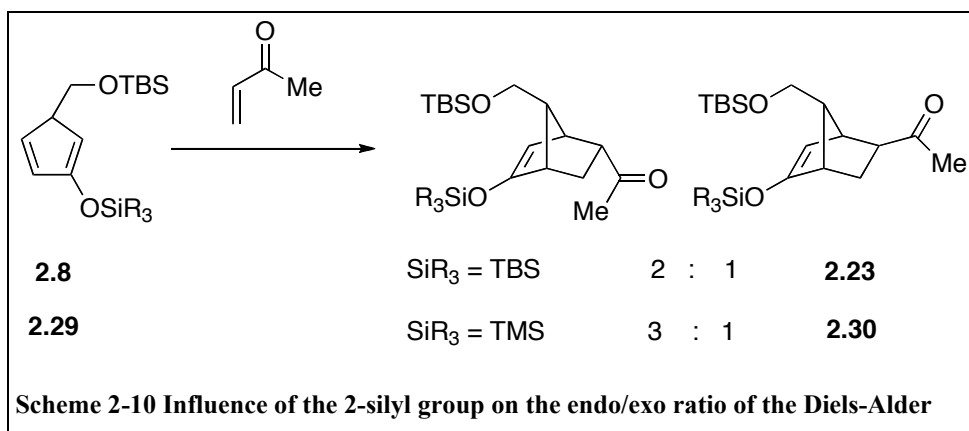
Due to the polarization of the diene's HOMO by the 2-silyloxy substituent, cycloaddition happens with predictable FMO control. In all cases, the electron-withdrawing group of the dienophile is in a 1,4 relationship to the silyloxy group on the cyclohexene ring formed during the Diels-Alder reaction. For example, the acrolein Diels-Alder adduct has the aldehyde and the silyl enol ether on positions 2 and 5, respectively, of the norbornene system (IUPAC nomenclature).

A competition experiment between the new diene and cyclopentadiene showed that the new diene reacts 2.3 times faster than cyclopentadiene for Diels-Alder cycloadditions. This is because the silyloxy group increases the energy of the diene's HOMO, making the diene more reactive in normal electron demand Diels-Alder cycloadditions. However, due to the steric bulk of the 5-silyloxymethane group, the new diene undergoes cycloaddition only on the face *anti* to this group. Since the new diene can undergo cycloaddition on only one of its two faces, as compared to cyclopentadiene having two reactive faces, the 2-silyloxy group in fact increases the reactivity of the diene system by about 4.6 fold (2.3 X 2).

It is interesting to compare the facial selectivity in our cycloadditions to the results of Burnell, who studied 5-substituted cyclopentadienes with a variety of substituents.⁵⁸ Burnell found that depending on the 5-substituent's size and electronic nature, the *syn/anti* facial selectivities would vary. However, all 5-substituted cyclopentadienes reported by Burnell produced at least some measurable amount of *syn* products with one dienophile or another. In the case of the new diene **2.8**, no *syn* cycloaddition product was ever detected.⁵⁹



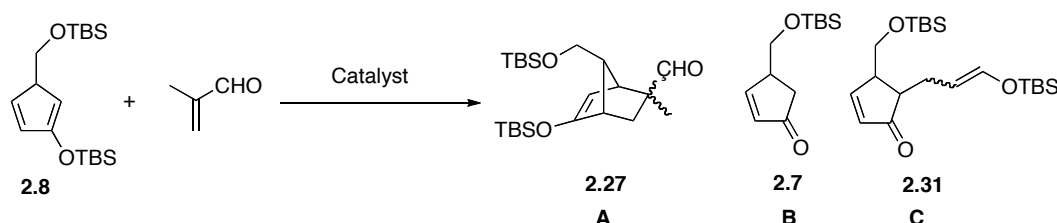
The endo/exo cycloaddition ratios observed with the new diene are very similar to those observed with cyclopentadiene, but are slightly more biased towards favoring the exo isomer. For example, methyl acrylate adds to cyclopentadiene with an endo/exo ratio of 3:1 while the new diene exhibits a selectivity of 2.3:1. Also, methacrolein adds to cyclopentadiene with a 1:3 ratio while it adds to the new diene in a 1:5 ratio. This is probably due to the 2-silyloxy group of the diene undergoing steric interaction with an endo substituent on the dienophile. In fact, the endo/exo ratio of the diene with methyl vinyl ketone changes from 2:1 to 3:1 when the 2-silyloxy substituent is changed from TBS to the smaller TMS.



2.2.4 Compatibility of the diene with Lewis acids

As can be seen from Table 2-1, methacrolein is a slow reacting dienophile, affording a low yield of the desired cycloaddition product due to the competing 1,5-H shift of the diene. We thus sought to increase the Diels-Alder rate through addition of a Lewis acid catalyst to activate the dienophile. Many types of Lewis acids were screened for activation of methacrolein in the course of its Diels-Alder

reaction with the new diene (see Table 2-2). The three main products that could be identified from the different reaction mixtures were the desired Diels-Alder product (**A**), the enone starting material coming from hydrolysis of the diene (**B**), and a Mukaiyama-Michael-type product (**C**).



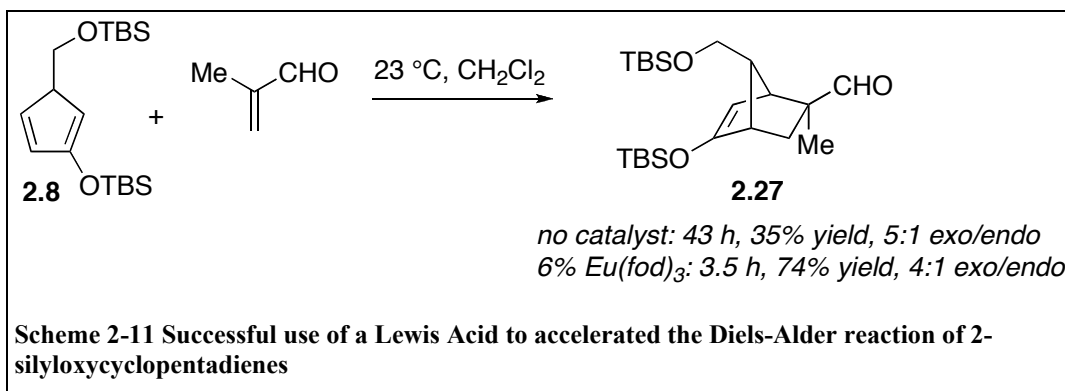
Potential Catalyst's category			
Catalyst	Temp. (Celcius)	Results	
Alkaline and alkaline earth:			
LiClO ₄	RT	1:1 A to C	
MgCl ₂	RT	no catalysis	
Early Transition Metals			
TiCl ₄	-40	decomposition	
Ti(O <i>i</i> Pr) ₄	RT	very slow catalysis to A	
Cp ₂ ZnCl ₂	RT	slow hydrolysis to B	
Y(OTf) ₃	RT	1:1 B to C	
Late Transition Metals			
Zn(OTf) ₂	RT	1:2 B to C	
FeCl ₃	RT	decomposition	
Main group metals			
Et ₂ AlCl	-40	A + decomposition	
AlMe ₃		A + decomposition	
SnCl ₄	RT	decomposition	
Main group non-metals			
BF ₃ ·Et ₂ O	-40	decomposition	
TBSOTf	-78	C + decomposition	
Lanthanides			
Ln(OTf) ₃	RT	A + C + decomposition	
CeCl ₃	RT	no catalysis	
Y(hfc) ₃	RT	A with rate acceleration	
Eu(fod) ₃	RT	A with rate acceleration	

Table 2-2 Screening of Lewis Acids to accelerate the Diels-Alder reaction of the 2-silyloxydiene

Strong Lewis acids, such as BF₃•Et₂O, SnCl₄ and TiCl₄ led to complete decomposition of the diene, even at low temperatures (-40 °C and beyond). The slightly less active AlMe₃ led to desired product formation along with significant

amounts of unidentifiable decomposition material. Other Lewis acids, especially those prone to generation of strong protic acid in the presence of adventitious water such as ytterbium(III)triflate, led to desilylation of the diene to starting enone, even when anhydrous handling techniques were used. Surprisingly, some Lewis acids such as lithium perchlorate promoted the formation of a new product: a Mukaiyama – Michael addition product (C) along with the desired Diels-Alder cycloadduct.

Fortunately, the use of lanthanide Lewis acids such as $\text{Eu}(\text{fod})_3$ and $\text{Y}(\text{hfc})_3$ led to the exclusive formation of the desired Diels-Alder product without any major side product. After optimization of the reaction conditions, it was found that 6% $\text{Eu}(\text{fod})_3$ lead to a 74% isolated yield of the desired methacrolein Diels-Alder cycloadduct after only 3.5 hours, as opposed to 35% after 43 hours for the uncatalyzed reaction. As expected, due to increased secondary orbital interactions in the transition state, the use of a Lewis acid increased the prevalence of the endo isomer (1:4 endo/exo for the L.A.-catalysed reaction versus 1:5 endo/exo ratio for the uncatalyzed cycloaddition). It is interesting to note that $\text{Eu}(\text{fod})_3$ was previously identified as a Lewis acid which was incapable of inducing a normal Mukaiyama aldol from a 2-silyloxy cyclopentadiene.⁶⁰ This results points out that a subtle electronic balance between the diene and dienophile is needed to favor the desired Diels-Alder product over the Mukaiyama-Michael product, while still catalyzing the reaction.



The isolated Mukaiyama-Michael product is similar in nature to the addition of the diene over azo dicarbonyl compounds (vide supra, product **2.20**). However, in this case the formation of the product directly in the reaction mixture could be

confirmed in the crude NMR. At this point, it is important to note that no definitive proof is available that any of the cycloaddition products presented in this chapter are formed from a concerted reaction (Diels-Alder) versus two, step-wise, Mukaiyama-Michael additions. However, the observation of endo-exo ratios for the products of silyloxy cyclopentadiene addition corresponding with the ratios obtained from the Diels-Alder reactions of cyclopentadiene (where only the Diels-Alder reaction can happen) strongly points towards a Diels-Alder mechanism.

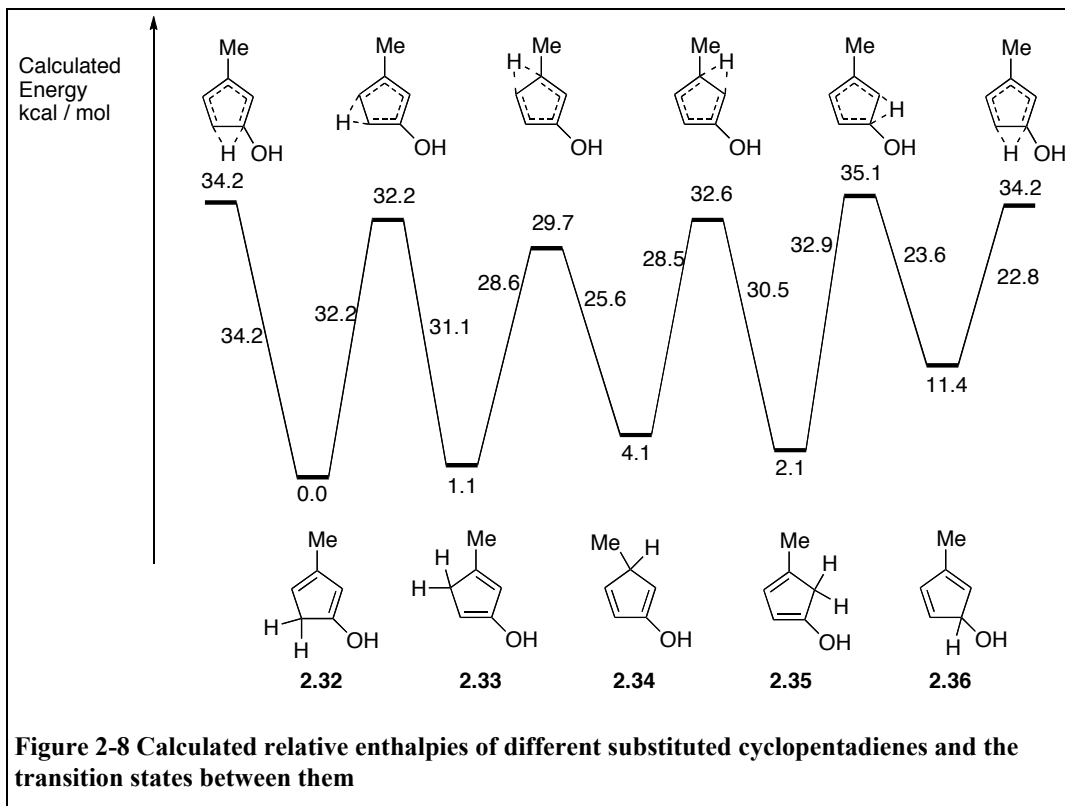
2.3 Synthesis and use of an enantioenriched 5-alkyl-2-silyloxy cyclopentadiene

Another advantage of the new diene over simple 5-substituted cyclopentadienes is that it is chiral. It thus became a goal to investigate if an enantiopure version of the diene could be synthesized and if this diene could conserve its enantiopurity long enough for cycloaddition.

2.3.1 Ab Initio calculations to determine the enantiostability of the diene

When considering to obtain the diene in enantiomerically enriched form, one concern that arose was that the diene might undergo 1,5-H shift and then a “retro 1,5-H shift” to regenerate the starting diene. Since this “retro-1,5-H shift” could occur from either of the two enantiotopic protons of the CH₂ atom of the cyclopentadiene, it could lead to racemization of the starting material. A DFT calculation at the B3LYP/6-31G* level of theory was thus performed to study the full energetic profile of the 1,5-H shifts around a 2-hydroxyl-cyclopentadiene (see Figure 2-8). This computer simulation predicted the correct direction of 1,5-H shift from the starting diene (vide supra) and predicted the “retro 1,5-H shift” to be about 3 kcal/mol higher in energy than the first sigmatropic shift. This energy difference means that the “retro 1,5-H shift” would be roughly 150 times slower than the forward shift, making the “retro 1,5-H shift problem” much less significant than the diene isomerization problem. In other words, for a reaction

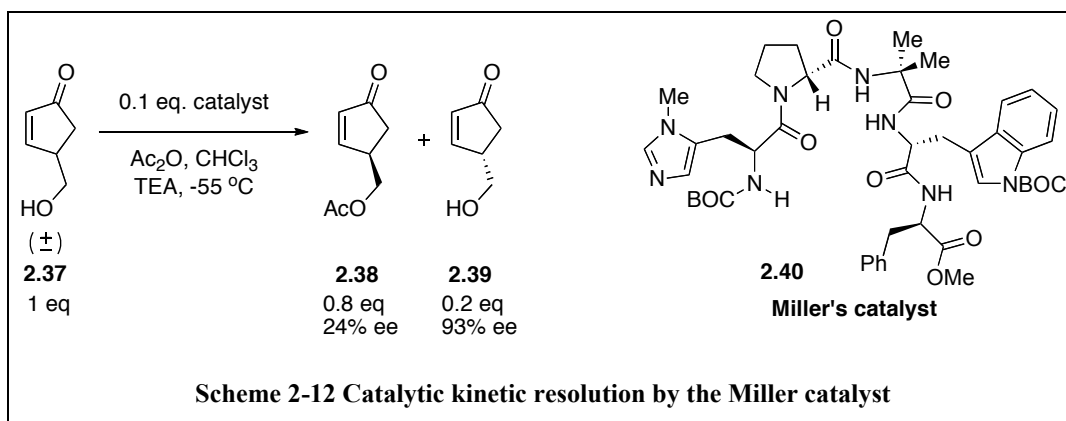
time in which the diene isomerization is low, the amount of diene undergoing “retro 1,5-H shift” will be minimal and should not influence the enantiomeric excess of the diene.



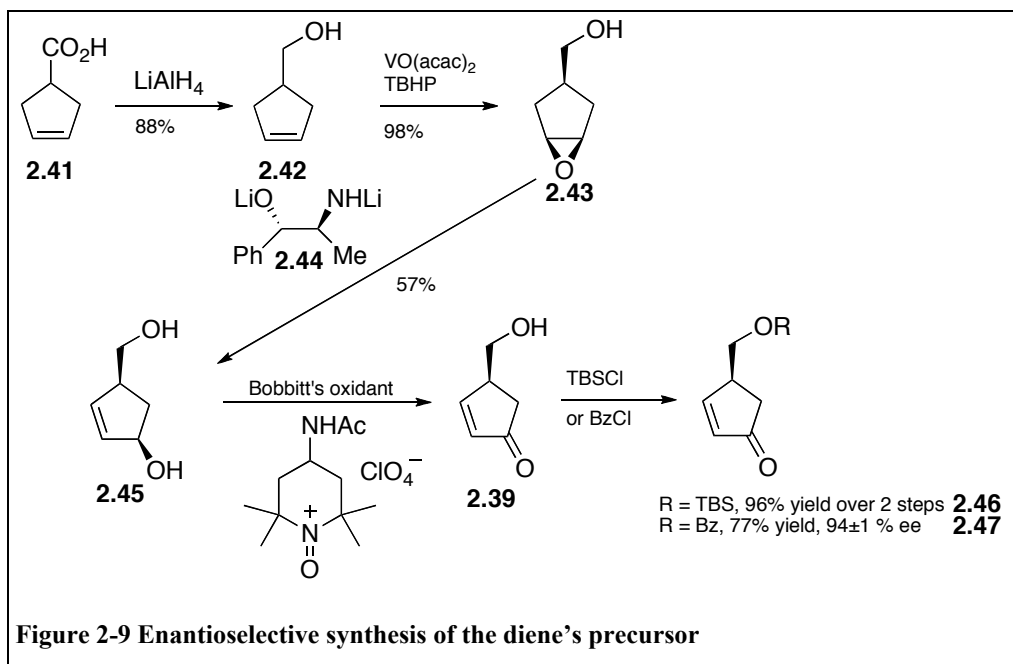
2.3.2 Enantioselective synthesis of the diene's precursor

With the encouraging computational results on the diene's enantioselectivity, it was decided to synthesize an enantioenriched version of the diene's enone precursor. To this end, we collaborated with several research groups in the hope of finding an efficient protocol for kinetic resolution of the enone alcohol **2.37**. Unfortunately, this proved to be an extremely challenging task as the chiral center is far away from the reactive primary alcohol. For instance, the Snapper-Hoveyda catalyst for kinetic resolution of alcohols through silylation yielded completely racemic product.⁶¹ The only catalyst that could perform any type of kinetic resolution was an unnatural pentapeptide **2.40** developed by Scott Miller.⁶² As can be seen from Scheme 2-12, kinetic resolution of enone **2.37** with 10 mol % of the catalyst **2.40** led to a 20% recovery of the enone **2.39** in 93% ee. Unfortunately,

due to the low selectivity (selectivity factor ~ 5), half an equivalent of the catalyst was needed to obtain one equivalent of the desired enone alcohol in 93% ee. On a practical scale, each gram of enantioenriched enone would require about 3.5 grams of resolving catalyst. Because the catalyst **2.40** is composed of a mix of *d*- and *l*- amino acids, along with non-natural amino acids (such as the alpha-methylalanine unit), the cost of obtaining a synthetically useful amount of the enantioenriched enone alcohol by this method would be prohibitive, and other non-catalytic methods were considered.

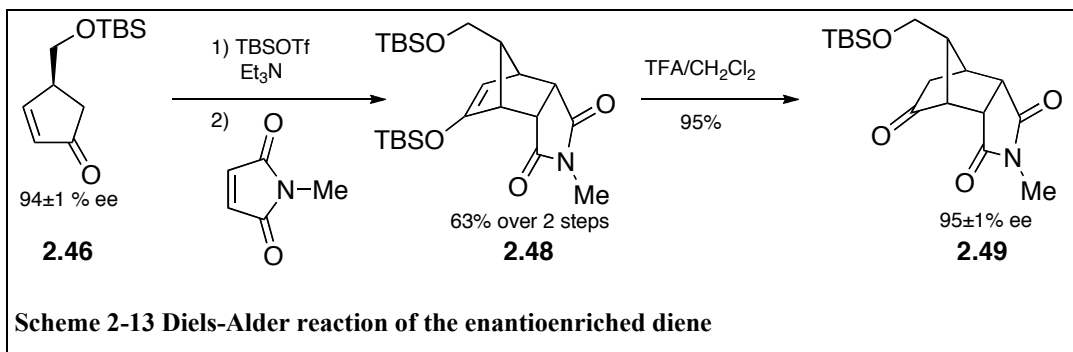


We therefore resorted to an enantioselective synthesis of chiral diol **2.45** using a desymmetrization protocol developed by Hodgson (see Figure 2-9). Cyclopent-3-ene carboxylic acid was reduced with lithium aluminum hydride to the corresponding alcohol **2.42**, which was then used as a directing group for a vanadium-catalyzed epoxidation of the alkene. The resulting meso epoxide **2.43** was treated with three equivalents of the bis-lithium salt of (1*S*, 2*R*)-norephedrine in order to promote an asymmetric deprotonation followed by an epoxide opening rearrangement, leading to the enantioenriched diol **2.45**, as reported by Hodgson.⁶³ The diol **2.45** was oxidized and protected as per the standard diene synthesis in order to obtain an enantioenriched diene precursor (*S*)-**2.46**. The enantiopurity of the diol was verified by selective oxidation of the secondary alcohol and protection of the primary alcohol as a benzoate ester (*S*)-**2.47** followed by HPLC analysis, revealing a 94% ee.



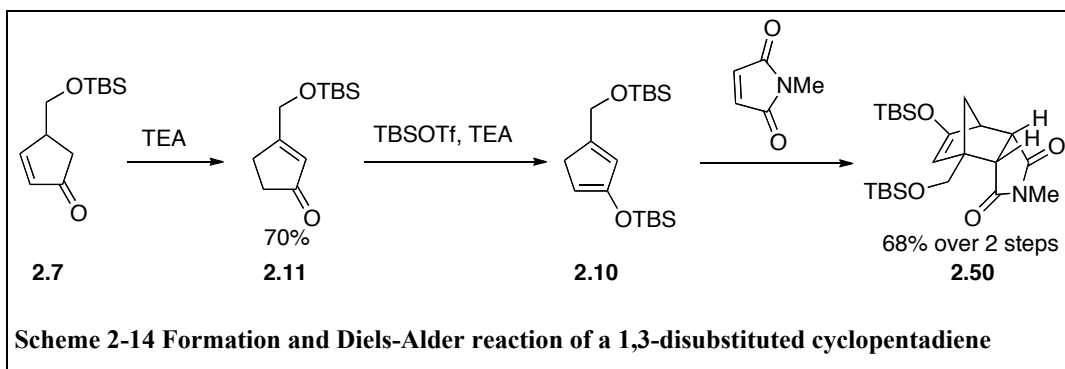
2.3.3 Synthesis and use of the enantioenriched diene

The enantioenriched enone precursor (*S*)-**2.46** was then treated under the standard enol silylation conditions to generate the diene and then reacted with *N*-methyl-maleimide for 1 hour to give Diels-Alder product **2.48** in 63 % yield. The silyl enol ether was then cleanly hydrolyzed with TFA to yield the corresponding ketone **2.49** in 95 % yield. This ketone was analyzed by chiral-phase HPLC and found to be 95 (± 1) % ee, showing that the diene does not undergo any racemization during the enol silylation step or before it undergoes the Diels-Alder reaction.



2.4 2-silyloxy-4-alkyl cyclopentadiene

Although we have focused on the reactions of diene **2.8**, the strategy of enolsilylation of substituted enones to provide stable substituted cyclopentadienes is a general one. As an example, the enone precursor **2.7** was treated with TEA and isomerized to the thermodynamically more stable trisubstituted conjugated enone **2.11**. This enone could be cleanly enolsilylated under the standard soft enolization conditions. This isomer was previously calculated (*vide supra*) to be more stable toward 1,5-H shift than the 5-alkyl-2-silyloxy isomer. The diene **2.10** indeed smoothly underwent Diels-Alder reaction with N-methyl maleimide, affording the desired cycloadduct **2.50** with a quaternary carbon stereocenter in 68% yield over two steps, proving that the new methodology is not limited to 5-alkyl-2-silyloxy cyclopentadienes.



2.5 Conclusion

It was found that enol silylation can be used to efficiently generate 5-substituted cyclopentadienes. It was observed that a silyloxy substituent on the diene will increase its LUMO energy, making it more stable towards 1,5-sigmatropic hydrogen shifts. This gain in stability was enough to allow for room-temperature manipulation of a 5-alkyl-2-silyloxy cyclopentadiene and subsequent Diels-Alder reaction. The silyloxy substituent impairs higher reactivity on the diene and allows for stereocontrol of the cycloaddition. The new diene is also compatible with the use of mild Lewis acids for dienophile activation. The new diene is chiral and will transfer the chiral information of the diene's precursor to

its Diels-Alder product. Finally, the enolsilylation methodology can be applied to stabilize other substituted cyclopentadienes.

2.6 References

-
- ⁵⁰ A) Hansson, L. and Carlson, R.; *Acta Chemica Scandinavica*, **1989**, *43*, 188 B) Plenio, H. and Aberle, C.; *Organometallics*, **1997**, *16*, 5959 C) Isakovic, L.; Ashenhurst, J.A.; Gleason, J. L.; *Organic Letters*, 2001, *3*, 4189
- ⁵¹ Brown, D. W.; Campbell, M. M.; Taylor, A. P.; Zhang, X.-a., *Tetrahedron Letters* **1987**, *28* (9), 985-988.
- ⁵² Wuts, Peter G. M. (editor) *Greene's protective groups in organic synthesis*. Hoboken, N.J. : Wiley-Interscience, **2007**, 1082p
- ⁵³ Saville-Stones, E. A.; Turner, R. M.; Lindell, S. D.; Jennings, N. S.; Head, J. C.; Carver, D. S., *Tetrahedron* **1994**, *50* (22), 6695-6704.
- ⁵⁴ Foresman, J.B. and Frisch, A. ; *Exploring Chemistry with Electronic Structure Methods, second edition*. Gaussian Inc. ; Pittsburg, 1996; 302 p.
- ⁵⁵ personal communications with professor K.N. Houk
- ⁵⁶ Isaacs, Neil S., 1934- Physical organic chemistry / Neil S. Isaacs. Burnt Mill, Harlow, Essex, England : Longman Scientific & Technical ; New York, NY : Wiley & Sons, 1995.
- ⁵⁷ W. H. Okamura, G.-Y. Shen, R.Tapia, *Journal of the American Chemical Society* **1986**, *108*, 5018
- ⁵⁸ Letourneau, J.E.; Wellman, M.A.; Burnell, D.J.; *J. Org. Chem.* **1997**, *62*, 7272
- ⁵⁹ Mehta, G.; Uma, R., *Accounts of Chemical Research* **2000**, *33* (5), 278-286.
- ⁶⁰ Brown, D. W.; Campbell, M. M.; Taylor, A. P.; Zhang, X.-a., *Tetrahedron Letters* **1987**, *28* (9), 985-988.
- ⁶¹ A) Zhao, Y.; Rodrigo, J.; Hoveyda, A. H.; Snapper, M. L., *Nature* **2006**, *443* (7107), 67-70. B) Zhao, Y.; Mitra, A. W.; Hoveyda, A. H.; Snapper, M. L., *Angewandte Chemie International Edition* **2007**, *46* (44), 8471-8474.
- ⁶² Lewis, C. A.; Miller, S. J., *Angewandte Chemie International Edition* **2006**, *45* (34), 5616-5619.
- ⁶³ A) Hodgson, D.M.; Witherington, J.; Moloney, B. A.; *Journal of the Chemical*

Society Perkin Transactions 1 **1994**, 3373 B) Hodgson, D.M.; Gibbs, Drew, M.
G. B. ; *Journal of the Chemical Society Perkin Transactions 1* **1999**, 3579 – 3590.

3 Efforts towards the total synthesis of the natural product palau'amine

3.1 Introduction

Natural sources seem to be an inexhaustible source of amazement and inspiration for organic chemists. Some natural products have structures that challenge our understanding of chemistry or fuel investigations on biological processes. The natural product palau'amine is one such molecule. It is a

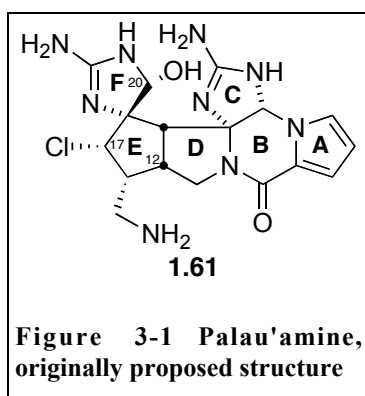


Figure 3-1 Palau'amine, originally proposed structure

hexacyclic, guanidine-containing marine alkaloid originally isolated in 1993 by Scheuer *et al.* from the marine sponge *stylotella aurantium*.^{64,65} Palau'amine was reported as having an impressive array of antibacterial, antifungal, anticancer and immunosuppressant properties. It is part of the family of pyrrole-imidazole alkaloids, which is believed to have biosynthetic origins from two

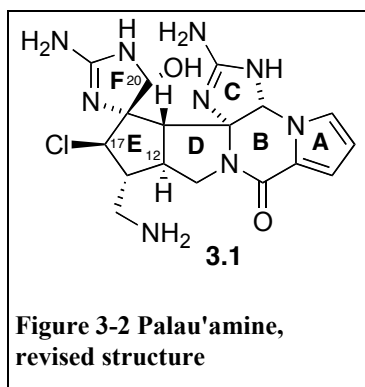
monomers of the natural product oroidin.⁶⁶

Like other members of its family, palau'amine is a natural product that exhibits a high nitrogen content. The structure and relative stereochemistry of the natural product were originally assigned from its high-resolution mass spectrum, IR spectrum and ¹H and ¹³C spectra. The absolute structure of palau'amine could not be determined as this natural product and its derivatives are not crystalline and no useful correlation could be established with other structures. The D-E ring junction was assigned as *cis* based on high ¹H NMR coupling constants and NOE. This assignment was further supported by the fact that 5-5 *cis* ring systems are thermodynamically favored.

Since the publication of its structure, palau'amine has attracted much attention in the synthetic community.⁶⁷ However, in 16 years of active research worldwide, the structure of palau'amine has not yielded to total synthesis. One of the challenging features of this structure is that cyclopentane ring E bears five

bulky substituents on the same face, one of them being a secondary chlorine atom. The high density of these functional groups adds to the synthetic challenge of the natural product.

The structure of palau'amine has undergone two revisions. In a minor revision, Scheuer *et al.* published in 1998 the full characterization data of palau'amine and revised the C20 aminal carbon stereocenter.⁶⁵ In 2007, three different research groups proposed a more significant structure revision.^{68,69,70} The isolation of new and related sponge natural products started the revision process and reassignment of the original NMR data was done using computational simulations. The new assignment adjusted the relative stereochemistry of C12,



C17 and C20. While C20 was reassigned back to the original 1993 proposed stereochemistry, reassignment of C17 and C12 significantly alters the structure of the molecule by decreasing the steric crowding in the vicinity of the strained E/D junction. This also means that the 5,5 ring junction of palau'amine is the thermodynamically unfavored trans isomer.⁷¹ Nevertheless, both the original and

revised structures of palau'amine present significant synthetic challenges.

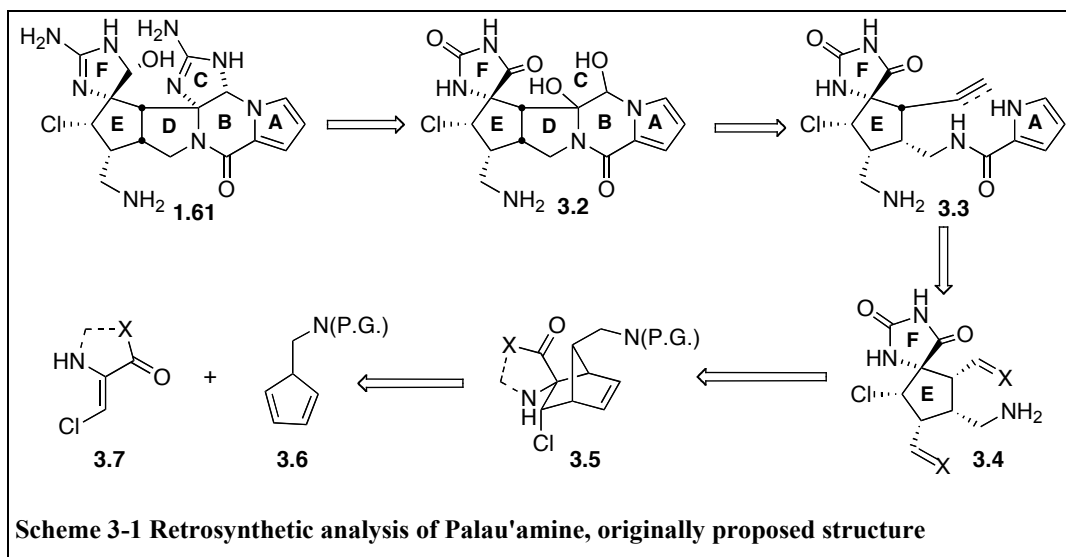
3.2 Retrosynthetic analysis of the palau'amine original structure

Our research group has been actively working on the synthesis of palau'amine.⁷² The most significant portion of our efforts has been directed towards the originally proposed structure of the molecule. One of the first structural features of palau'amine that an observer will notice is the unbalanced distribution of structural complexity. The relatively simple ABCD rings of palau'amine are essentially the structure of the natural product phakellin, which has previously been synthesized in a few steps from oroidin by Büchi in 1982, with later improvements by other groups.^{73,74} However, the hexasubstituted E ring presents a significant synthetic challenge. With a fully substituted α -face, a high

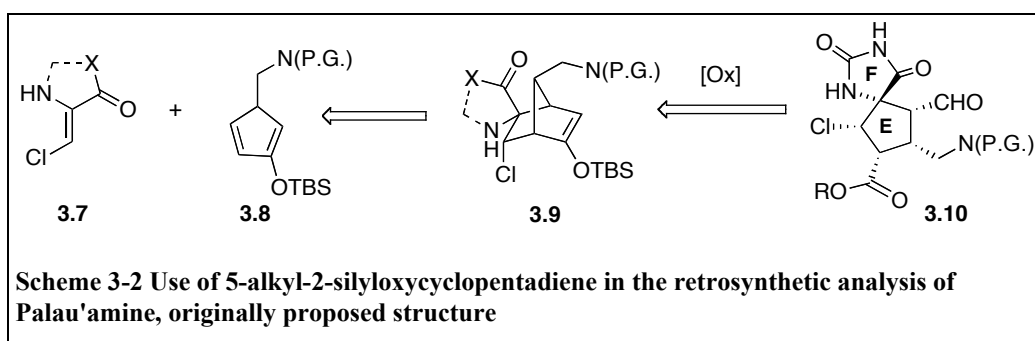
degree of steric strain is expected in this part of the molecule. Also, of the eight stereocenters of the molecule, five are located on this ring. Since the E ring is expected to cause the most challenge during total synthesis, it would be wise to address it early in the synthetic approach.

In considering a synthetic strategy for palau'amine, the C and F guanidine-based rings are disconnected first to afford a structure **3.2** with fewer reactive functional groups (Scheme 3-1). Subsequent disconnection of the ABD rings leads to a central cyclopentane core **3.3** of dense functionality. This dense functionality will inevitably be linked with steric strain. Slowly building this strain by stepwise insertion of many groups into a core structure would be a risky path: as the core would get more sterically crowded, inserting more functional groups into a tight chemical space would become increasingly difficult, if not impossible. The alternative would be to use a powerful synthetic transformation to build in one step a structure of high steric strain.

Few reactions are able to build structures of high complexity and strain at the same time; one of them is the Diels-Alder reaction. Because of the highly favorable energetics of the reaction generating two new C-C σ bonds from two C-C π bonds, the generation of strained structures is potentially achievable. For example, norbornene is a significantly more reactive alkene than average due to steric strain. Norbornenes are readily available from Diels-Alder reactions between cyclopentadiene and dienophiles. Thus, if the two X groups from Scheme 3-1, molecule **3.4**, are brought together, a norbornene scaffold is obtained. It was thus decided to build the dense cyclopentane ring E of palau'amine by a Diels-Alder reaction of a 5-substituted cyclopentadiene with an appropriately substituted dienophile, followed by oxidative ring opening at the double bond of the norbornene scaffold.



As discussed in Chapter 2, we have already developed a highly versatile method for the generation and use of 5-substituted cyclopentadienes. In the context of palau'amine total synthesis, this methodology would offer several advantages. First, the diene would guarantee cycloaddition *anti* to the 5-substituent, as required in Scheme 3-1. Second, the reactive diene would allow the Diels-Alder to proceed at room temperature, therefore permitting the use of a variety of mildly reactive dienophiles. Thirdly, the two carbons of the resulting norbornene's double bond would be at different oxidation states, therefore differentiating the two groups generated after oxidative cleavage. This would allow for easier manipulation of the desired substituted cyclopentadiene. Because of the advantages of the newly developed 5-substituted cyclopentadiene methodology, it was applied to our palau'amine total synthesis efforts (see Scheme 3-2 for the retrosynthetic analysis.)



3.3 Synthesis of the original palau'amine E ring structure

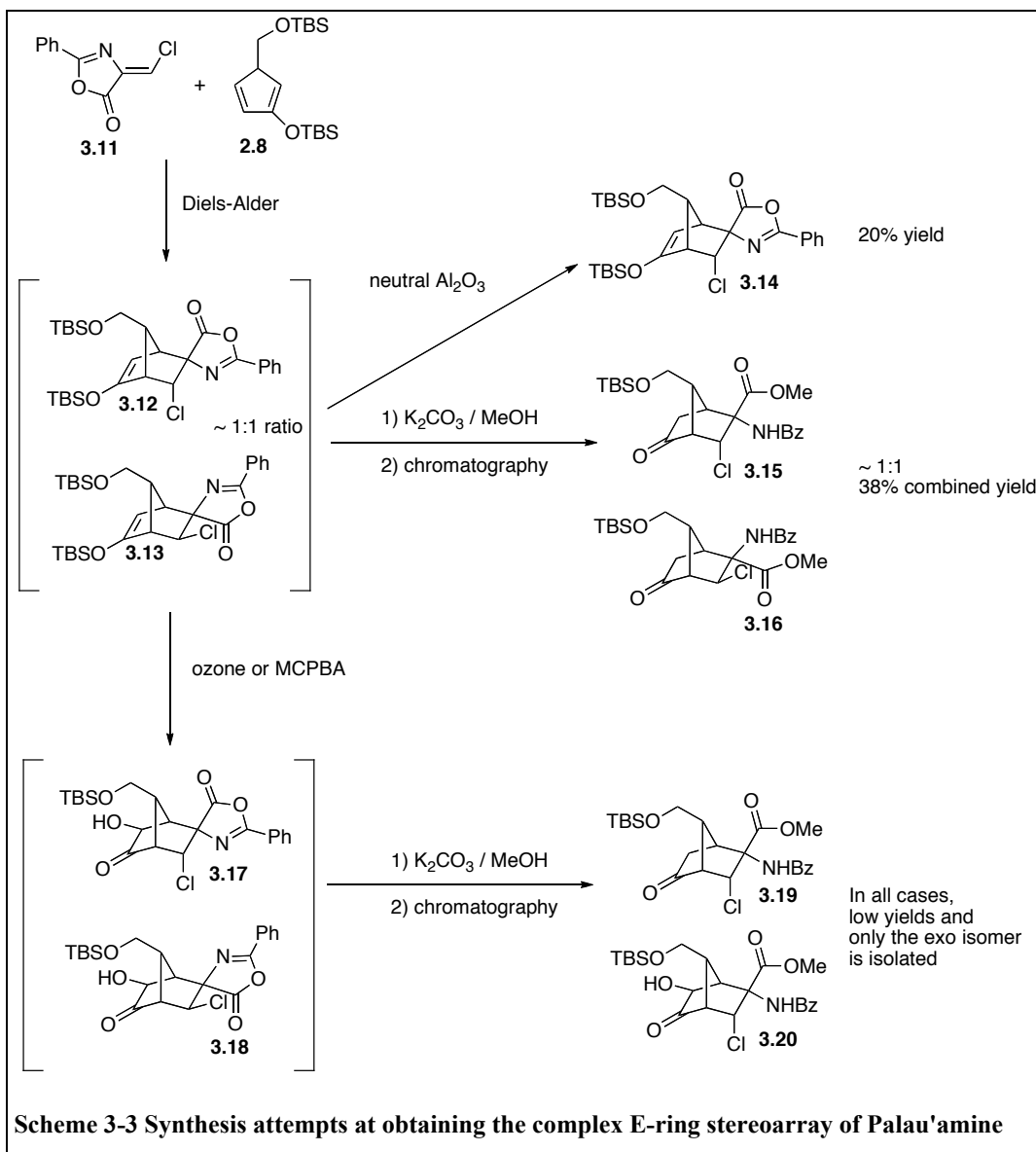
In order to test our retrosynthetic scheme for the synthesis of the cyclopentane core of palau'amine, it was decided to use the same 2-silyloxy-5-silyloxymethylcyclopentadiene system already developed and available. It was envisioned that in later synthesis attempts, the side-chain silyloxy group of the diene could be modified to a more appropriate protected nitrogen substituent.

The dienophile chosen for study was chloromethyleneoxazolone **3.11**, a reactive dienophile that had been reported by Bland *et al.*⁷⁵ Simple mixing of diene **2.8** and oxazolone **3.11** in solvent at 23 °C was sufficient to induce the Diels-Alder to proceed, and the dienophile was completely consumed within one hour. From NMR analysis of the crude reaction mixture, three major products were evident and were tentatively assigned as the endo and exo desired cycloaddition products along with a third, unidentified component. Chromatography of the reaction mixture under a multitude of conditions led to significant decomposition. Only the exo (as defined by the electron-withdrawing ester group on the dienophile) cycloaddition product could be isolated in a low 20% yield.

In the hope of isolating both the endo and exo products, the cycloaddition mixture was exposed to alkaline conditions (K_2CO_3 / MeOH) leading to the isolation of two products in low yield, tentatively assigned as the endo and exo cycloaddition products where the silyl enol ethers have been hydrolyzed to the ketone and the oxazolone hydrolytically cleaved to the benzoyl amide and methyl ester. However, significant decomposition material was again observed. One possible source of decomposition is silyl enol ether hydrolysis and subsequent Mukaiyama reaction of the resulting ketone with a second equivalent of silyl enol ether.

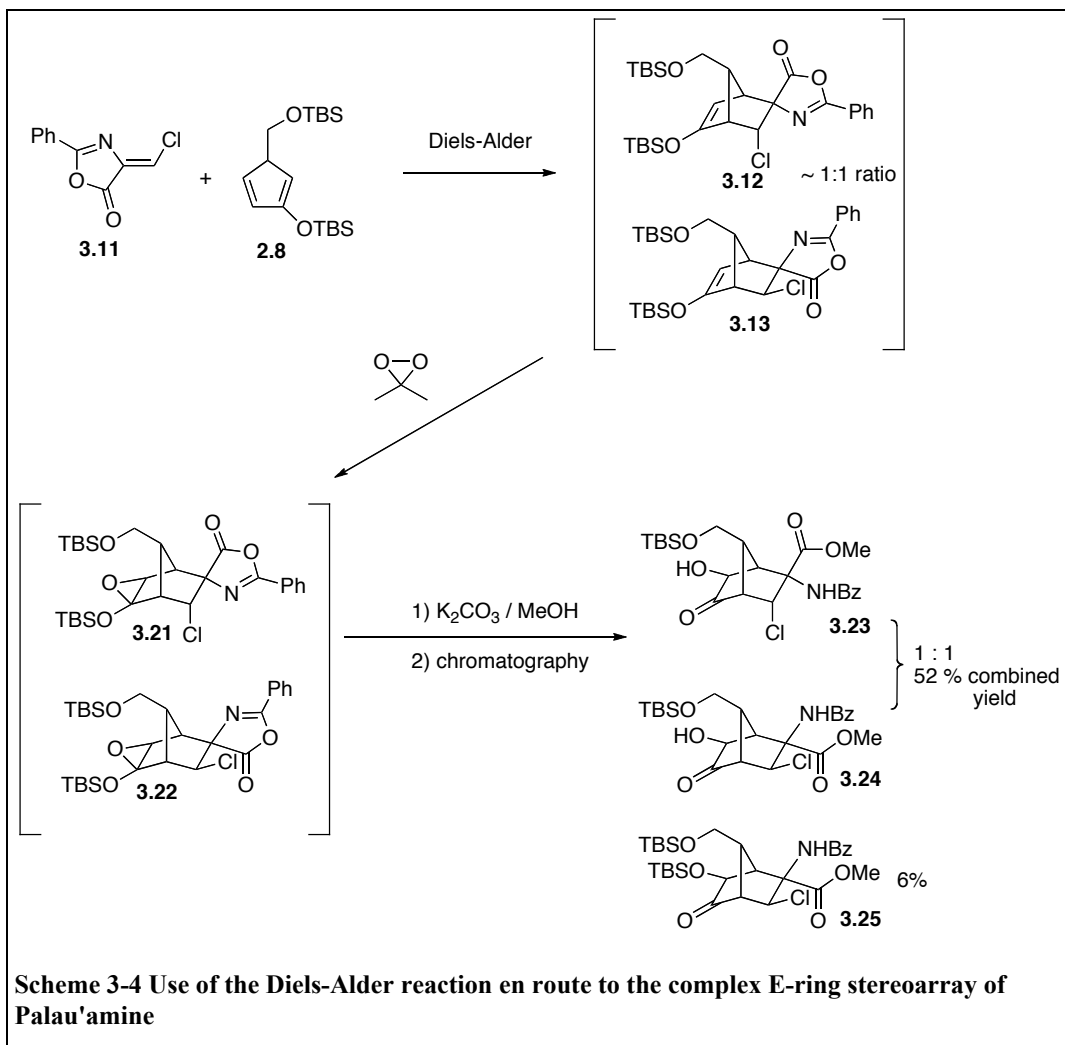
Since direct isolation of the cycloaddition products was not practical, direct oxidation of the reaction mixture was attempted. Treatment of the silyl enol ether with ozone gas, followed by hydrolysis of the oxazolone (K_2CO_3 / MeOH), gave a low isolated yield of the desired alpha-hydroxy ketone exo isomer.⁷⁶ However, products corresponding to the silyl enol ether hydrolysis to the ketone were

continually observed. The undesired hydrolysis could be traced back to adventitious moisture in the ozone oxidation step. Attempted drying of the ozone gas with a cold trap did not change the results.



We searched for alternatives to ozone in the oxidation of the silyl enol ether. Most unexpectedly, the use of MCPBA also lead to significant hydrolysis product.⁷⁷ Milder and drier oxidation conditions were thus needed. The silyl enol ether was therefore treated with a solution of dimethyldioxirane to effect epoxidation of the alkene.⁷⁸ The resulting product was immediately hydrolyzed with $K_2CO_3/MeOH$ and gratifyingly the desired endo and exo products could be

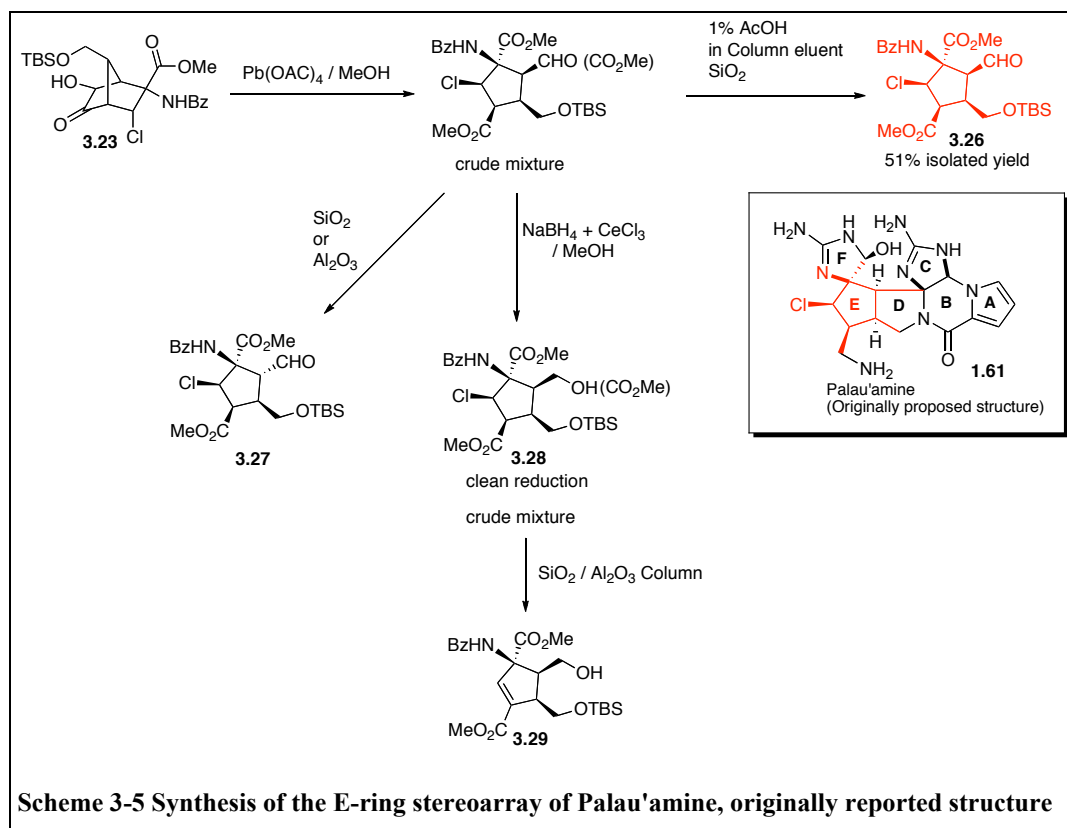
obtained in a 1:1 ratio and a combined isolated yield of 52 %, along with a small amount of silyl migration endo product (6%).



Having the α -hydroxy exo product **3.23** in hand, the oxidative cleavage of the norbornane skeleton would lead to the desired cyclopentane core of palau'amine. Lead tetraacetate in methanol was found to easily cleave the hydroxy-ketone. The resulting aldehyde-methyl ester oxidation product was relatively clean, but was contaminated with a small amount of overoxidation product of the aldehyde (~85:15 product to overoxidation product, complete conversion and no other side material). Unfortunately, purification of the final aldehyde proved problematic. While the product could be passed through a very short silica gel plug without ill effect, chromatography of the reaction mixture led

to the complete epimerization of the aldehyde to **3.27**. In order to avoid this epimerization, the crude aldehyde was cleanly reduced under the Luche conditions to the corresponding alcohol **3.28** with no observable epimerization. However, attempted purification of the alcohol product **3.28** under a variety of conditions led to the elimination of the chloride to form an α/β unsaturated ester cyclopentene **3.29**. The highly sterically strained nature of the cyclopentane makes it a very unstable system under many conditions.

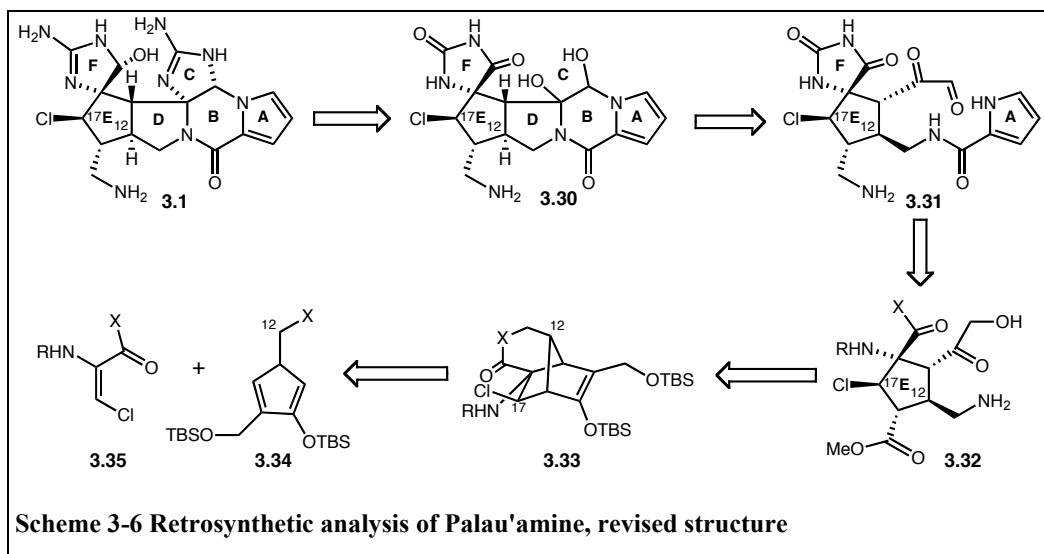
Our experiments seemed to indicate that the desired aldehyde would epimerize under basic, but not necessarily acidic conditions, as exemplified by the successful Luche reduction. Therefore, a chromatographic solvent system with 1% acetic acid was tested and enabled the isolation of the desired aldehyde **3.26** in pure form for characterization, albeit in a low 51% yield due to inevitable decomposition. The nature of the desired product was thus ascertained. These results were published and were the second example, only a few months after Gin's synthesis, of a methodology for obtaining the fully substituted scaffold of the E ring of the originally proposed structure of palau'amine.⁷⁹



Scheme 3-5 Synthesis of the E-ring stereoarray of Palau'amine, originally reported structure

3.4 Exploration of synthesis avenues for the E ring of the corrected structure of palau'amine

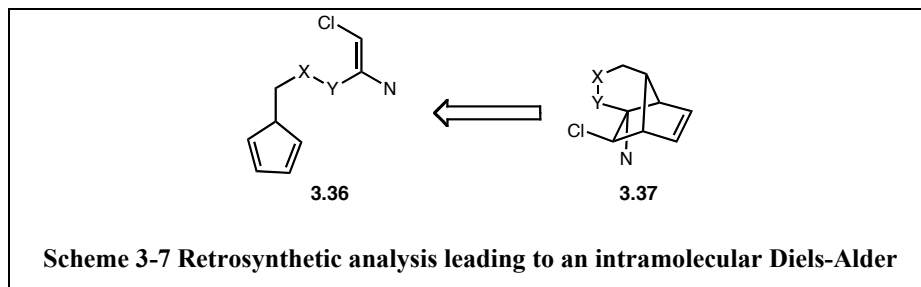
In addition to our work on the originally proposed structure of palau'amine, we sought to adapt our strategy such that it could be applied to the revised structure. The revised structure involves a change of two stereocenters: the chlorine-bearing stereocenter C-17 and the ring junction C-12. In our original synthetic plan, the C-17 stereocenter was set during the Diels-Alder cycloaddition and was controlled from the dienophile's double bond's *cis* geometry. Changing from a *cis* to a *trans* dienophile would therefore allow access to the newly proposed C-17 stereochemistry. Access to a *trans* dienophile is not expected to be difficult and many synthetic options are available. For example, the oxazolone dienophile **3.11** used for the synthesis of the original E-ring stereoarray was reported to undergo UV-promoted double bond isomerization to its *trans* stereochemistry.⁸⁰



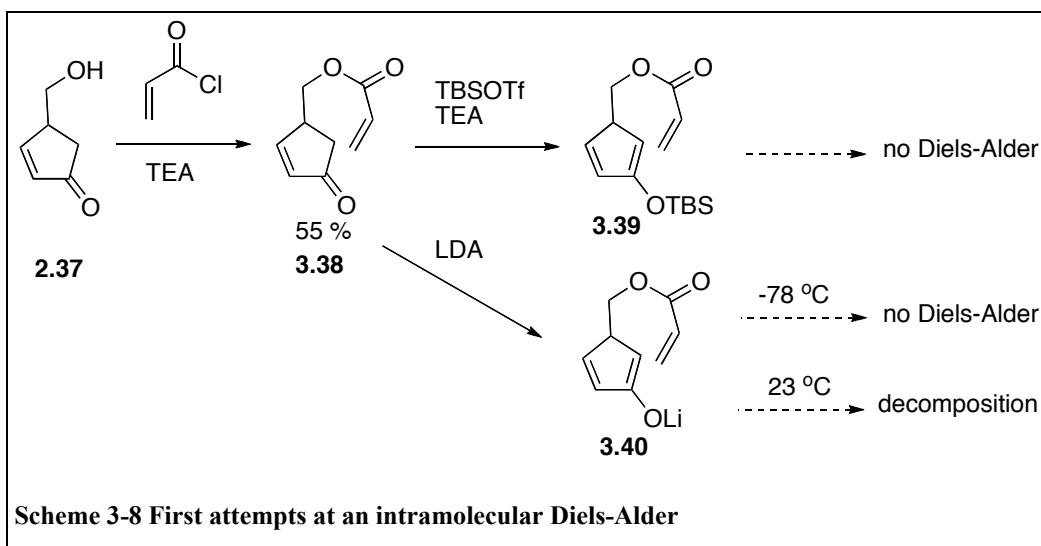
Scheme 3-6 Retrosynthetic analysis of Palau'amine, revised structure

The absolute stereochemistry of the C-12 stereocenter in our synthesis of the original E-ring stereoarray was set by approach of the dienophile away from the silyloxy methyl group (*vide supra*). While it could be possible to adjust this stereocenter after cycloaddition through an oxidation-epimerization pathway, it would be more efficient to obtain the desired relative stereochemistry directly from the Diels-Alder reaction. While unlikely in an intermolecular cycloaddition,

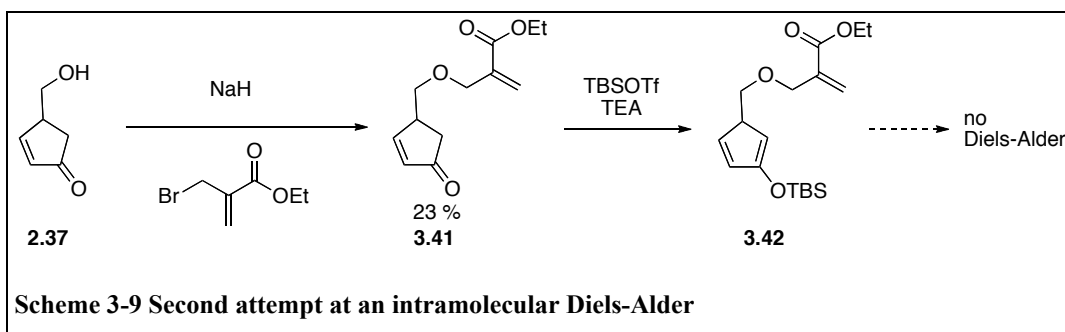
a properly devised intramolecular Diels-Alder might force the dienophile to approach the diene *syn* to the 5-substituent (see Scheme 3-7).



Initial experiments have been performed to probe the possibility of an intramolecular Diels-Alder reaction. The free alcohol of 4-(hydroxymethyl)cyclopent-2-enone **2.37** was acylated with acryloyl chloride in an unoptimized yield of 55%. The standard procedure for silyloxydiene synthesis was applied and the formation of the diene could be confirmed by ^1H NMR. However, after 2 days, no trace of a Diels-Alder product could be observed. The formation of the lithium enolate of the enone precursor was also attempted, in order to generate a more reactive diene or perhaps induce a double Michael addition reaction. However, no Diels-Alder product formed upon enolization at $-78\text{ }^\circ\text{C}$ (LDA) and decomposition occurred upon warming of the lithium enolate to room temperature (see Scheme 3-8). Lewis acid catalysis of this intramolecular reaction has not been attempted yet.

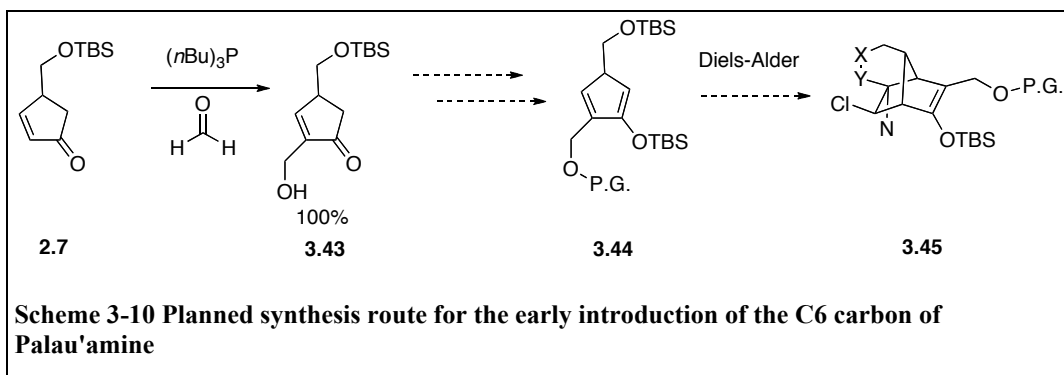


With the hypothesis that the ester carbonyl was preventing the formation of the desired conformation for Diels-Alder reaction, a new dienophile was linked to the diene system. The free alcohol of 4-(hydroxymethyl)cyclopent-2-enone **2.37** was alkylated with ethyl 2-(bromomethyl)acrylate in an unoptimized yield of 23 %. From this enone, the diene was generated under the standard conditions. However, no Diels-Alder product could be observed under these conditions. It is known that intramolecular Diels-Alder reactions of 5-substituted cyclopentadienes are optimal when the tether length between the diene and dienophile is two atoms long (vide supra, section 1.1.2.4). Further work needs to be done on this intramolecular Diels-Alder reaction for the palau'amine total synthesis, notably with Lewis acid catalysis (vide supra, section 2.2.4).



3.4.1 Carbon C6 installation

In our synthesis of the E-ring of the original structure of palau'amine, carbon C10 was obtained as an aldehyde. From this aldehyde, it was planned to later install carbon C6 by a methylenation reaction. However, a more convergent synthesis would be achieved through an earlier incorporation of this carbon, before the key Diels-Alder step. This could be done using a Morita-Baylis-Hillman reaction directly on the diene's enone precursor. This first step was successfully performed on the 4-alkyl cyclopent-2-enone **2.7** with formaldehyde as the electrophile and tri-*n*-butyl phosphine as a catalyst, giving the product **3.43** in quantitative yield (see Scheme 3-10).⁸¹ While only this step has been performed so far, this synthetic avenue might be re-visited in the future once more synthetic exploration has been done on the synthesis of the revised 5,5-*trans* D-E ring junction.



3.5 Conclusion

A methodology was developed to access the “all-*cis*” cyclopentane stereoarray of the E-ring of the originally proposed structure of the natural product palau'amine. The methodology relies on a Diels-Alder reaction to build the high steric strain of the structure, followed by a multi-step oxidative opening of the resulting norbornene system. This methodology is currently being modified to allow for the synthesis of the corrected structure of palau'amine.

3.6 References

- ⁶⁴ Kinnel, R.B.; Gehrken, H.-P. ; Scheuer, P. J. ; *Journal of the American Chemical Society* **1993**, *115*, 3376;
- ⁶⁵ Kinnel, R. B. ; Gehrken, H.-P. ; Swali, R. ; Skoropowski, G. ; Scheuer, P. J. ; *The Journal of Organic Chemistry* **1998**, *63*, 3281.
- ⁶⁶ Hoffmann, H.; Lindel, T.; *Synthesis*, **2003**, *12*, 1753
- ⁶⁷ Jacquot, D.E.N.; Lindel, T; *Current Organic Chemistry*, **2005**, *9*, 1551
- ⁶⁸ Kobayashi, H.; Kitamura, K.; Nagai, K.; Nakao, Y.; Fusetani, N.; van Soest, R. W. M.; Matsunaga, S., *Tetrahedron Letters* **2007**, *48* (12), 2127-2129.
- ⁶⁹ Grube, A.; Kock, M., *Angewandte Chemie International Edition* **2007**, *46* (13), 2320-2324.

-
- ⁷⁰ Buchanan, M. S.; Carroll, A. R.; Addepalli, R.; Avery, V. M.; Hooper, J. N. A.; Quinn, R. J., *The Journal of Organic Chemistry* **2007**, 72 (7), 2309-2317.
- ⁷¹ Kock, M.; Grube, A.; Seiple, I. B.; Baran, P. S., *Angewandte Chemie International Edition* **2007**, 46 (35), 6586-6594.
- ⁷² Cernak, T. A.; Gleason, J. L., *The Journal of Organic Chemistry* **2007**, 73 (1), 102-110.
- ⁷³ Foley, L. H.; Buchi, G. *Journal of the American Chemical Society* **1982**, 104, 1776-1777.
- ⁷⁴ A) Wiese, K. J.; Yakushijin, K.; Horne, D. A., *Tetrahedron Letters* **2002**, 43 (29), 5135-5136. B) Nakadai, M.; Harran, P. G., *Tetrahedron Letters* **2006**, 47 (23), 3933-3935.
- ⁷⁵ Bland, J. M.; Stammer, C. H.; Varughese, K. I., *The Journal of Organic Chemistry* **2002**, 49 (9), 1634-1636.
- ⁷⁶ A) Clark, R. D.; Heathcock, C. H., *Tetrahedron Letters* **1974**, 15 (23), 2027-2030. B) Clark, R. D.; Heathcock, C. H., *The Journal of Organic Chemistry* **1976**, 41 (8), 1396-1403.
- ⁷⁷ Almansa, C.; Carceller, E.; Moyano, A.; Serratosa, F., *Tetrahedron* **1986**, 42 (13), 3637-3648.
- ⁷⁸ Lachance, H.; St-Onge, M.; Hall, D. G., *The Journal of Organic Chemistry* **2005**, 70 (10), 4180-4183.
- ⁷⁹ Bultman, M. S. ; Ma, J.; Gin, D. Y. ; *Angewandte Chemie International Edition*. **2008**, 47, 6821
- ⁸⁰ Clerici, F.; Gelmi, M. L.; Gambini, A., *The Journal of Organic Chemistry* **1999**, 64 (16), 5764-5767.
- ⁸¹ Ito, H.; Takenaka, Y.; Fukunishi, S.; Iguchi, K., *Synthesis* **2005**, 2005 (18), 3035-3038.

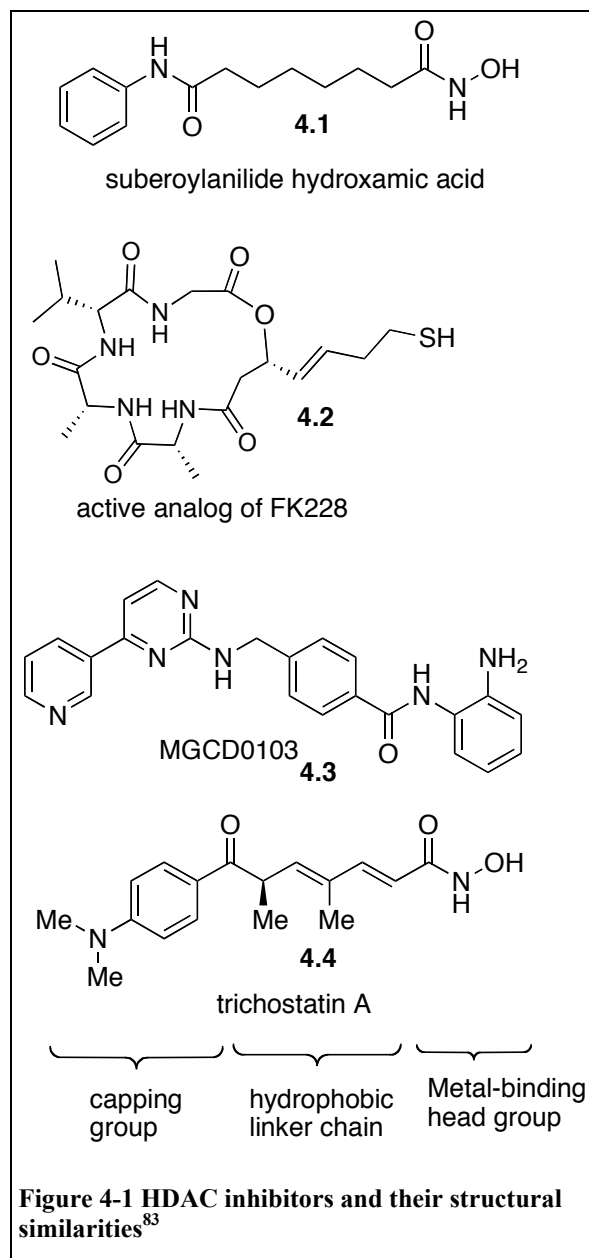
Part B

4 Synthesis of the multiple ligand drug triciferol, agonist of the nuclear vitamin D receptor and inhibitor of histone deacetylases

4.1 Rational design of triciferol

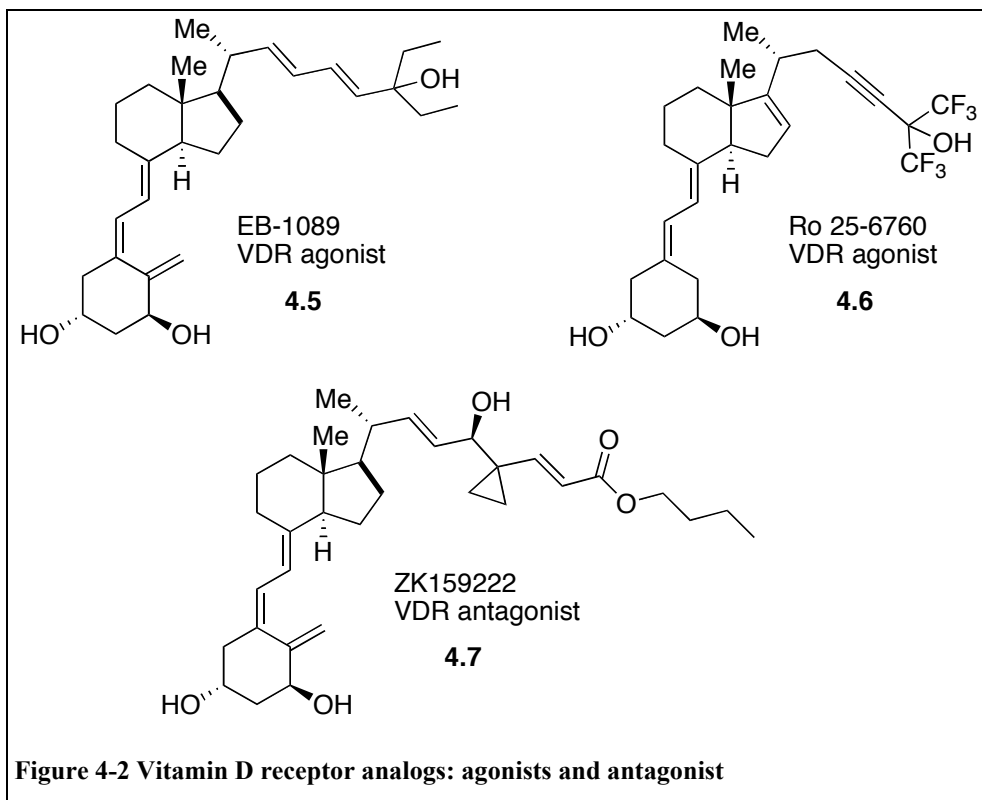
It was found by our collaborators that 1,25D₃ and TSA have synergistic effects as anti-cancer agents. Because of the advantages of multiple ligands drugs, it was decided to combine the properties of both molecules into one single entity, a multiple ligand drug. In order to choose the optimal type of multiple ligand design (tethered, linked, fused or fully merged), a deeper understanding of both biologicals targets was needed. 1,25D₃ is an agonist of the vitamin D nuclear receptor. TSA is an inhibitor of histone deacetylase (HDAC) enzymes.

The targeted HDAC enzymes are zinc metalloproteases.⁸² The zinc atom is found at the bottom of a long and narrow hydrophobic pocket. As can be seen from Figure 4-1, many inhibitors of HDACs follow the general pattern of a head group, a linker and a capping group. The HDACi head is constituted of a metal binding group to deactivate the metalloprotease enzyme. The head and cap groups are joined by a hydrophobic linker. Finally, the capping group interacts with the HDAC surface, which is open and flexible, therefore tolerating a wide variety of capping end groups. All of these HDACi regions would need to be incorporated in the new multiple ligand drug.

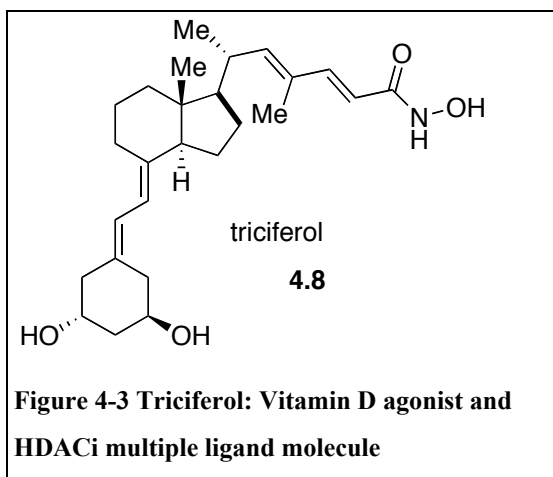


The vitamin D receptor pocket is more restrictive to potential ligands. Because the ligand binding domain of the vitamin D receptor completely encapsulates the ligand upon binding, successful analogs of vitamin D have a structure and size very similar to the parent hormone. As can be seen from Figure 4-2, some variation is tolerated in the top chain of the vitamin.⁸⁴ However, too long a top chain might lead to a molecule which binds to the vitamin D receptor but prevents the recruitment of co-activators, such as the antagonist ZK159222.

Also of note, the A-ring exo-methylene moiety is non-essential for binding and its deletion only leads to a small loss in binding affinity.⁸⁵



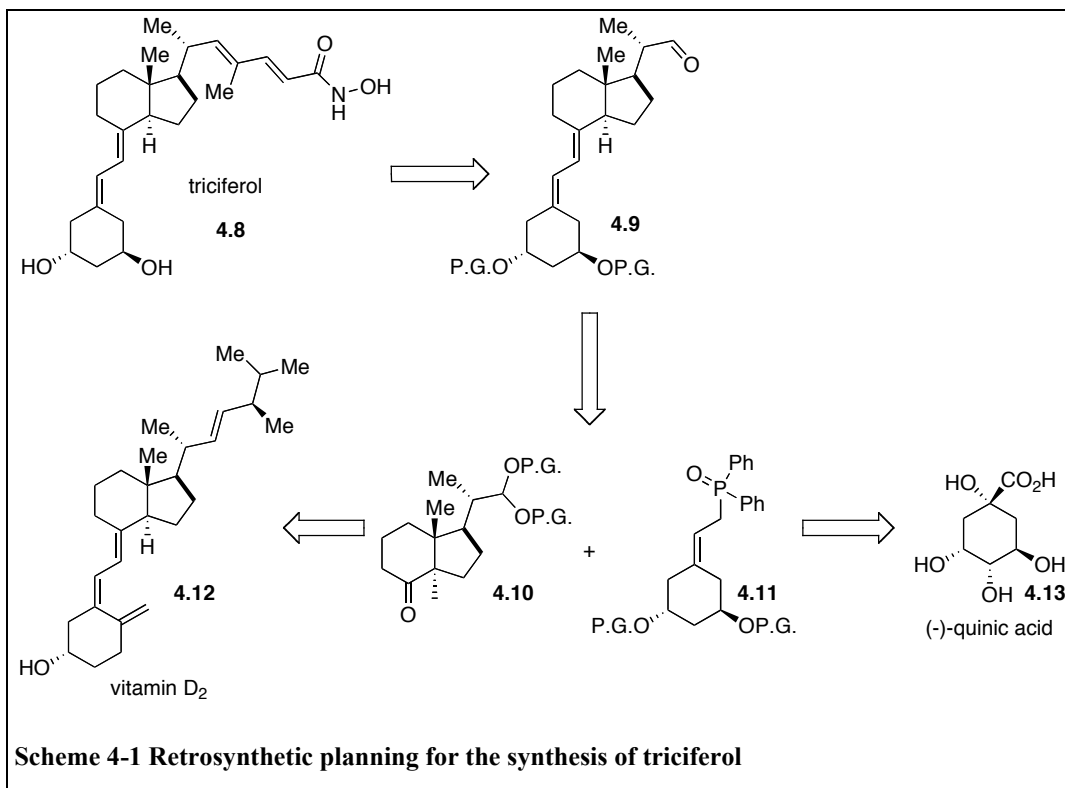
The tolerated variability of vitamin D analogs at the side chain prompted us to merge there the HDACi functionality. Because of the high potency of TSA, a similar structure was chosen for the HDAC part of the multiple ligand: a conjugated diene chain ending with a hydroxamic acid. Since analogs such as EB-



1089 and Ro 25-6760 are well tolerated by the vitamin D receptor, the conjugated diene was expected to be tolerated. It was expected that either the NH or OH of the hydroxamic acid of **4.8** would form a hydrogen bond to the vitamin D receptor in a way similar to the C-25 alcohol of the native ligand 1,25D₃.

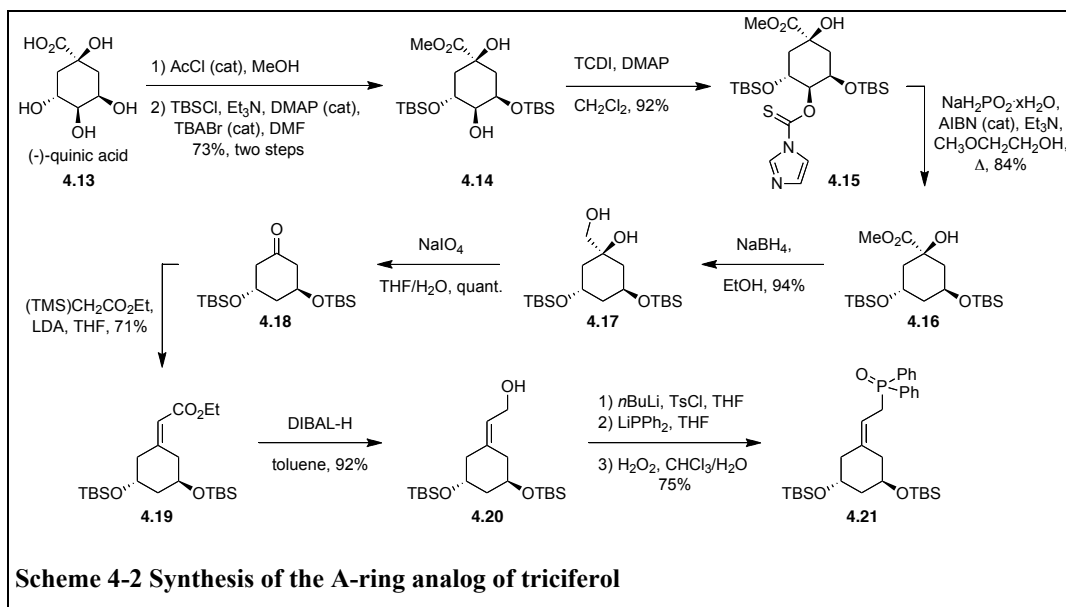
The vitamin D core was also envisioned as a possible capping group for the HDACi structure requirement, since a variety of cap groups are tolerated in HDACi. For synthetic accessibility considerations, and because it is non-essential for high binding affinity to the vitamin D receptor, the A-ring exo-methylene moiety would not be included in the multiple ligand. With all of those considerations in mind, the structure of the first 1,25D₃/HDAC hybrid was envisioned as presented in Figure 4-3.

The retrosynthetic analysis of triciferol is presented in Scheme 4-1. The C-D ring core of triciferol was envisioned as coming from a degradation product of vitamin D₂. The A-ring would originate from the commercially available natural product (-)-quinic acid. Finally, the top chain would be elaborated late in the synthesis, in order to minimize the handling of the hydroxamic acid moiety. The chosen retrosynthetic scheme relies entirely on enantiopure chiral starting materials as the source of chirality in the final molecule. This minimizes the number of synthetic steps needed and alleviates the need to separate enantiomers.



4.2 Synthesis of triciferol

The synthesis of the A-ring moiety of triciferol was adapted from a procedure by DeLuca *et al.*⁸⁶ (-)-Quinic acid was submitted to a Fisher esterification in methanol, yielding the desired product quantitatively. Bis-protection of the sterically less hindered secondary alcohols at the 3- and 5-positions was achieved in 73% yield by treatment with two equivalents of TBSCl. The remaining free secondary alcohol was acylated with thiocarbonyl diimidazole to afford thiocarbamate **4.15** in 92% yield. Radical deoxygenation of the thiocarbamate with sodium hypophosphite as the hydrogen donor led, in 84% yield, to the alpha-hydroxy ester **4.16**, which was reduced with sodium borohydride to the vicinal diol in high yield. This diol was oxidatively cleaved with sodium periodate to yield the ketone **4.18** in quantitative yield. The 3,5-disilyloxycyclohexanone product is unstable to base and tends to undergo elimination of the silyloxy groups to yield phenol, especially under conditions for standard Wittig or Horner couplings. However, an aldol/Peterson olefination sequence on the ketone afforded the desired conjugated ester in 71% yield. From the intermediate **4.19**, reduction of the ester with DIBAL-H led to the allylic alcohol in high yield. This alcohol was converted to **4.21**, a precursor for Horner coupling, in 75% yield over three steps by a sequence of tosylation of the alcohol, displacement of this leaving group by a phosphine and oxidation of the phosphine to the phosphine oxide. The A-ring analog and Horner coupling partner **4.21** was thus obtained in 11 steps in 26% overall yield from quinic acid.

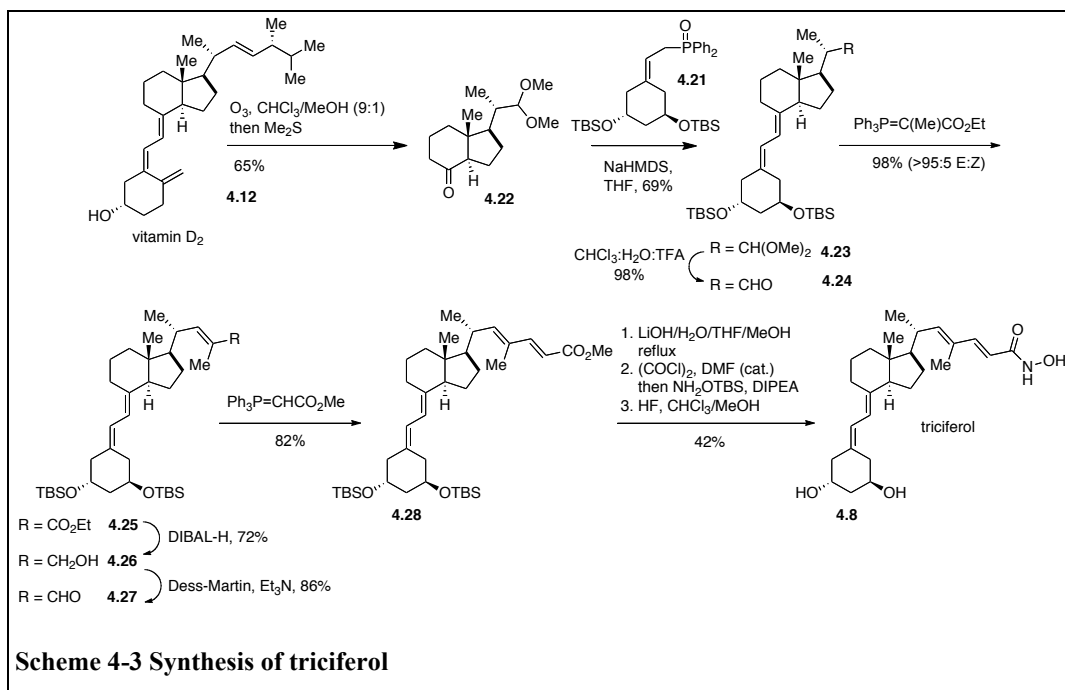


The core of the secosteroidal portion of triciferol is obtained by ozonolytic degradation of vitamin D₂ in a mixture of chloroform and methanol (9:1). After decomposition of the intermediate trioxolane with dimethyl sulfide, dimethylacetal product **4.22** was isolated in 65% yield. The *in-situ* ketalization in this process is probably catalyzed by trace acid in the chloroform solvent. Coupling of secosteroidal core **4.22** to an A-ring analog is complicated by the sensitivity of the stereocenter α to the ketone. Base-catalysed enolization of the ketone will lead to the epimerization of the stereocenter at the ring junction; in this system, the 5-6 *cis* ring junction is thermodynamically more stable than the vitamin D 5-6 *trans* system. To complete the secosteroid synthesis, A-ring analog **4.21** is coupled *via* a mildly basic Horner reaction to ketone **4.22** to afford diene **4.23** in 69% yield. The diene was obtained exclusively with the *E* stereochemistry, as was expected from previous syntheses of vitamin D structures.⁸⁷

In preparation for side-chain extension, acidic deprotection of the dimethylacetal revealed aldehyde **4.24** in 95% yield. Elongation of the top side-chain started with a stabilized Wittig reaction, yielding the *trans* conjugated ester **4.25** in high yield. Reduction of the ester with DIBAL-H led to the allylic alcohol in 72% yield. Oxidation of the free alcohol with the Dess-Martin reagent gave the

conjugated aldehyde **4.27** in good yield. Further elongation of the side-chain was performed with a second stabilized Wittig reaction, affording mainly the *trans* alkene in 82% yield. Gratifyingly, the undesired minor *cis* alkene formed in the Wittig reaction could be separated by careful chromatography before the final sequence leading to triciferol. This was essential as a removal was impossible at later stages.

With the fully elongated chain of product **4.28** in hand, conversion of the ester to the desired hydroxamic acid could be performed. First, the ester **4.28** was saponified and, after a simple extraction, the highly pure acid was carried forward. The acid was converted to an acyl chloride and then immediately coupled with an O-silyl hydroxylamine. This protocol was found to be superior to other standard peptide coupling strategies, which led to low conversion and side products. Also, the use of O-silyl hydroxylamine was found superior to simple hydroxylamine, possibly because of the low water content and high solubility in organic media of the former. Following hydroxamic acid formation, the silyl groups of the vitamin D analog were carefully deprotected using hydrofluoric acid in methanol/acetonitrile, yielding triciferol in 42% isolated yield from the ester **4.28**. Triciferol was thus obtained in 10 linear steps and 9% overall yield starting from vitamin D₂.



4.2.1 Isolation of triciferol

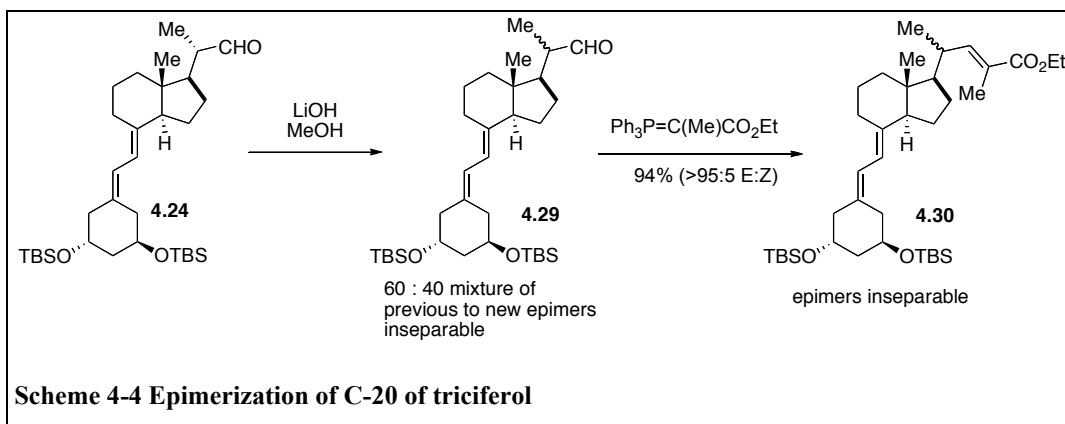
The final isolation of triciferol proved especially challenging. Indeed, purification of triciferol using standard silica gel led to the isolation of a red oil from a streaking band on the TLC. This isolation was difficult to reproduce and sometimes would yield minimal amounts of the desired product. Nevertheless, the red oil had properties corresponding with the expected product and was submitted for preliminary biological testing. Initial tests performed in the laboratory of professor John White were promising. However, the results of the biological tests proved irreproducible over time and investigation of the triciferol sample showed complete decomposition after a few months, even though the sample was kept at low temperature between manipulations. Upon re-synthesis of a fresh batch of triciferol, the TLC isolation was replaced by a reverse-phase semi-preparative HPLC isolation. In contrast to purification on silica, HPLC purification yielded a white solid as the main product. This solid had spectral properties very similar to the red oil previously isolated. Using this new information, a purification of a larger amount of the crude triciferol was attempted using standard column

chromatography with a reverse-phase stationary phase (Octadecyl-functionalized silica gel) and a water-methanol mobile phase. Again, a white powder was obtained. Submission of a sample of this powder to TLC led to a streaking red band as in the original isolation of triciferol. The white powder of triciferol was solubilized in DMSO- d_6 and left at room temperature, in the dark. No sign of decomposition could be detected by ^1H NMR after one year. All of these results leads us to hypothesize that exposure of the hydroxamic acid of triciferol to silica gel results in metal ion complexation. Hydroxamic acids are known to be efficient metal chelators, especially for iron. A representative from our silica gel supplier (SiliCycle $\text{\textcircled{R}}$) confirmed that metal ions are present in trace quantities in the standard silica gel we obtain from them. Complexation of a metal ion by the hydroxamic acid of triciferol probably accelerates the decomposition of the drug, leading to the irreproducible biological results. Reverse phase silica can be pre-washed with large quantities of deionized water, greatly reducing its trace metal content. Upon testing of the white powder form of triciferol, biological test results were reproducible and could be used to investigate the properties of the new molecule in living systems. The final isolation of triciferol by a method that does not expose the molecule to trace metal ions was therefore key in obtaining reproducible and reliable results.

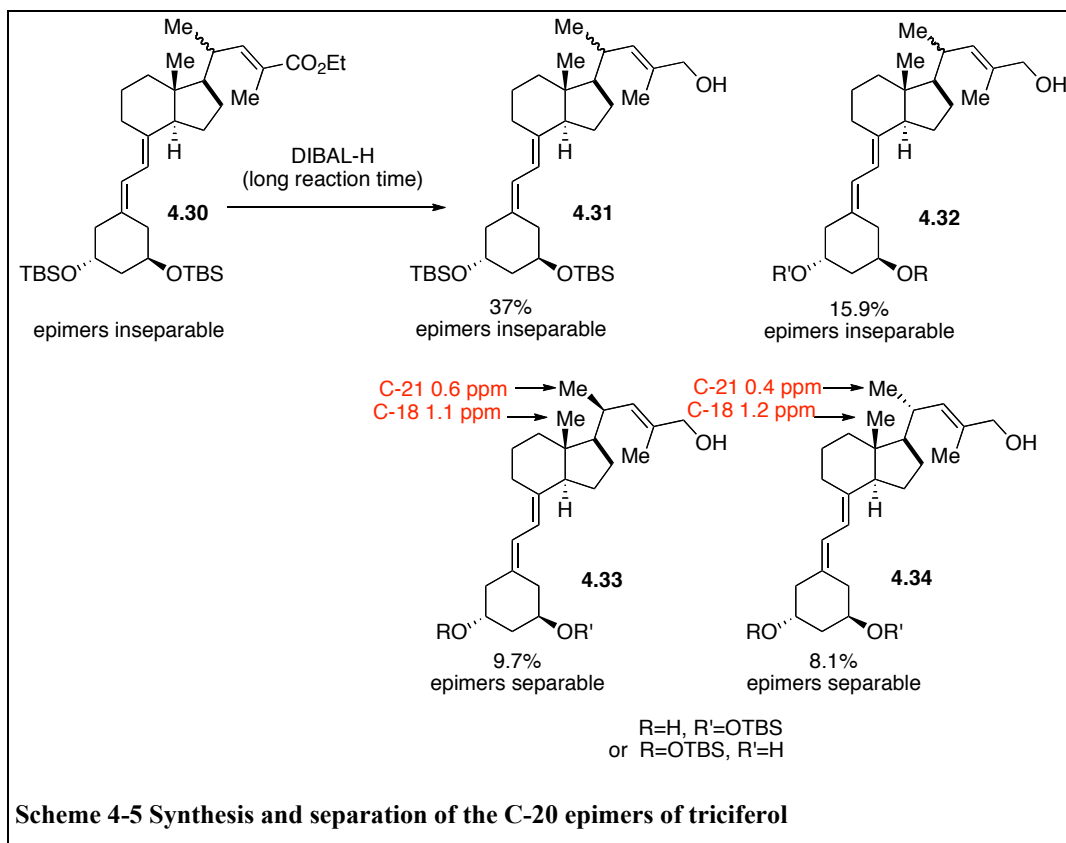
4.2.2 Synthesis of C-20 *epi*-triciferol precursor

An important concern in organic synthesis is the purity of the products being isolated. It came as a concern to our research group that during any of the top-chain elongation steps, the C-20 stereocenter might be partially or completely epimerized, as is occasionally the case in Wittig couplings (vide supra for a discussion of alpha center epimerization in the A-ring coupling). One would expect such an event to be detectable by ^1H NMR. However, synthesizing a C-20 epimer of triciferol was the only way of addressing this question with certainty. From the deprotection product **4.24**, base-catalyzed epimerization α to the aldehyde was attempted using lithium hydroxide in methanol. The crude mixture had a complex ^1H NMR spectrum, suggestive of the presence of multiple

products. However, chromatography was unsuccessful at separating these products. NMR data obtained later (vide infra) allowed us to identify this crude product as an inseparable mixture of C-20 epimers in a 3:2 ratio favoring the starting epimer. These epimers were subjected to the first Wittig olefination and yielded the desired conjugated esters **4.30**. However, the epimers could still not be separated by chromatography.



When attempting to reduce the ester **4.30** using DIBAL-H, too long a reaction time led to partial desilylation of the A-ring alcohols, as can be seen from Scheme 4-5. Of the many reduced products obtained, two were of high interest, as they were separable C-20 epimers with only one silyl group (**4.33**, **4.34**). Interestingly enough, when both silyl groups are present (**4.31**) or absent, the C-20 epimers cannot be separated. As well, of the two possible regioisomers where one silyl group is present on the A-ring, only one regioisomer will lead to separable C-20 epimers while the other regioisomer will lead to an inseparable mixture (**4.32**). Comparison of the ^1H NMR spectra of epimers **4.33** and **4.34** showed characteristic chemical shift differences between their C-18 and C-21 methyl groups, which could be traced back to the complex ^1H NMR of the epimerized aldehyde **4.29**. This information allowed us to further confirm that no C-20 epimer was present in triciferol or its synthetic precursors.



4.3 Biological results with triciferol

Triciferol was tested by our collaborators in the laboratory of professor John White. The results have already been published, and will be summarized here.

The binding of triciferol to the vitamin D receptor was first tested in a fluorescence polarization assay. Triciferol displayed a binding affinity to the vitamin D receptor of 87 nm, as compared to 32 nm with 1,25D₃. Triciferol thus retains much affinity for the receptor, despite the significant changes made to the top chain. This result is in accord with our hypothesis that the critical hydrogen bonding of 1,25D₃ to the vitamin D receptor would be maintained with the hydroxamic acid functionality of triciferol.

The activity of triciferol was further tested in cell systems for the activation of vitamin D related genes. The first assay performed was a luciferase reporter gene assay. In this assay, a plasmid containing the vitamin D response element gene followed by the luciferase gene was transfected into a cell line. The exposure of

this cell line to 1,25D₃ or triciferol resulted in the binding of the small molecules to the vitamin D nuclear receptor, recruitment of co-factors and transcription of the luciferase gene, causing the cells to emit light. In this assay, triciferol was approximately as active as 1,25D₃. However, this assay is not quantitative and a second assay was performed. In this second assay, the ability of triciferol to activate the *cyp24* gene was investigated. The activation of this gene is an exquisitely sensitive marker for vitamin D agonism. CYP24 is an enzyme that catabolizes the destruction of vitamin D₃. It is produced in cells as a feedback loop to prevent overstimulation of gene transcription. The *cyp24* gene assay analyzes the cellular level of mRNA corresponding with the CYP24 protein. In this assay, triciferol was approximately 10 % as potent as 1,25D₃ in promoting the transcription of the *cyp24* gene. These results prove that triciferol is an agonist of the vitamin D nuclear receptor, acting as 1,25D₃ in promoting the cellular machinery to transcribe vitamin D related genes.

Next, the ability of triciferol to act as an HDAC inhibitor was investigated. N-Boc-(N-Ac)-Lysine conjugated to a fluorescent group was exposed to cell lysates. The HDACs in the cell lysates then initiates the cleavage of the fluorescent group from the histone mimic, resulting in a detectable fluorescence of the medium. The inhibition of the HDACs by TSA and triciferol was then tested. In this assay, triciferol was about 10 % as potent as TSA as and HDAC inhibitor. This result confirms the ability of triciferol to act as an HDAC inhibitor.

The potential of triciferol to act as an anti-cancer agent was tested on several types of cancer cells. Triciferol was significantly more potent than 1,25D₃ or TSA alone in preventing the growth of the SCC4 and MDA-MB231 cancer cell lines. Even more impressive, against MCF-7 breast cancer cells, triciferol (100 nM) was more effective at inducing cell death than a combination of 1,25D₃ (100nM) and TSA (15nM). The lower concentration of TSA relative to triciferol in this experiment was used to compensate for the 10-fold greater potency of TSA against HDAC. In the SCC4 cell line, the morphology of the cells treated with triciferol was drastically different from the cells treated with 1,25D₃ but similar to cells cotreated with 1,25D₃ and TSA. Cells treated with 1,25D₃ or TSA alone

appeared as normal SCC4 cells, whereas cells treated with triciferol varied in size and shape, occasionally were multinucleated or had intercellular tubulin bridges. All of these effects are consistent with a disruption of mytosis by triciferol. These results were extremely encouraging and prompted further studies, notably on the exact HDAC that triciferol inhibits.

There are multiple HDACs responsible for cellular functions. As was previously mentioned, many of them are responsible for histone acetylation and thus gene regulation. However, HDACs are not limited to this role. HDAC6, for example, is notably responsible for the deacetylation of tubulin during cellular division.⁸⁸ While triciferol was found to inhibit histone deacetylation, tests showed it to be an even more potent inhibitor of tubulin deacetylation. This could explain the unusual cell morphologies found when using triciferol, and very probably contributes to its antiproliferative effects.

Triciferol was thus found to be both a vitamin D receptor agonist and an HDAC inhibitor. This ability to be a ligand for multiple targets allows triciferol alone to be an effective anticancer agent *in vitro*. Triciferol was found to prevent the proliferation of cancer cells through disruption of mytosis.

4.4 Conclusion

Starting from a knowledge of the mechanism of action and the pharmacophoric requirements of two drugs with synergistic effects, 1,25D₃ and an HDAC inhibitor, a new molecule with both functions was designed. The new potential drug, triciferol, is a multiple ligand of the “fully merged” type. It was synthesized from the vitamin D₂ core on which an A-ring diol was coupled, followed by building a conjugated top chain ending with a hydroxamic acid. This functionality was extremely sensitive to exposure to trace metals and could only be purified using reverse phase silica chromatography. Pure triciferol was successfully tested for both vitamin D receptor activation and HDAC inhibition. It also showed promising anti-cancer properties.

This project is currently being continued by other students. While more biological studies are being performed on triciferol, new 1,25D₃/HDACi hybrid

molecules are being synthesized. As a notable expansion of the project, the side chain conjugated hydroxamic acid of triciferol is being replaced with other zinc binding groups.

4.5 References

⁸² Hooper, N. M., Editor, *Zinc metalloproteases in health and disease*. CRC press; London, 1996; 350 pp.

⁸³ A) FK228 analog : Yurek-George, A.; Cecil, A. R. L.; Mo, A. H. K.; Wen, S.; Rogers, H.; Habens, F.; Maeda, S.; Yoshida, M.; Packham, G.; Ganesan, A., *Journal of Medicinal Chemistry* **2007**, *50* (23), 5720-5726. B) For MGCD0103 : Fournel, M.; Bonfils, C.; Hou, Y.; Yan, P. T.; Trachy-Bourget, M.-C.; Kalita, A.; Liu, J.; Lu, A.-H.; Zhou, N. Z.; Robert, M.-F.; Gillespie, J.; Wang, J. J.; Ste-Croix, H. I. n.; Rahil, J.; Lefebvre, S.; Moradei, O.; Delorme, D.; MacLeod, A. R.; Besterman, J. M.; Li, Z., *Molecular Cancer Therapeutics* **2008**, *7* (4), 759-768.

⁸⁴ Guyton, K. Z.; Kensler, T. W.; Posner, G. H., *Annual Review of Pharmacology and Toxicology* **2001**, *41* (1), 421-442.

⁸⁵ Ono, Y.; Kashiwagi, H.; Esaki, T.; Tadakatsu, T.; Sato, H.; Fujii, N., *Journal of Combinatorial Chemistry* **2007**, *9* (4), 711-716.

⁸⁶ Perlman, K.L.; Swenson, R.E.; Paaren, H.E.; Schnoes, H.K., DeLuca, H.F. *Tetrahedron Letters* **1991**, *32*, 7663

⁸⁷ Lythgoe, B.; Moran, T. A.; Nambudiry, M. E. N.; Tideswell, J.; Wright, P.W.; *Journal of the Chemical Society, Perkin Transactions 1* **1978**, 590-595.

⁸⁸ Valenzuela-Fernandez, A.; Cabrero, J. R. N.; Serrador, J. M.; Sanchez-Madrid, F., *Trends in Cell Biology* **2008**, *18* (6), 291-297.

5 Contributions to knowledge

- A new 5-substituted cyclopentadiene with improved thermal stability towards 1,5-H shift is disclosed. Racemic and enantioselective syntheses of the new diene have been developed.
- The origins of the new cyclopentadiene's stability have been investigated and are ascribed, using FMO theory, to an increase in the LUMO energy of the diene. Using the FMO theory also allowed to explain phenomena observed by other authors in the acceleration or deceleration of 1,5-H shift in dienes.
- The new diene was found to undergo Diels-Alder reaction at room temperature with many dienophiles, yielding products of high complexity. For slow reacting dienophiles, the use of an europium Lewis acid was found to accelerate the cycloaddition without causing side reactions with the new diene.
- The new diene is enantiostable and delivers products of equal enantiomeric excess.
- The developed Diels-Alder methodology with the new diene was applied to the synthesis of the highly functionalized E-ring of the originally proposed structure of the natural product palau'amine. This led to the second published synthesis for this complex cyclopentane stereoarray, 15 years after the publication of the structure of the natural product.
- The structures of vitamin D₃ and the HDAC inhibitor trichostatin A were merged into one molecule, triciferol. Triciferol was obtained from semi-synthesis starting from Vitamin D₂ and (-)-quinic acid.
- The instability of triciferol was identified as coming from trace metal contamination of the hydroxamic acid moiety during silica gel chromatography. Purification of hydroxamic acids using reverse phase chromatography was found to prevent this issue.
- In accord with our original design, triciferol was found to be both an agonist of the vitamin D₃ receptor and an HDAC inhibitor. Because of these properties, triciferol was also found to be an effective anti-cancer drug *in vitro*.

6 Appendix 1 Experimental section

General Procedures. All reactions were performed in flame-dried or oven-dried round bottom flasks fitted with rubber septa under a positive pressure of argon with magnetic stirring, unless otherwise noted. Liquids and solutions were transferred *via* syringe or stainless steel cannula. Analytical thin-layer chromatography was performed using glass plates pre-coated with 0.25 mm 230-400 mesh silica gel impregnated with a fluorescent indicator (254 nm). Thin layer chromatography plates were visualized by exposure to ultraviolet light and/or by exposure to an aqueous solution of potassium permanganate, followed by heating. Organic solutions were concentrated by rotary evaporation at ~15 Torr (water aspirator). Flash column chromatography was performed as described by Still *et al.*⁸⁹ using Silicycle 60 Å silica gel (230-400 mesh) or Brockman type IV (10% water by weight) neutral alumina.

Materials. Commercial reagents and solvents were used as received with the following exceptions. Triethylamine, dichloromethane, and diisopropylamine were distilled from calcium hydride at 760 Torr under an atmosphere of nitrogen. Tetrahydrofuran was distilled from sodium benzophenone ketyl at 760 Torr under an atmosphere of dinitrogen. ACS grade methanol was stored over freshly activated 3Å molecular sieves. CDCl₃ was stored over freshly activated 4 Å molecular sieves. Dimethylacetylene dicarboxylate, acrolein, methyl vinyl ketone, chloroacrylonitrile, acrylonitrile, methyl acrylate and methacrolein were passed through a short column of basic alumina before use. Solutions of *n*-butyllithium were titrated in Et₂O using 2,2-dipyridyl as indicator. Dimethyldioxirane was prepared according to the procedure by Adam⁹⁰.

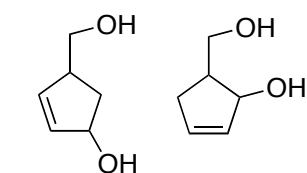
Instrumentation. Proton nuclear magnetic resonance (¹H NMR) and carbon nuclear magnetic resonance (¹³C NMR) spectra were recorded with a Varian Unity-500 (500 MHz), Varian Mercury-400 (400 MHz), or Varian Mercury-300 (300 MHz) NMR spectrometer. Proton chemical shifts are reported in parts per million (δ scale) downfield from tetramethylsilane and are referenced to residual protium in the NMR solvent (CHCl₃: δ 7.26, C₆D₆: 7.15). Data is

reported as follows: chemical shift [multiplicity (s = singlet, br s = broad singlet, d = doublet, t = triplet, m = multiplet), integration, coupling constant(s) in Hertz]. Carbon chemical shifts are reported in parts per million (δ scale) downfield from tetramethylsilane and are referenced to the carbon resonances of the solvent (CDCl₃: δ 77.0, C₆D₆: δ 128.0). Infrared spectra were recorded with a Nicolet Avatar 360 FTIR spectrometer. Melting points (MP) were obtained on a Gallenkamp melting point apparatus in open capillaries and are uncorrected. High-resolution mass spectroscopy was performed by Dr. Alain LeSimple (Mass Spectrometry Unit at McGill University) in positive ion electrospray mode with an IonSpec 7.0 tesla FTMS (Lake Forest, CA) calibrated with polyethylene glycol.

DFT simulations

Computer calculations were performed using the Gaussian 03 software at the B3LYP/6-31G* level of theory⁹¹. Transition states were identified by the presence of a single negative eigenvalue in frequency calculations and visually confirmed by inspection of their vibrational frequency. Energies are reported in kcal/mol and are corrected for zero-point energy. Energies were obtained from the Gaussian output file under “sum of electronic and zero-point energies”. For the generation of Figures 2.3-2.6, the energies reported are the lowest activation energies found for the 1,5-H shift in each system, regardless of the direction of the hydrogen shift (towards or away from the substituent).

Preparation of (hydroxymethyl)cyclopentanol isomers 2.5-2.6

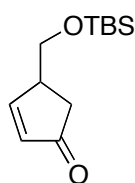


Chemical Formula: C₆H₁₀O₂
Molecular Weight: 114.14240

Paraformaldehyde (88g, 2.93 mol, 3.22 eq.) was suspended in 95% formic acid (500 g, 10.3 mol, 11.3 eq.) and heated to reflux in an oil bath at 100 °C. After 1 h, the resulting clear solution was cooled to - 10 °C, and *p*-toluenesulfonic acid monohydrate (0.30 g, 1.6 mmol, 0.17 eq.) was added in one portion. An addition funnel was affixed to the flask, and freshly distilled cyclopentadiene (60 g, 0.91 mol, 1 eq.) was added dropwise over 1 h.

The mixture was allowed to warm to room temperature and slowly turned black. After 14 h, the resulting black solution was cooled to $-10\text{ }^{\circ}\text{C}$ and a solution of aqueous sodium hydroxide (10 M, 1.2 L, 12 mol, 13 eq.) was added slowly over a period of 5 h while maintaining the reaction temperature below $0\text{ }^{\circ}\text{C}$. At this point, the reaction was comprised of an amber solution with a black sludge floating at the top. The black sticky sludge was removed by filtering the solution three times through a large Buchner funnel. The black residue was also washed with distilled water (500 mL) and the washings combined with the filtrate. The amber filtrate was acidified to pH 5 using hydrochloric acid (1 M) and then evaporated to dryness using a rotary evaporator (otherwise sodium formate will not be removed in the subsequent trituration). The resulting yellow solid was triturated with acetonitrile (3 x 500 mL) and filtered. The amber acetonitrile solution was then concentrated in vacuo, yielding 76.5 g of an amber oil. The oil was distilled under reduced pressure (bp $95\text{ }^{\circ}\text{C}$ at 0.2 torr) yielding 44.4 g (0.39 mol, 43%) of a clear, pale yellow oil which was an approximate 3:2 mixture of 1,4 and 1,3 diols, in agreement with Saville-Stones *et al.*⁹²

4-((*tert*-butyldimethylsilyloxy)methyl)cyclopent-2-enone **2.7**

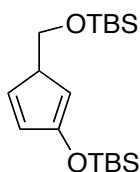


Chemical Formula: $\text{C}_{12}\text{H}_{22}\text{O}_2\text{Si}$
Molecular Weight: 226.38738

To a solution of (hydroxymethyl)cyclopentanol isomers **2.5-2.6** (16.0 g, 0.14 mol, 1 eq.) in dichloromethane (250 mL, A.C.S. grade solvent, no further drying necessary) at $23\text{ }^{\circ}\text{C}$ was added Bobbitt's oxidant, 4-acetamido-2,2,6,6-tetramethyl-1-oxopiperidinium perchlorate **2.6**⁹³, (49.8 g, 0.16 mol, 1.14 eq.) in small portions over 20 min. After the addition was complete, the vigorously stirred yellow suspension was diluted with dichloromethane (500 mL). After 3.5 h, the suspension was filtered to remove white and yellow solids and the filtrate was concentrated in vacuo, providing an orange oil. To a solution of the orange oil in dichloromethane (1 L) at $23\text{ }^{\circ}\text{C}$ were added sequentially, imidazole (15.9g, 0.234 mol, 1.64 eq.), *t*-butyldimethylsilyl chloride (31.1 g, 0.206 mol, 1.47 eq.), and (4-dimethylamino)pyridine (0.29g, 2.4 mmol, 0.017 eq.). The resulting

solution was stirred at 23 °C for 4 h, during which it turned cloudy yellow and a white solid precipitated. The reaction was then washed successively with distilled water (1L), hydrochloric acid (1 M, 1 L), distilled water (1 L), saturated aqueous NaHCO₃ solution (1L) and brine (1L). The organic phase was dried over Na₂SO₄, filtered, and concentrated in vacuo to a pale brown oil which was purified by flash chromatography on silica gel using a solvent gradient (from hexanes → 15% ethyl acetate in hexanes) yielding the product as a colorless oil (14.4 g, 0.0635mol, 45%) R_f = 0.27 (10 % ethyl acetate in hexanes). ¹H NMR (300 MHz, CDCl₃) δ 7.65 (dd, 1H, *J* = 5.8, 2.5), 6.18 (dd, 1H, *J* = 5.6, 2.1), 3.71 (dd, 1H, *J* = 9.8, 5.6), 3.58 (dd, 1H, *J* = 9.6, 6.6), 3.10 (m, 1H), 2.41 (dd, 1H, *J* = 18.7, 6.6), 2.08 (dd, 1H, *J* = 18.7, 2.2), 0.84 (s, 9H), 0.01 (s, 6H); ¹³C NMR (125 MHz, CDCl₃) δ 209.9, 166.2, 135.1, 65.0, 44.4, 37.7, 26.0, 18.4, -5.2, -5.3; IR (film) ν 2954, 2929, 1717, 2857, 1717, 1472, 1254, 1184, 1094, 838, 777 cm⁻¹; HRMS (FTMS): *m/z* calcd. for (M+H⁺) = 227.1460, found = 227.1462.

Preparation of *tert*-butyl((3-(*tert*-butyldimethylsilyloxy)cyclopenta-2,4-dienyl)methoxy)dimethylsilane under soft enolization conditions 2.8

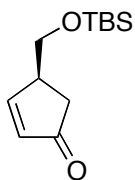


Chemical Formula: C₁₈H₃₆O₂Si₂
Molecular Weight: 340.64824

To a stirred solution of enone **2.7** (100 mg, 0.442 mmol, 1 eq.) in dichloromethane (2 mL) at -10 °C (ice-acetone bath) was added triethylamine (90 μL, 0.65 mmol, 1.46 eq.) followed by freshly distilled *t*-butyldimethylsilyltriflate (130 μL, 0.57 mmol, 1.28 eq.). After 1.5 h, the resulting yellow solution was diluted with ethyl acetate (10 mL) and washed with aqueous pH 7 buffer (2 x 3 mL) and brine (3 mL). The organic phase was dried over Na₂SO₄, filtered, and concentrated under reduced pressure using a rotary evaporator with a water bath at 23 °C to afford diene **2.8** as a pale yellow oil. Analysis by ¹H NMR spectroscopy indicated that the reaction had proceeded in ≥95% conversion. The diene was used without further purification. The diene isomerizes at room temperature with a half life of 37 h (see below for more experimental details on this calculation) and thus was not

allowed to stand for prolonged periods of time. ^1H NMR (400 MHz, CDCl_3) δ 6.39 (ddd, 1H, $J = 1.2, 1.9, 5.5$), 6.18 (1H, dt, $J = 1.2, 5.5$), 5.21 (dd, 1H, $J = 1.9, 3.8$), 3.59 (dd, 1H, $J = 7.8, 9.4$), 3.48 (dd, 1H, $J = 8.4, 9.2$), 3.24 (td, 1H, $J = 1.3, 8.1$), 0.95 (s, 9H), 0.91 (s, 9H), 0.19 (s, 6H), 0.06 (s, 6H); ^{13}C NMR (125 MHz, CDCl_3) δ 156.7, 136.5, 132.3, 107.0, 64.0, 53.1, 25.9, 25.7, 18.4, 18.2, -4.7, -5.4; IR (film) ν 2956, 2859, 1607, 1254, 838 cm^{-1} ; HRMS (ESI): m/z calcd. for $(\text{M}+\text{H}^+) = 341.2327$, found = 341.2327.

Preparation of enantiomerically enriched (*S*)-4-((*tert*-butyldimethylsilyloxy)methyl)cyclopent-2-enone **2.46**



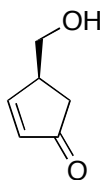
(1*R*,4*S*)-4-(hydroxymethyl)cyclopent-2-enol (**2.45**)

was obtained following the procedure by Hodgson *et al.*⁶³ using (1*S*,2*R*)-(+)-norephedrine. This enantioenriched diol was then oxidized and protected using the same procedure as described

Chemical Formula: $\text{C}_{12}\text{H}_{22}\text{O}_2\text{Si}$
Molecular Weight: 226.38738

above, giving the desired product in 96% yield over 2 steps. The enantiopurity of the product was inferred by protection of the intermediate primary alcohol as the benzoate ester **2.47** and analysis of the product by chiral HPLC (*vide infra*).

Preparation of enantiomerically enriched (*S*)-4-(hydroxymethyl)cyclopent-2-enone **2.39**



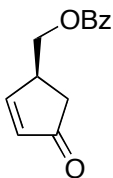
This compound is obtained as the intermediate in the two-step procedure written above. It may be purified by silica gel chromatography as a colorless oil (10% iso-propanol in dichloromethane). R_f (50%

Chemical Formula: $\text{C}_6\text{H}_8\text{O}_2$
Molecular Weight: 112.12652

ethyl acetate in hexanes) 0.13 ^1H NMR (400 MHz, CDCl_3) δ 7.70 (dd, 1H, $J = 5.9, 2.3$), 6.21 (dd, 1H, $J = 5.9, 2.0\text{Hz}$), 3.70 (m, 2H), 3.16 (m, 1H), 2.73 (m, OH), 2.47 (dd, 1H, $J = 19.0, 6.5$), 2.15 (dd, 1H, $J = 18.8, 2.3$); ^{13}C NMR (125 MHz, CDCl_3) δ 210.9, 166.9, 135.1, 64.2, 44.5, 37.9; IR (film) ν 3407, 2927, 2872, 1707, 1671, 1585, 1407, 1350, 1189, 1060.0, 1032, 941, 787 cm^{-1} ; HRMS (ESI): m/z calcd. for $(\text{M}+\text{H}^+) = 113.05971$, found =

113.05969. The enantiopurity of this product was inferred by chiral HPLC analysis of its benzoate ester (vide infra).

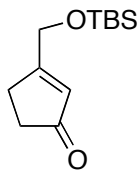
Preparation of enantiomerically enriched (*S*)-(4-oxocyclopent-2-enyl)methyl benzoate 2.47



Chemical Formula: C₁₃H₁₂O₃
Molecular Weight: 216.23258

To a solution of (*S*)-4-(hydroxymethyl)cyclopent-2-enone (21.5 mg, 0.19 mmol, 1 eq.) in dichloromethane (2.0 mL) at 0 °C were added pyridine (50 μL, 0.62 mmol, 3.25 eq.), (4-dimethylamino)pyridine (2.9mg, 0.024mmol, 0.12 eq.) and benzoyl chloride (65 μL, 0.56 mmol, 3.0 eq.). The reaction was left to warm to room temperature for 2 h, diluted with ethyl acetate (20 mL), washed with hydrochloric acid (1 M, 2 x 10 mL), saturated aqueous Na₂CO₃ solution (10 mL) and brine (10 mL), and then was dried over Na₂SO₄, filtered and concentrated in vacuo. The residue was purified by flash chromatography on silica gel using a solvent gradient (from 20% ethyl acetate in hexanes → 40% ethyl acetate in hexanes) yielding the product as a colorless oil (31.6mg, 0.15 mmol, 77%). *R_f*(20% ethyl acetate in hexanes) 0.13 ¹H NMR (500 MHz, CDCl₃) δ 7.99 (d, 2H, *J* = 8.1), 7.70 (dd, 1H, *J* = 5.6, 2.2), 7.56 (t, 1H, *J* = 7.4), 7.44 (t, 2H, *J* = 7.7), 6.30 (dd, 1H, *J* = 5.6, 1.7), 4.49 (dd, 1H, *J* = 11.0, 5.9), 4.37 (dd, 1H, *J* = 10.9, 6.0), 3.44 (m, 1H), 2.61 (dd, 1H, *J* = 18.48 6.8), 2.29 (dd, 1H, *J* = 18.8, 2.2); ¹³C NMR (125 MHz, CDCl₃) δ 208.6, 166.5, 164.0 (2 C), 136.0, 133.6, 129.8, 128.7, 65.8, 41.2, 38.0; IR (film) ν 1716, 1451, 1315, 1272, 1178, 1114, 1070, 1026, 785, 712 cm⁻¹; HRMS (ESI): *m/z* calcd. for (M+Na⁺) = 239.06787, found = 239.06777. The enantiopurity of the product (94 ± 1 % enantiomeric excess) was determined by HPLC with a Chiralpak AD-H column (Hexanes : 2-propanol , 99:1), 23 °C, UV 210nm, 2.0 mL/min; major enantiomer *t_R*=24.9min, minor enantiomer *t_R*=22.1 min.

3-((*tert*-butyldimethylsilyloxy)methyl)cyclopent-2-enone **2.11**

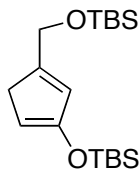


Chemical Formula: C₁₂H₂₂O₂Si
Molecular Weight: 226.38738

A solution of enone **2.7** (353.15 mg, 1.56 mmol, 1 eq.) in anhydrous ethanol (4 mL) and triethylamine (2 mL) was refluxed for 46 h then concentrated in vacuo. The residue was purified by flash chromatography on silica gel using a solvent gradient (from 5 % ethyl acetate in hexanes → 25 % ethyl acetate in hexanes) yielding the product **7** (247 mg, 70%) as a white amorphous solid (mp: 65-67 °C). R_f (20% ethyl acetate in hexanes) 0.28; ¹H NMR (400 MHz, CDCl₃) δ 6.16 (t, 1H, *J* = 1.4), 4.46 (s, 2H), 2.56 (m, 1H), 2.44 (m, 1H), 0.93 (s, 9H), 0.10 (s, 6H); ¹³C NMR (125 MHz, CDCl₃) δ 209.4, 181.4, 128.4, 63.2, 35.0, 27.8, 25.7, 18.3, -5.5; IR (film) ν 2929, 2856, 1699, 1669, 1626, 1432, 1262, 839, 777cm⁻¹; HRMS (ESI): *m/z* calcd. for (M+H⁺) = 227.14618, found = 227.14617.

Alternatively, enone **2.11** can be obtained from samples of diene **2.8** which have been left at room temperature for a few days (usually four). Dilution of those samples in a solution of 10% *p*-toluenesulfonic acid in ethyl acetate-water (10:1) and stirring for 30 min yielded the enone **2.11** after purification by flash chromatography (ethyl acetate : hexanes, 10:90).

tert-butyl((3-((*tert*-butyldimethylsilyloxy)cyclopenta-1,3-dienyl)methoxy)dimethylsilane **2.10**



Chemical Formula: C₁₈H₃₆O₂Si₂
Molecular Weight: 340.64824

To a stirred solution of enone **2.11** (101 mg, 0.444 mmol, 1 eq.) in dichloromethane (2 mL) at -10 °C (ice-acetone bath) were added, first, triethylamine (90 μL, 0.65 mmol, 1.46 eq.) then freshly distilled *t*-butyldimethylsilyltriflate (130 μL, 0.57 mmol, 1.27 eq.). After 1.5 h, the resulting yellow solution was diluted with ethyl acetate (10 mL) and washed with aqueous pH 7 buffer (2 x 3 mL) and brine (3 mL). The

organic phase was dried over Na₂SO₄, filtered and concentrated under reduced pressure using a rotary evaporator with a water bath at 23 °C to afford diene **6** as a pale yellow oil. Analysis by ¹H NMR spectroscopy indicated that the reaction had proceeded in ≥95% conversion. The diene was used without further purification. ¹H NMR (500 MHz, CDCl₃) δ 6.06 (s, 1H), 5.13 (s, 1H), 4.44 (s, 2H), 2.86 (s, 2H), 0.94 (s, 9H), 0.91 (s, 9H), 0.18 (s, 6H), 0.07 (s, 6H).

General procedure for the Diels-Alder cycloadditions

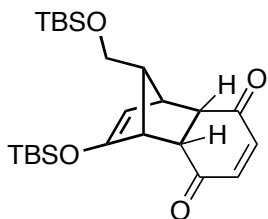
To the neat diene **2.8**, prepared as described above from enone **2.7** (100 mg, 0.44 mmol, 1 eq.), was added a solution of the dienophile (1.33 mmol, 3 eq.) in dichloromethane (0.9 mL). This solution was stirred at 23 °C. Upon complete consumption of **2.8**, the crude solution was immediately loaded on a neutral alumina column (Brockman type IV) and purified by flash chromatography using a solvent gradient (from hexanes → 10 % ethyl acetate in hexanes) [exception: the para-quinone cycloadduct **2.14** was best purified by standard silica gel column chromatography using the same solvent gradient].

The Diels-Alder adducts were characterized fully using 2D NMR to ascertain the nature of the *endo* and *exo* cycloadducts.

Representative procedure for the Lewis-Acid catalyzed Diels-Alder cycloaddition

To the neat diene **2.8**, prepared as described above from enone **2.7** (100 mg, 0.44 mmol, 1 eq.), were added sequentially, at 23 °C, a solution of methacrolein (110 μL, 1.33 mmol, 3.00 eq.) in dichloromethane (0.9 mL) then Europium(III)-tris(1,1,1,2,2,3,3-heptafluoro-7,7-dimethyl-4,6-octanedionate) (27.3 mg, 0.026 mmol, 0.06 eq.). After 3.5 h, the crude solution was loaded on a neutral alumina column and purified by flash chromatography using a solvent gradient (from hexanes → 2 % ethyl acetate in hexanes) yielding **2.27** (136 mg, 74%, 4:1 ratio of *exo* and *endo* cycloadducts) as a colorless oil.

(1*RS*, 2*SR*, 7*RS*, 8*RS*, 11*RS*)-9-(*tert*-butyldimethylsilyloxy)-11-((*tert*-butyldimethylsilyloxy)methyl)-tricyclo[6.2.1.0^{2,7}]undec-4,9-diene-3,6-dione 2.14

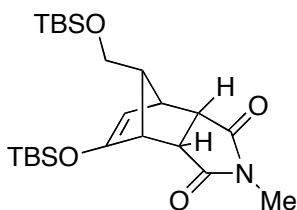


Chemical Formula: C₂₄H₄₀O₄Si₂
Molecular Weight: 448.74

The Diels-Alder reaction was carried out following the general procedure described above (reaction time : 10 min). The product was purified by flash chromatography on silica gel using a solvent gradient (from hexanes → 20 % ethyl acetate in hexanes) yielding the endo product as a

pale yellow amorphous solid (134 mg, 66%) m.p. : transition to a glassy wax at 63-66 °C, true melting at 110-115 °C. R_f (20 % ethyl acetate in hexanes) 0.45 ¹H NMR (400 MHz, CDCl₃) δ 6.61 (d, 1H, *J* = 10.3), 6.56 (d, 1H, *J* = 10.3), 4.51 (d, 1H, *J* = 3.1), 3.61 (d, 2H, *J* = 7.2), 3.21-3.31 (m, 3H), 3.09 (m, 1H), 2.01 (t, 1H, *J* = 7.1), 0.86 (s, 9H), 0.85 (s, 9H), 0.11 (s, 3H), 0.02 (s, 3H), 0.01 (s, 6H); ¹³C NMR (125 MHz, CDCl₃) δ 199.7, 197.9, 157.9, 142.2, 142.0, 98.6, 60.2, 60.0, 54.2, 50.9, 49.0, 48.6, 25.9, 25.3, 18.3, 17.7, -4.8, -5.3, -5.38, -5.39; IR (film) ν 2928, 2857, 1667, 1661, 1255, 1120, 1096, 1074, 880, 837, 782 cm⁻¹; HRMS (ESI): *m/z* calcd. for (M+Na⁺) = 471.23628, found = 471.23521.

(1*RS*, 2*SR*, 6*RS*, 7*RS*, 10*RS*)-8-(*tert*-butyldimethylsilyloxy)-10-((*tert*-butyldimethylsilyloxy)methyl)-4-methyl-4-azatricyclo[5.2.1.0^{2,6}]dec-8-ene-3,5-dione 2.21



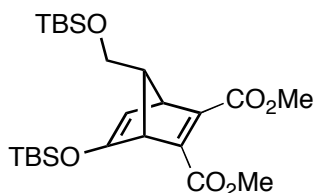
Chemical Formula: C₂₃H₄₁NO₄Si₂
Molecular Weight: 451.75

The Diels-Alder reaction was carried out following the general procedure described above (reaction time : 30 min). The product was purified by neutral alumina chromatography and the resulting solid was left under high vacuum (<0.5 torr) for 3 h to

remove residual N-methylmaleimide. The endo product was obtained as a white solid (158 mg, 79%). m.p. : 86-94 °C R_f (20 % ethyl acetate in hexanes) 0.34; ¹H NMR (400 MHz, CDCl₃) δ 4.46 (d, 1H, *J* = 2.4), 3.59 (d, 2H, *J* = 7.3), 3.30 (m,

2H), 3.11 (m, 1H), 2.97 (m, 1H), 2.83 (s, 3H), 2.11 (t, 1H, $J = 7.3$), 0.86 (s, 9H), 0.85 (s, 9H), 0.11 (s, 3H), 0.03 (s, 3H), -0.01 (s, 6H); ^{13}C NMR (100 MHz, CDCl_3) δ 178.0, 177.6, 157.7, 96.6, 64.3, 60.3, 50.1, 48.5, 46.0, 44.8, 25.9, 25.3, 24.5, 18.3, 17.8, -5.28, -5.30, -5.37, -5.39; IR (film) ν 2953, 2930, 2858, 1751, 1704, 1431, 1379, 1276, 1257, 1131, 1089, 839, 779 cm^{-1} ; HRMS (ESI): m/z calcd. for $(\text{M}+\text{Na}^+) = 474.24718$, found = 474.24585.

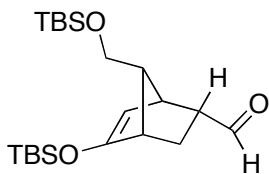
(1*RS*,4*RS*,7*RS*)-dimethyl 5-(*tert*-butyldimethylsilyloxy)-7-((*tert*-butyldimethylsilyloxy)methyl)bicyclo[2.2.1]hepta-2,5-diene-2,3-dicarboxylate 2.22



Chemical Formula: $\text{C}_{24}\text{H}_{42}\text{O}_6\text{Si}_2$
Molecular Weight: 482.76

The Diels-Alder reaction was carried out following the general procedure described above (reaction time : 45 min). After neutral alumina chromatography, the product was isolated as a colorless oil (169 mg, 79%). ^1H NMR (500 MHz, CDCl_3) δ 5.10 (s, 1H), 3.78 (s, 3H), 3.77 (s, 3H), 3.66 (dd, 2H, $J = 6.8, 2.4$), 3.56 (m, 1H), 3.33 (m, 1H), 2.96 (t, 1H, $J = 6.8$), 0.92 (s, 9H), 0.88 (s, 9H), 0.16 (s, 3H), 0.12 (s, 3H), 0.02 (s, 6H); ^{13}C NMR (125 MHz, CDCl_3) δ 169.6, 165.8, 165.1, 156.4, 151.4, 102.8, 82.7, 62.3, 58.4, 53.1, 52.0, 51.9, 26.1, 25.7, 18.5, 18.2, -4.6, -4.7, -5.2; IR (film) ν 2953, 2931, 2858, 1718, 1617, 1293, 1256, 1207, 1068, 840, 781 cm^{-1} ; HRMS (ESI): m/z calcd. for $(\text{M}+\text{Na}^+) = 505.24176$, found = 505.24071

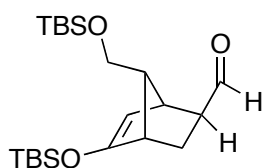
(1*RS*,2*RS*,4*SR*,7*RS*)-5-(*tert*-butyldimethylsilyloxy)-7-((*tert*-butyldimethylsilyloxy)methyl)bicyclo[2.2.1]hept-5-ene-2-carbaldehyde 2.16



Chemical Formula: $\text{C}_{21}\text{H}_{40}\text{O}_3\text{Si}_2$
Molecular Weight: 396.71

The Diels-Alder reaction was carried out following the general procedure described above (reaction time : 2 h). After neutral alumina chromatography, a colorless oil was isolated as a 1.6:1 mixture of endo and exo cycloadducts (125 mg, 71%). The endo and exo cycloadducts could

be separated by silica gel chromatography using a solvent gradient (from hexanes → ethyl acetate : hexanes, 20:80). R_f (20 % ethyl acetate in hexanes) 0.55 ^1H NMR (Major isomer : endo) (400 MHz, C_6D_6) δ 9.31 (d, 1H, $J = 1.2$), 4.29 (d, 1H, $J = 2.7$), 3.58 (dd, 1H, $J = 7.4, 10.2$), 3.53 (dd, 1H, $J = 7.4, 10.2$), 2.78 (m, 1H), 2.51-2.41 (m, 2H), 1.77 (dd, 1H, $J = 12.1, 4.3$), 1.71 (t, 1H, $J = 7.0$), 1.53 (ddd, 1H, $J = 3.9, 9.0, 12.1$), 0.94 (s, 9H), 0.88 (s, 9H), 0.07 (s, 3H), 0.05 (s, 3H), 0.02 (s, 6H); ^{13}C NMR (100 MHz, C_6D_6) δ 201.6, 160.6, 96.5, 61.0, 60.6, 55.0, 48.1, 45.0, 27.6, 25.8, 25.4, 18.2, 17.7, -5.0, -5.3, -5.52, -5.53; IR (film) ν 2955, 2931, 2887, 2858, 1463, 1302, 1277, 1253, 1139, 1103, 1070, 903, 838, 779 cm^{-1} ; HRMS (ESI): m/z calcd. for $(\text{M}+\text{H}^+) = 397.25942$, found = 397.25790.

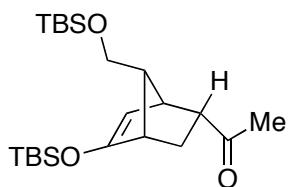


Chemical Formula: $\text{C}_{21}\text{H}_{40}\text{O}_3\text{Si}_2$
Molecular Weight: 396.71

^1H NMR (Minor isomer : exo) R_f (20 % ethyl acetate in hexanes) 0.60 (400 MHz, C_6D_6) δ 9.45 (d, 1H, $J = 1.6$), 4.38 (d, 1H, $J = 3.1$), 3.59 (d, 2H, $J = 7.4$), 2.70 (m, 1H), 2.46 (m, 1H), 2.06 (dd, 1H, $J = 3.1, 7.8$), 1.94-1.83 (m, 2H), 1.32 (dd, 1H, $J =$

9.0, 12.1), 0.92 (s, 9H), 0.89 (s, 9H), 0.07 (s, 3H), 0.02 (s, 3H), 0.01 (s, 6H); ^{13}C NMR (100 MHz, C_6D_6) δ 201.3, 161.2, 100.5, 61.0, 57.8, 55.3, 47.2, 44.7, 26.9, 25.8, 25.4, 18.2, 17.8, -4.9, -5.1, -5.5; IR (film) ν 2955, 2931, 2886, 2858, 1721, 1615, 1470, 1327, 1254, 1103, 1078, 839, 779 cm^{-1} ; HRMS (ESI): m/z calcd. for $(\text{M}+\text{H}^+) = 397.25942$, found = 397.25868.

1-((1*RS*,2*RS*,4*SR*,7*RS*)-5-(*tert*-butyldimethylsilyloxy)-7-((*tert*-butyldimethylsilyloxy)methyl)bicyclo[2.2.1]hept-5-en-2-yl)ethanone 2.23

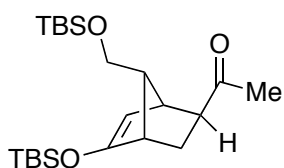


Chemical Formula: $\text{C}_{22}\text{H}_{42}\text{O}_3\text{Si}_2$
Molecular Weight: 410.73808

The Diels-Alder reaction was carried out following the general procedure described above (reaction time : 2 h). After chromatography on neutral alumina, a colorless oil was isolated as a 2:1 mixture of endo and exo cycloadducts (123 mg, 67%). The endo and exo cycloadducts could

be separated by silica gel chromatography using a solvent gradient (from hexanes → ethyl acetate : hexanes, 20:80). (Major isomer : endo) R_f (20 % ethyl acetate in

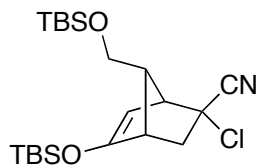
hexanes) 0.53 ¹H NMR (400 MHz, C₆D₆) δ 4.31 (d, 1H, *J* = 2.9), 3.67 (dd, 1H, *J* = 7.3, 9.8), 3.60 (dd, 1H, *J* = 7.3, 9.8), 2.80 (m, 1H), 2.55-2.46 (m, 2H), 2.03 (dd, 1H, *J* = 11.7, 3.9), 1.81 (t, 1H, *J* = 7.3), 1.68 (s, 3H), 1.51 (ddd, 1H, *J* = 3.4, 8.8, 11.7), 0.96 (s, 9H), 0.91 (s, 9H), 0.14 (s, 3H), 0.13 (s, 3H), 0.05 (s, 6H); ¹³C NMR (100 MHz, C₆D₆) δ 205.4, 160.7, 95.9, 61.6, 61.2, 54.8, 48.0, 46.6, 28.1, 27.5, 25.8, 25.4, 18.2, 17.8, -4.9, -5.3, -5.5; IR (film) ν 2955, 2931, 2886, 2858, 1712, 1615, 1359, 1334, 1254, 1123, 1081, 838, 781 cm⁻¹; HRMS (ESI): *m/z* calcd. for (M+H⁺) = 411.27507, found = 411.27404



Chemical Formula: C₂₂H₄₂O₃Si₂
Molecular Weight: 410.74

(Minor isomer : exo) *R_f* (20 % ethyl acetate in hexanes) 0.65 ¹H NMR (400 MHz, C₆D₆) δ 4.50 (d, 1H, *J* = 3.4), 3.69 (m, 2H), 2.75 (m, 1H), 2.52 (m, 1H), 2.22 (dd, 1H, *J* = 3.9, 11.7), 2.17 (t, 1H, *J* = 7.3), 2.03 (dt, 1H, *J* = 11.7, 3.9), 1.75 (s, 3H), 1.42 (dd, 1H, 8.8, 11.7), 0.94 (s, 9H), 0.92 (s, 9H), 0.11 (s, 3H), 0.08 (s, 3H), 0.03 (s, 3H), 0.02 (s, 3H); ¹³C NMR (100 MHz, C₆D₆) δ 201.2 161.2, 101.0, 61.2, 57.6, 55.2, 47.1, 46.0, 28.8, 25.8, 25.4, 18.2, 17.8, -4.8, -5.0, -5.5; IR (film) ν 2955, 2931, 2887, 2858, 1708, 1616, 1359, 1328, 1254, 1171, 1102, 1073, 839, 779 cm⁻¹; HRMS (ESI): *m/z* calcd. for (M+H⁺) = 411.27507, found = 411.27455

(1*RS*,2*RS*,4*SR*,7*SR*)-5-(*tert*-butyldimethylsilyloxy)-7-((*tert*-butyldimethylsilyloxy)methyl)-2-chlorobicyclo[2.2.1]hept-5-ene-2-carbonitrile 2.24

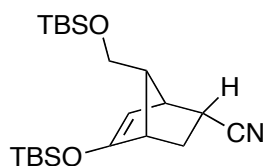


Chemical Formula: C₂₁H₃₈ClNO₂Si₂
Molecular Weight: 428.16

The Diels-Alder reaction was carried out following the general procedure described above (reaction time : 3.5 h). After neutral alumina chromatography, a colorless oil was isolated as an inseparable mixture of exo and endo cycloadducts in a 3.2 : 1 ratio (139 mg, 73%). The endo and exo isomers were assigned by ¹H-¹³C coupling constants. ¹H NMR (Major isomer, exo nitrile) *R_f* (20 % ethyl acetate in hexanes) 0.68 (400 MHz, C₆D₆) δ 4.36 (d, 1H, *J* = 3.1), 3.41 (d, 2H, *J* = 7.0), 3.00 (m, 1H), 2.31 (m, 1H), 2.26-2.20 (m, 2H), 1.57

(d, 1H, $J = 13.3$), 0.89 (s, 9H), 0.83 (s, 9H), 0.02 (s, 3H), -0.01 (s, 3H), -0.04 (s, 3H), -0.05 (s, 3H); ^{13}C NMR (100 MHz, C_6D_6) δ 161.1, 121.0, 96.3, 60.5, 59.4, 59.0, 56.6, 48.1, 45.5, 25.7, 25.2, 18.1, 17.6, -5.1, -5.4, -5.6, -5.7; IR (film) ν 2955, 2932, 2886, 2859, 1619, 1471, 1362, 1337, 1256, 1131, 1089, 841, 781 cm^{-1} ; HRMS (ESI): m/z calcd. for $(\text{M}+\text{H}^+)$ = 428.22079, found = 428.21982. The identities of the major and minor isomers were assigned based on the observed ^1H - ^{13}C coupling constants for the nitrile carbon. Major isomer: exo nitrile (ddd, $J = 5.8, 2.5, 2.4$ Hz). Minor isomer : endo nitrile (dd, $J = 5.0, 2.0$ Hz).

(1*RS*,2*RS*,4*SR*,7*RS*)-5-(*tert*-butyldimethylsilyloxy)-7-((*tert*-



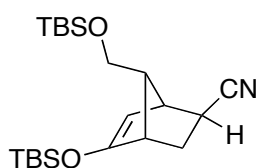
Chemical Formula:

$\text{C}_{21}\text{H}_{39}\text{NO}_2\text{Si}_2$

Molecular Weight: 393.71086

butyldimethylsilyloxy)methyl)bicyclo[2.2.1]hept-5-ene-2-carbonitrile 2.25

The Diels-Alder reaction was carried out following the general procedure described above (reaction time : 20 h). After chromatography, a colorless oil was isolated as a 1.2:1 mixture of endo and exo cycloadducts (118 mg, 67%). The endo and exo cycloadducts could be separated by silica gel chromatography using a solvent gradient (from hexanes \rightarrow 20 % ethyl acetate in hexanes). ^1H NMR (Major isomer : endo) R_f (20 % ethyl acetate in hexanes) 0.60 (500 MHz, C_6D_6) δ 4.63 (d, 1H, $J = 2.9$), 3.46 (m, 2H), 2.61 (m, 1H), 2.35 (m, 1H), 2.18 (dt, 1H, $J = 3.4, 8.8$), 1.53 (ddd, 1H, $J = 3.4, 9.3, 12.7$), 1.40-1.30 (m, 2H), 0.93 (s, 9H), 0.91 (s, 9H), 0.17 (s, 3H), 0.13 (s, 3H), 0.00 (s, 6H); ^{13}C NMR (125 MHz, C_6D_6) δ 161.3, 122.4, 97.5, 61.0, 60.0, 47.7, 46.9, 32.6, 30.7, 26.0, 25.6, 18.4, 18.0, -4.8, -5.2, -5.36, -5.40; IR (film) ν 2954, 2931, 2886, 2859, 1616, 1336, 1256, 1123, 1083, 878, 838, 781 cm^{-1} ; HRMS (ESI): m/z calcd. for $(\text{M}+\text{H}^+)$ = 394.25976, found = 394.25891



Chemical Formula:

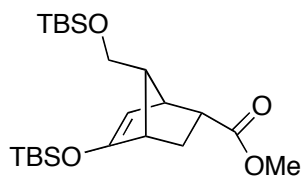
$\text{C}_{21}\text{H}_{39}\text{NO}_2\text{Si}_2$

Molecular Weight: 393.71086

^1H NMR (Minor isomer : exo) R_f (20 % ethyl acetate in hexanes) 0.65 (500 MHz, C_6D_6) δ 4.13 (d, 1H, $J = 3.1$), 3.52 (d, 2H, $J = 7.4$), 2.66 (m, 1H), 2.38 (m, 1H), 2.18 (t, 1H, $J = 7.4$), 1.72 (dd, 1H, $J = 3.9, 9.0$), 1.63 (dt, 1H, $J = 3.9, 12.1$), 1.32 (dd, 1H,

$J = 9.0, 12.1$), 0.96 (s, 9H), 0.87 (s, 9H), 0.04 (s, 3H), 0.03 (s, 3H), -0.03 (s, 6H); ^{13}C NMR (125 MHz, C_6D_6) δ 160.7, 122.7, 99.5, 60.9, 59.0, 48.3, 47.3, 32.2, 30.4, 26.0, 25.5, 18.4, 18.0, -4.8, -5.0, -5.29, -5.32; IR (film) ν 2955, 2931, 2886, 2858, 1616, 14.71, 1333, 1254, 1103, 1076, 838, 780 cm^{-1} ; HRMS (ESI): m/z calcd. for $(\text{M}+\text{H}^+) = 394.25976$, found = 394.25910

(1*RS*,2*RS*,4*SR*,7*RS*)-methyl 5-(*tert*-butyldimethylsilyloxy)-7-((*tert*-butyldimethylsilyloxy)methyl)bicyclo[2.2.1]hept-5-ene-2-carboxylate 2.26

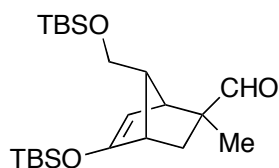


Chemical Formula: $\text{C}_{22}\text{H}_{42}\text{O}_4\text{Si}_2$
Molecular Weight: 426.74

The Diels-Alder reaction was carried out following the general procedure described above (reaction time : 24 h). After neutral alumina chromatography, a colorless oil was isolated as a

2.3:1 mixture of endo and exo cycloadducts (122 mg, 65%). The endo cycloadduct could be isolated pure after silica gel chromatography using a solvent gradient (from hexanes \rightarrow 20 % ethyl acetate in hexanes). R_f (20 % ethyl acetate in hexanes) 0.69 ^1H NMR (Major isomer : endo) (400 MHz, C_6D_6) 4.55 (d, 1H, $J = 3.1$), 3.63 (m, 2H), 3.13 (s, 3H), 3.07 (m, 1H), 2.80 (m, 1H), 2.49 (m, 1H), 1.95 (dd, 1H, $J = 4.3, 12.1$), 1.82-1.69 (m, 2H), 0.94 (s, 9H), 0.91 (s, 9H), 0.14 (s, 3H), 0.13 (s, 3H), -0.02 (s, 3H), -0.03 (s, 3H); ^{13}C NMR (100 MHz, C_6D_6) δ 173.8, 160.6, 97.3, 61.2, 61.1, 50.6, 47.9, 46.6, 46.3, 29.5, 25.8, 25.5, 18.2, 17.8, -4.9, -5.3, -5.50, -5.52; IR (film) ν 2954, 2931, 2858, 1740, 1616, 1255, 838, 780 cm^{-1} ; HRMS (ESI): m/z calcd. for $(\text{M}+\text{H}^+) = 427.26999$, found = 427.26893.

(1*RS*,2*SR*,4*SR*,7*RS*)-5-(*tert*-butyldimethylsilyloxy)-7-((*tert*-butyldimethylsilyloxy)methyl)-2-methylbicyclo[2.2.1]hept-5-ene-2-



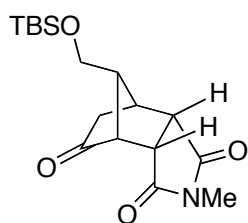
Chemical Formula: $\text{C}_{22}\text{H}_{42}\text{O}_3\text{Si}_2$
Molecular Weight: 410.74

carbaldehyde 2.27

The Diels-Alder reaction was carried out following the general procedure described above (reaction time : 43 h). After neutral alumina chromatography, a colorless oil was isolated as an

inseparable 5:1 mixture of exo and endo cycloadducts (65 mg, 35%). ^1H NMR (Major isomer : exo) R_f (20 % ethyl acetate in hexanes) 0.62 (500 MHz, CDCl_3) δ 9.68 (s, 1H), 4.56 (d, 1H, $J = 3.4$), 3.62 (m, 2H), 2.62 (m, 1H), 2.45 (m, 1H), 2.38 (dd, 1H, $J = 12.2, 3.91$), 1.94 (t, 1H, $J = 7.1$), 1.04 (s, 3H), 1.00 (d, 1H, $J = 12.2$), 0.93 (s, 9H), 0.86 (s, 9H), 0.19 (s, 3H), -0.17 (s, 3H), 0.00 (s, 6H); ^{13}C NMR (125 MHz, CDCl_3) δ 206.1, 162.1, 96.9, 61.5, 59.7, 57.2, 49.5, 48.6, 35.0, 26.2, 25.8, 20.3, 18.6, 18.2, -4.4, -4.5, -5.1; IR (film) ν 2955, 2931, 2859, 1723, 1616, 1256, 1100, 839, 780 cm^{-1} ; HRMS (ESI): m/z calcd. for $(\text{M}+\text{H}^+)$ = 411.27507, found = 411.27507.

Preparation of enantiomerically enriched (1*S*, 2*S*, 6*R*, 7*R*, 10*R*)-10-((*tert*-butyldimethylsilyloxy)methyl)-4-methyl-4-azatricyclo[5.2.1.0^{2,6}]decane-3,5,8-trione **2.49**

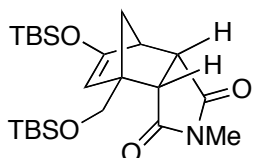


Chemical Formula: $\text{C}_{17}\text{H}_{27}\text{NO}_4\text{Si}$
Molecular Weight: 337.48608

To a sample of enantioenriched **2.46** (30.0 mg, 0.0658 mmol, 1 eq., obtained in two steps from enolization of (*S*)-**4** and Diels-Alder reaction with *N*-methylmaleimide), was added a solution of trifluoroacetic acid in dichloromethane (0.5% v/v, 1.0 mL) at 23 °C. After 10 min, the solution was diluted with ethyl acetate (10 mL), washed with saturated aqueous NaHCO_3 (5 mL) and brine (5 mL), dried over Na_2SO_4 , filtered and concentrated in vacuo to provide pure **12** (21.3 mg, 95% yield) as a colorless oil. R_f (50 % ethyl acetate in hexanes) 0.52 ^1H NMR (400 MHz, CDCl_3) δ 3.66 (dd, 1H, $J = 6.0, 11.0$), 3.58 (t, 1H, $J = 9.5$), 3.45 (m, 2H), 3.11 (m, 1H), 2.95 (m, 1H), 2.91 (s, 3H), 2.47 (m, 1H), 2.37 (dd, 1H, $J = 4.2, 19.2$), 0.85 (s, 9H), 0.012 (s, 3H), 0.006 (s, 3H); ^{13}C NMR (125 MHz, CDCl_3) δ 211.1, 176.6, 175.0, 60.4, 55.2, 53.5, 47.6, 46.0, 39.0, 37.6, 26.0, 24.9, 18.4, -5.3, -5.4; HRMS (ESI): m/z calcd. for $(\text{M}+\text{NH}_4^+)$ = 355.20476, found = 355.20512. IR (film): 2979, 2927, 1737, 1711, 1378, 1254, 1149, 842 cm^{-1} ; The enantiopurity of the product (95 \pm 1 % enantiomeric excess) was determined by HPLC with a Chiralpak AD-H column (6% iso-propanol in

hexanes), 23 °C, UV 210nm, 1.0 mL/min; major enantiomer t_r =17.2min, minor enantiomer t_r =12.1 min.

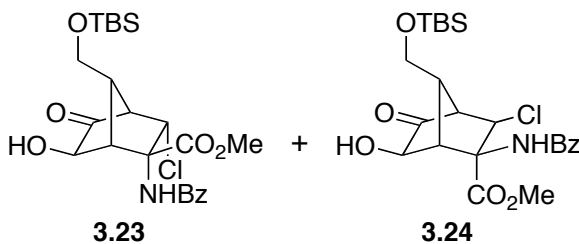
(1*RS*, 2*SR*, 6*SR*, 8*SR*)-8-(*tert*-butyldimethylsilyloxy)-1-((*tert*-butyldimethylsilyloxy)methyl)-4-methyl-4-azatricyclo[5.2.1.0^{2,6}]dec-8-ene-3,5-dione **2.50**



Chemical Formula: C₂₃H₄₁NO₄Si₂
Molecular Weight: 451.74694

To a solution of diene **2.10**, prepared as described above from enone **2.11** (100.5 mg, 0.44 mmol, 1 eq.), in dichloromethane (0.9 mL), was added N-methyl maleimide (148.2 mg, 1.33 mmol, 3 eq.) at 23 °C. After 30 min, the yellow reaction mixture was loaded on a neutral alumina column (Brockman type IV) and purified by flash chromatography using a solvent gradient (from hexanes → 6 % ethyl acetate in hexanes), yielding the product **2.50** as a glassy solid (135.4 mg, 0.30 mmol, 68% yield) m.p. : 97-99 °C. R_f (20 % ethyl acetate in hexanes) 0.49 ¹H NMR (400 MHz, CDCl₃) δ 4.40 (s, 1H), 4.08 (d, 1H, J = 10.6), 3.89 (d, 1H, J = 10.2), 3.32 (m, 2H), 3.02 (m, 1H), 2.82 (s, 3H), 1.64 (dd, 1H, J = 1.6, 8.6), 1.58 (d, 1H, J = 8.2), 0.88 (s, 9H), 0.87 (s, 9H), 0.10 (s, 3H), 0.08 (s, 3H), 0.06 (s, 3H), 0.03 (s, 3H); ¹³C NMR (100 MHz, CDCl₃) δ 178.1, 177.0, 159.9, 101.3, 62.4, 59.1, 52.4, 48.5, 47.6, 46.9, 25.9, 25.4, 24.4, 18.3, 17.9, -5.2, -5.4; IR (film): 2932, 2858, 1704, 1612, 1431, 1339, 1253, 1096, 877, 838, 781 cm⁻¹; HRMS (ESI): m/z calcd. for (M+H⁺) = 452.26469, found = 452.26460

Preparation of cycloadducts 3.23 and 3.24



Chemical Formula: C₂₃H₃₂ClNO₆Si
Molecular Weight: 482.04178

To the neat diene **2.8** (0.50 mmol, 1.4 eq.) was added a solution of (*Z*)-4-(chloromethylene)-2-phenyloxazol-5(4*H*)-one **3.11**⁹⁴ (75.3mg, 0.36 mmol, 1 eq.) in dichloromethane (900 μL) at 23 °C. The reaction immediately

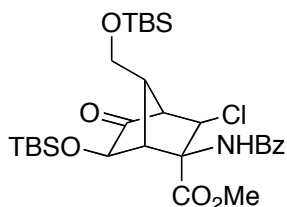
turned red. After 1 h, the reaction was filtered through a short plug of neutral alumina (Brockman type IV), eluting with hexanes (5 mL). The filtrate was cooled to $-78\text{ }^{\circ}\text{C}$ and a freshly prepared solution of dimethyldioxirane (9 mL of 0.06 M dimethyldioxirane in acetone, 0.54 mmol, 1.5 eq.) was added. After 1 h, the reaction was left to warm to $23\text{ }^{\circ}\text{C}$, during which time the red solution gradually turned to yellow. The solution was then evaporated in vacuo and redissolved in methanol (5 mL), to which was added K_2CO_3 (49.6 mg, 0.36 mmol, 1.0 eq.). The suspension was stirred at room temperature for 45 min then diluted with ethyl acetate (20 mL) and washed with saturated NH_4Cl solution (5 mL) and brine (5 mL) then dried over Na_2SO_4 , filtered and concentrated in vacuo. The product was purified by flash chromatography on silica gel using a solvent gradient (from 10 % ethyl acetate in hexanes \rightarrow 50 % ethyl acetate in hexanes) yielding the products **3.24** (47.7 mg, 0.099 mmol, 28%) and **3.23** (39.8 mg, 0.083 mmol, 23 %) as pale yellow oils.

Product **3.24** R_f (50 % ethyl acetate in hexanes) 0.50 ^1H NMR (500 MHz, CDCl_3) δ 7.77 (d, 2H, $J = 6.8$), 7.53 (m, 1H), 7.43 (m, 2H), 6.80 (m, NH), 5.20, (s, 1H), 4.49 (m, OH), 4.07 (dd, 1H, $J = 11.7, 3.4$), 4.00 (dd, 1H, $J = 11.7, 4.9$), 3.76 (s, 3H), 3.61 (dd, 1H, $J = 9.0, 2.2$), 2.97 (br s, 1H), 2.95 (br s, 1H), 2.81 (m, 1H), 0.89 (s, 9H), 0.10 (s, 3H), 0.08 (s, 3H); ^{13}C NMR (125 MHz, CDCl_3) δ 210.0, 169.6, 167.6, 132.9, 132.2, 128.7, 127.2, 70.2, 67.8, 61.8, 61.2, 60.2, 54.9, 53.3, 48.0, 25.7, 18.3, -5.8, -5.9; IR (film) ν 3352, 2953, 2931, 2858, 1763, 1740. 1644, 1527, 1487, 1314, 1106, 1078, 838, 781, 715 cm^{-1} ; HRMS (ESI): m/z calcd. for $(\text{M}+\text{H}^+)$ = 482.17602, found = 482.17588.

Product **3.23** R_f (50 % ethyl acetate in hexanes) 0.63 ^1H NMR (500 MHz, CDCl_3) δ 7.78 (d, 2H, $J = 7.8$), 7.54 (m, 1H), 7.45 (m, 2H), 7.19 (m, NH), 4.95, (d, 1H, $J = 4.9$), 4.18 (d, OH, $J = 8.8$), 4.00 (dd, 1H, $J = 11.5, 4.6$), 3.93 (m, 2H), 3.77 (s, 3H), 3.47 (br s, 1H), 2.96(m, 1H), 2.72 (br s, 1H), 0.88 (s, 9H), 0.08 (s, 3H), 0.06 (s, 3H); ^{13}C NMR (125 MHz, CDCl_3) δ 210.6, 171.7, 167.5, 132.9, 132.6, 129.0, 127.4, 70.2, 63.1, 61.5, 60.6, 58.5, 53.7, 52.0, 46.6, 26.0, 18.6, -5.57, -5.61; IR (film) ν 3372, 2954, 2931, 2885, 2857, 1765, 1740, 1652, 1520, 1483, 1436,

1293, 1251, 1142. 1088, 1038, 839, 780, 716 cm^{-1} ; HRMS (ESI): m/z calcd. for $(M+\text{Na}^+) = 504.1580$ found = 504.1580

(1*RS*,2*RS*,4*RS*,6*RS*,7*SR*)-methyl 2-benzamido-6-(*tert*-butyldimethylsilyloxy)-7-((*tert*-butyldimethylsilyloxy)methyl)-3-chloro-5-oxobicyclo[2.2.1]heptane-2-carboxylate 3.25

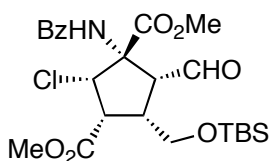


Chemical Formula: $\text{C}_{29}\text{H}_{46}\text{ClNO}_6\text{Si}_2$
Molecular Weight: 596.30264

This product is isolated as a minor side-product in 3 to 9% yield as a colorless oil after the above sequence leading to **3.23** and **3.24**. R_f (50 % ethyl acetate in hexanes) 0.75. ^1H NMR (500 MHz, CDCl_3) δ 7.82

(d, 2H, $J = 7.8$), 7.55 (m, 1H), 7.48 (m, 2H), 6.75 (m, NH), 5.18, (s, 1H), 3.93 (dd, 1H, $J = 10.9, 5.7$), 3.79 (s + m, 4H), 3.69 (m, 1H), 2.96 (br s, 1H), 2.90 (br s, 1H), 2.80 (m, 1H), 0.89 (s, 9H), 0.88, (s, 9H), 0.10 (s, 3H), 0.09 (s, 3H), 0.08 (s, 3H), 0.04 (s, 3H); ^{13}C NMR (125 MHz, CDCl_3) δ 209.8, 170.1, 167.5, 133.2, 132.5, 129.0, 127.5, 71.3, 67.7, 62.4, 61.1, 60.6, 54.2, 53.3, 49.8, 26.1, 26.0, 25.8, 18.5, 18.3, -4.6, -5.1, -5.2; IR (film) ν 2954, 2930, 2857, 1767, 1739, 1643, 1528, 1253, 1148. 1099, 838, 780cm^{-1} ; HRMS (ESI): m/z calcd. for $(M+\text{H}^+) = 596.26250$, found = 596.26200.

(1*SR*,2*SR*,3*RS*,4*SR*,5*RS*)-dimethyl 1-benzamido-4-((*tert*-butyldimethylsilyloxy)methyl)-2-chloro-5-formylcyclopentane-1,3-dicarboxylate 3.26

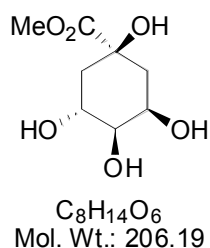


Chemical Formula:
 $\text{C}_{24}\text{H}_{34}\text{ClNO}_7\text{Si}$
Molecular Weight:
512.06776

Lead(IV)acetate (73.0 mg, 0.165 mmol, 3.7 eq.) was added to a solution of **3.23** (21.0 mg, 0.044mmol, 1 eq.) in dry methanol (2 mL) at -10°C . The resulting yellow solution was stirred at -10°C for 90 min then lifted off the cooling bath for 10 min, during which time the solution turned orange. At this point, the reaction was diluted with ethyl acetate (15 mL) and washed with a saturated aqueous solution of NH_4Cl (5 mL) and brine (5 mL). The organic layer was dried over Na_2SO_4 , filtered, and

concentrated *in vacuo* to give the crude product (23.0 mg) as a pale yellow oil (^1H NMR and HRMS analysis of the sample indicated contamination due to overoxidation of the aldehyde moiety to the methyl ester). The product was purified by a short flash chromatography column on silica gel using a solvent gradient (from 2 % ethyl acetate in hexanes \rightarrow 10 % ethyl acetate in hexanes; the solvent always contained 1% acetic acid by volume to prevent product decomposition) yielding the product as a pale yellow oil (11.5 mg, 0.0225 mmol, 51%) R_f (50 % ethyl acetate in hexanes) 0.60 ^1H NMR (500 MHz, CDCl_3) δ 9.78 (d, 1H, $J = 1.5$), 8.61 (s, NH), 7.89 (d, 2H, $J = 7.5$), 7.54 (t, 1H, $J = 7.0$), 7.47 (m, 2H), 4.86 (d, 1H, $J = 7.5$), 4.02 (dd, 1H, $J = 7.5, 10.0$), 3.91 (m, 1H), 3.82-3.72 (m, 8H), 2.97 (m, 1H), 0.85 (s, 9H), 0.03 (s, 6H), ^{13}C NMR (125 MHz, CDCl_3) δ 199.6, 171.34, 171.25, 167.3, 132.9, 132.4, 128.9, 127.6, 68.4, 62.5, 60.1, 55.6, 53.7, 52.5, 51.5, 45.0, 25.9, 18.3, -5.4. IR (film) ν 2954, 2857, 1739, 1666, 1520, 1484, 1438, 1256, 1210, 1180, 1084, 839, 779, 744 cm^{-1} ; HRMS (ESI): m/z calcd. for $(\text{M}+\text{H}^+)$ = 512.18659, found = 512.18712.

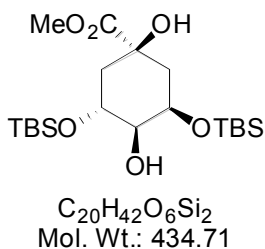
Methyl (3*R*,5*R*)-1,3,4,5-tetrahydroxycyclohexanecarboxylate.²¹



AcCl (2.044 g, 1.850 mL, 26.02 mmol) was added to a stirring solution of MeOH (37 mL) in a flame dried, round bottom flask charged with argon at 0 °C. (-)-Quinic acid (**4.13**, 10.00 g, 52.04 mmol, purchased from Sigma-Aldrich) was added to the mixture, and the suspension stirred for 16 h while warming to room temperature. The solid reactant dissolved as the reaction proceeded to afford a pale yellow solution. The reaction mixture was concentrated *in vacuo*, the residue redissolved in CHCl_3 , and then concentrated again (this process was repeated three times to remove the excess MeOH via azeotropic distillation). The product was isolated as a viscous yellow oil in quantitative yield (10.80 g, 52.38 mmol). R_f = 0.10 (30% EtOAc in hexanes); ^1H NMR (300 MHz, CD_3CN) δ 4.04-3.97 (1H, m), 3.96-3.84 (1H, m), 3.65 (3H, s), 3.34-3.26 (1H, m), 2.09-1.88 (3H, m), 1.74-1.63 (1H, m), 4

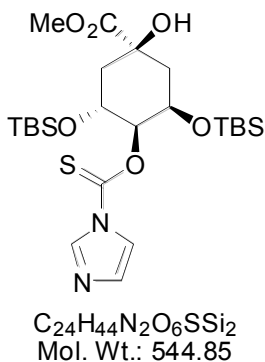
exchangeable protons unobserved; ^{13}C NMR (75 MHz, CD_3CN) δ 175.0, 76.7 (2C), 71.3, 67.6, 53.0, 42.1, 38.0.

Methyl (3*R*,5*R*)-3,5-bis[*tert*-butyl(dimethyl)silyloxy]-1,4-dihydroxycyclohexanecarboxylate. 4.14²¹



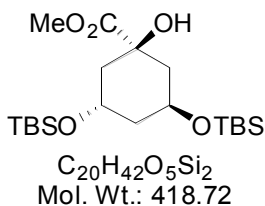
Methyl (3*R*, 5*R*)-1,3,4,5-tetrahydroxycyclohexanecarboxylate (Quinic acid methyl ester, *vide supra*) (10.73 g, 52.04 mmol) was dissolved in DMF (200 mL), in a flame dried round bottom flask flushed with argon. To this stirring solution was added DMAP (0.6358 g, 5.204 mmol), TBABr (1.730 g, 5.204 mmol), and TBSCl (17.26 g, 114.5 mmol). The flask was sealed with a rubber septum and cooled to 0 °C, at which point Et_3N (11.85 g, 16.30 mL, 117.1 mmol) was added to the reaction via syringe. A fine white precipitate formed upon addition of the amine. The reaction was stirred under argon for 16 h while warming to room temperature. The reaction mixture was then filtered to remove the precipitate, the filtrate diluted with EtOAc (200 mL) and extracted with sat. NH_4Cl (3 x 100 mL), distilled H_2O (100 mL) and brine (100 mL). The organic layer was then separated, dried (MgSO_4), and concentrated *in vacuo* to provide the crude product as a yellow, viscous oil. Compound 4.14 was isolated as a fluffy white solid via FCC (30% EtOAc in hexanes) in 73% yield (16.42 g, 37.76 mmol). R_f = 0.60 (30% EtOAc in hexanes); ^1H NMR (400 MHz, CDCl_3) δ 4.52 (1H, br s), 4.36 (1H, dt, J = 4.5, 2.5 Hz), 4.11 (1H, ddd, J = 13.0, 8.5, 4.5 Hz), 3.76 (3H, s), 3.42 (1H, dt, J = 8.5, 2.5 Hz), 2.32 (1H, d, J = 2.5 Hz), 2.18 (1H, ddd, J = 13.0, 4.5, 2.5 Hz), 2.09 (1H, dd, J = 14.0, 2.5 Hz), 2.01 (1H, ddd, J = 14.0, 4.5, 2.5 Hz), 1.82 (1H, dd, J = 13.0, 10.5 Hz), 0.90 (18H, d, J = 6.0 Hz), 0.15 (6H, d, J = 7.0 Hz), 0.11 (6H, d, J = 5.0 Hz); ^{13}C NMR (100 MHz, CDCl_3) δ 173.8, 76.3, 76.1, 71.6, 68.7, 52.8, 42.8, 38.0, 26.1 (6C), 18.4 (2C), -4.0, -4.3, -4.4, -4.7.

Methyl (3*R*, 5*R*)-3,5-bis[*tert*-butyl(dimethyl)silyloxy]-1-hydroxy-4-[(1*H*-imidazol-1-ylcarbonothioyl)oxy]cyclohexanecarboxylate . 4.15



Compound **4.14** (5.534 g, 12.73 mmol) was dissolved in CH_2Cl_2 (14 mL) in a flamed dried round bottom flask. To this stirring solution was added DMAP (0.1555 g, 1.273 mmol) and TCDI (3.402 g, 19.09 mmol) which dissolved into solution after several hours of stirring. The reaction vessel was sealed with a rubber septum and flushed with argon, and the reaction mixture stirred at room temperature for 3 days. The reaction mixture was then concentrated to provide the crude product as a dark orange viscous oil, which was directly loaded on the silica gel. Compound **4.15** was isolated as a pale yellow viscous oil via FCC (gradient 30% to 50% EtOAc in hexanes) in 92% yield (6.401 g, 11.75 mmol). $R_f = 0.20$ (30% EtOAc in hexanes); 1H NMR (300 MHz, $CDCl_3$) δ 8.28 (1H, s), 7.54 (1H, s), 6.95 (1H, s), 5.43 (1H, dd, $J = 8.5, 3.0$ Hz), 4.61-4.54 (2H, m), 4.50-4.41 (1H, m), 3.70 (3H, s), 2.27-2.13 (2H, m), 2.04-1.92 (2H, m), 0.82 (9H, s), 0.70 (9H, s), 0.01 (3H, s), 0.00 (3H, s), -0.05 (3H, s), -0.17 (3H, s); ^{13}C NMR (75 MHz, $CDCl_3$) δ 183.6, 173.2, 137.0, 130.7, 117.7, 86.0, 75.1, 68.3, 65.4, 52.7, 43.0, 38.0, 25.8, 25.7 (2C), 25.5 (2C), 25.4, 17.8, 17.7, -4.2, -4.7, -4.9, -5.6.

Methyl (3*S*,5*S*)-3,5-bis[*tert*-butyl(dimethyl)silyloxy]-1-hydroxy-cyclohexanecarboxylate 4.16

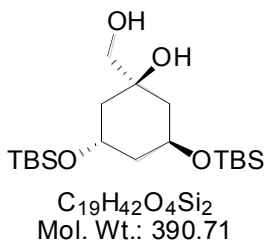


Compound **4.15** (9.490 g, 17.42 mmol) and $NaH_2PO_2 \cdot xH_2O$ (7.660 g, 87.09 mmol) were dissolved in 2-methoxy-ethanol (230 mL) under argon in a flamed dried round bottom flask equipped with a reflux condenser, and heated to reflux using a heating mantle. In a separate flask, AIBN (0.5714 g, 3.484 mmol) was dissolved in 2-methoxy-ethanol (20 mL) and Et_3N (approx. 2 mL) was added to this solution until a pH of 8 was obtained. Half of the AIBN solution was added to the refluxing reaction

mixture. The reaction was refluxed for 3 h with addition of the second half of the AIBN solution after 1 h. The reaction mixture was then cooled to room temperature, diluted with EtOAc (200 mL) and extracted with sat. NH₄Cl (3 x 100 mL), distilled H₂O (100 mL) and brine (100 mL). The organic layer was separated, dried (MgSO₄), and concentrated *in vacuo* to provide the crude product as a clear viscous oil. Compound **4.16** was isolated as a white solid via FCC (30% EtOAc in hexanes) in 84% yield (6.110 g, 14.59 mmol). *R*_f = 0.60 (30% EtOAc in hexanes); ¹H NMR (300 MHz, CDCl₃) δ 4.76 (1H, s), 4.43-4.37 (1H, m), 4.32 (1H, tt, *J* = 11.0, 4.5 Hz), 3.76 (3H, s), 2.25-2.16 (1H, m), 2.09-1.99 (1H, m), 1.97-1.92 (2H, m), 1.71 (1H, dd, *J* = 13.0, 11.0 Hz), 1.51-1.42 (1H, m), 0.90 (9H, s), 0.88 (9H, s), 0.12 (3H, s), 0.10 (3H, s), 0.07 (6H, s); ¹³C NMR (75 MHz, CDCl₃) δ 174.3, 70.0, 63.7, 52.8, 44.9, 42.4, 39.7, 38.6, 26.2 (3C), 26.0 (3C), 18.5, 18.1, -4.2, -4.3, -4.7, -4.8.

(3*S*,5*S*)-3,5-bis[*tert*-butyl(dimethyl)silyloxy]-1-(hydroxymethyl) cyclohexanol

4.17²¹



Compound **4.16** (6.110 g, 14.59 mmol) was dissolved in EtOH (150 mL) in a round bottom flask, and cooled to 0 °C. NaBH₄ (1.656 g, 43.78 mmol) was added to the stirring solution. After 30 min of stirring at 0 °C, the reaction mixture was warmed to room temperature

and stirred overnight. The reaction mixture was then quenched with sat. NH₄Cl (50 mL) and diluted with EtOAc (100 mL). The layers were separated and the aqueous layer extracted with EtOAc (2 x 50 mL). The combined organic layers were further extracted with sat. NH₄Cl (2 x 50 mL), distilled H₂O (50 mL) and brine (50 mL), separated, dried (MgSO₄), and concentrated *in vacuo* to give the crude product as a translucent grey solid in 94% yield (5.368 g, 13.74 mmol). The diol **4.17** was carried forward without further purification. *R*_f = 0.40 (30% EtOAc in hexanes); ¹H NMR (300 MHz, CDCl₃) δ 4.58 (1H, s), 4.42-4.26 (2H, m), 3.44-3.28 (2H, m), 2.21 (1H, dd, *J* = 8.5, 4.5 Hz), 2.10-1.85 (3H, m), 1.50-1.36 (2H, m), 1.27 (1H, dd, *J* = 12.5, 11.0 Hz), 0.92 (9H, s), 0.90 (9H, s), 0.13

(3H, s), 0.12 (3H, s), 0.09 (6H, s); ^{13}C NMR (75 MHz, CDCl_3) δ 74.7, 71.0, 70.0, 64.2, 44.1, 43.0, 38.1, 26.2 (3C), 25.1 (3C), 18.4, 18.0, -4.3, 4.4, -4.7, -5.0.

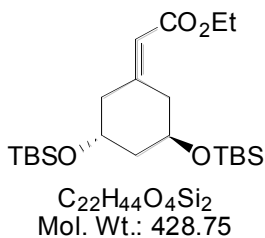
(3*S*,5*S*)-3,5-bis[*tert*-butyl(dimethyl)silyloxy]-cyclohexanone **4.18**



To a stirring solution of **4.17** (5.368 g, 13.74 mmol) in THF (100 mL), cooled to 0 °C, was added an aqueous solution of NaIO_4 (4.408 g, 20.61 mmol) (50 mL). A fine, white precipitate formed as the reaction proceeded.

The reaction mixture was then warmed to room temperature and stirred over night. The reaction mixture was then diluted with distilled H_2O until all of the precipitate dissolved. The layers were separated and the aqueous layer extracted with EtOAc (2 x 50 mL). The organic layers were combined and extracted with sat. NH_4Cl (2 x 50 mL), distilled H_2O (50 mL) and brine (50 mL), then dried (MgSO_4), and concentrated *in vacuo* to provide the crude product as a white crystalline solid in quantitative yield (4.938 g, 13.77 mmol). The ketone **4.18** was carried forward without further purification. $R_f = 0.40$ (10% EtOAc in hexanes); ^1H NMR (300 MHz, CDCl_3) δ 4.34 (2H, m), 2.55 (2H, dd, $J = 14.0, 4.0$ Hz), 2.35 (2H, ddd, $J = 14.0, 7.0, 1.0$ Hz), 1.94 (2H, t, $J = 5.5$ Hz), 0.87 (18H, s), 0.07 (6H, s), 0.06 (6H, s); ^{13}C NMR (75 MHz, CDCl_3) δ 207.7, 67.0 (2C), 50.4 (2C), 42.3, 25.9 (6C), 18.2 (2C), -4.6 (2C), -4.7 (2C).

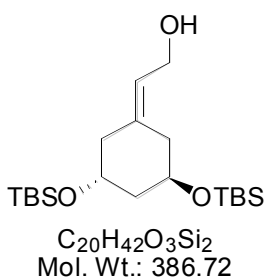
Ethyl ((3*R*,5*R*)-3,5-bis[*tert*-butyl(dimethyl)silyloxy]-cyclohexylidene)acetate **4.19**



In a flame dried round bottom flask cooled to -78 °C under argon, *n*-BuLi (8.610 mmol) was added to a solution of *i*-Pr₂NH (0.8712 g, 8.610 mmol) in THF (100 mL). The mixture was suspended above the ice bath for 15 min, then recooled to -78 °C. Ethyl-(trimethylsilyl)acetate (1.656 g, 10.33 mmol) was added to the stirring reaction mixture, and the reaction vessel was

again suspended above the ice bath for 15 min and recooled to -78 °C. Finally, a solution of **4.18** (2.471 g, 6.888 mmol) in THF (30 mL) was slowly cannulated into the reaction flask over a period of 30 min. The reaction mixture was then stirred at -78 °C for another 3 h, quenched with sat. NH₄Cl (50 mL) and warmed to room temperature. The layers were separated and the aqueous layer extracted with EtOAc (3 x 50 mL). The combined organic layers were extracted with distilled H₂O (50 mL) and brine (50 mL), dried (MgSO₄), and concentrated *in vacuo* to provide the crude product. Compound **4.19** was isolated as a clear oil via FCC (gradient 10% to 20% EtOAc in hexanes) in 71% yield (2.103 g, 4.905 mmol). *R*_f = 0.70 (10% EtOAc in hexanes); ¹H NMR (300 MHz, CDCl₃) δ 5.70 (1H, s), 4.20-4.08 (4H, m), 3.06 (1H, dd, *J* = 13.5, 6.0 Hz), 2.79 (1H, dd, *J* = 13.5, 3.5 Hz), 2.40 (1H, dd, *J* = 13.0, 3.5 Hz), 2.16 (1H, dd, *J* = 13.0, 8.0 Hz), 1.88-1.78 (1H, m), 1.76-1.66 (1H, m), 1.28 (3H, t, *J* = 7.0 Hz), 0.88 (9H, s), 0.86 (9H, s), 0.06 (12H, m); ¹³C NMR (75 MHz, CDCl₃) δ 166.4, 156.7, 117.5, 68.2, 68.1, 59.8, 46.3, 43.4, 37.7, 26.1 (3C), 26.0 (3C), 18.4, 18.3, 14.6, -4.5 (2C), -4.7 (2C).

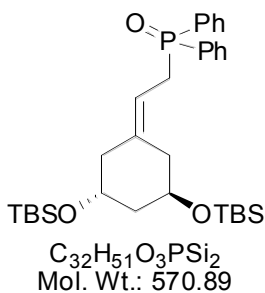
2-((3*R*,5*R*)-3,5-bis[*tert*-butyl(dimethyl)silyloxy]cyclohexylidene)ethanol **4.20**



In a flame dried round bottom flask, cooled to -78 °C under argon, DIBAL-H (12.26 mmol) was added to a solution of **4.19** (2.103 g, 4.905 mmol) in toluene (50 mL). The reaction mixture was warmed to room temperature and stirred for another 3 h. The reaction mixture was then cooled to 0 °C and diluted with Et₂O (50 mL). To this stirring solution was sequentially added distilled H₂O (0.5 mL), 1M NaOH (0.5 mL), and more distilled H₂O (1.2 mL). The reaction mixture was warmed to room temperature and stirred for 30 min. MgSO₄ (5 g) was added to the mixture, and the reaction stirred for another 30 min. The reaction mixture was filtered to remove the insoluble by-products, and the filtrate concentrated to provide compound **15** in 92% yield (1.726 g, 4.463 mmol) as a translucent grey solid. The allylic alcohol **4.20** was carried forward without further purification. *R*_f = 0.20 (10% EtOAc in hexanes); ¹H NMR (300 MHz, CDCl₃) δ 5.60 (1H, t, *J*

= 7.0 Hz), 4.18-4.10 (2H, m), 4.06-3.96 (2H, m), 2.40-2.30 (2H, m), 2.18 (1H, dd, $J = 13.5, 3.0$ Hz), 2.06 (1H, dd, $J = 12.0, 9.0$ Hz), 1.87-1.78 (1H, m), 1.69-1.59 (1H, m), 1.43 (1H, br s), 0.89 (18H, s), 0.07 (6H, s), 0.06 (3H, s), 0.05 (3H, s); ^{13}C NMR (75 MHz, CDCl_3) δ 138.4, 125.4, 68.3, 68.1, 58.5, 45.8, 43.6, 36.8, 26.1 (6C), 18.4 (2C), -4.5 (4C).

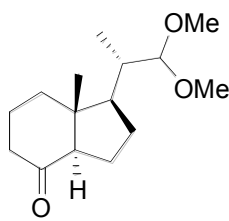
**[2-((3*R*,5*R*)-3,5-bis[*tert*-butyl(dimethyl)silyloxy]cyclohexylidene)ethyl]
(diphenyl)phosphine oxide **4.21****



In a flame dried round bottom flask under argon atmosphere, a 2.15 M solution of *n*-BuLi in hexanes (1.47 mL, 3.16 mmol, 1.05 eq.) was added to a stirred solution of **4.20** (1.11 g, 3.01 mmol, 1 eq.) in THF (12 mL) at 0 °C. To this mixture was added via cannula, a solution of freshly recrystallized *p*-toluenesulfonylchloride (602 mg, 3.16 mmol, 1.05 eq.) in THF (6 mL). The reaction was stirred at 0 °C for 2.5 hours. To this solution was added over a period of 30 min, a bright red solution of LiPPh₂, prepared separately in a separate flame dried flask under argon by adding a 2.15 M solution of *n*-BuLi in hexanes (1.54 mL, 3.31 mmol, 1.10 eq.) to a solution of HPPH₂ (0.575 mL, 3.31 mmol, 1.10 eq.) in THF (5 mL). The reaction mixture was allowed to stir at 0 °C for 1 h then warmed to room temperature. The reaction mixture was concentrated, and the residue dissolved in CHCl_3 (25 mL) and distilled H_2O (25 mL). To this mixture was added a 50% aqueous solution of H_2O_2 (1.73 mL, 30 mmol, 9.97 eq.), and the reaction mixture was stirred at room temperature for 3 h. The reaction was quenched with sat. NaHCO_3 (25mL), the layers separated, and the aqueous layer extracted with CH_2Cl_2 (3 x 30 mL). The combined organic layers were extracted with brine (30 mL), then dried (MgSO_4), filtered, and concentrated *in vacuo*. The residue was purified by FCC on silica gel using a 1:1 ethyl acetate - hexanes mixture as eluent. The product was further recrystallized from diethyl ether to give **4.21** as a white solid in 75% yield (1.2888 g, 2.26 mmol). $R_f = 0.30$ (30% EtOAc in hexanes); ^1H NMR (300 MHz, CDCl_3) δ 7.71-7.58 (4H, m),

7.46-7.33 (6H, m), 5.22 (1H, ddd, $J = 14.0, 7.0, 7.0$ Hz), 3.91 (2H, m), 3.11 (1H, ddd, $J = 15.0, 8.0, 8.0$ Hz), 2.99 (1H, ddd, $J = 15.0, 8.0, 8.0$ Hz), 2.22-2.12 (1H, m), 2.00-1.79 (3H, m), 1.60 (2H, dd, $J = 5.0, 5.0$ Hz), 0.80 (9H, s), 0.78 (9H, s), -0.04 (3H, s), -0.05 (6H, s), -0.06 (3H, s); ^{13}C NMR (75 MHz, CDCl_3) δ 139.20 (d, $J = 12.0$ Hz), 133.00 (d, $J = 98.0$ Hz), 132.70 (d, $J = 98.0$ Hz), 131.90 (2C), 131.30 (2C, d, $J = 9.5$ Hz), 131.20 (2C, d, $J = 9.5$ Hz), 128.70 (2C, d, $J = 11.5$ Hz), 128.6 (2C, d, $J = 11.5$ Hz), 113.90 (d, $J = 8.5$ Hz), 68.0, 67.7, 45.3, 43.6, 37.4, 30.7 (d, $J = 70.0$ Hz), 26.2 (3C), 26.1 (3C), 18.5, 18.4, -4.4 (4C).

(1R, 3aR, 7aR)-1-[(1S)-2,2-dimethoxy-1-methylethyl]-7-methyl-octahydro-4H-inden-4-one 4.22

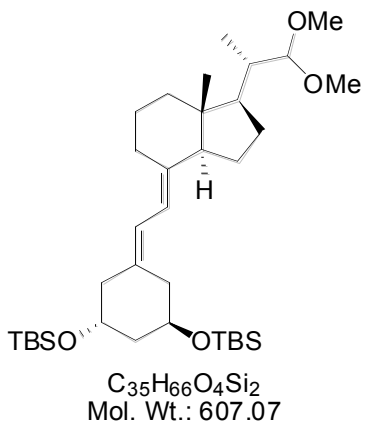


$\text{C}_{15}\text{H}_{26}\text{O}_3$
Mol. Wt.: 254.37

Ozone gas was bubbled through a solution of vitamin D₂ (17, ergocalciferol, **4.121**) (2.7071 g, 6.82 mmol, 1 eq.) in MeOH (72 mL) and CHCl_3 (8 mL) at -78 °C until a dark blue color persisted and then left for another hour. Argon was then bubbled through the reaction mixture until the solution turned clear. Me_2S (3.0 mL, 41 mmol, 6.0 eq.) was added to the reaction mixture at -78 °C, and the reaction stirred for 1 hour, then warmed to room temperature and stirred for another 30 min. The conversion of the keto-aldehyde to the keto-acetal was carefully monitored by thin layer chromatography on silica gel (eluent: 1:4 ethyl acetate to hexanes). The reaction was immediately stopped upon appearance of a third spot indicating the epimerization of the C14 stereocenter. The reaction mixture was then concentrated and the crude loaded directly onto silica gel. Compound **4.22** was isolated via silica gel column chromatography (1:4 ethyl acetate to hexanes) in 65 % yield (1.1313 g, 4.45mmol) as a clear oil. $R_f = 0.40$ (20% EtOAc in hexanes); ^1H NMR (400 MHz, CDCl_3) δ 4.09 (1H, d, $J = 2.5$ Hz), 3.40 (3H, s), 3.35 (3H, s), 2.43 (1H, dd, $J = 11.0, 7.5$ Hz), 2.28-2.15 (2H, m), 2.10-1.95 (2H, m), 1.92-1.82 (2H, m), 1.76-1.58 (4H, m), 1.57-1.47 (1H, m), 1.43-1.33 (1H, m), 0.95 (3H, d, $J = 6.5$ Hz), 0.61 (3H, s); ^{13}C NMR (100 MHz, CDCl_3) δ 211.6, 108.8, 61.6, 57.0, 56.1, 52.7, 50.1, 41.2, 39.4, 39.0, 27.2, 24.2, 19.4, 12.6, 12.1; IR

(film) ν 2956, 1714, 1461, 1381, 1142, 1070, 959 cm^{-1} ; LRMS (ESI): m/z (rel. intensity) = 255 [38, (M + H)⁺], 223 (100), 191 (12), 107 (5), 74 (6); HRMS (ESI): m/z calcd. for [(M + H)⁺] = 255.1955, found = 255.1954.

(1R, 3R, 7E, 17₋)- 1, 3-bis[*tert*-butyl(dimethyl)silyloxy]-17[(1S)- 2,2-dimethoxy- 1- methylethyl]- 9,10-secoestra- 5, 7-diene 4.23

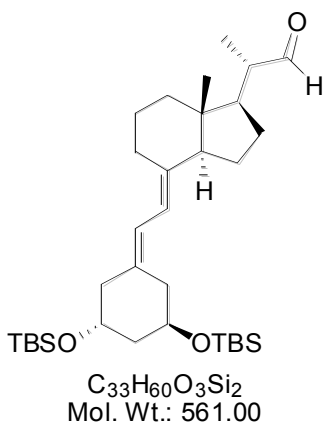


In a flame dried round bottom flask, cooled to -78 °C under argon, NaHMDS (2.574 mmol) was added to a solution of **4.21** (1.469 g, 2.574 mmol) in THF (30 mL). The reaction vessel was suspended above the ice bath for 5 min, then recooled to -78 °C. A solution of **4.22** (0.6235 g, 2.451 mmol) in THF (10 mL) was cannulated into the reaction mixture over a period of 15 min. The reaction mixture was left to stir at -78 °C for

1 h, followed by warming to room temperature over a period of 30 min, and quenching with sat. NH_4Cl (25 mL). The layers were separated and the aqueous layer extracted with EtOAc (2 x 25mL). The organic layers were combined and extracted with sat. NH_4Cl (2 x 25 mL), distilled H_2O (25 mL) and brine (25 mL), then dried (MgSO_4) and concentrated *in vacuo* to give the crude product. Compound **4.23** was isolated via FCC (20% EtOAc in hexanes) as a clear amorphous solid in 69% yield (1.027 g, 1.691 mmol). R_f = 0.70 (10% EtOAc in hexanes); ^1H NMR (300 MHz, CDCl_3) δ 6.16 (1H, d, J = 11.0 Hz), 5.82 (1H, d, J = 11.0 Hz), 4.15 (1H, d, J = 2.0 Hz), 4.13-4.02 (2H, m), 3.45 (3H, s), 3.39 (3H, s), 2.88-2.76 (1H, m), 2.46-2.33 (2H, m), 2.30-2.22 (1H, m), 2.16-1.50 (13H, m), 1.44-1.34 (2H, m), 0.98 (3H, d, J = 6.5 Hz), 0.89 (9H, s), 0.88 (9H, s), 0.56 (3H, s), 0.07 (12H, m); ^{13}C NMR (75 MHz, CDCl_3) δ 140.6, 133.8, 121.8, 116.3, 109.2, 68.3, 68.2, 57.2, 56.0, 55.9, 52.5, 46.2, 46.0, 44.0, 40.7, 40.1, 37.1, 29.0, 27.4, 26.1 (6C), 23.6, 22.6, 18.4 (2C), 12.3, 12.2, -4.3, -4.4, -4.5, -4.6; IR (film) ν 2951, 1739, 1619, 1471, 1361, 1254, 1187, 1089, 1026, 960, 921, 836 cm^{-1} ; LRMS (EI): m/z (rel. intensity) = 608 (10), 607 (20, M⁺), 592 (12), 590 (22), 576

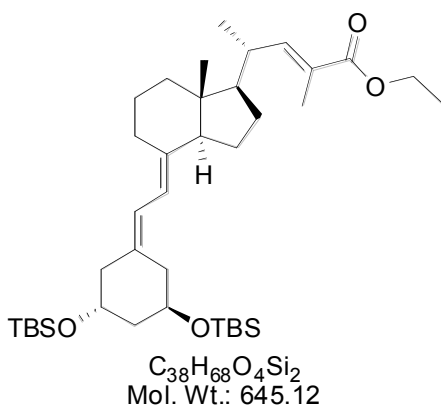
(21), 575 (51), 574 (100), 534 (8), 533 (19), 518 (9), 458 (59), 442 (96), 239 (13), 237 (11); HRMS (EI): m/z calcd. for (M^+) = 606.4499, found = 606.4490.

(2*S*)-2-((1*R*,3*R*,7*E*,17_)-1,3-bis[*tert*-butyl(dimethyl)silyloxy]-9,10-secoestra-5,7-dien-17-yl)propanal 4.24



Trifluoroacetic acid (0.8 mL, 11 mmol, 24 eq.) was added to a vigorously stirred solution of **4.23** (273.0 mg, 0.450 mmol, 1 eq.) in $CHCl_3$ (4.8 mL) and distilled H_2O (2.4 mL) at 0 °C. The mixture rapidly turned purple, then blue-green, then colorless. The reaction was monitored by thin layer chromatography on silica gel plates (eluent: 1:9 ethyl acetate to hexanes). After 25 minutes, the starting material spot completely converted to a new spot. The reaction was quenched with sat. $NaHCO_3$ (15 mL), the layers were separated and the aqueous layer extracted with EtOAc (2 x 15 mL). The organic layers were combined and extracted with sat. $NaHCO_3$ (2 x 15 mL), distilled H_2O (10 mL) and brine (10 mL), then dried ($MgSO_4$), filtered and concentrated in vacuo to give the crude product **4.24** as a clear oil in 89% yield (225.5 mg, 0.402 mmol). This product was carried forward without further purification. R_f = 0.75 (10% EtOAc in hexanes); 1H NMR (300 MHz, $CDCl_3$) δ 9.58 (1H, d, J = 3.0 Hz), 6.16 (1H, d, J = 11.0 Hz), 5.83 (1H, d, J = 11.0 Hz), 4.17-4.02 (2H, m), 2.89-2.80 (1H, m), 2.46-2.22 (4H, m), 2.16-1.92 (4H, m), 1.84-1.54 (8H, m), 1.48-1.35 (2H, m), 1.14 (3H, d, J = 6.5 Hz), 0.89 (9H, s), 0.87 (9H, s), 0.60 (3H, s), 0.06 (12H, m); ^{13}C NMR (75 MHz, $CDCl_3$) δ 204.9, 139.7, 134.3, 121.6, 116.7, 68.3, 68.1, 55.7, 51.6, 50.0, 46.3 (2C), 43.9, 40.5, 37.0, 28.9, 26.8, 26.1 (6C), 23.5, 22.9, 18.4 (2C), 13.9, 12.8, -4.3, -4.4, -4.5, -4.6; IR (film) ν 2953, 2706, 1726, 1619, 1472, 1361, 1255, 1089, 1052, 1026, 1006, 960, 920, 836 cm^{-1} ; LRMS (EI): m/z (rel. intensity) = 560 (15, M^+), 503 (20), 428 (75), 371 (20), 301 (30), 239 (25), 147 (35), 133 (45), 74 (100); HRMS (EI): m/z calcd. for (M^+) = 560.4081, found = 560.4085.

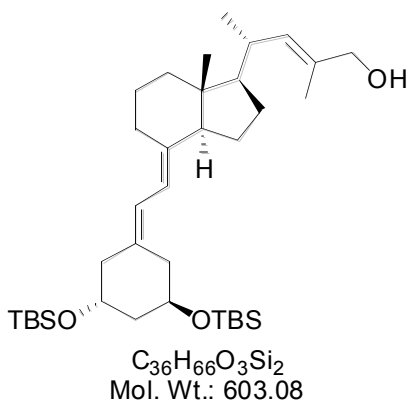
Ethyl (2*E*,4*R*)-4-((1*R*,3*R*,7*E*,17_)-1,3-bis[*tert*-butyl-(dimethyl)silyloxy]-9,10-secoestra-5,7-dien-17-yl)-2-methylpent-2-enoate **4.25**



Ethyl 2-(triphenylphosphoranylidene)propanoate (0.3805 g, 1.050 mmol) was added to a solution of **4.24** (0.5610 g, 1.000 mmol) in toluene (10 mL) in a round bottom flask. The flask was fitted with a reflux condenser and the reaction mixture heated to reflux for 16 h by means of a heating mantle. The reaction mixture was concentrated, and the residue dissolved in

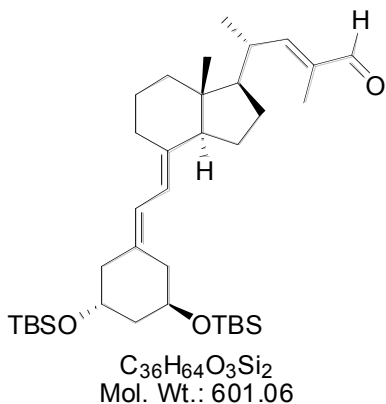
hexanes to precipitate out the triphenylphosphine oxide by-product. The suspension was filtered and the filtrate concentrated and loaded directly onto silica gel. Compound **4.25** was isolated via FCC (10% EtOAc in hexanes) as a clear oil in 98% yield (0.6322 g, 0.98 mmol). $R_f = 0.60$ (5% EtOAc in hexanes); 1H NMR (300 MHz, $CDCl_3$) δ 6.58 (1H, dd, $J = 11.0$ Hz), 6.15 (1H, d, $J = 11.0$ Hz), 5.82 (1H, d, $J = 11.0$ Hz), 4.19 (2H, q, $J = 7.0$ Hz), 4.13-4.05 (2H, m), 2.88-2.79 (1H, m), 2.62-2.49 (1H, m), 2.43-2.30 (3H, m), 2.18-1.97 (3H, m), 1.88 (3H, d, $J = 1.5$ Hz), 1.83-1.63 (6H, m), 1.60-1.50 (4H, m), 1.46-1.36 (1H, m), 1.31 (3H, t, $J = 7.0$ Hz), 1.05 (3H, d, $J = 6.5$ Hz), 0.90 (9H, s), 0.89 (9H, s), 0.62 (3H, s), 0.07 (12H, m); ^{13}C NMR (75 MHz, $CDCl_3$) δ 168.7, 147.7, 140.2, 134.1, 125.0, 121.8, 116.6, 68.4, 68.3, 60.5, 56.6, 56.4, 46.2, 46.0, 44.1, 40.9, 37.3, 36.2, 29.0, 27.3, 26.2 (6C), 23.8, 22.6, 19.6, 18.4 (2C), 14.6, 13.0, 12.8, -4.3, -4.4 (2C), -4.5; IR (film) ν 2953, 2929, 2856, 1711, 1471, 1362, 1255, 1194, 1090, 1051, 1026, 960, 921, 835 cm^{-1} ; LRMS (EI): m/z (rel. intensity) = 644 (20, M^+), 587 (20), 512 (40), 455 (10), 371 (10), 301 (15), 239 (35), 113 (45), 74 (100); HRMS (EI): m/z calcd. for (M^+) = 644.4656, found = 644.4646.

(2*E*,4*R*)-4-((1*R*,3*R*,7*E*,17_)-1,3-bis[*tert*-butyl-(dimethyl)silyloxy]-9,10-secoestra-5,7-dien-17-yl)-2-methylpent-2-en-1-ol 4.26



A 1.0 M solution of DIBAL-H in toluene (1.2 mL, 1.2 mmol, 3.0 eq.) was added to a solution of rigorously dried **4.25** (258.1 mg, 0.400 mmol, 1 eq.) in toluene (6 mL) at 0 °C. The reaction was left to slowly warm to room temperature overnight. The reaction was then cooled to 0 °C and diluted with Et₂O (3.3 mL). To the stirring reaction was sequentially added distilled H₂O (0.040 mL), 1M NaOH (0.040 mL), and more distilled H₂O (0.16 mL). The reaction was warmed to room temperature and stirred for 30 min. MgSO₄ was added to the mixture, and the reaction was stirred for another 30 min. The reaction was filtered to remove the insoluble by-products, and the filtrate concentrated. The crude product was purified by silica gel column chromatography using a gradient starting from 1:9 ethyl acetate to hexanes and ending with 1:4 ethyl acetate to hexanes, providing product **4.26** in 72% yield (172.5 mg, 0.29 mmol). R_f = 0.30 (10% EtOAc in hexanes); ¹H NMR (400 MHz, CDCl₃) δ 6.17 (1H, d, *J* = 11.0 Hz), 5.81 (1H, d, *J* = 11.0 Hz), 5.21 (1H, d, *J* = 10.0 Hz), 4.13-4.04 (2H, m), 3.99 (2H, s), 2.88-2.79 (1H, m), 2.43-2.34 (3H, m), 2.32-2.26 (1H, m), 2.11 (1H, dd, *J* = 13.0, 8.0 Hz), 2.05-1.95 (2H, m), 1.83-1.63 (4H, m), 1.70 (3H, s), 1.59-1.47 (3H, m), 1.42-1.12 (5H, m), 0.99 (3H, d, *J* = 6.5 Hz), 0.89 (9H, s), 0.88 (9H, s), 0.60 (3H, s), 0.07 (12H, m); ¹³C NMR (100 MHz, CDCl₃) δ 140.6, 133.8, 133.3, 131.5, 121.8, 116.3, 69.5, 68.3, 68.1, 57.0, 56.5, 46.2, 45.8, 43.9, 40.8, 37.1, 35.3, 29.0, 27.7, 26.2 (6C), 23.7, 22.5, 20.8, 18.4 (2C), 14.4, 12.7, -4.3, -4.4 (2C), -4.5; IR (film) ν 3348, 2952, 1619, 1471, 1361, 1255, 1090, 1025, 961, 906, 836 cm⁻¹; LRMS (EI): *m/z* (rel. intensity) = 602 (25, M⁺), 470 (25), 371 (10), 301 (25), 237 (30), 143 (30), 74 (100); HRMS (EI): *m/z* calcd. for (M⁺) = 602.4550, found = 602.4542.

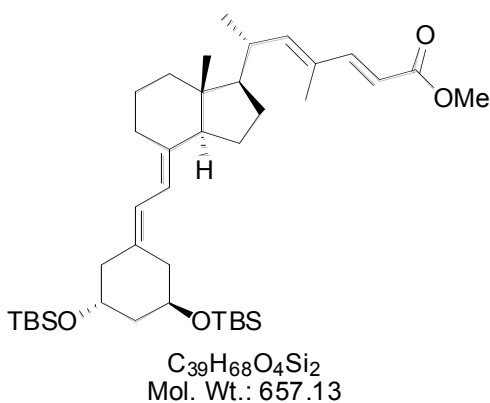
(2E,4R)-4-((1R,3R,7E,17_)-1,3-bis[*tert*-butyl-(dimethyl)silyloxy]-9,10-secoestra-5,7-dien-17-yl)-2-methylpent-2-enal **4.27**



Dess-Martin periodinane (0.4988 g, 1.176 mmol) was added to a stirring solution of **4.26** (0.5674 g, 0.9408 mmol) in CH_2Cl_2 (10 mL). The reaction mixture was stirred for 1 h at room temperature, then diluted with Et_2O (20 mL) and quenched with sat. $NaHCO_3$ (40 mL) and sat. $Na_2S_2O_3$ (10 mL). The reaction mixture was stirred until the milky white organic layer

became clear (approx. 1 h). The layers were separated and the aqueous layer extracted with Et_2O (2 x 25mL). The organic layers were combined and extracted with distilled H_2O (25 mL) and brine (25 mL), then dried ($MgSO_4$), and concentrated *in vacuo* to give the crude product. Compound **4.27** was isolated via FCC (10% $EtOAc$ in hexanes) as a translucent amorphous solid in 86% yield (0.4863 g, 0.8091 mmol). $R_f = 0.70$ (10% $EtOAc$ in hexanes); 1H NMR (400 MHz, $CDCl_3$) δ 9.37 (1H, s), 6.29 (1H, d, $J = 10.5$ Hz), 6.16 (1H, d, $J = 11.0$ Hz), 5.82 (1H, d, $J = 11.0$ Hz), 4.15-4.05 (2H, m), 2.88-2.81 (1H, m), 2.79-2.70 (1H, m), 2.42-2.34 (2H, m), 2.30-2.24 (1H, m), 2.16-1.98 (3H, m), 1.78 (3H, s), 1.76-1.51 (9H, m), 1.46-1.20 (2H, m), 1.10 (3H, d, $J = 6.5$ Hz), 0.89 (9H, s), 0.88 (9H, s), 0.62 (3H, s), 0.06 (12H, m); ^{13}C NMR (75 MHz, $CDCl_3$) δ 195.9, 160.3, 139.9, 136.5, 134.2, 121.7, 116.6, 68.2, 68.1, 56.2, 56.1, 46.2, 46.1, 43.9, 40.7, 37.1, 36.6, 28.9, 27.3, 26.1 (6C), 23.6, 22.5, 19.4, 18.4 (2C), 12.7, 9.9, -4.3, -4.4, -4.5, -4.6; IR (film) ν 2952, 2956, 1690, 1469, 1253, 1086, 1051, 1024, 959, 920, 834 cm^{-1} ; LRMS (EI): m/z (rel. intensity) = 600 (5, M^+), 468 (20), 301 (5), 277 (100), 201 (20), 199 (20), 183 (20), 149 (20), 77 (45); HRMS (EI): m/z calcd. for (M^+) = 600.4394, found = 600.4387.

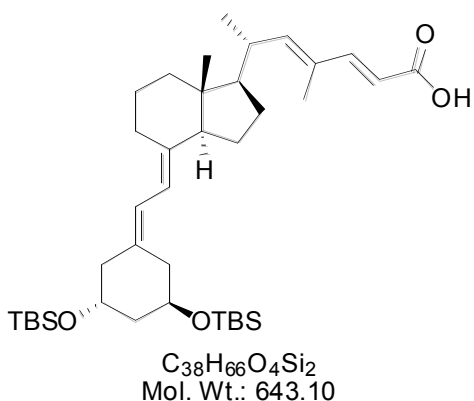
Methyl-(2*E*,4*E*,6*R*)-6-((1*R*,3*R*,7*E*,17_)-1,3-bis-[*tert*-butyl(dimethyl)silyloxy]-9,10-secoestra-5,7-dien-17-yl)-4-methylhepta-2,4-dienoate **4.28**



Methyl (triphenylphosphoranylidene)acetate (0.2840 g, 0.8496 mmol) was added to a solution of **4.27** (0.4863 g, 0.8091 mmol) in toluene (8 mL) in a round bottom flask. The flask was fitted with a reflux condenser, and the reaction mixture heated to reflux for

16 h by means of a heating mantle. The reaction mixture was concentrated, and the residue dissolved in hexanes to precipitate out the triphenylphosphine oxide by-product. The suspension was then filtered, and the filtrate concentrated and loaded directly onto silica gel. Compound **4.28** was isolated via FCC (10% EtOAc in hexanes) as a clear oil in 95% yield (0.5051 g, 0.7686 mmol). $R_f = 0.70$ (10% EtOAc in hexanes); 1H NMR (400 MHz, $CDCl_3$) δ 7.30 (1H, d, $J = 16.0$ Hz), 6.16 (1H, d, $J = 11.0$ Hz), 5.80 (1H, d, $J = 11.0$ Hz), 5.78 (1H, d, $J = 16.0$ Hz), 5.71 (1H, d, $J = 10.0$ Hz), 4.12-4.03 (2H, m), 3.75 (3H, s), 2.86-2.78 (1H, m), 2.62-2.52 (1H, m), 2.40-2.33 (2H, m), 2.30-2.24 (1H, m), 2.11 (1H, dd, $J = 13.0, 8.0$ Hz), 2.06-1.96 (2H, m), 1.80 (3H, s), 1.75-1.62 (5H, m), 1.58-1.30 (5H, m), 1.20-1.10 (1H, m), 1.02 (3H, d, $J = 6.5$ Hz), 0.88 (9H, s), 0.87 (9H, s), 0.59 (3H, s), 0.06 (12H, m); ^{13}C NMR (100 MHz, $CDCl_3$) δ 168.0, 150.5, 148.7, 140.3, 133.9, 129.8, 121.7, 116.4, 115.1, 68.3, 68.1, 56.6, 56.3, 51.7, 46.2, 45.9, 43.9, 40.7, 37.1, 36.3, 28.9, 27.5, 26.1 (6C), 23.6, 22.5, 20.1, 18.4 (2C), 12.9, 12.7, -4.3, -4.4 (2C), -4.5; IR (film) ν 2952, 2856, 1721, 1622, 1435, 1361, 1312, 1254, 1169, 1088, 1024, 960, 919, 835 cm^{-1} ; LRMS (EI): m/z (rel. intensity) = 656 (10, M^+), 599 (15), 524 (25), 301 (20), 237 (25), 125 (30), 93 (85), 74 (100); HRMS (EI): m/z calcd. for (M^+) = 656.4656, found = 656.4645.

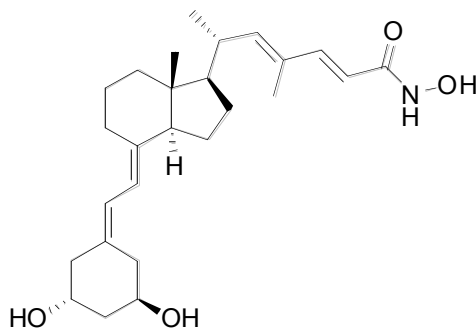
(2E,4E,6R)-6-((1R,3R,7E,17_)-1,3-bis[*tert*-butyl-(dimethyl)silyloxy]-9,10-secoestra-5,7-dien-17-yl)-4-methylhepta-2,4dienoic acid



LiOH·H₂O (11.8 mg, 0.281 mmol, 7.47 eq.) was added to a stirring solution of **4.28** (24.7 mg, 0.0376 mmol, 1 eq.) in THF (1 mL), MeOH (0.4 mL) and H₂O (0.4 mL). The reaction vessel was fitted with a reflux condenser, and the reaction brought to reflux for 2.5 h. The reaction was cooled to room temperature and diluted with EtOAc (10 mL), then

quenched with a pH 1 solution of KHSO₄ (10 mL). The layers were separated and the aqueous layer further extracted with EtOAc (5 mL). The organic layers were combined and extracted with brine (5 mL), then dried (MgSO₄), and concentrated *in vacuo* to give the crude product. This product was carried forward without further purification. If desired, this carboxylic acid product **4.29** can be purified by FCC (1:1 ethyl acetate to hexanes). $R_f = 0.30$ (20% EtOAc in hexanes); ¹H NMR (300 MHz, CDCl₃) δ 10.00-9.30 (1H, br s), 7.39 (1H, d, $J = 15.5$ Hz), 6.16 (1H, d, $J = 11.0$ Hz), 5.82 (2H, m), 5.78 (1H, d, $J = 15.5$ Hz), 4.15-4.00 (2H, m), 2.87-2.78 (1H, m), 2.63-2.53 (1H, m), 2.44-2.24 (3H, m), 2.16-1.96 (3H, m), 1.83 (3H, s), 1.82-1.36 (11H, m), 1.04 (3H, d, $J = 6.5$ Hz), 0.89 (9H, s), 0.88 (9H, s), 0.60 (3H, s), 0.06 (12H, m); ¹³C NMR (75 MHz, CDCl₃) δ 173.1, 152.7, 149.8, 140.3, 134.0, 129.9, 121.7, 116.5, 114.8, 68.3, 68.1, 56.6, 56.3, 46.2, 46.0, 43.9, 40.7, 37.1, 36.4, 28.9, 27.5, 26.1 (6C), 23.6, 22.5, 20.1, 18.4 (2C), 12.9, 12.7, -4.3, -4.4, -4.5, -4.6; IR (film) ν 3000 (br), 2956, 1686, 1618, 1417, 1254, 1207, 1088, 1026, 908, 834, 801 cm⁻¹; LRMS (ESI): m/z (rel. intensity) = 681 [6, (M + K)⁺], 665 [79, (M + Na)⁺], 643 (11, M⁺), 641 (20), 519 (18), 512 (27), 511 (100), 510 (11), 509 (39), 497 (11), 397 (41), 381 (13), 380 (16), 379 (64); HRMS (ESI): m/z calcd. for [(M + H)⁺] = 643.4572, found = 643.4572.

(2E,4E,6R)-6-[(1R,3R,7E,17_)-1,3-dihydroxy-9,10secoestra-5,7-dien-17-yl]-N-hydroxy-4-methylhepta-2,4-dienamide 4.8 (tricerol)



C₂₆H₃₉NO₄
Mol. Wt.: 429.59

Oxalyl chloride (5.0 μ l, 0.059mmol, 1.57 eq.) was added to a solution of the rigorously dried crude product **4.29** (approximately 0.0376 mmol, 1 eq.) and N,N-dimethylformamide (0.6 μ l, 7.7 micromole, 0.2 eq.) in dry dichloromethane (1 mL) at 0 °C. The reaction mixture rapidly turned yellow and was left stirring at 0 °C for 90 minutes, at which time N,N-diisopropylethylamine (21 μ l, 0.12 mmol, 3.2 eq.) was added followed by a solution of O-(*tert*-butyldimethylsilyl)hydroxylamine (11.9 mg, 0.081 mmol, 2.15 eq.) in dry dichloromethane (0.235 mL). The reaction was left to stir at 0 °C for 2 hours and then at room temperature for an additional 2 hours. The reaction was quenched by diluting with ethyl acetate (10 mL) and a 1M citric acid aqueous solution (10 mL). The layers were separated and the aqueous layer further extracted with ethyl acetate (5 mL). The combined organic layers were extracted with distilled water (5 mL) and brine (5 mL, then dried (MgSO₄), filtered and concentrated *in vacuo*. This crude product was dissolved in CDCl₃ (0.5 mL) and CD₃CN (0.5 mL) and then placed in a plastic vial. To this solution was added a 48 wt. % HF aqueous solution (50 μ l) followed by an additional 50 μ l after 2.5 hours (total 2.8 mmol, 73 eq.). The reaction was monitored by ¹H NMR and TLC and was complete after 4 hours. The reaction was quenched by diluting with ethyl acetate (10 mL) and a 1M citric acid aqueous solution (10 mL). The layers were separated and the aqueous layer was further extrated with ethyl acetate (5 mL). The combined organic layers were washed with distilled water (5 mL) and brine (5 mL), then dried with MgSO₄, filtered and evaporated *in vacuo*. The crude product was

purified by means of octadecyl-functionalized reverse phase silica gel column chromatography using a solvent gradient starting from distilled water with 0.05 % trifluoroacetic acid and ending with pure methanol. The product **4.8** was isolated as a white amorphous solid in 41% yield (6.6 mg, 0.015 mg) from the methyl ester 24. $R_f = 0.30$ [(88: 10:2) CH_2Cl_2 :MeOH: CH_3COOH]; ^1H NMR (300 MHz, CD_3OD) δ 7.17 (1H, d, $J = 13.0$ Hz), 6.20 (1H, d, $J = 10.5$ Hz), 5.93-5.66 (3H, m), 4.08-3.94 (2H, m), 2.88-2.80 (1H, m), 2.64-2.55 (2H, m), 2.44-2.36 (1H, m), 2.24-2.11 (2H, m), 2.08-1.95 (2H, m), 1.99 (3H, s), 1.79 (3H, s), 1.70-1.35 (8H, m), (3H, d, $J = 6.0$ Hz), 0.63 (3H, s), 4 exchangeable protons unobserved; ^{13}C NMR (75 MHz, CD_3OD) δ 166.8, 147.9, 146.9, 141.6, 133.9, 130.9, 123.2, 117.1, 115.5, 67.9, 67.6, 57.9, 57.3, 46.9, 45.4, 42.7, 41.7, 37.6, 37.1, 29.8, 28.2, 24.5, 23.3, 20.5, 13.2, 12.9; IR (film) ν 3221 (br), 2929, 2869, 1645, 1611, 1446, 1377, 1043, 976 cm^{-1} ; LRMS (ESI): m/z (rel. intensity) = 859 [9, $(2\text{M} + \text{H})^+$], 452 [17, $(\text{M} + \text{Na})^+$], 430 [100, $(\text{M} + \text{H})^+$], 412 (8), 397 (10), 390 (8); HRMS (ESI): m/z calcd. for $[(\text{M} + \text{H})^+] = 430.2952$, found = 430.2952.

6.1 References

-
- ⁸⁹ Still, W.C.; Kahn, M.; Mitra, A. *The Journal of Organic Chemistry* **1978**, *43*, 2923
- ⁹⁰ Adam, W.; Bialas, J.; Hadjarapoglou, L. *Chemische Berichte* **1991**, *124*, 2377
- ⁹¹ Gaussian 03, Revision C.02, Frisch, M. J.; Trucks, G. W.; Schlegel, H. B.; Scuseria, G. E.; Robb, M. A.; Cheeseman, J. R.; Montgomery, Jr., J. A.; Vreven, T.; Kudin, K. N.; Burant, J. C.; Millam, J. M.; Iyengar, S. S.; Tomasi, J.; Barone, V.; Mennucci, B.; Cossi, M.; Scalmani, G.; Rega, N.; Petersson, G. A.; Nakatsuji, H.; Hada, M.; Ehara, M.; Toyota, K.; Fukuda, R.; Hasegawa, J.; Ishida, M.; Nakajima, T.; Honda, Y.; Kitao, O.; Nakai, H.; Klene, M.; Li, X.; Knox, J. E.; Hratchian, H. P.; Cross, J. B.; Bakken, V.; Adamo, C.; Jaramillo, J.; Gomperts, R.; Stratmann, R. E.; Yazyev, O.; Austin, A. J.; Cammi, R.; Pomelli, C.; Ochterski, J. W.; Ayala, P. Y.; Morokuma, K.; Voth, G. A.; Salvador, P.; Dannenberg, J. J.; Zakrzewski, V. G.; Dapprich, S.; Daniels, A. D.; Strain, M. C.;

Farkas, O.; Malick, D. K.; Rabuck, A. D.; Raghavachari, K.; Foresman, J. B.; Ortiz, J. V.; Cui, Q.; Baboul, A. G.; Clifford, S.; Cioslowski, J.; Stefanov, B. B.; Liu, G.; Liashenko, A.; Piskorz, P.; Komaromi, I.; Martin, R. L.; Fox, D. J.; Keith, T.; Al-Laham, M. A.; Peng, C. Y.; Nanayakkara, A.; Challacombe, M.; Gill, P. M. W.; Johnson, B.; Chen, W.; Wong, M. W.; Gonzalez, C.; and Pople, J. A.; Gaussian, Inc., Wallingford CT, 2004.

⁹² Saville-Stones, E. A.; Turner, R. M.; Lindell, S. D.; Jennings, N. S.; Head, J. C.; Carver, D. S. *Tetrahedron*, **1994**, *50*, 6695.

⁹³ Bobbitt, J. M. *The Journal of Organic Chemistry*. **1998**, *63*, 9367.

⁹⁴ Clerici, F.; Gelmi, M. L.; Gambini, A. *The Journal of Organic Chemistry* **1999**, *64*, 5764

7 Appendix 2 Publications

The following article is a reprint of the article:

Tavera-Mendoza, L. E.; Quach, T. D.; Dabbas, B.; Hudon, J.; Liao, X.; Palijan, A.; Gleason, J. L.; White, J. H., Incorporation of histone deacetylase inhibition into the structure of a nuclear receptor agonist. *Proceedings of the National Academy of Sciences* **2008**, *105* (24), 8250-8255.

© Copyright 2008 National Academy of Sciences, U.S.A.

Incorporation of histone deacetylase inhibition into the structure of a nuclear receptor agonist

Luz E. Tavera-Mendoza*, Tan D. Quach[†], Basel Dabbas[‡], Jonathan Hudon[‡], Xiaohong Liao[†], Ana Palijan[‡], James L. Gleason^{†§}, and John H. White*^{‡§}

Departments of *Medicine and [†]Physiology, McIntyre Building, McGill University, 3655 Drummond Street, Montreal, QC, Canada H3G 1Y6; and [‡]Department of Chemistry, Otto Maass Building, McGill University, 801 Sherbrooke Street West, Montreal, QC, Canada H3A 2K6

Edited by Pierre Chambon, Institut de Génétique et de Biologie Moléculaire et Cellulaire, Strasbourg, France, and approved April 1, 2008 (received for review September 29, 2007)

1,25-dihydroxyvitamin D₃ (1,25D) regulates gene expression by signaling through the nuclear vitamin D receptor (VDR) transcription factor and exhibits calcium homeostatic, anticancer, and immunomodulatory properties. Histone deacetylase inhibitors (HDACis) alter nuclear and cytoplasmic protein acetylation, modify gene expression, and have potential for treatment of cancer and other indications. The function of nuclear receptor ligands, including 1,25D, can be enhanced in combination with HDACi. We designed triciferol, a hybrid molecule in which the 1,25D side chain was replaced with the dienyl hydroxamic acid of HDACi trichostatin A. Triciferol binds directly to the VDR, and functions as an agonist with 1,25D-like potency on several 1,25D target genes. Moreover, unlike 1,25D, triciferol induces marked tubulin hyperacetylation, and augments histone acetylation at concentrations that largely overlap those where VDR agonism is observed. Triciferol also exhibits more efficacious antiproliferative and cytotoxic activities than 1,25D in four cancer cell models *in vitro*. The bifunctionality of triciferol is notable because (i) the HDACi activity is generated by modifying the 1,25D side chain without resorting to linker technology and (ii) 1,25D and HDACi have sympathetic, but very distinct biochemical targets; the hydrophobic VDR ligand binding domain and the active sites of HDACs, which are zinc metalloenzymes. These studies demonstrate the feasibility of combining HDAC inhibition with nuclear receptor agonism to enhance their therapeutic potential.

HDAC inhibitors | multiple ligands | vitamin D

The biologically active metabolite of vitamin D₃, 1,25-dihydroxyvitamin D₃ (1,25D, **1**) (Fig. 1), is best known as a primary regulator of calcium homeostasis (1, 2). However, 1,25D also controls cell differentiation and proliferation through binding to the nuclear vitamin D receptor (VDR) (NR1H1), which regulates histone acetylation, chromatin remodeling and recruitment of RNA polymerase II and ancillary factors required for target gene transcription (2). In addition to their calcium homeostatic properties, 1,25D analogs have therapeutic potential in treatment of hyperproliferative disorders, such as cancer and psoriasis (2, 3). 1,25D analogs may also be effective in treatment of a range of disorders with autoimmune components such as multiple sclerosis, type 1 diabetes and Crohn's disease, an inflammatory bowel disorder (2, 4). Moreover, 1,25D is also a direct inducer of antimicrobial innate immunity (5–7), a finding that has provided a molecular genetic basis for its activity against *Mycobacterium tuberculosis* infections (8).

Recent studies demonstrated combinatorial effects of trichostatin A (TSA, **2**; Fig. 1), a histone deacetylase inhibitor (HDACi), and 1,25D on the proliferation of 1,25D-resistant cancer cells (ref. 9 and L.E.T.-M., B.D., and J.H.W. unpublished results). HDACis, including TSA and suberoylanilide hydroxamic acid (SAHA, **5**) (Fig. 1), regulate the acetylation state of histones and other nuclear and nonnuclear proteins. Like VDR agonists, HDACis modulate gene expression and induce cell cycle arrest, cellular differentiation, and/or apoptosis (10–12),

and so they have been investigated as treatments for cancer. The potential of HDACis as therapeutics is underscored by the recent approval of SAHA, under the trade name Zolinza, for treatment of cutaneous T cell lymphoma (13).

In developing therapies against human disease, it is often advantageous to target two or more sympathetic biological targets. The potential advantages of this approach include targeting sympathetic biochemical pathways involved in a disease, limiting the development of resistance and reducing dosages of more toxic drugs. Classical examples include combining reverse transcriptase inhibitors with protease inhibitors in the treatment of AIDS (14) or coadministration of niacin with a statin in the treatment of hypercholesterolemia (15). Although many examples exist where combination therapy involves administration of multiple drugs, there is growing interest in developing “multiple ligands,” single chemical entities that interact with multiple biological targets (16). Although achieving appropriate dosing against individual targets is more readily achieved with separate chemical agents, a multiple ligand may have significant advantages. Development of a multiple ligand simplifies analysis of dose/toxicity relationships and pharmacokinetic profiles, holds the potential to localize activity against one target based on affinity for a second target (17), and can improve adherence to a treatment regimen.

Based on the observed synergy between 1,25D and TSA, we sought to combine VDR agonist activity and HDAC inhibition within a single molecule. This presented a significant design challenge. Although many multiple ligands have been designed to interact with two related biological targets [e.g., vasopeptidase inhibitors, which are dual inhibitors of zinc metalloproteases neprilysin and angiotensin converting enzyme (18)], few have been rationally designed to interact with two markedly different biological targets. In the case of targeting of both the VDR and HDACs, metalloenzyme inhibition would need to be incorporated into the structure of a lipophilic nuclear receptor agonist (19). Further increasing the challenge, 1,25D is fully enclosed within the VDR binding pocket and thus a fully merged structure with overlapping pharmacophores would be necessary. In this article, we describe the design, synthesis, and biochemical characterization of triciferol, a multiple ligand agent that combines VDR agonism and HDAC inhibition to enhance the cytostatic and cytotoxic activities of 1,25D.

Author contributions: L.E.T.-M., T.D.Q., B.D., J.H., X.L., and A.P. performed research; J.L.G. and J.H.W. designed research; J.L.G. and J.H.W. analyzed data; and J.L.G. and J.H.W. wrote the paper.

The authors declare no conflict of interest.

This article is a PNAS Direct Submission.

Freely available online through the PNAS open access option.

§To whom correspondence may be addressed. E-mail: jim.gleason@mcgill.ca or john.white@mcgill.ca.

This article contains supporting information online at www.pnas.org/cgi/content/full/0709279105/DCSupplemental.

© 2008 by The National Academy of Sciences of the USA

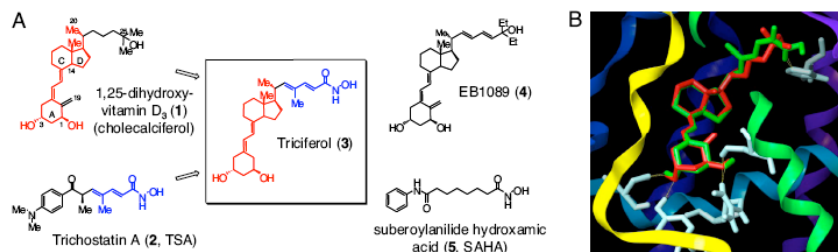


Fig. 1. Design of triciferol. (A) Structures of 1,25D (1) and TSA (2), which are merged into triciferol (3). 1,25D analog EB1089 (4), HDAC SAHA (5) are also shown. (B) Triciferol is fully enclosed within the VDR ligand binding domain pocket. Ribbon diagram of the VDR backbone with overlays of docking of 1,25D (red) and triciferol (green). Note that a portion of helix 3 (in green) has been removed for clarity. Key hydrogen bonding amino acids are shown in white. Hydrogen bonds are indicated by fine lines.

Results

Design of Triciferol. Triciferol (3) (Fig. 1) was designed with the aid of structure/activity data for both 1,25D and its analogs, and HDACis TSA and SAHA. Numerous 1,25D analogs, including seocalcitol (EB1089, 4) (Fig. 1), have revealed that the VDR can accommodate structures with alterations in side chain substitution and length (19–21), as long as critical hydrogen bonds are maintained at all three hydroxyl groups. HDACis, such as TSA and SAHA, are composed of highly variable “cap” structures that bind at the surfaces of HDACs, coupled via a linking chain to hydroxamic acids (22, 23) or other groups (24) that chelate active site zinc ions. Triciferol combines the secosteroidal backbone of 1,25D with the dienyl hydroxamic acid of TSA. It was expected that the hydroxamic acid would act as a surrogate for the 25OH group and establish hydrogen bonds to His-305 and/or His-397 in the VDR ligand binding pocket, an essential element of 1,25D binding to the receptor (19). Indeed, optimal docking solutions (AutoDock 3.0, FITTED 2.0) indicated that triciferol should bind to the VDR in an orientation roughly similar to 1,25D (25, 26), with the side chain hydroxamic acid rotated

relative to the 25-hydroxyl of 1,25D, but still forming a strong hydrogen bond between the hydroxamate OH and His-397 (Fig. 1B). The secosteroidal core overlays almost exactly that of VDR-bound 1,25D, maintaining hydrogen bonds to the 1- and 3-OH groups (27). The computational models predicted that the affinity of triciferol for VDR should be similar to that of 1,25D and EB1089. No preliminary modeling was conducted on the HDAC binding site because of poor handling of zinc-hydroxamic acid interactions in all modeling methods. However, given the breadth of HDACi cap group structures reported (22–24), it was reasonable to expect that the secosteroidal core of triciferol could serve effectively in this capacity when combined with the known affinity of the dienyl hydroxamic acid for HDACs.

Synthesis and Bifunctional Activity of Triciferol. Triciferol was synthesized in 10 steps (Fig. 2) from vitamin D₂ (6) and A-ring phosphine oxide 8 (28), after a general sequence of ozonolytic degradation of vitamin D₂, installation of the A-ring via Horner coupling, extension of the side chain by sequential Wittig olefination and hydroxamic acid formation via the acid chloride

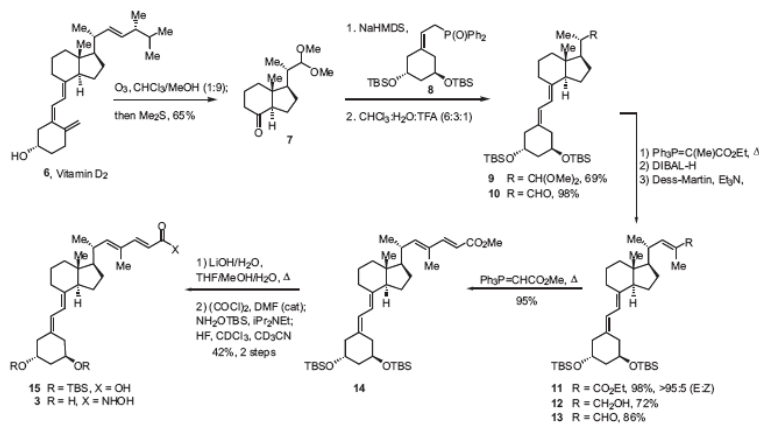


Fig. 2. Schematic representation of key elements of the synthesis of triciferol (see *SI Materials and Methods* and *Scheme S1* for details of synthesis).

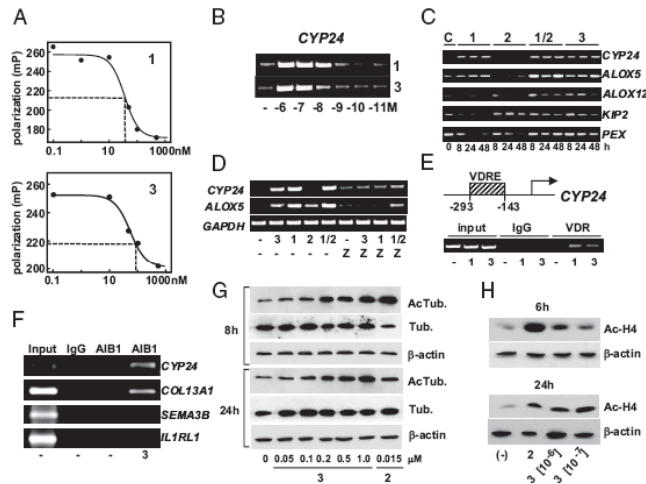


Fig. 3. VDR agonist and HDACi activities of triciferol. (A) Triciferol binds directly to the VDR ligand binding domain. Fluorescence polarization competition assays comparing displacement of a fluorescent tracer from the VDR ligand binding domain are shown. (mP, milli-polarization units; see *SI Materials and Methods* for assay details). Estimated IC₅₀s for 1,25D and triciferol in the assay were 32 and 87 nM, respectively. (B) Dose-response analysis of induction of *cyp24* expression by 1,25D (1) and triciferol (3). (C) Comparison of the regulation of 1,25D target genes by 100 nM 1,25D (1), 15 nM TSA (2), 1,25D and TSA together (1+2), and 100 nM triciferol (3). (D) VDR antagonist ZK159222 blocks triciferol-induced expression of 1,25D target genes *cyp24* and *alox5*. Cells were treated with vehicle (-), 1,25D (1), TSA (2), triciferol (3), and/or ZK159222 (Z), as indicated. (E) (Upper) Schematic representation of the proximal human *cyp24* promoter. (Lower) Analysis of induction by 100 nM 1,25D (1) or triciferol (3) of VDR binding to the 1,25D-responsive region of the human *cyp24* promoter by ChIP assay. (F) Re-ChIP analysis of recruitment induced by triciferol of the coactivator AIB1 to 1,25D target genes in MCF-7 cells, which overexpress AIB1 (36). The VDR was immunoprecipitated from extracts prepared for ChIP assays and reimmunoprecipitated with an antibody directed against AIB1. (G) Western blot analysis of dose-dependent induction of tubulin acetylation in SCC4 cells by triciferol (3) in SCC4 cells. Blots were probed for both total tubulin and actin as controls. (H) Western analysis of induction of histone H4 acetylation after 8 or 24 h of treatment with TSA (2) or triciferol (3), as indicated. See *SI Materials and Methods* for details.

[Fig. 2; see [supporting information \(SI\) Materials and Methods](#) for complete details]. Direct binding of triciferol to the VDR was assessed by using a fluorescence polarization competition (FPC) assay, which revealed that triciferol competed for tracer binding with an apparent IC₅₀ of 87 nM or ≈ 3 -fold higher than that of 1,25D (32 nM) (Fig. 3A). VDR agonism of triciferol was tested initially by using a 1,25D-sensitive reporter gene assay, which revealed agonist activity comparable to that of 1,25D at 100 nM (Fig. S1). VDR agonism was also assessed in human squamous carcinoma SCC4 cells (29, 30) by analyzing induction of the gene encoding CYP24 (Fig. 3B), the enzyme that initiates 1,25D catabolism (1, 2). Triciferol induced strong *cyp24* expression and was within a factor of ≈ 10 as potent as 1,25D, in good agreement with the results of the FPC assay.

We compared further the capacity of triciferol and a combination of 1,25D and TSA to regulate the expression of a series of 1,25D₃ target genes (31, 32) in SCC4 cells over 48 h. This revealed profiles of gene regulation by triciferol that are more similar to those of 1,25D and TSA in combination than 1,25D alone (Fig. 3C). *Cyp24* was completely unresponsive to TSA, and its induction by 1,25D, 1,25D and TSA or triciferol did not differ substantially. However, in many cases, the magnitude of gene expression observed in the presence of triciferol differed markedly from that of 1,25D under conditions where TSA was active on its own or where it substantially enhanced 1,25D₃-dependent gene regulation (*cdkn1c/kip2*, *alox12*, and *pex*). Notably, unlike 1,25D, triciferol induced a marked up-regulation of the gene

encoding cyclin-dependent kinase inhibitor p57^{KIP2} (*cdkn1c/kip2*), whose expression is lost during oral SCC progression (33). Induction of *cyp24* and *alox5* by triciferol was markedly inhibited by the VDR antagonist ZK159222 (Fig. 3D), consistent with a VDR-driven mechanism of gene regulation. Furthermore, treatment with either 1,25D or triciferol markedly enhanced VDR binding to the promoter-proximal VDRE region (34) of the *cyp24* promoter, as assessed by chromatin immunoprecipitation (ChIP) assay (Fig. 3E), consistent with their similar effects on *cyp24* induction. In other ChIP assays, triciferol also induced VDR binding to the VDRE (32) in the *col13a1* gene (data not shown). Moreover, re-ChIP experiments revealed that triciferol induced recruitment of the p160 coactivator AIB1 (35) to VDR-bound target genes (Fig. 3F). Taken together, the results above show that triciferol is a VDR agonist with a gene regulatory profile that is distinct from that of 1,25D.

In preliminary assays with an acetylated colorimetric substrate (36), triciferol showed clear inhibitory activity (Fig. S2). In control experiments in SCC4 squamous carcinoma cells, 1,25D alone at concentrations as high as 1 μ M did not alter tubulin or histone acetylation and had no substantial effect on hyperacetylation induced by TSA (Fig. S3). In contrast, treatment of SCC4 cells with triciferol induced a marked dose-dependent increase in levels of acetylated α -tubulin (Fig. 3G) and enhanced acetylation of histone H4 (Fig. 3H). Tubulin hyperacetylation (Fig. 3G) was visible after 8 h of incubation with triciferol concentrations as low as 50 nM, and plateaued at a concentration of

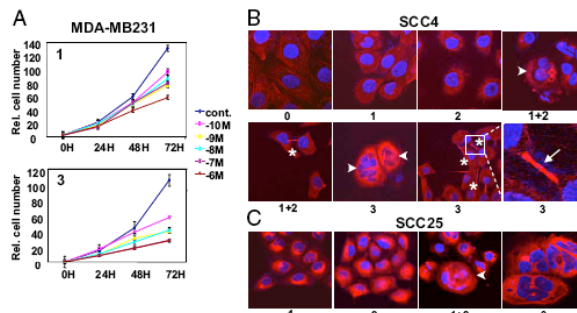


Fig. 4. Analysis of the antiproliferative and cytotoxic activities of triciferol. (A) Comparison of the dose-dependent effects of 1,25D (1) and triciferol (3) on proliferation of human MDA-MB231 breast cancer cells. Growth inhibition by triciferol was statistically significantly different from that of 1,25D at concentrations of 1 nM or above. (B) 1,25D (1) and TSA (2) in combination or triciferol (3) alone induces morphological changes in human SCC4 cells associated with mitotic catastrophe. Multinucleated cells are indicated by arrowheads. Cells joined by tubulin “bridges” are indicated by asterisks. (Lower Right) Higher magnification image of the adjacent panel of a tubulin bridge (arrow) joining two cells. (C) Experiments similar to those in B showing multinucleation (arrowheads) in human SCC25 cells treated with 1,25D (1) and TSA (2) in combination or triciferol (3). Immunocytochemistry on SCC4 and SCC25 cells was performed by using rabbit anti-human α/β tubulin. All samples were counterstained with Hoechst dye. See *SI Materials and Methods* for details.

≈ 200 nM, concentrations that largely overlap those where VDR agonism is observed (Fig. 3B).

Triciferol Exhibits Enhanced Cytostatic and Cytotoxic Activities. We compared further the capacity of triciferol and 1,25D to control proliferation and viability of cancer cell lines. Triciferol was significantly more efficacious in suppressing the proliferation of estrogen receptor-negative human MDA-MB231 breast cancer cells (Fig. 4A). Similar results were obtained in human SCC4 cells (data not shown). 1,25D treatment decreased the numbers of SCC4 cells in S phase of the cell cycle, and induced a partial accumulation in G_0/G_1 . In contrast, triciferol reduced the number of cells in S, but induced an accumulation in G_2/M , effects that were similar to those induced by 1,25D and TSA together (Fig. S4).

Given the marked effect of triciferol on tubulin acetylation and the association of tubulin acetylation with microtubule stabilization, we analyzed the effects of various treatments on tubulin morphology in SCC4 cells to determine whether treatment with triciferol disrupted microtubule dynamics. Treatment with 1,25D or TSA alone did not induce distinct morphological changes (Fig. 4B), whereas treatment with 1,25D and TSA together produced a range of effects, including large variations in cell size and shape, asymmetric cell divisions and occasional multinucleated cells (Fig. 4B, arrowheads, and data not shown). Unlike 1,25D, triciferol also induced the formation of multinucleated cells (Fig. 4B, arrowheads). Moreover, 1,25D and TSA in combination or triciferol alone induced formation of numerous intercellular tubulin “bridges” (Fig. 4B, asterisks), reminiscent of collapsed telophase mitotic spindles (Fig. 4B, arrow). In contrast, although triciferol or 1,25D and TSA in combination induced frequent multinucleation in well differentiated SCC25 head and neck squamous carcinoma cells (Fig. 4C), we found no evidence for formation of intercellular tubulin bridges. The observations of partial G_2/M arrest, formation of multinucleated cells, and collapsed mitotic spindles in the presence of triciferol are consistent with death by mitotic failure in SCC4 cells. Note that none of the treatments markedly induced the expression of markers of apoptosis, such as annexin V, although triciferol markedly enhanced the capacity of UV light, which induces apoptosis in SCC4 cells, to induce annexin V expression (Fig. S5).

Tavera-Mendoza et al.

The cytotoxic properties of triciferol were further analyzed in the human MCF-7 breast cancer cell model. MCF-7 cells are estrogen receptor α -positive and are sensitive to autophagic cell death induced by a number of agents including antiestrogens and EB1089 (37, 38). Treatment of MCF-7 cells with triciferol induced ≈ 2.5 -fold higher rates of cell death than equimolar amounts of 1,25D (Fig. S4). Staining for annexin V indicated that the elevated cell death was not due to apoptosis (Fig. S6). Rather, 1,25D and TSA combined, or triciferol induced markedly enhanced formation of autophagosomes in MCF-7 cells, as judged by lysotracker red staining (Fig. 5B), consistent with autophagy.

Discussion

Nuclear receptor ligands, such as 1,25D, have attracted intensive interest in the pharmaceutical industry because of their diverse physiological functions, clinical relevance, and synthetic accessibility. HDACs have therapeutic potential on their own and enhance the function of other therapeutics, including nuclear receptor ligands, in both experimental cancer models and in the clinic (39, 40). For example, HDACs augment the therapeutic effects of retinoids in retinoid-resistant promyelocytic leukemia (39) and have been shown to enhance the sensitivity of breast cancers cells to antiestrogens (41, 42). Our results demonstrate that triciferol functions as a multiple ligand with combined VDR agonist and HDAC antagonist activities. As a VDR agonist, it acts on several target genes with a potency within an order of magnitude of that of 1,25D, but with a gene regulatory profile closer to that of 1,25D and TSA in combination than to 1,25D alone. These studies also underline the flexibility in design of potential HDACi, because the secosteroidal backbone of triciferol is capable of playing the role of the HDACi “cap” structure. Intriguingly, fusion of the dienyl hydroxamic acid of TSA to the secosteroidal backbone of vitamin D alters HDACi specificity as triciferol appears to be more selective for inducing tubulin hyperacetylation than TSA, and future experiments will be needed to establish activity of triciferol against specific HDAC isozymes.

A significant concern when designing multiple ligands is the difficulty in matching potency for individual targets. Importantly, we found that triciferol induces protein hyperacetylation

PNAS | June 17, 2008 | vol. 105 | no. 24 | 8253

CHEMISTRY

BIOCHEMISTRY

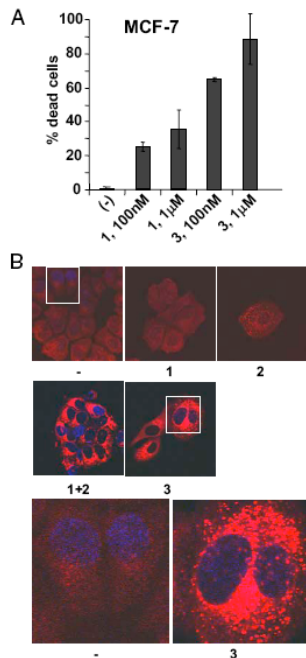


Fig. 5. Comparison of autophagic cell death induced by 1,25D and triciferol in human MCF-7 breast cancer cells. (A) MCF-7 cell death induced by 1,25D (1) or triciferol (3) as measured by trypan blue exclusion assay. (B) Analysis of formation of autophagosomes in MCF-7 cells treated with vehicle (-), 1,25D (1), TSA (2), 1,25D and TSA together (1+2), or triciferol (3). (Lower) Magnifications of the boxed regions of control or triciferol-treated cells. See *SI Materials and Methods* for details.

in a concentration range largely overlapping that where VDR agonism is observed, and that this hyperacetylation is sustained over at least 24 h. Thus, it might be expected that it would function as an effective multiple ligand *in vivo*. Indeed, triciferol exhibited enhanced cytostatic properties relative to 1,25D in

poorly differentiated breast and squamous carcinoma lines and displayed enhanced cytotoxic properties in the MCF-7 breast cancer line. Moreover, although treatment with 1,25D or TSA alone did not have marked effects on SCC4 cell morphology, triciferol induced morphological changes that were very similar to those seen with combined treatment with 1,25D and TSA. Taken together, these data show that triciferol acts as a multiple ligand with significantly enhanced properties relative to either 1,25D or TSA alone in the models tested. The data also suggest that triciferol may exhibit enhanced therapeutic potential relative to 1,25D or other analogues.

Although we have focused here on cancer models, compounds like triciferol may have enhanced activities against other indications targeted by 1,25D or its analogs, such as psoriasis (2), microbial infections (5–8), or autoimmune conditions, such as inflammatory bowel diseases (4). An important next step is to compare the therapeutic index of triciferol with that of 1,25D in animal models of disease and, in particular, determine whether triciferol, like other 1,25D analogs (43), lacks the undesirable calcemic properties of 1,25D.

In conclusion, the above studies demonstrate the synthetic feasibility of combining HDAC inhibition with VDR agonism in 1,25D analogs to enhance their therapeutic potential. Triciferol is unique in that it is a fully merged structure targeting two radically different and biochemically distinct proteins (a metalloenzyme and a nuclear receptor ligand binding domain), and provides proof-of-principle that a second biochemical activity can be incorporated into the agonist structure of a nuclear receptor ligand.

Materials and Methods

Synthesis of Triciferol. See *SI Materials and Methods* for a detailed protocol describing the synthesis of triciferol, including spectroscopic analysis of intermediates.

Molecular and Cell Biology. All cells used in this study were purchased from the American Type Culture Collection and cultured under recommended conditions. See *SI Materials and Methods, Cell and Molecular Biology* for details of all molecular and cell biology protocols, including tissue culture, cell viability assays, and microscopy, RT/PCR analysis, chromatin immunoprecipitation assays, Western blot analysis, and HDAC colorimetric assays.

ACKNOWLEDGMENTS. We thank Dr. Jing Liu and XiaoFeng Wang of the McGill University High Throughput Screening Facility for their assistance with the fluorescence polarization competition assay and Drs. Andreas Steinmeyer and Ekkehard May (Bayer Schering Pharma) for their generous gift of ZK159222. This work was supported by a scholarship from the Montreal Centre for Experimental Therapeutics in Cancer (L.E.T.-M.), a McGill University Health Centre scholarship (to B.D.), a Natural Sciences and Engineering Research Council Postgraduate Scholarship (to J.H.), a Natural Sciences and Engineering Research Council Undergraduate Summer Research Award (to X.L.), and a Proof-of-Principle grant from the Canadian Institutes of Health Research (to J.H.W. and J.L.G.). J.H.W. is a Chercheur-Boursier National of the Fonds de Recherche en Santé du Québec.

- Feldman D, Glorieux FH, Pike JW (1997) *Vitamin D* (Academic, New York).
- Lin R, White JH (2004) The pleiotropic actions of vitamin D. *BioEssays* 26:21–28.
- Masuda S, Jones G (2006) Promise of vitamin D analogues in the treatment of hyper-proliferative conditions. *Mol Cancer Ther* 5:797–808.
- Lim WC, Hanauer SB, Li YC (2005) Mechanisms of disease: Vitamin D and inflammatory bowel disease. *Nature Clin Practice Gastroenterol Hepatol* 2:308–315.
- Wang TT, et al. (2004) 1,25-dihydroxyvitamin D3 is a direct inducer of antimicrobial peptide gene expression. *J Immunol* 173:2909–2912.
- Zaslav FM (2005) Sunlight, vitamin D, and the innate immune defenses of the human skin. *J Invest Dermatol* 125:XXV–XXVII.
- Liu PT, Krutzik SR, Modlin RL (2007) Therapeutic implications of the TLR and VDR partnership. *Trends Mol Med* 13:117–124.
- Liu PT, et al. (2006) Toll-like receptor triggering of a vitamin D-mediated human antimicrobial response. *Science* 311:1770–1773.
- Khanim FL, et al. (2004) Altered SMRT levels disrupt vitamin D-3 receptor signalling in prostate cancer cells. *Oncogene* 23:6712–6725.
- Kim SC, et al. (2006) Substrate and functional diversity of lysine acetylation revealed by a proteomics survey. *Mol Cell* 23:607–618.
- McLaughlin F, La Thangue NB (2004) Histone deacetylase inhibitors open new doors in cancer therapy. *Biochem Pharm* 68:1139–1144.
- Villar-Garea A, Esteller M (2004) Histone deacetylase inhibitors: Understanding a new wave of anticancer agents. *Int J Cancer* 112:171–178.
- Xu WS, Parmigiani RB, Marks PA (2007) Histone deacetylase inhibitors: Molecular mechanisms of action. *Oncogene* 26:5541–5552.
- Wang Z, Bennett EM, Wilson DJ, Salomon C, Vince R (2007) Rationally designed dual inhibitors of HIV reverse transcriptase and integrase. *J Med Chem* 50:3416–3419.
- Tsalamandris C, Panagiotopoulos S, Sinha A, Cooper ME, Jerums G (1994) Complementary effects of pravastatin and nicotinic acid in the treatment of combined hyperlipidaemia in diabetic and non-diabetic patients. *J Cardiovasc Risk* 1:231–239.
- Morphy R, Rankovic Z (2005) Designed multiple ligands. An emerging drug discovery paradigm. *J Med Chem* 48:6523–6543.
- Meunier B (2008) Hybrid Molecules with a Dual Mode of Action: Dream or Reality. *Acc Chem Res* 41:69–77.
- Bralet J, Schwartz J-C (2001) Vasopeptidase inhibitors: An emerging class of cardiovascular drugs. *Trends Pharm Sci* 22:16–109.

19. Rochel N, Wurtz JM, Mitschler A, Klahlolz B, Moras D (2000) The crystal structure of the nuclear receptor for vitamin D bound to its natural ligand. *Mol Cell* 5:173–179.
20. Hansen CM, Hamberg KJ, Binderup E, Binderup L (2000) Seocalcitol (EB1089): A vitamin D analogue of anti-cancer potential. Background, design, synthesis, pre-clinical and clinical evaluation. *Curr Pharm Des* 6:803–828.
21. Tochlini-Vaentini G, Rochel N, Wurtz JM, Moras D (2004) Crystal structures of the vitamin D nuclear receptor liganded with the vitamin D side chain analogues calcipotriol and seocalcitol, receptor agonists of clinical importance. Insights into a structural basis for the switching of calcipotriol to a receptor antagonist by further side chain modification. *J Med Chem* 47:1956–1961.
22. Monneret C (2005) Histone deacetylase inhibitors. *Eur J Med Chem* 40:1–13.
23. Marson CM, et al. (2004) Stereodefined and polyunsaturated inhibitors of histone deacetylase based on (2E,4E)-5-arylpenta-2,4-dienoic acid hydroxamides. *Biorg Med Chem Lett* 14:2477–2481.
24. Suzuki T, Miyata N (2005) Non-hydroxamate histone deacetylase inhibitors. *Curr Med Chem* 12:2867–2880.
25. Morris GM, et al. (1998) Automated docking using a Lamarckian genetic algorithm and an empirical binding free energy function. *J Comp Chem* 19:1639–1662.
26. Corbell CR, Englebienne P, Moitesier N (2007) Docking ligands into flexible and solvated macromolecules. 1. Development and validation of FITTED 1.0. *J Chem Info Mod* 47:435–449.
27. Fujihima T, et al. (2000) Efficient synthesis and biological evaluation of all A-ring diastereomers of 1 α ,25-dihydroxyvitamin D₃ and its 20-epimer. *Biorg Med Chem Lett* 8:123–134.
28. Perlman KL, Siciński RR, Schnoes HK, DeLuca HF (1990) 1 α ,25-Dihydroxy-19-norvitamin D₃, a novel vitamin D-related compound with potential therapeutic activity. *Tetrahedron Lett* 31:1823–1824.
29. St John LS, Sauter ER, Herlyn M, Litwin S, Adler-Storthz K (2000) Endogenous p53 gene status predicts the response of human squamous cell carcinomas to wild-type p53. *Cancer Gene Ther* 7:749–756.
30. Akutsu N, et al. (2001) Regulation of gene expression by 1 α ,25-dihydroxyvitamin D₃ and its analog EB1089 under growth inhibitory conditions in squamous carcinoma cells. *Mol Endocrinol* 15:1127–1139.
31. Lin R, et al. (2002) Expression profiling in squamous carcinoma cells reveals pleiotropic effects of vitamin D₃ signaling on cell proliferation, differentiation and immune system regulation. *Mol Endocrinol* 16:1243–1256.
32. Wang TT, et al. (2005) Large-scale *in silico* and microarray-based genomic screening of 1,25-dihydroxyvitamin D₃ target genes. *Mol Endocrinol* 19:2685–2695.
33. Fan GK, Chen J, Ping F, Geng Y (2006) Immunohistochemical analysis of P57(kip2), p53 and hsp60 expressions in premalignant and malignant oral tissues. *Oral Oncology* 42:147–153.
34. Chen KS, DeLuca HF (1995) Cloning of the human 1 α ,25-dihydroxyvitamin D-3 24-hydroxylase gene promoter and identification of two vitamin D-responsive elements. *Biochim Biophys Acta* 1263:1–9.
35. Anzick SL, et al. (1997) AIB1, a steroid receptor coactivator amplified in breast and ovarian cancer. *Science* 277:965–968.
36. Wegener D, Wirsching F, Riester D, Schwienhorst A (2003) A fluorogenic histone deacetylase assay well suited for high-throughput activity screening. *Chem and Biol* 10:61–68.
37. Bursch W, et al. (1996) Active cell death induced by the anti-estrogens tamoxifen and ICI 164 384 in human mammary carcinoma cells (MCF-7) in culture: The role of autophagy. *Carcinogenesis* 17:1595–1607.
38. Hoyer-Hansen M, Bastholm L, Mathiasen IS, Elling F, Jaattela M (2005) Vitamin D analog EB1089 triggers dramatic lysosomal changes and Bedin 1-mediated autophagic cell death. *Cell Death Diff* 12:1297–1309.
39. Minucci S, Pelicci PG (2006) Histone deacetylase inhibitors and the promise of epigenetic (and more) treatments for cancer. *Nat Rev Cancer* 6:38–51.
40. Drummond DC, et al. (2004) Clinical development of histone deacetylase inhibitors as anticancer agents. *Ann Rev Pharmacol Toxicol* 45:495–528.
41. Alao JP, et al. (2004) Histone deacetylase inhibitor trichostatin A represses estrogen receptor alpha-dependent transcription and promotes proteasomal degradation of cyclin D1 in human breast carcinoma cell lines. *Clin Cancer Res* 10:8094–8104.
42. Jang ER, et al. (2004) The histone deacetylase inhibitor trichostatin A sensitizes estrogen receptor alpha-negative breast cancer cells to tamoxifen. *Oncogene* 23:1724–1736.
43. Ma YF, et al. (2006) Identification and characterization of noncalcemic, tissue-selective, nonsteroidal vitamin D receptor modulators. *J Clin Invest* 116:892–904.

CHEMISTRY

BIOCHEMISTRY

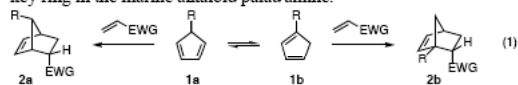
In the following pages is the pre-peer reviewed version of the following article :

Hudon, J.; Cernak, T. A.; Ashenurst, J. A.; Gleason, J. L., Stable 5-Substituted Cyclopentadienes for the Diels-Alder Cycloaddition and their Application to the Synthesis of Palau'amine13. *Angewandte Chemie International Edition* **2008**, *47* (46), 8885-8888.

Stable 5-Substituted Cyclopentadienes for the Diels-Alder Cycloaddition and their Application to Palau'amine Synthesis.

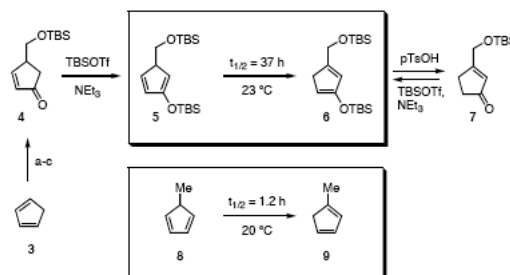
Jonathan Hudon, Timothy A. Cernak, James A. Ashenhurst and James L. Gleason*

The Diels-Alder cycloaddition is one of the most fundamental synthetic transformations and has played a cornerstone role in countless total syntheses. Surprisingly, cyclopentadiene, the most common diene employed in asymmetric synthesis methods, is used only rarely in total syntheses and substituted variants, with the notable exception of Corey's landmark synthesis of the prostaglandins, are almost never used.¹ Substituted cyclopentadienes, particularly those substituted at the 5-position, are very attractive substrates as they lead to structures of high complexity and can provide functional handles for further transformation.² The main obstacle to their use is the need to prepare, isolate and employ the diene at temperatures ≤ 0 °C to prevent facile 1,5-sigmatropic shift which can lead to mixtures of cycloadducts (e.g. eq. 1).^{1,2,3} While this problem may be circumvented in certain instances by removing the offending hydrogen, no direct solution to this long-standing problem has been reported.⁴ In this communication, we demonstrate that the incorporation of a 2-silyloxy group greatly stabilizes 5-substituted cyclopentadienes toward 1,5-sigmatropic shift, for the first time making their use practical for Diels-Alder cycloadditions conducted at room temperature. We further demonstrate the potential of this method by applying it towards the synthesis of a key ring in the marine alkaloid palau'amine.



5-Substituted cyclopentadiene **5** is easily prepared by enolsilylation of 4-substituted cyclopentenone **4** (Scheme 1). The latter is prepared from cyclopentadiene following an easily scalable, three-step procedure involving a Prins reaction with formaldehyde, selective allylic oxidation with Bobbit's reagent and 1° alcohol protection.^{5,6} Silyl enol ether formation from **4** may be accomplished under either soft (R_3SiOTf , NEt_3) or hard (LDA, R_3SiCl) enolization conditions. Either the TBS, TES or TMS silyl enol ether may be prepared, with the former being preferred due to increased hydrolytic stability of the diene and subsequent cycloadducts. Regardless of the means of enol ether preparation, the

cross-conjugated diene is formed exclusively and may be isolated by simple extractive workup and used directly in subsequent cycloadditions.



Scheme 1. Synthesis of stable 5-substituted cyclopentadiene **5**. a) HCHO, HCO₂H, TsOH, NaOH (43%, 55:45 regioisomers); b) 4-acetamido-2,2,6,6-tetramethyl-1-oxopiperidinium perchlorate. c) TBSOTf, imidazole; regioisomer separation (45%, two steps).

Diene **5** undergoes 1,5-sigmatropic shift of hydrogen at a considerably slower rate than normal 5-substituted cyclopentadienes. Monitoring **5** by ¹H NMR in d₆-benzene demonstrated that it rearranges with a half-life of 37 h at 23 °C and it was found that **5** could be stored at -20 °C for up to a month with no significant rearrangement or dimerization observed. By contrast 5-methylcyclopentadiene is reported to rearrange with a half life of only 1.2 h at 20 °C, indicating a greater than 30-fold increase in stability upon incorporation of the 2-silyloxy group.⁷ Although the rearrangement product could not be separated from **5**, its ¹H NMR in the rearrangement process, the isolation of enone **7** upon mild acid workup and regeneration upon enolsilylation of **7** were fully consistent with **6** as the major rearrangement product. The increased stability of **5** undoubtedly arises from donation of electron density from the silyloxy substituent.⁸ Density functional calculations at the B3LYP/6-31G* level showed a reasonable correlation between the predicted activation enthalpy for 1,5-shift and the electron donating ability of substituents at the 2-position of the diene (See Supporting Information for details).^{9,10}

Diene **5** proved to be highly competent in Diels-Alder cycloadditions with a wide variety of dienophiles under very mild conditions (0.5 M **5**, 1.5 M dienophile, CH₂Cl₂, 23 °C, Table 1). The cycloadducts were isolated as the versatile silyl enol ethers after chromatography on neutral alumina (Brockman Grade IV). Cycloadditions were rapid with dienophiles such as benzoquinone, *N*-methylmaleimide and dimethylacetylene dicarboxylate and were highly endo-selective in the former two cases. Cycloadditions with slightly less reactive dienophiles such as acrolein, methyl vinyl ketone and chloroacrylonitrile also proceeded efficiently at room temperature in just 2-4 hours. Finally, reaction of **5** with acrylonitrile and methyl acrylate also afforded good yields of cycloadducts even with extended reaction times (20-24 h) at room

[*] J.L. Gleason, J. Hudon, T.A. Cernak, J.A. Ashenhurst
Department of Chemistry
McGill University
801 Sherbrooke St. West, Montreal, QC, Canada H3A 2K6
Fax: 514-398-3797
E-mail: jim.gleason@mcgill.ca

[**] This work was supported by the Natural Science and Engineering Research Council (NSERC). JH thanks NSERC and Le Fonds Québécois de la Recherche sur la Nature et les Technologies (FQRNT) for pre-doctoral fellowships. TAC thanks FQRNT for a pre-doctoral fellowship. JAA thanks the Walter C. Sumner Foundation for a pre-doctoral fellowship.

Supporting information for this article is available on the WWW under <http://www.angewandte.org> or from the author.

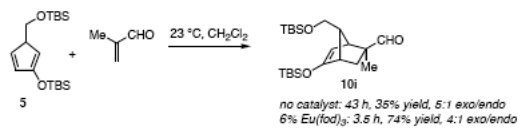
temperature, conditions that would clearly not be suitable for simple 5-substituted cyclopentadienes. In all cases, the cycloadditions proceeded with excellent diastereofacial selectivity, with approach of the dienophile opposite to the 5-silyloxymethyl group, and with endo/exo ratios comparable to those observed with cyclopentadiene.¹¹

Table 1. Diels-Alder cycloadditions of 5-substituted cyclopentadiene **5**.^[a]

Dienophile	Product	<i>t</i> (h)	yield ^[b] (%)	endo:exo
		0.15	66	>95:5
		0.5	79	>95:5
		0.75	79	
		2	71	1.6:1
		4	67	2:1
		3.5	73	3.2:1
		20	68	1.2:1
		24	65	2.3:1

[a] Reactions carried out with excess dienophile (3 equiv) in dichloromethane at a diene concentration of 0.5 M at 23 °C. [b] Isolated overall yield (endo + exo) starting from enone **4**.

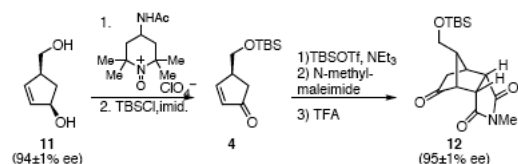
Diene **5** is compatible with the use of mild Lewis acids. Cycloaddition of **5** with methacrolein proceeds very slowly at room temperature, affording only a 35% isolated yield of **10i** after 43 h (Scheme 2). However, use of 6% Eu(fod)₃ as catalyst allowed the reaction to proceed to completion in just 3.5 h at 23 °C affording a 74% yield of cycloadduct **10i** as a 4:1 exo/endo mixture.¹²



Scheme 2. Lewis acid catalysis with diene **5**.

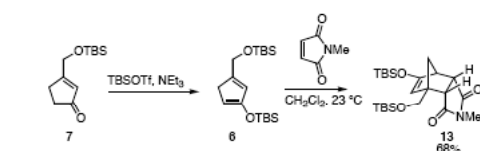
Diene **5** offers an additional advantage over simple 5-substituted cyclopentadienes in that it is chiral and, as can be seen in Table 1, it provides excellent regioselectivity and diastereofacial control with

respect to both the 2- and 5-substituents. Diene **5** may be prepared in enantiomerically enriched form from **11** (94±1% ee), available by the procedure of Hodgson,¹³ by selective allylic oxidation and silylation.⁶ Cycloaddition of enantiomerically enriched **5** with *N*-methylmaleimide followed by selective desilylation of the enol ether afforded ketone **12** as a single diastereomer in 95%±1% ee, indicating that the diene does not racemize during formation nor via successive reversible 1,5-sigmatropic shifts.



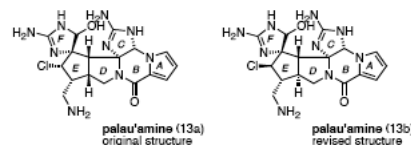
Scheme 3. Preparation and use of enantioenriched diene.

The concept of stabilization by a silyloxy group is not limited to diene **5**. Diene **6**, produced cleanly by enolsilylation of enone **7**, is even more stable than **5** to [1,5]-sigmatropic shift (Scheme 4).¹⁴ Exposure of **6** to *N*-methylmaleimide for 0.5 h under our standard cycloaddition conditions affords endo cycloadduct **13** in 68% yield as a single regio- and diastereomer. Presumably this silyloxy stabilization can be incorporated in other diene substitution patterns.



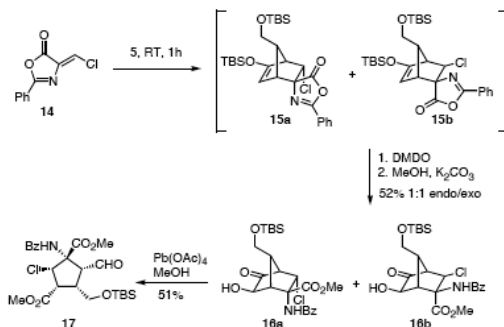
Scheme 4. 2,4-Disubstituted cyclopentadiene **6** in a Diels-Alder cycloaddition.

As a demonstration of the synthetic utility of **5**, we applied it towards a significant synthetic challenge presented by the oroidin alkaloid palau'amine.¹⁵ This marine alkaloid, isolated from *Stylotella aurantium*, possesses a hexacyclic structure containing two guanidine-containing rings and a densely functionalized E-ring, the stereochemistry about which has been a matter of significant debate.¹⁶ The original structure assignment suggested that the D-E ring junction was *cis*-fused and that the chlorine in the E-ring was on the α -face (as in **13a**).¹⁵ Several groups have recently proposed that the D-E ring fusion is *trans* and that the chlorine is on the β -face (**13b**).¹⁷ Both of these stereoarrays represent significant synthetic challenges. Despite significant efforts by many research groups, the original all-*cis* stereoarray in the E-ring of the originally reported structure has never yielded to synthesis.



One potential route to the E-ring stereochemistry in the original structure is via cycloaddition of a 5-substituted cyclopentadiene with

a β -chlorodehydroalanine derivative, followed by oxidative ring-opening of the cycloadduct.¹⁸ We found that cycloaddition of **5** with chloromethyleneoxazolone **14**¹⁹ proceeds rapidly in dichloromethane at room temperature (Scheme 5). The resulting 1:1 mixture of cycloadducts was not stable to chromatography and thus was treated directly with dimethylsiloxane followed by methanolysis of the oxazolone to afford hydroxy ketones **16a** and **16b** in 52% combined yield over three steps. Subsequent cleavage of the hydroxy ketone in **16a** with lead tetraacetate in methanol afforded the hexasubstituted cyclopentane **17** which possesses the same stereochemistry as the E-ring in **13a**. This is the first successful example of the preparation of the palau'amine E-ring with the all-*cis* stereochemistry.



Scheme 5. Application of **5** to the synthesis of the palau'amine E-ring.

In conclusion, we have shown that 2-silyloxy substitution markedly stabilizes 5-substituted cyclopentadienes towards 1,5-sigmatropic shift, allowing facile preparation and efficient use of this important class of dienes. Furthermore, the diene may easily be prepared in enantiomerically enriched form and undergoes cycloaddition with excellent regio- and diastereocontrol with no loss of enantiopurity. It is expected that this versatile new diene will find application in complex molecule synthesis.²⁰

Received: ((will be filled in by the editorial staff))
Published online on ((will be filled in by the editorial staff))

Keywords: Diels-Alder cycloaddition · sigmatropic shift · palau'amine

- [1] a) Corey, E. J.; Weinschenker, N. M.; Schaaf, T. K.; Huber, W. *J. Am. Chem. Soc.* **1969**, *91*, 5675. For a recent exquisite example which takes advantage of differential reactivity of 1- and 2-substituted cyclopentadienes, see: b) Li, P.; Payette, J.N.; Yamamoto, H. *J. Am. Chem. Soc.* **2007**, *129*, 9534. c) Payette, J.N.; Yamamoto, H. *J. Am. Chem. Soc.* **2007**, *129*, 9536.
- [2] For other examples of 5-substituted cyclopentadienes in Diels-Alder cycloadditions, see: a) Letourneau, J.E.; Wellman, M.A.; Burnell, D.J. *J. Org. Chem.* **1997**, *62*, 7272. b) Wellman, M.A.; Burry, L.C.; Letourneau, J.E.; Bridson, J.N.; Miller, D.O.; Burnell, D.J. *J. Org. Chem.* **1997**, *62*, 939. c) King, S.B.; Ganem, B. *J. Am. Chem. Soc.* **1994**, *116*, 562. d) Goering, B.K.; Ganem, B.K. *Tetrahedron Lett.* **1994**, *35*, 6997. e) McClinton, M.A.; Sik, V. *J. Chem. Soc. Perkin I* **1992**, 1891. f) Franck-Neumann, M.; Sedrati, M. *Tetrahedron Lett.* **1983**, *24*, 1391. g) Breslow, R.; Hoffman Jr., J.M.; Perchonock, C.

- Tetrahedron Lett.* **1973**, *14*, 3723. h) Winstein, S.; Shatavsky, M.; Norton, C.; Woodward, R.B. *J. Am. Chem. Soc.* **1955**, *77*, 4183.
- [3] (a) Kresze, G.; Schulz, G.; Walz, H. *Ann. Chem.* **1963**, *45*, 666. (b) Mironov, V. A.; Sobolev, E. V.; Elizarova, A. N. *Tetrahedron* **1963**, *19*, 1939. c) McNeil, D.; Vogt, B.R.; Sudol, J.J.; Theodoropoulos, S.; Hedaya, E. *J. Am. Chem. Soc.* **1974**, *96*, 4673. An exception are 5-halocyclopentadienes which are reported to rearrange at slower rates. See Ref 2g.
- [4] For examples of 6-substituted fulvenes, see: a) Brown, E. D.; Clarkson, R.; Leeney, T. J.; Robinson, G. E. *Chem. Commun.* **1974**, 642. b) Yates, P.; Lokensgard, J. P. *Synth Commun.* **1975**, *5*, 37-42. For intramolecular trapping, see: c) Ohkita, M.; Kawai, H.; Tsuji, T. *J. Chem. Soc. Perkin I*, **2002**, 366. For examples of spirobicyclo[4.2.0]heptadienes where 1,5-shift is not possible, see d) Corey, E. J.; Shimer, C. S.; Volante, R. P.; Cyr, C. R. *Tetrahedron Lett.* **1975**, *16*, 1161-4. e) Attah-Poku, S. K.; Gallacher, G.; Ng, A. S.; Taylor, L. E. B.; Alward, S. J.; Fallis, A. G. *Tetrahedron Lett.* **1983**, *24*, 677-80. f) Gonzalez, A. G.; Darias, J.; Diaz, F. *Tetrahedron Lett.* **1984**, *25*, 2697-700. g) Starr, J. T.; Koch, G.; Carreira, E. M. *J. Am. Chem. Soc.* **2000**, *122*, 8793-8794.
- [5] a) Bajorek, J.S.; Battaglia, R.; Pratt, G.; Sutherland, J.K. *J. Chem. Soc. Perkin I* **1974**, 1243; b) Saville-Stones, E.A.; Turner, R.M.; Lindell, S.D.; Jennings, N.S.; Head, J.C.; Carver, D.S. *Tetrahedron*, **1994**, *50*, 6695.
- [6] Bobbitt, J.M. *J. Org. Chem.* **1998**, *63*, 9367. CAUTION! The perchlorate salt is reported to be explosive. It can be replaced by the tetrafluoroborate salt. See: Bobbitt, J.M. *Chem. Eng. News* **1999**, *77*, 6.
- [7] Maclean, S.; Haynes, P. *Tetrahedron* **1965**, *21*, 2329.
- [8] Methyl groups at either the 1- or 2-position have been reported to slow sigmatropic shift in 5-substituted cyclopentadienes, but their preparation is problematic. See Ref. 7 and a) McLean, S.; Haynes, P. *Tetrahedron*, **1965**, *21*, 2313. Electron withdrawing groups have been reported to accelerate 1,5-hydrogen shifts. See b) Okamura, W. H.; Shen, G.-Y.; Tapia, R. *J. Am. Chem. Soc.* **1986**, *108*, 5018.
- [9] Frisch, M. J. et al. *Gaussian 03*, revision C.02, Gaussian Inc., Wallingford, CT, 2004.
- [10] Calculations at the MPW1K level of theory produced similar results. For MPW1K calculations on the 1,5-shift of hydrogen, see Shelton, G.R.; Hrovat, D.A.; Bordon, W.T. *J. Am. Chem. Soc.* **2007**, *129*, 164.
- [11] Stereochemistry was assigned by NOE analysis in all cases except for **10f** which was assigned by comparison of ³J H-C coupling. In contrast to simple 5-substituted cyclopentadienes (see ref 2a), no cycloadducts arising from addition syn to the 5-silyloxymethyl group were observed.
- [12] Strong Lewis acids such as BF₃·OEt₂ and TiCl₄ were not compatible, resulting in significant decomposition of the diene.
- [13] (a) Hodgson, D.M.; Witherington, J.; Moloney, B. A. *J. Chem. Soc. Perkin Trans. I* **1994**, 3373; (b) Hodgson, D. M.; Gibbs, A. R.; Drew, M. G. B. *J. Chem. Soc. Perkin Trans. I* **1999**, 3579-3590.
- [14] Enone **7** is conveniently prepared by NEt₃ induced isomerization of **4**.
- [15] (a) Kinnel, R. B.; Gehrken, H.-P.; Scheuer, P. J. *J. Am. Chem. Soc.* **1993**, *115*, 3376; (b) Kinnel, R. B.; Gehrken, H.-P.; Swali, R.; Skoropowski, G.; Scheuer, P. J. *J. Org. Chem.* **1998**, *63*, 3281.
- [16] For recent reviews of synthetic studies towards palau'amine, see: (a) Jacquot, D. E. N.; Lindel, T. *Curr. Org. Chem.* **2005**, *9*, 1551; (b) Hoffmann, H.; Lindel, T. *Synthesis* **2003**, 1753; (c) Jin, Z. *Nat. Prod. Rep.* **2006**, *23*, 464.
- [17] (a) Grube, A.; Kock, M. *Angew. Chem. Int. Ed.* **2007**, *46*, 2320; (b) Buchanan, M. S.; Carroll, A. R.; Addelpalli, R.; Avery, V. M.; Hooper, J. N. A.; Quinn, R. J. *J. Org. Chem.* **2007**, *72*, 2309; (c) Kobayashi, H.; Kitamura, K.; Nagai, K.; Nakao, Y.; Fusetani, N.; van Soest, R. W. M.; Matsunaga, S. *Tetrahedron Lett.* **2007**, *48*, 2127; (d) Buchanan, M. S.; Carroll, A. R.; Quinn, R. J. *Tetrahedron Lett.* **2007**, *48*, 4573; (e) Lanman, B.A.; Overman, L.E.; Paulini, R.; White, N.S. *J. Am. Chem. Soc.* **2007**, *129*, 12896.
- [18] For model studies using cyclopentadiene in place of **6**, see: Cernak, T.A.; Gleason, J.L. *J. Org. Chem.* **2008**, *73*, 102.
- [19] Bland, J.M.; Stammer, C.H.; Varughese, K.I. *J. Org. Chem.* **1984**, *49*, 1634

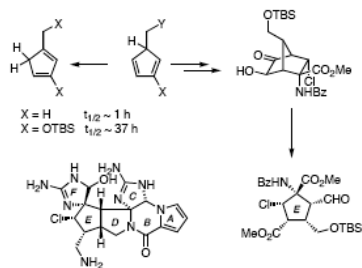
[20] For application in a [6+4] tropone cycloaddition towards the core of CP-225,917, see Ashenurst, J.A.; Gleason, J.L. *Tetrahedron. Lett.*

2008, 49, 504.

Diels-Alder Cycloadditions

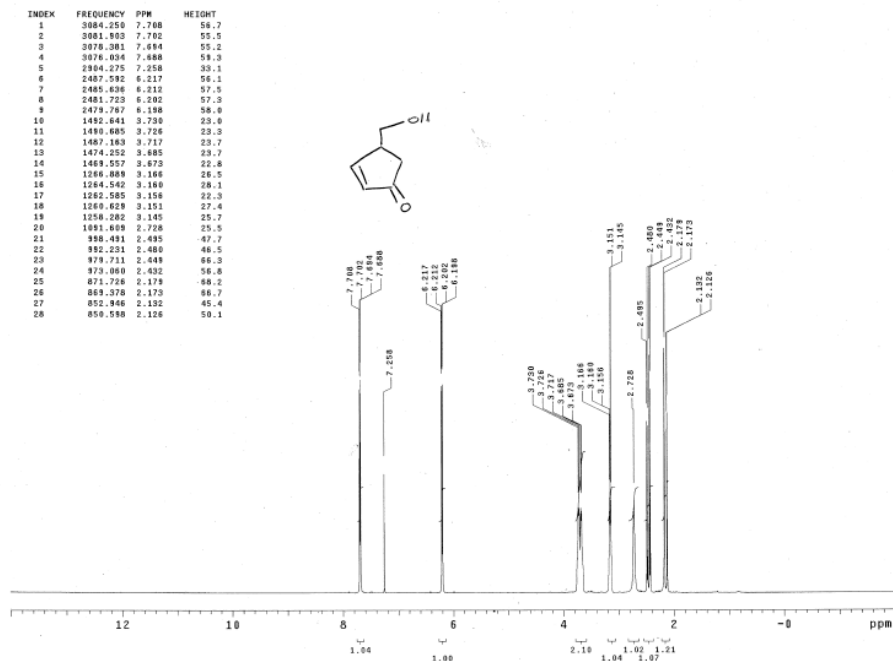
Jonathan Hudon, Timothy A. Cernak,
James A. Ashenurst and James L.
Gleason* _____ **Page – Page**

**Stable 5-Substituted
Cyclopentadienes for the Diels-Alder
Cycloaddition and their Application
to Palau'amine Synthesis.**

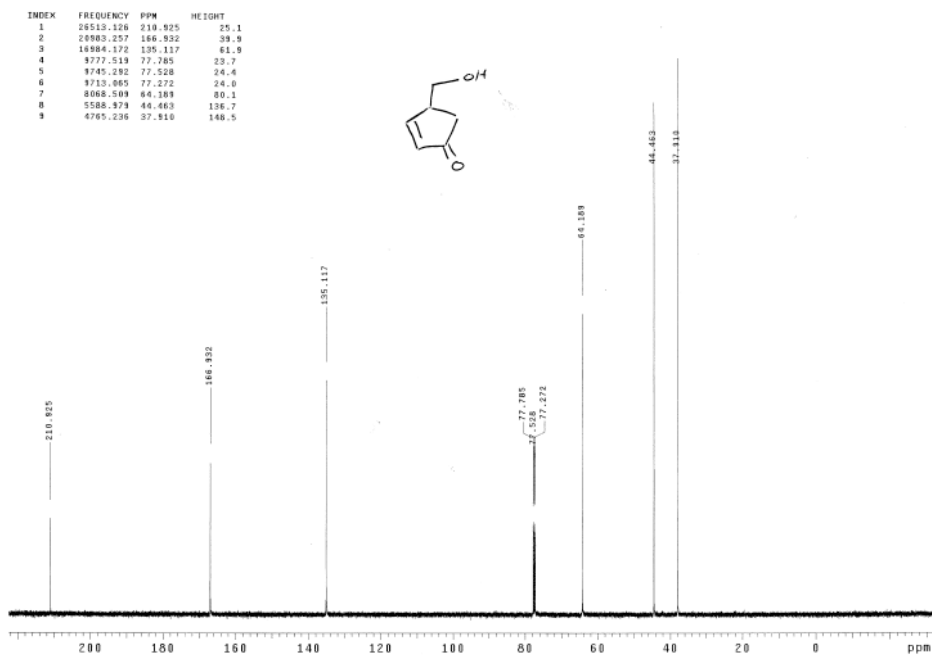


Putting the brakes on a hydride shift: The incorporation of a 2-silyloxy group increases both the stability and reactivity of 5-substituted cyclopentadienes, facilitating their preparation and use. Application to the *E*-ring stereoarray in palau'amine is described.

9 Appendix 3 Selected NMR spectra

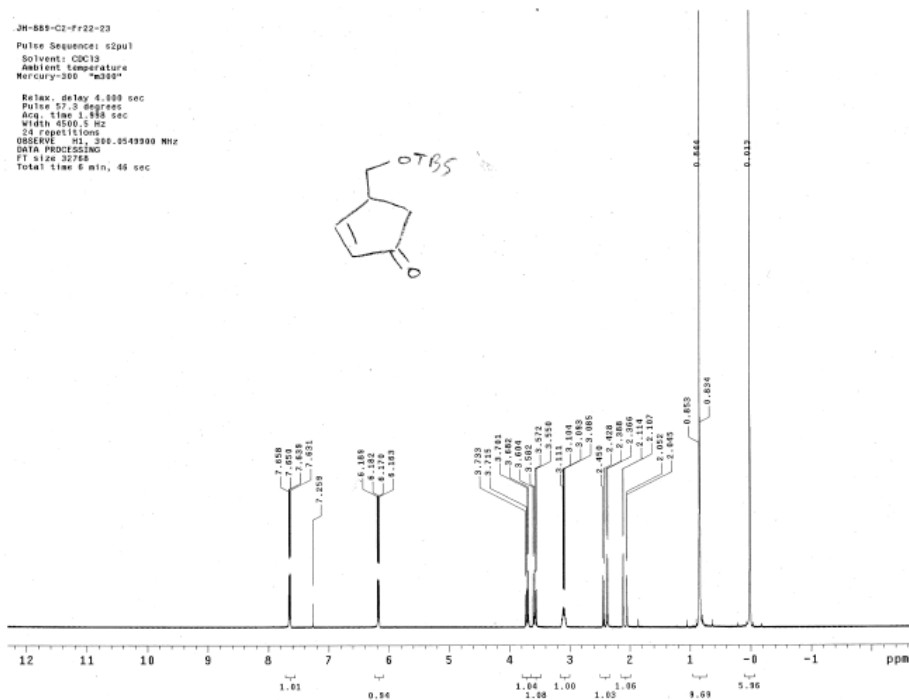


Spectrum A ^1H NMR of 4.39



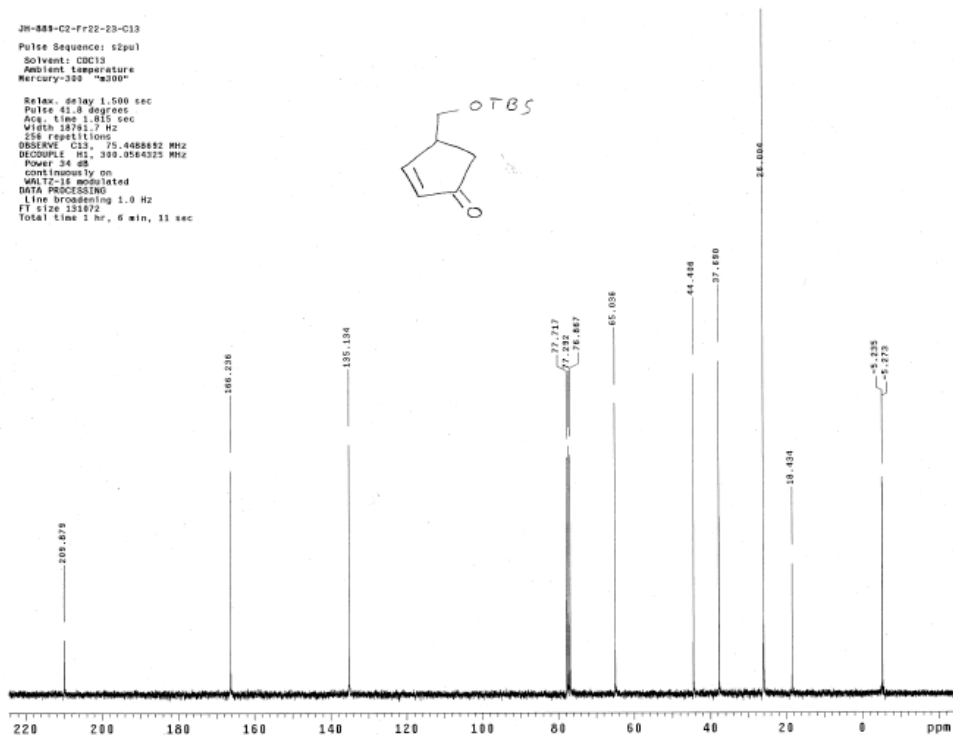
Spectrum B ^{13}C NMR

JH-885-C2-Fr22-23
 Pulse Sequence: s2pu1
 Solvent: CDCl3
 Ambient temperature
 Mercury-300 "m300"
 Relax. delay 4.899 sec
 Pulse 57.3 degrees
 Acq. time 1.888 sec
 Width 4590.3 Hz
 24 Repetitions
 OBSERVE F1: 300.2549900 MHz
 DATA PROCESSING
 FT size 32768
 Total time 6 min, 46 sec

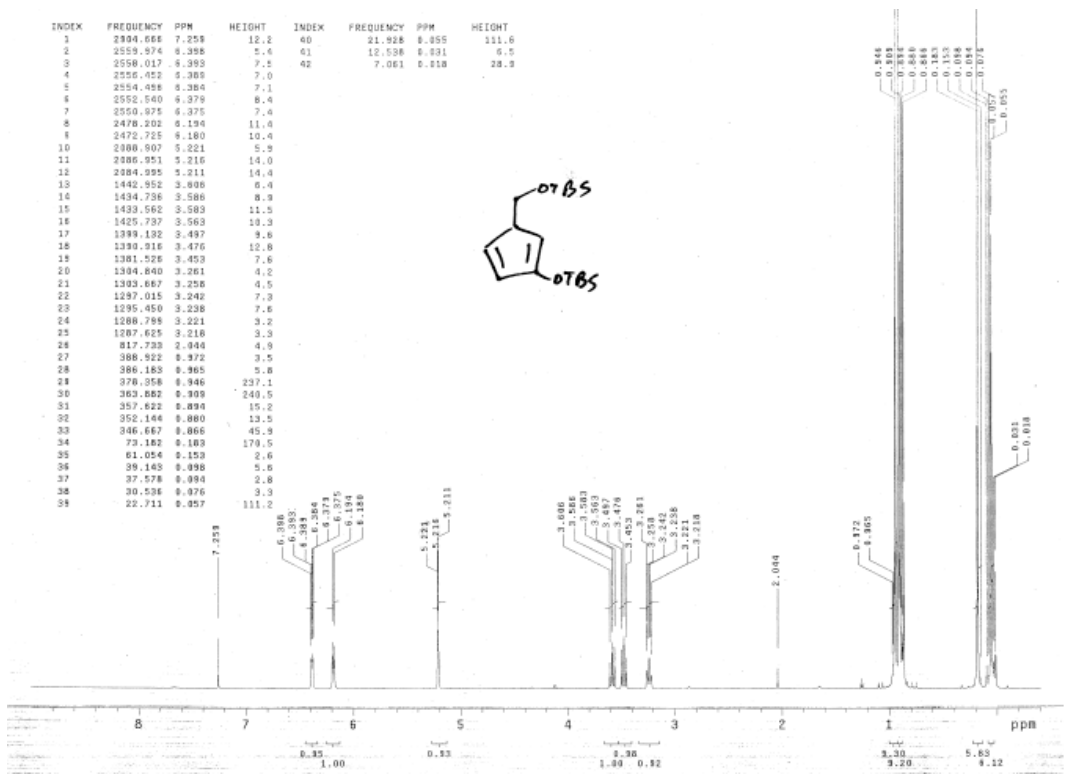


Spectrum C ¹H NMR of 2.7

JH-885-C2-Fr22-23-C13
 Pulse Sequence: s2pu1
 Solvent: CDCl3
 Ambient temperature
 Mercury-300 "m300"
 Relax. delay 1.500 sec
 Pulse 41.0 degrees
 Acq. time 1.815 sec
 Width 18761.7 Hz
 258 Repetitions
 OBSERVE F1: 75.4408892 MHz
 DECOUPLE F2: 300.2549325 MHz
 Power 34 dB
 Continuous ly on
 WALTZ-16 modulated
 DATA PROCESSING
 Line broadening 1.0 Hz
 FT size 151872
 Total time 1 hr, 6 min, 11 sec

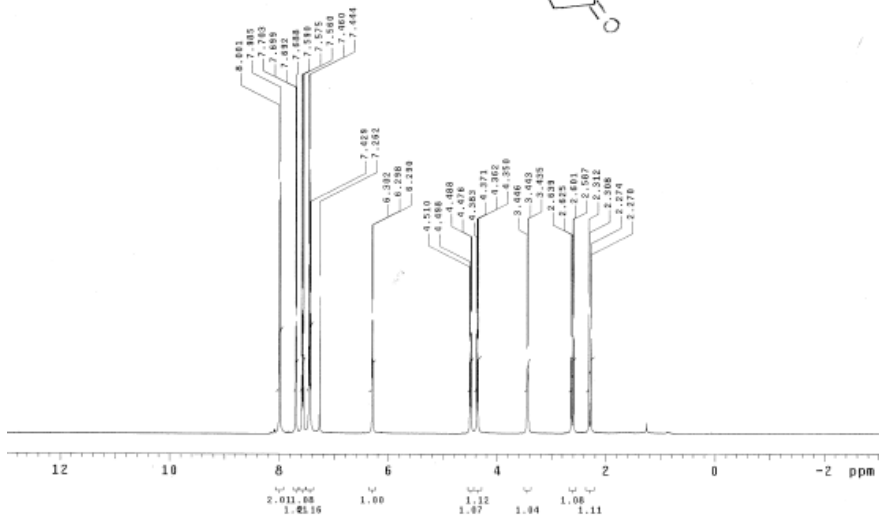
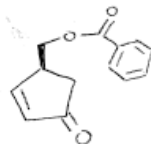


Spectrum D ¹³C NMR of 2.7



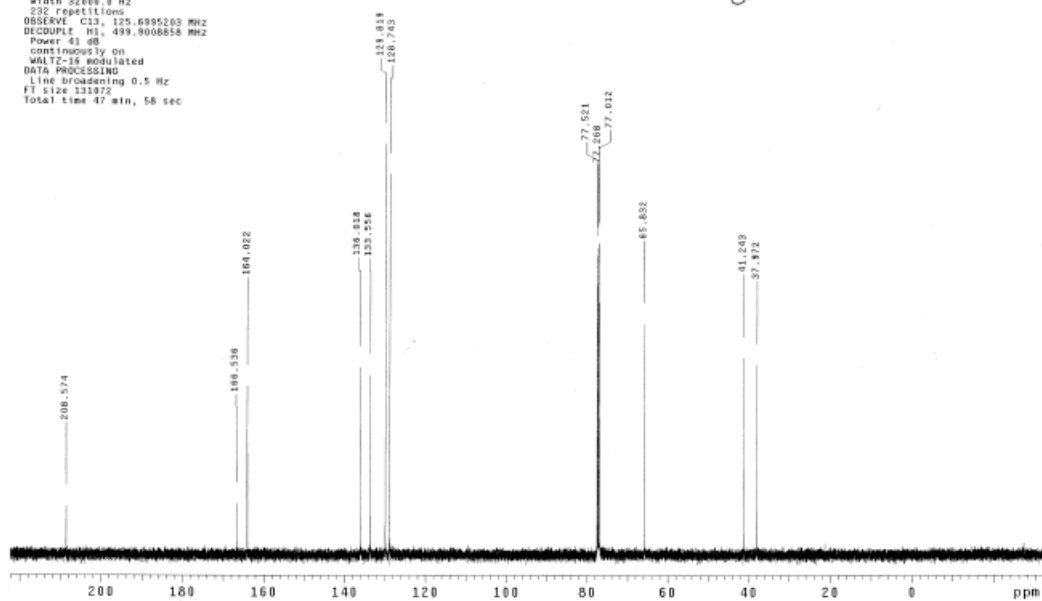
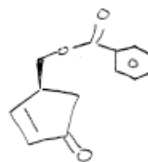
Spectrum E ¹H NMR of 2.8

JH-664-C2
 Pulse Sequence: s2pul
 Solvent: CDCl3
 Ambient temperature
 UNITY-500 "dante"
 Relax. delay 4.000 sec
 Pulse 43.4 degrees
 Acq. time 1.692 sec
 Width 8990.0 Hz
 8 repetitions
 OBSERVE H1, 499.8183900 MHz
 DATA PROCESSING
 FT size 95536
 Total time 6 min, 17 sec



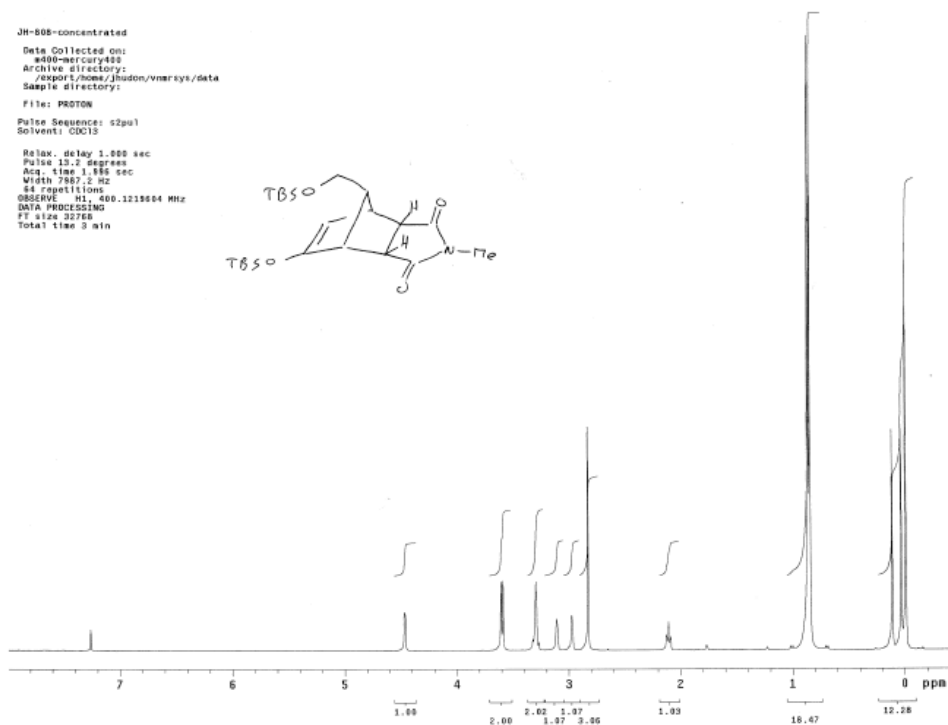
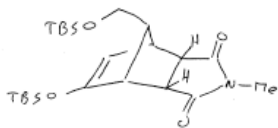
Spectrum F ¹H NMR of 2.47

JH-664-C2-C13
 Pulse Sequence: s2pul
 Solvent: CDCl3
 Ambient temperature
 User: J-14-87
 UNITY-500 "dante"
 Relax. delay 1.500 sec
 Pulse 42.9 degrees
 Acq. time 1.380 sec
 Width 82000.0 Hz
 232 repetitions
 OBSERVE C13, 125.6995203 MHz
 DECOUPLE H1, 499.8008858 MHz
 Power 41.00
 continuously on
 WALTZ-16 modulated
 DATA PROCESSING
 Line broadening 0.5 Hz
 FT size 131872
 Total time 47 min, 58 sec



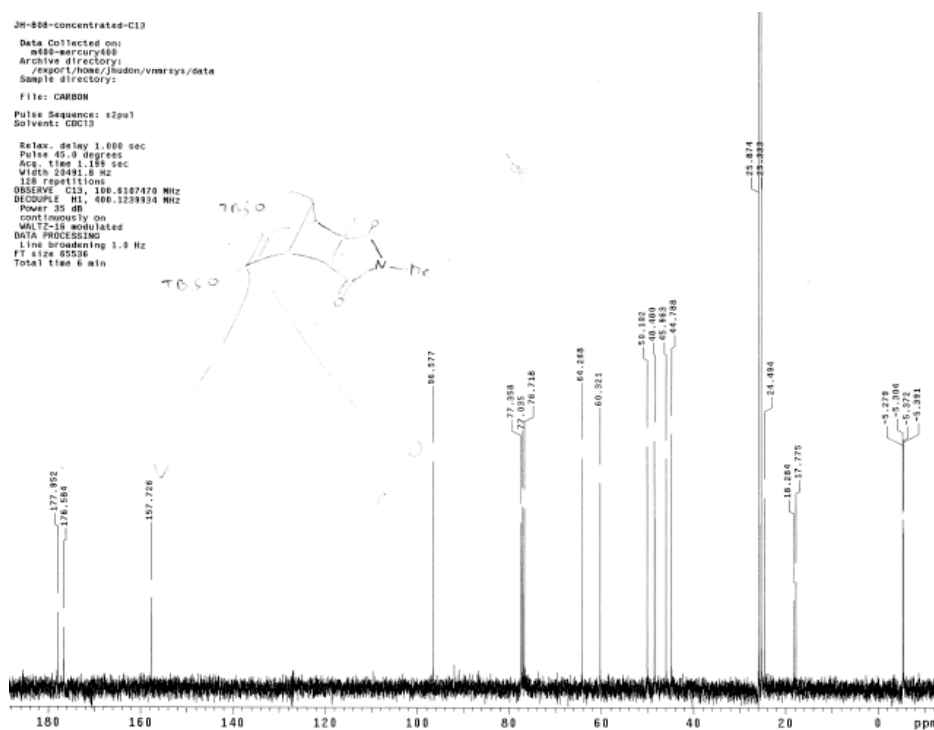
Spectrum G ¹³C NMR of 2.47

JH-808-concentrated
 Date Collected on: m808-mercury800
 Archive directory: /export/home/jhadon/vmrsys/data
 Sample directory:
 File: PROTON
 Pulse Sequence: s2pu1
 Solvent: CDCl3
 Relax. delay 1.000 sec
 Pulse 13.2 degrees
 Acq. time 1.995 sec
 Width 7867.2 Hz
 64 repetitions
 OBSERVE H1, 400.1215604 MHz
 DATA PROCESSING
 FT size 32768
 Total time 9 min



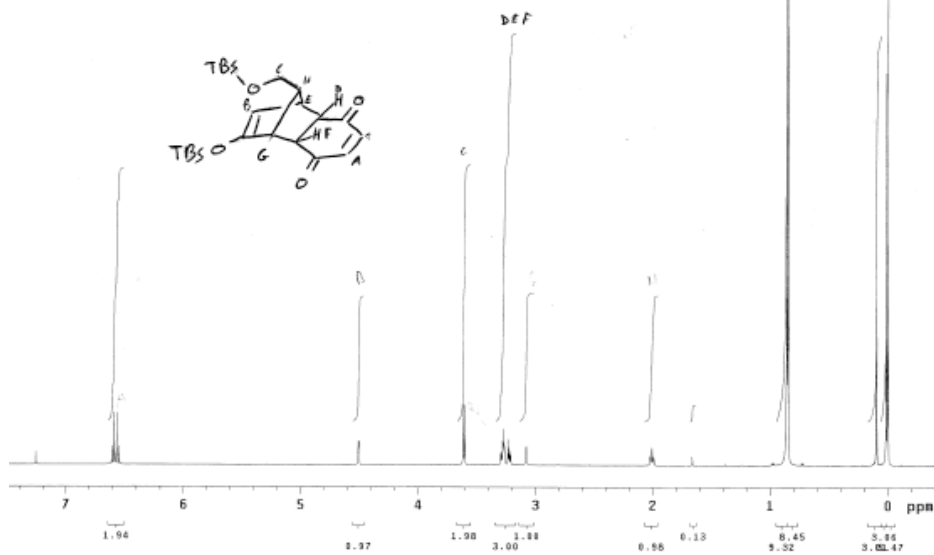
Spectrum H ^1H NMR of 2.21

JH-808-concentrated-C13
 Date Collected on: m808-mercury800
 Archive directory: /export/home/jhadon/vmrsys/data
 Sample directory:
 File: CARBON
 Pulse Sequence: s2pu1
 Solvent: CDCl3
 Relax. delay 1.000 sec
 Pulse 45.0 degrees
 Acq. time 1.195 sec
 Width 23481.6 Hz
 128 repetitions
 OBSERVE C13, 100.6207470 MHz
 DECOUPLE H1, 400.1228934 MHz
 Power 35 dB
 continuous by on
 WALTZ-16 modulated
 DATA PROCESSING
 Line broadening 1.0 Hz
 FT size 65536
 Total time 6 min



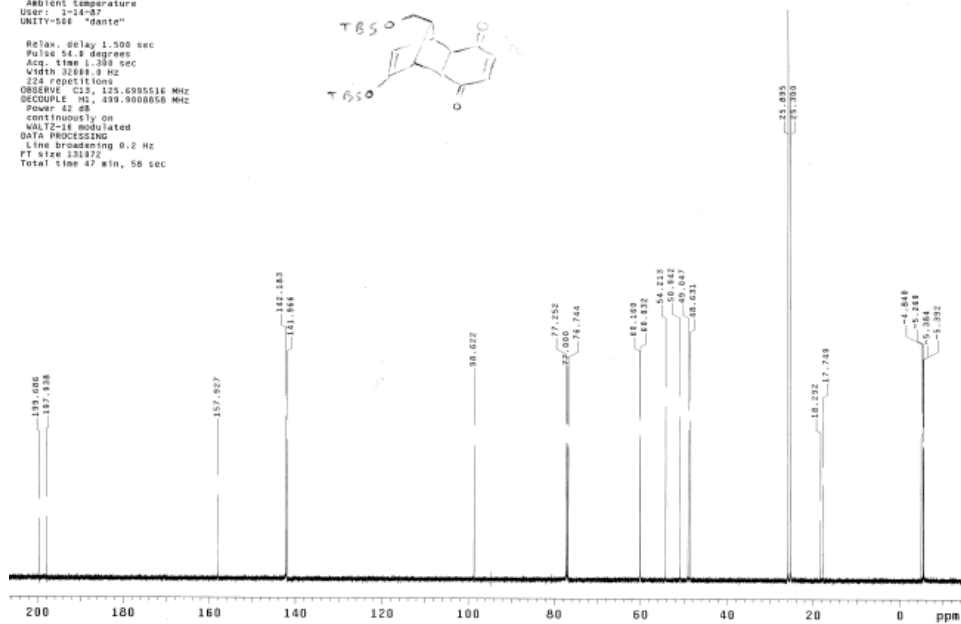
Spectrum I ^{13}C NMR of 2.21

JH-644-A-Fr48-51
 Pulse Sequence: s2pul
 Solvent: CDCl3
 Ambient temperature
 UNITY-500 "dante"
 Relax. delay 4.000 sec
 Pulse 32.4 degrees
 Acq. time 1.992 sec
 Width 5999.0 Hz
 3 repetitions
 OBSERVE M1, 499.8983908 MHz
 DATA PROCESSING
 FT size 32768
 Total time 9 min, 47 sec



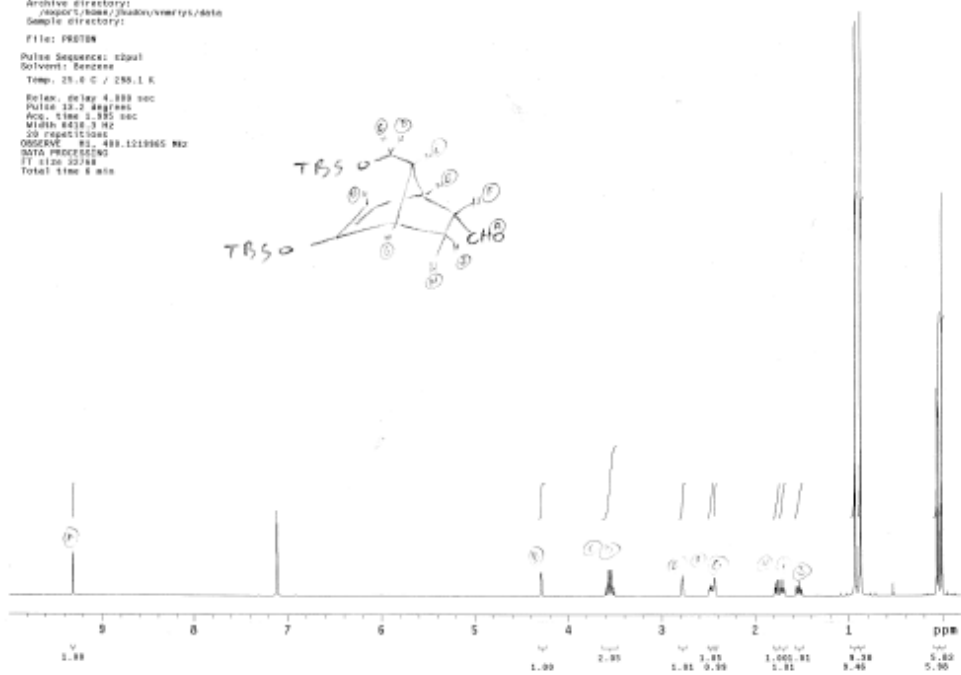
Spectrum J ^1H NMR of 2.14

JH-644-A-Fr48-51-C13
 Pulse Sequence: s2pul
 Solvent: CDCl3
 Ambient temperature
 User: J-14-87
 UNITY-500 "dante"
 Relax. delay 1.000 sec
 Pulse 54.4 degrees
 Acq. time 1.399 sec
 Width 32684.0 Hz
 224 repetitions
 OBSERVE C13, 125.6085516 MHz
 DECOUPLE M1, 499.9008858 MHz
 Power 12 dB
 continuously on
 VOLTAGE is modulated
 DATA PROCESSING
 Line broadening 0.2 Hz
 FT size 131972
 Total time 47 min, 58 sec



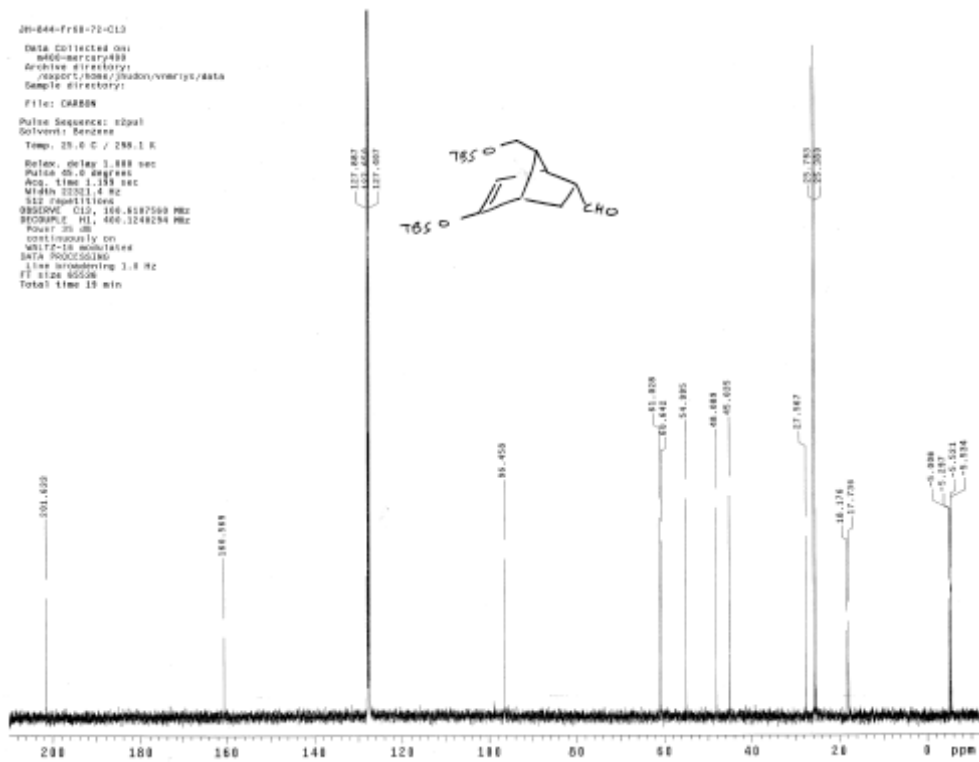
Spectrum K ^{13}C NMR of 2.14

2H-644-FR58-72
 Data Collected on:
 m400-mercury400
 Archive directory:
 /nsport/home/jhudson/vnmrjz/data
 Sample directory:
 File: PROTEN
 Pulse Sequence: zgpg30
 Solvent: Benzene
 Temp: 25.0 C / 298.1 K
 Relax. delay: 4.389 sec
 Pulse: 12.2 degrees
 Acq. time: 3.395 sec
 Width: 8424.9 Hz
 20 repetitions
 OBSERVE: H1, 400.121865 MHz
 DATA PROCESSING
 F1 size: 32768
 Total time: 8 min



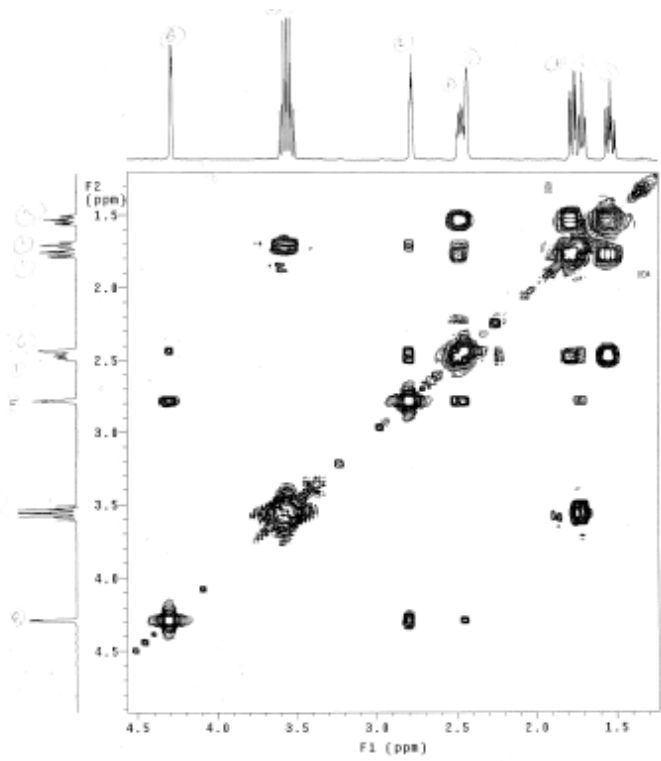
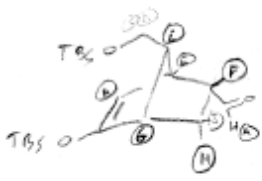
Spectrum L ^1H NMR of 2.16 endo

2H-644-FR58-72-013
 Data Collected on:
 m400-mercury400
 Archive directory:
 /nsport/home/jhudson/vnmrjz/data
 Sample directory:
 File: CARRBN
 Pulse Sequence: zgpg30
 Solvent: Benzene
 Temp: 25.0 C / 298.1 K
 Relax. delay: 3.888 sec
 Pulse: 20.0 degrees
 Acq. time: 3.395 sec
 Width: 8424.9 Hz
 512 repetitions
 OBSERVE: C13, 100.626250 MHz
 P1: 0.000000 sec
 PCORRECT: HI, 400.1248294 MHz
 Power: 20 dB
 continuously on
 WALTZ-16 modulated
 DATA PROCESSING
 Line broadening: 1.8 Hz
 FT size: 65536
 Total time: 15 min



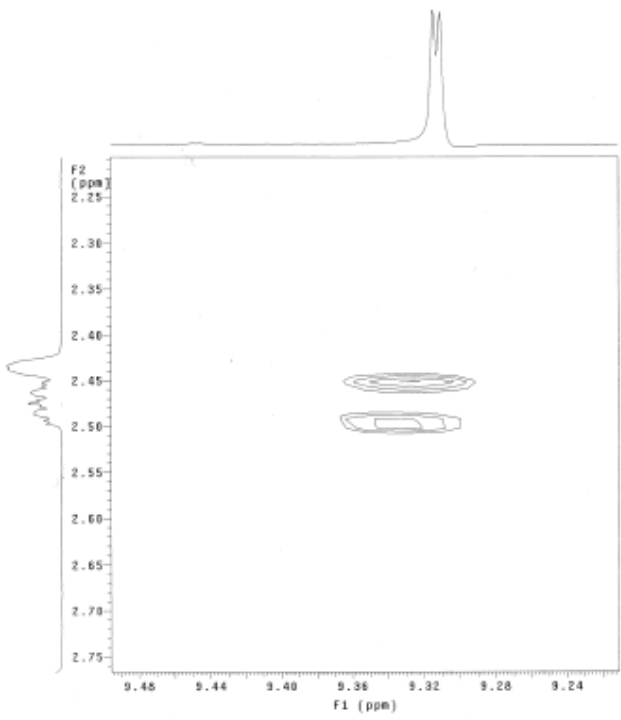
Spectrum M ^{13}C NMR of 2.16 endo

24-899-F088-72-COSY
 Data Collected on:
 WBB9-mw/cu/y666
 Archive directory:
 /report/home/1/hodon/vnmr/ps/data
 Sample directory:
 File: g000Y
 Pulse Sequence: gCOSY
 Solvent: Benzene
 Temp: 25.9 C / 299.1 K
 Relax. delay: 1.000 sec
 Acq. time: 0.150 sec
 Width: 8166.7 Hz
 SF width: 4083.7 Hz
 # repetitions: 8
 328 Increments
 OBSERVED: 600.1218965 MHz
 DATA PROCESSING:
 Size: 2k11 0.875 sec
 F1: DATA PROCESSING
 Size: 2k11 0.831 sec
 F1 size: 2048 x 2048
 Total time: 21 min



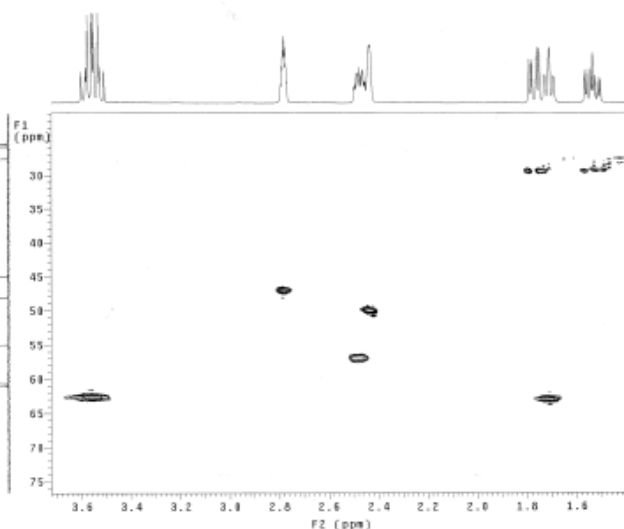
Spectrum N 2D COSY NMR of 2.16 endo (part 1)

24-899-F088-72-COSY
 Data Collected on:
 WBB9-mw/cu/y666
 Archive directory:
 /report/home/1/hodon/vnmr/ps/data
 Sample directory:
 File: g000Y
 Pulse Sequence: gCOSY
 Solvent: Benzene
 Temp: 25.9 C / 299.1 K
 Relax. delay: 1.000 sec
 Acq. time: 0.150 sec
 Width: 8166.7 Hz
 SF width: 4083.7 Hz
 # repetitions: 8
 328 Increments
 OBSERVED: 600.1218965 MHz
 DATA PROCESSING:
 Size: 2k11 0.875 sec
 F1: DATA PROCESSING
 Size: 2k11 0.831 sec
 F1 size: 2048 x 2048
 Total time: 21 min



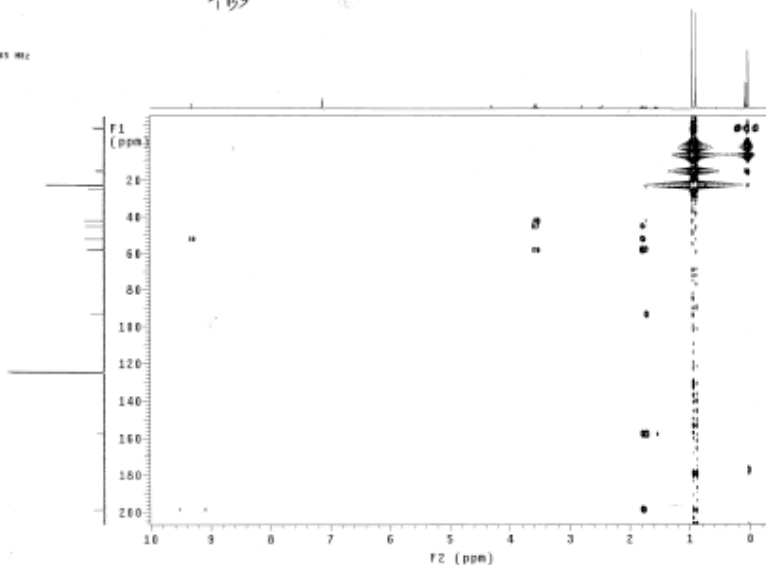
Spectrum O 2D COSY NMR of 2.16 endo (part 2)

20-000-1766-72-0000
 Data Collected on:
 400-MERCUY400
 Archive directory:
 /export/home/jhuang/wmwy/data
 Sample directory:
 File: qhmqc
 Pulse Sequence: qhmqc
 Solvent: Benzene
 Temp: 25.0 C / 298.1 K
 Relax delay: 1.000 sec
 Acq. time: 0.150 sec
 Width: 4166.7 Hz
 2D Width: 22221.4 Hz
 4 repetitions
 1 x 64 increments
 ORIGIN: HI, 400.1218885 MHz
 PROCESSED: C13, 100.6207176 MHz
 Power: 10 dB
 on during acquisition
 off during delay
 GMP-1 disabled
 DATA PROCESSING
 Sg. size: 6411 x 1.00 sec
 Skipped by: 0.150 sec
 F2: 100.6207176 MHz
 Sg. size: 6411 x 0.020 sec
 Skipped by: 0.020 sec
 F1: size: 1024 x 2.000
 Total time: 11 min



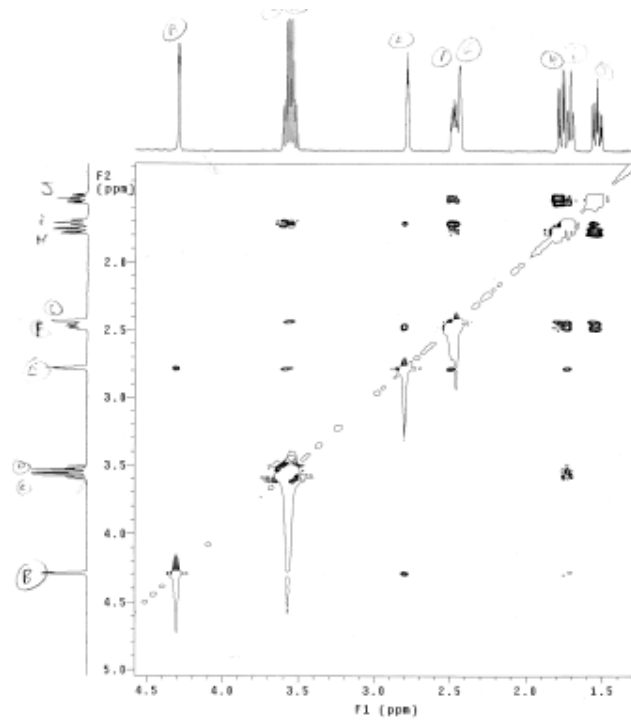
Spectrum P 2D HMQC NMR of 2.16 endo

20-000-1766-72-0000
 Data Collected on:
 400-MERCUY400
 Archive directory:
 /export/home/jhuang/wmwy/data
 Sample directory:
 File: qhmbc
 Pulse Sequence: qhmbc
 Solvent: Benzene
 Temp: 25.0 C / 298.1 K
 Relax delay: 1.000 sec
 Acq. time: 0.150 sec
 Width: 4166.7 Hz
 2D Width: 22221.4 Hz
 4 repetitions
 128 increments
 ORIGIN: HI, 400.1218885 MHz
 DATA PROCESSING
 Sine bell: 0.075 sec
 F2: 100.6207176 MHz
 Sine bell: 0.060 sec
 F1: size: 1024 x 2.040
 Total time: 12 min



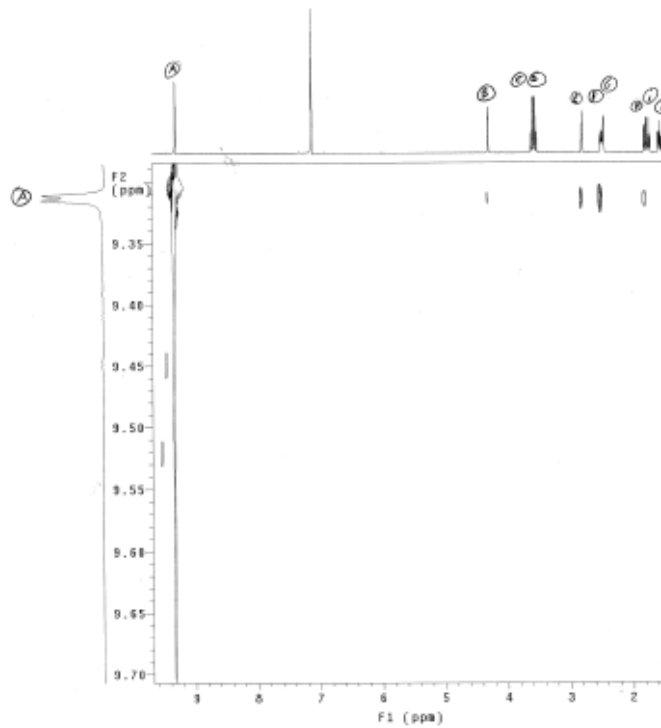
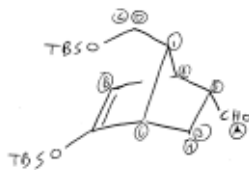
Spectrum Q 2D HMBC NMR Of 2.16 endo

20-044-FR68-72-NOESY
 Data Collected on:
 msl0-mercury400
 Archive directory:
 .report/home/jhuang/vnmrpy/data
 Sample directory:
 File: NOESY
 Pulse Sequence: NOESY
 Solvent: Benzene
 Temp: 25.4 C / 298.1 K
 Relax. delay: 2.000 sec
 Mixing: 0.700 sec
 Acq. Time: 0.150 sec
 Width: 4166.7 Hz
 2D Width: 4166.7 Hz
 4 repetitions
 2 x 256 increments
 CHANNEL: H1, 400.121965 MHz
 DATA PROCESSING
 Sg. time shift: 0.150 sec
 Shifted by: -0.150 sec
 F1 SFO: 400.121965 MHz
 Sg. time shift: 0.056 sec
 Shifted by: -0.056 sec
 FT size: 4096 x 4096
 Total time: 1 hr, 44 min



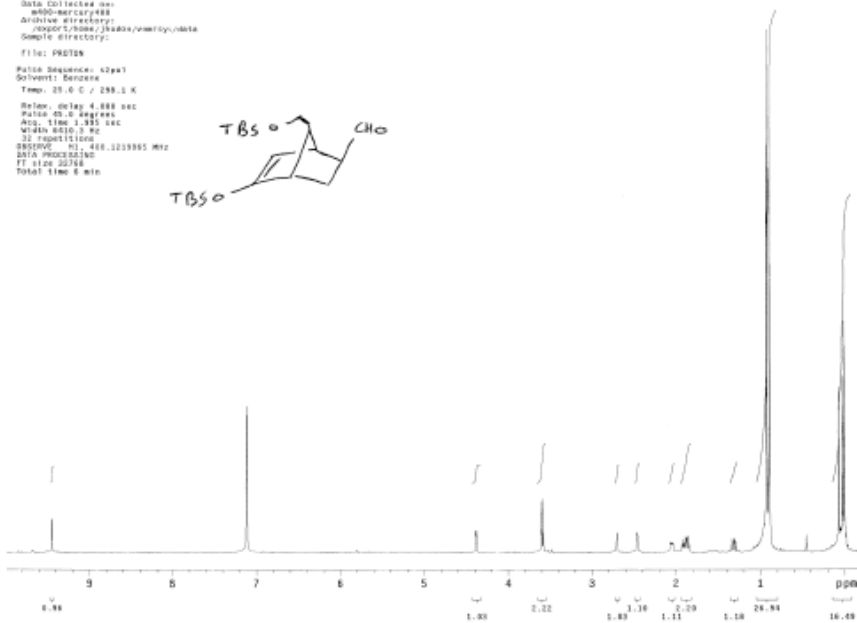
Spectrum R 2D NOESY NMR of 2.16 endo (part 1)

20-044-FR68-73-NOESY
 Data Collected on:
 msl0-mercury400
 Archive directory:
 .report/home/jhuang/vnmrpy/data
 Sample directory:
 File: NOESY
 Pulse Sequence: NOESY
 Solvent: Benzene
 Temp: 25.3 C / 298.1 K
 Relax. delay: 2.000 sec
 Mixing: 0.700 sec
 Acq. Time: 0.150 sec
 Width: 4166.7 Hz
 2D Width: 4166.7 Hz
 4 repetitions
 2 x 256 increments
 CHANNEL: H1, 400.121965 MHz
 DATA PROCESSING
 Sg. time shift: 0.150 sec
 Shifted by: -0.150 sec
 F1 SFO: 400.121965 MHz
 Sg. time shift: 0.096 sec
 Shifted by: -0.096 sec
 FT size: 4096 x 4096
 Total time: 1 hr, 44 min



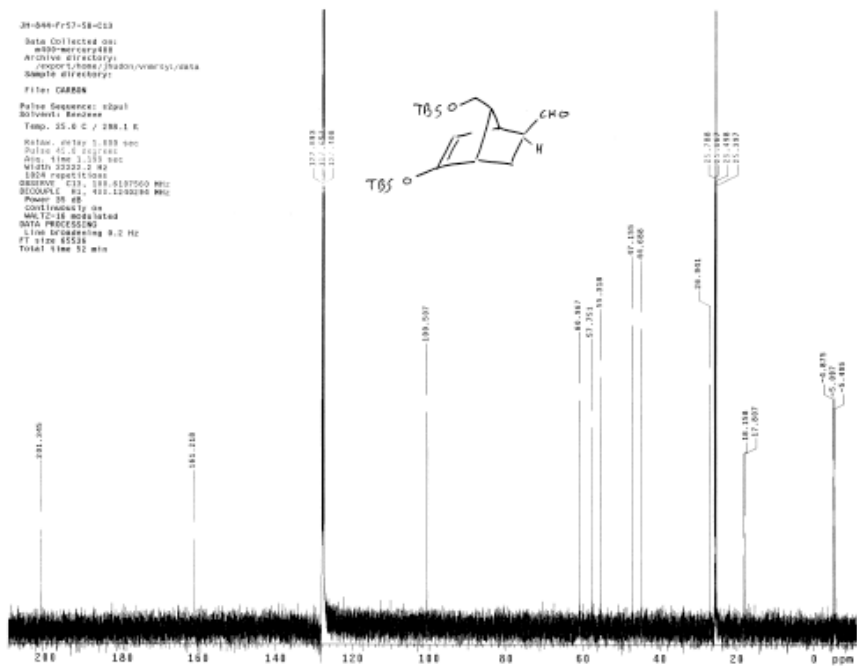
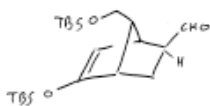
Spectrum S 2D NOESY NMR of 2.16 endo (part 2)

JH-046-Fr57-58
 Data Collected on:
 m90-mercury400
 Analysis directory:
 _export/home/jh046/vw/rsy/data
 Sample directory:
 File: P00708
 Pulse Sequence: zgpg30
 Solvent: Benzene
 Temp: 29.0 C / 299.1 K
 Relax: delay 4.000 sec
 Pulse: 12.0 degrees
 Acq. time 1.395 sec
 Width 6553.0 Hz
 32 repetitions
 OBSERVE: H1, 400.323395 MHz
 DATA PROCESSING
 FT size 22784
 Total time 8 min



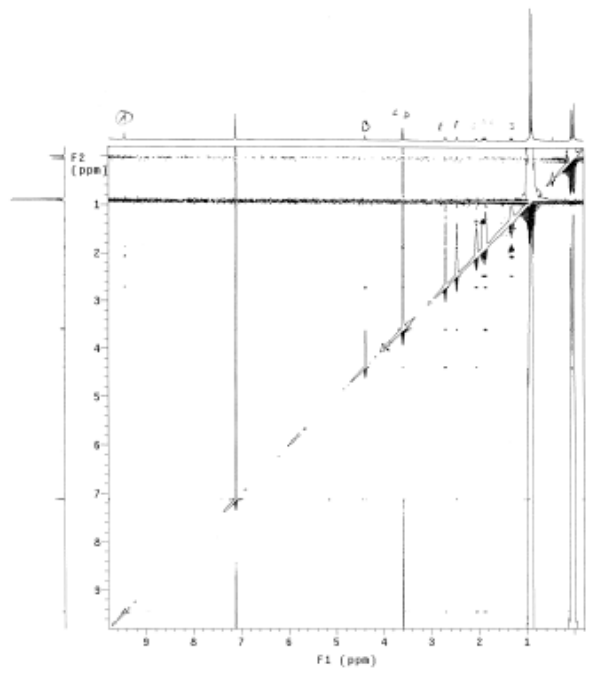
Spectrum T ¹H NMR of 2.16 exo

JH-046-Fr57-58-013
 Data Collected on:
 m90-mercury400
 Analysis directory:
 _export/home/jh046/vw/rsy/data
 Sample directory:
 File: C0008
 Pulse Sequence: zgpg30
 Solvent: Benzene
 Temp: 29.0 C / 299.1 K
 Relax: delay 1.000 sec
 Pulse: 45.0 degrees
 Acq. time 1.395 sec
 Width 32282.2 Hz
 328 repetitions
 OBSERVE: C13, 101.6197500 MHz
 SOLVENT: H1, 400.323395 MHz
 Power: 28 dB
 Continuum by on
 MSLT-18 H051614
 DATA PROCESSING
 1 line expanding 9.2 Hz
 FT size 85538
 Total time 32 min



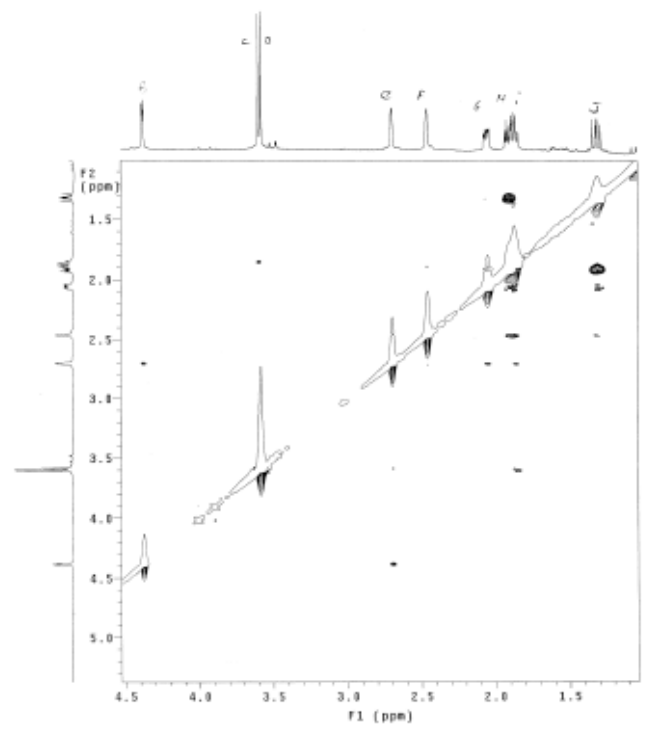
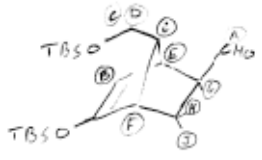
Spectrum U ¹³C NMR of 2.16 exo

JH-046-F157-58-NOESY
 Date Collected on: 4/20/2004
 Archive directory: report/home/jhadon/vnmrxy/data
 Sample directory:
 File: NOESY
 Pulse Sequence: NOESY
 Solvent: Benzene
 Temp: 25.8 C / 298.1 K
 Relax. delay: 2.000 sec
 Mixing: 0.750 sec
 Acq. Time: 0.150 sec
 Width: 4000.0 Hz
 TD: 65536
 SFO: 400.136363 MHz
 # repetitions: 4
 2 x 154 increments
 OBSERVE: H1, 400.136363 MHz
 DATA PROCESSING
 Sg. size: 6411 x 150 sec
 Shifted by: -0.150 sec
 F1 DATA PROCESSING
 Sg. size: 6411 x 150 sec
 Shifted by: -0.150 sec
 FT size: 4096 x 4096
 Total time: 1 hr, 44 min

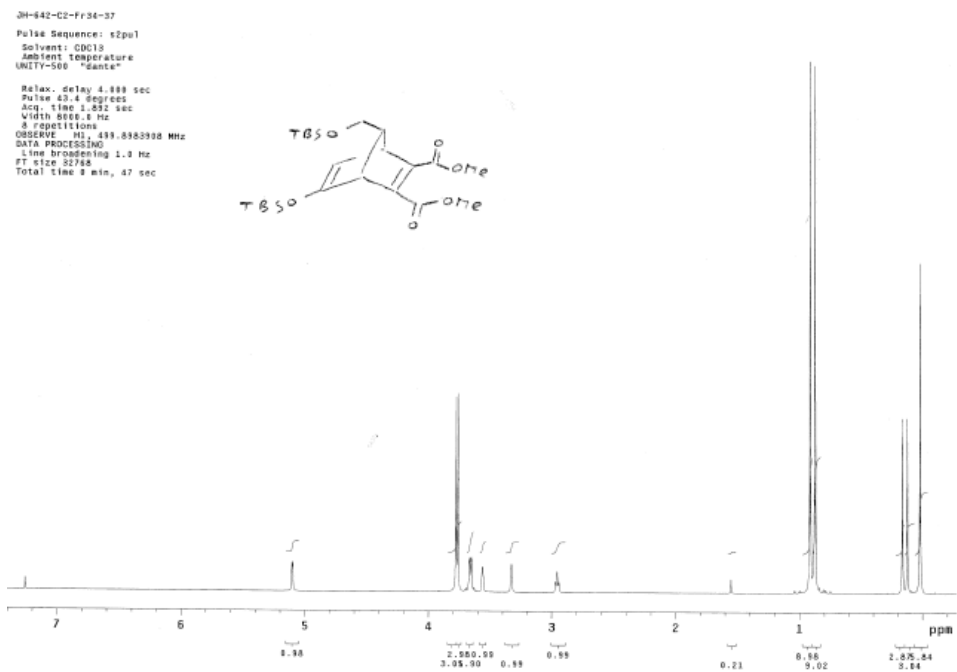


Spectrum V 2D NOESY NMR of 2.16 exo (part 1)

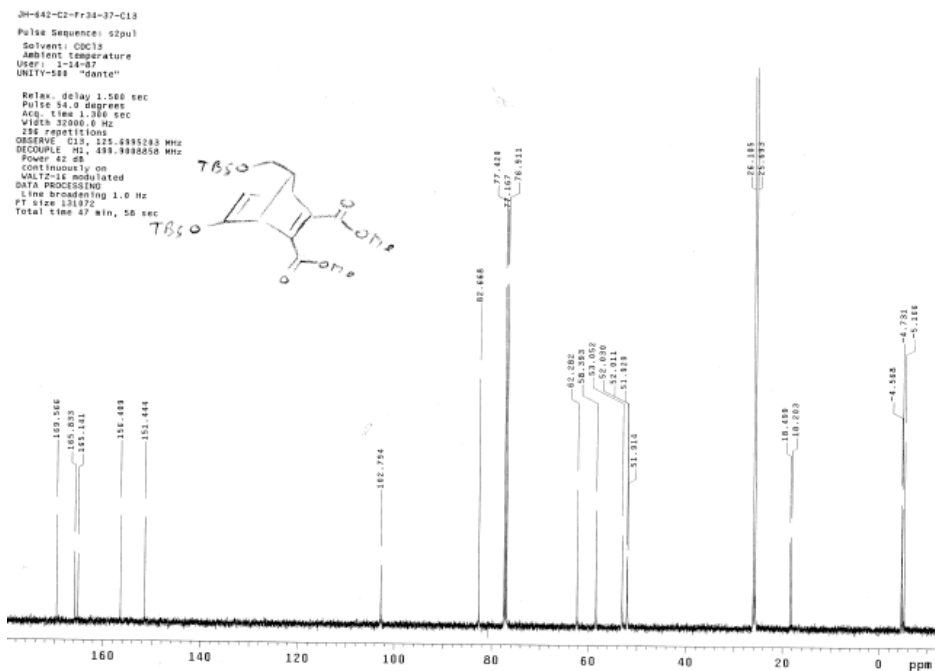
JH-046-F157-58-NOESY
 Date Collected on: 4/20/2004
 Archive directory: report/home/jhadon/vnmrxy/data
 Sample directory:
 File: NOESY
 Pulse Sequence: NOESY
 Solvent: Benzene
 Temp: 25.0 C / 298.1 K
 Relax. delay: 2.000 sec
 Mixing: 0.750 sec
 Acq. Time: 0.150 sec
 Width: 4000.0 Hz
 TD: 65536
 SFO: 400.136363 MHz
 # repetitions: 4
 2 x 154 increments
 OBSERVE: H1, 400.136363 MHz
 DATA PROCESSING
 Sg. size: 6411 x 150 sec
 Shifted by: -0.150 sec
 F1 DATA PROCESSING
 Sg. size: 6411 x 150 sec
 Shifted by: -0.150 sec
 FT size: 4096 x 4096
 Total time: 1 hr, 44 min



Spectrum W 2D NOESY NMR of 2.16 exo (part 2)

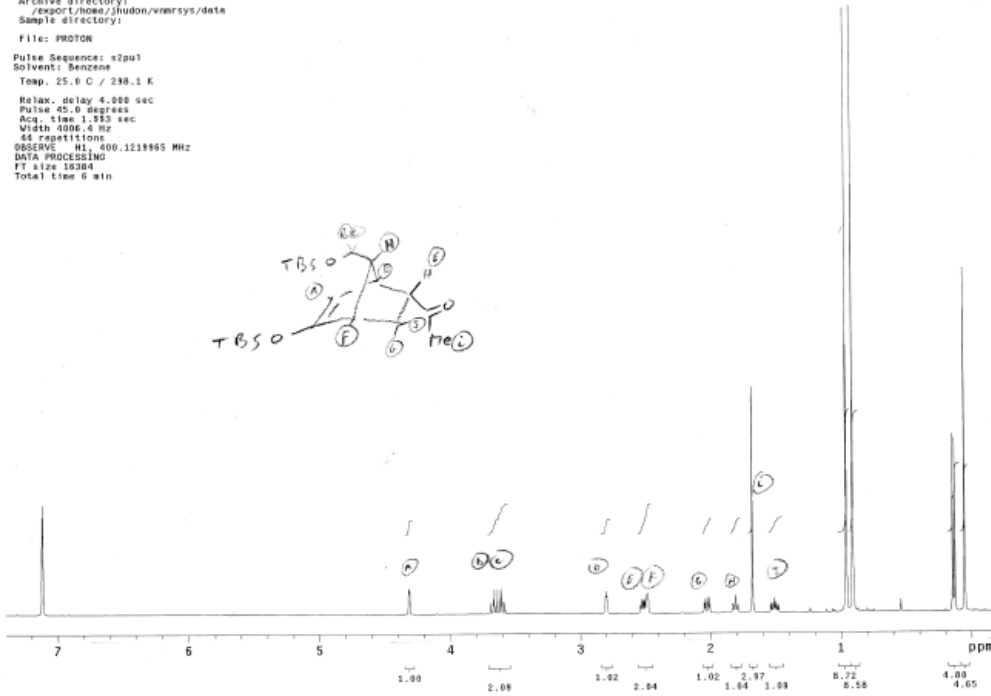


Spectrum X ¹H NMR of 2.22



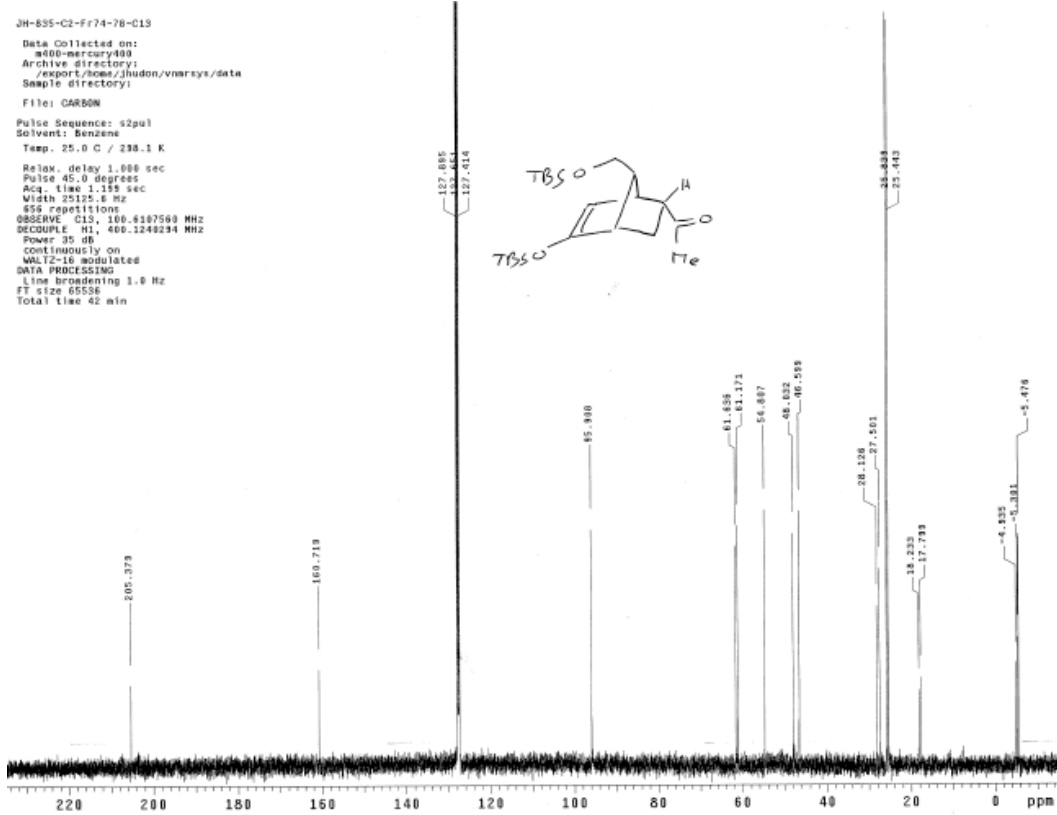
Spectrum Y ¹³C NMR of 2.22

JH-835-C2-Fr74-78
 Data Collected on:
 m488-mercury400
 Archive directory:
 /export/home/jhudon/vnmrsys/data
 Sample directory:
 File: PROTON
 Pulse Sequence: s2pu1
 Solvent: Benzene
 Temp. 25.0 C / 298.1 K
 Relax. delay 4.000 sec
 Pulse 45.0 degrees
 Acq. time 1.533 sec
 Width 9006.4 Hz
 44 repetitions
 OBSERVE H1, 400.1218965 MHz
 DATA PROCESSING
 FT size 16384
 Total time 5 min

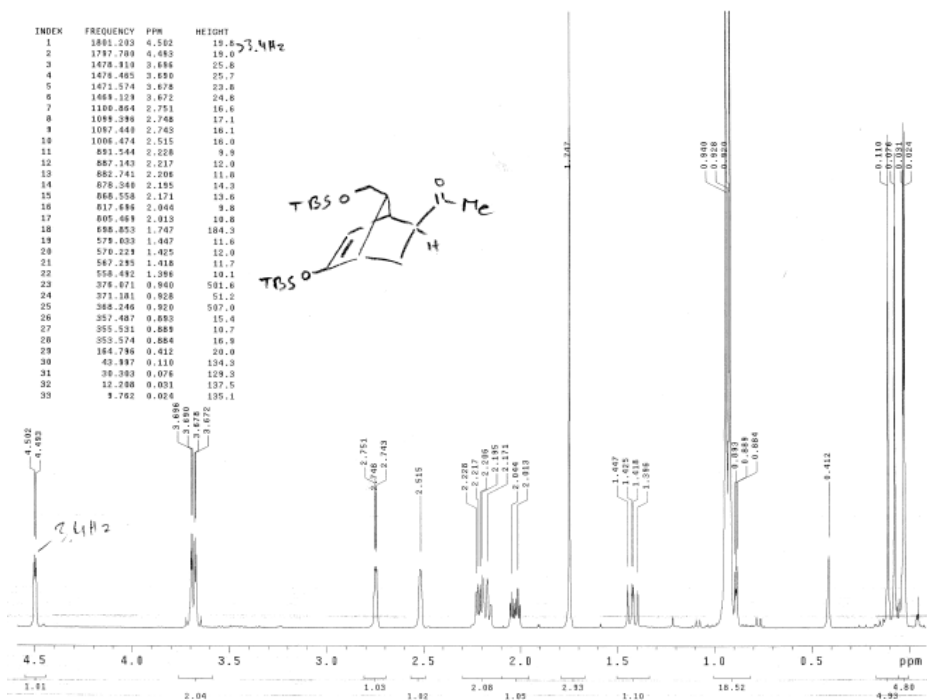


Spectrum Z ¹H NMR of 2.23 endo

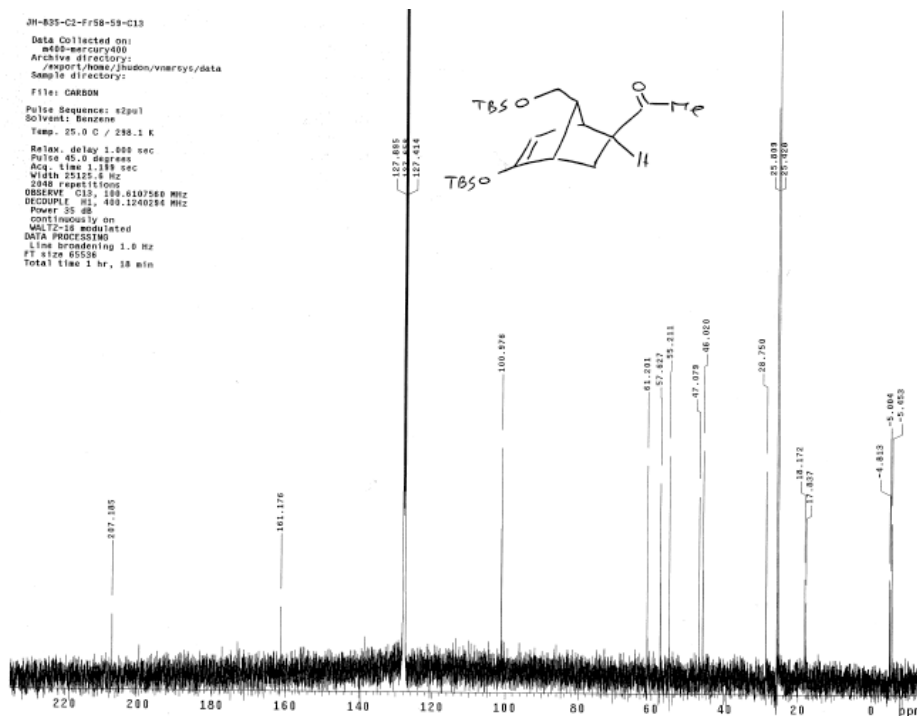
JH-835-C2-Fr74-78-C13
 Data Collected on:
 m488-mercury400
 Archive directory:
 /export/home/jhudon/vnmrsys/data
 Sample directory:
 File: CARBON
 Pulse Sequence: s2pu1
 Solvent: Benzene
 Temp. 25.0 C / 298.1 K
 Relax. delay 1.000 sec
 Pulse 45.0 degrees
 Acq. time 1.135 sec
 Width 25125.8 Hz
 555 repetitions
 OBSERVE C13, 100.6187560 MHz
 DECOUPLE H1, 400.1248294 MHz
 Power 35 db
 continuously on
 WALTZ-16 modulated
 DATA PROCESSING
 Line broadening 1.0 Hz
 FT size 65536
 Total time 42 min



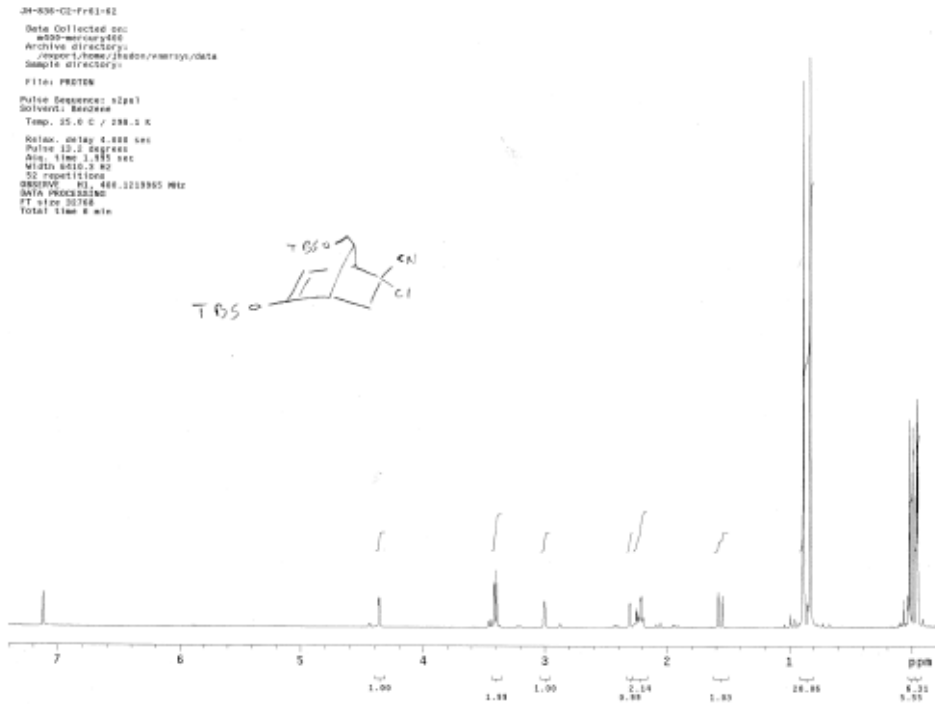
Spectrum AA ¹³C NMR of 2.23 endo



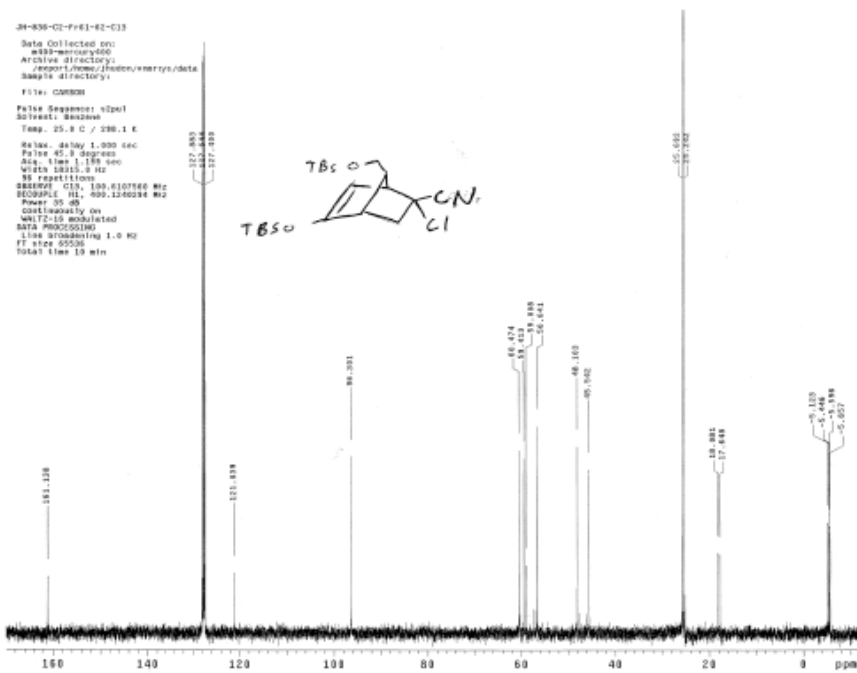
Spectrum BB ^1H NMR of 2.23 exo



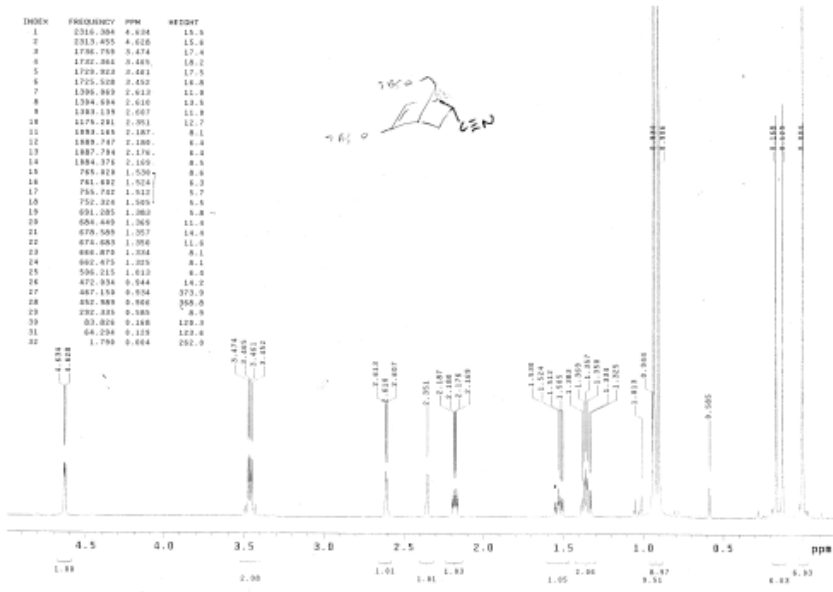
Spectrum CC ^{13}C NMR of 2.23 exo



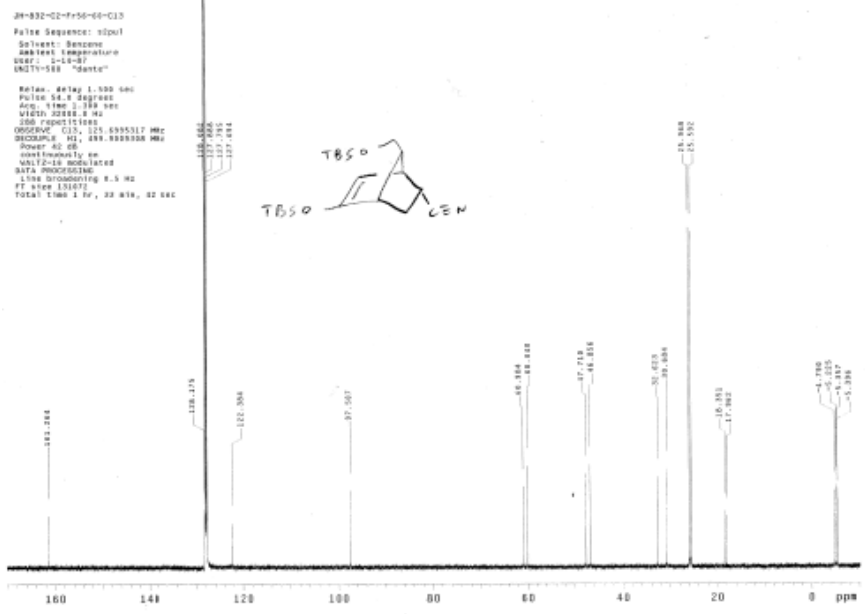
Spectrum DD ^1H NMR of 2.24 exo



Spectrum EE ^{13}C NMR of 2.24 exo

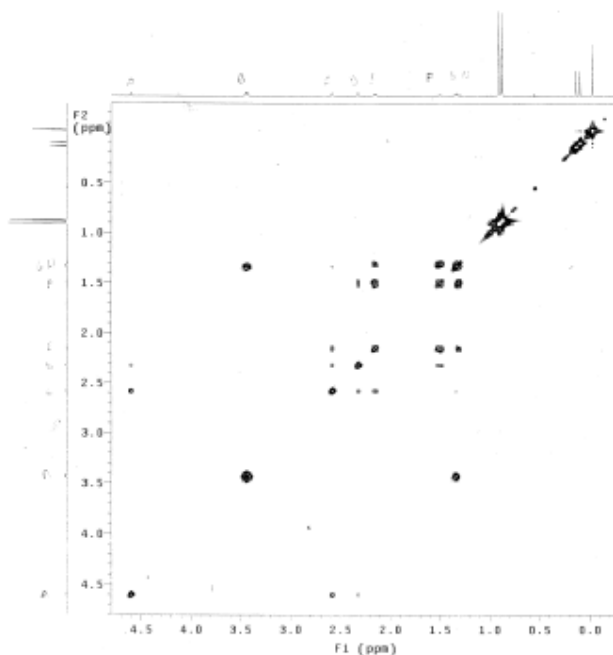
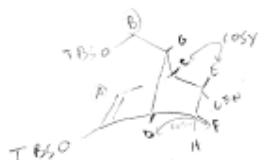


Spectrum FF ¹H NMR of 2.25 endo



Spectrum GG ¹³C NMR of 2.25 endo

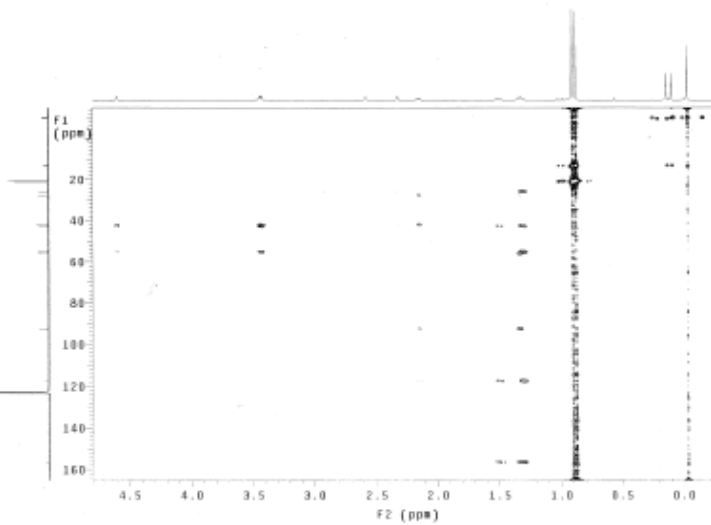
STANDARD PROTON PARAMETERS
 Pulse Sequence: gpcsy
 Solvent: Benzene
 Ambient Temperature
 NS01-000 "danta"
 Relax. delay 1.000 sec
 Acq. time 0.201 sec
 VPROB 2DPR010 Hz
 2D WIDTH 2048.0 Hz
 S REPERTITIONS
 S2 REPERTITIONS
 OBSERVE H1, 499.0564350 MHz
 DATA PROCESSING
 Size 8k11 0.100 sec
 F1 DATA PROCESSING
 Size 8k11 0.050 sec
 F1 size 2048 x 2048
 Total time 23 min, 30 sec



Spectrum HH 2D COSY NMR of 2.25 endo

STANDARD PROTON PARAMETERS
 Pulse Sequence: gpmc
 Solvent: Benzene
 Ambient Temperature
 User: 214-01
 UNITY-000 "danta"
 Relax. delay 1.000 sec
 Acq. time 0.201 sec
 VPROB 2DPR010 Hz
 2D WIDTH 2280.1 Hz
 S REPERTITIONS
 S2 REPERTITIONS
 OBSERVE H1, 499.0564350 MHz
 DATA PROCESSING
 Size 8k11 0.100 sec
 F1 DATA PROCESSING
 Size 8k11 0.050 sec
 F1 size 2048 x 4096
 Total time 44 min, 43 sec

3H-83D-C2-F-56-60-HN6C



Spectrum II 2D HMBC NMR of 2.25 endo

24-832-CI-F156-00-NOESY

Pulse Sequence: NOESY

Software: MARIANA

Temp: 25.0 C / 290.1 K

UNITY-500 "delta"

Relax. delay 2.000 sec

Mixing 0.700 sec

Acq. time 0.200 sec

NUC1 201.0 MHz

2D Width 2547.0 Hz

0 repetitions

2 x 204 increments

OSSEKVC H1.459.0004358 MHz

DATA PROCESSING

SI. SINE DELT 0.001 sec

Swapped by -0.201 sec

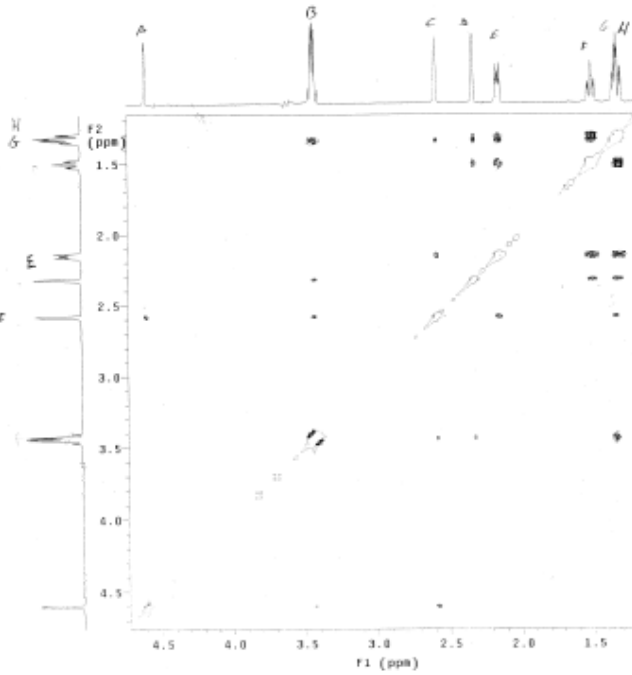
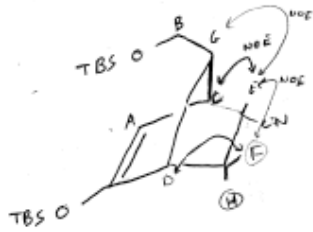
F1 SINE MODULATED

Sq. sine delT 0.157 sec

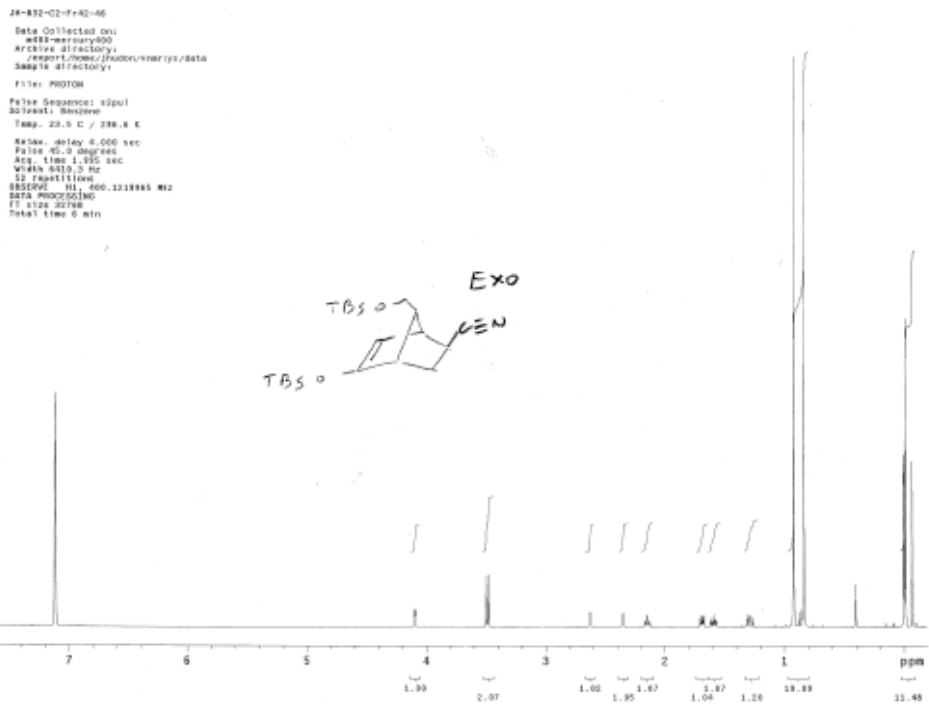
Swapped by -0.157 sec

F2 SINE MODULATED

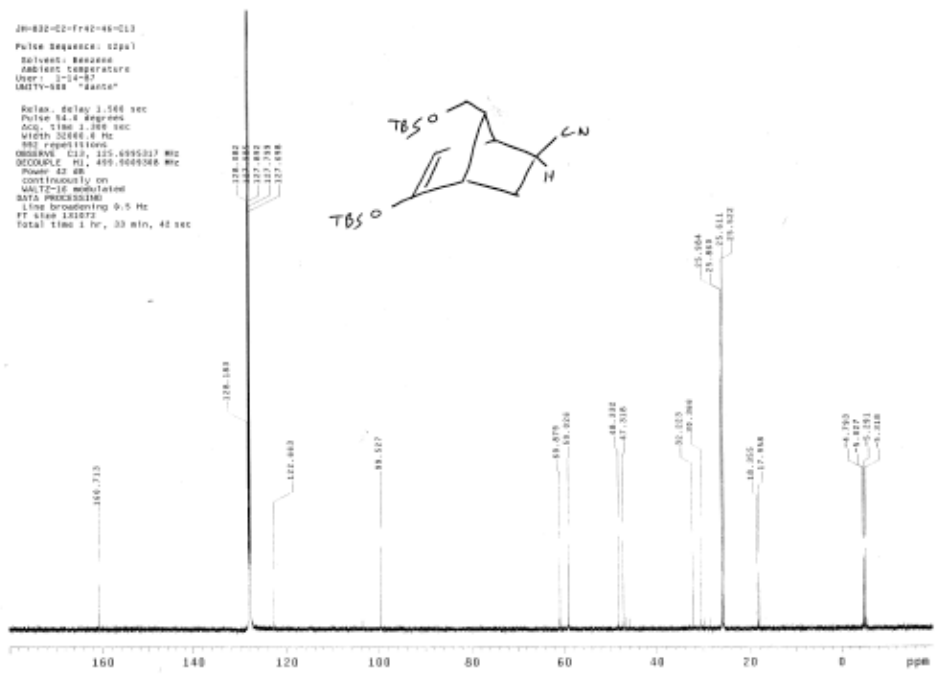
Total time 3 hr, 24 min, 0 sec



Spectrum JJ 2D NOESY NMR of 2.25 endo



Spectrum KK ¹H NMR of 2.25 exo

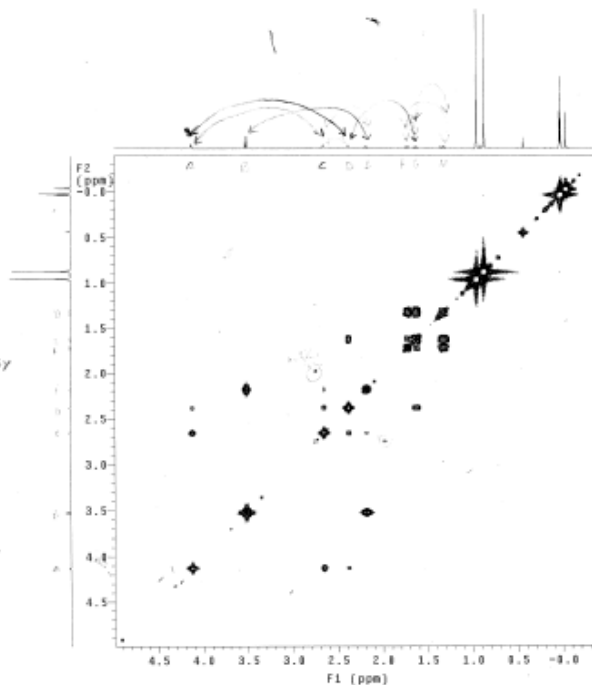
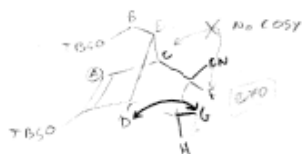


Spectrum LL ¹³C NMR of 2.25 exo

```

24-832-C2-F102-08-COSY
Data Collected on:
m60-mrcaisy00
Archive directory:
...expert/home/jfrabon/mrcaisy/data
Sample directory:
File: gCOSY
Pulse Sequence: gCOSY
Solvent: Benzene
Temp: 26.4 C / 299.1 K
Relax: delay 1.900 sec
AQ: 0.186 s 8.00 sec
Width: 2355.2 Hz
2D Width: 2355.2 Hz
0 repetitions
128 increments
OSCILL: 49.1218031 MHz
DATA PROCESSING:
Sfr: sine bell 8.875 sec
F1 (DATA PROCESSING)
Sfr: sine bell 8.935 sec
FT size 2048 x 2048
Total time 22 min

```



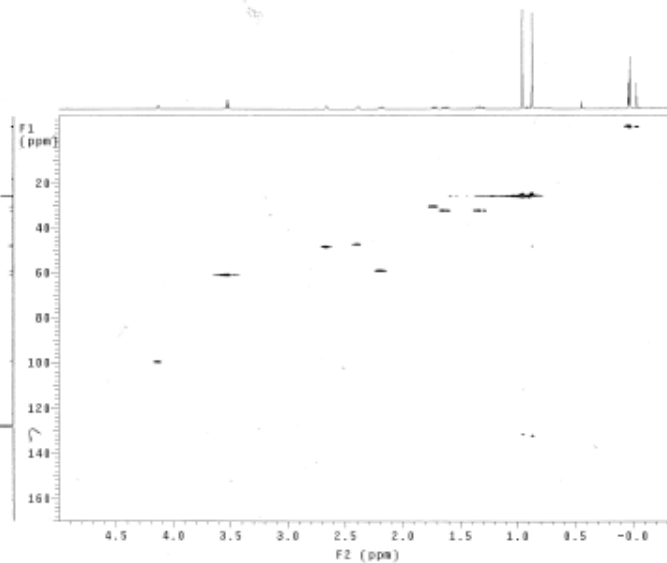
Spectrum MM 2D COSY NMR of 2.25 exo

24-832-C2-F102-08 - HMQC

```

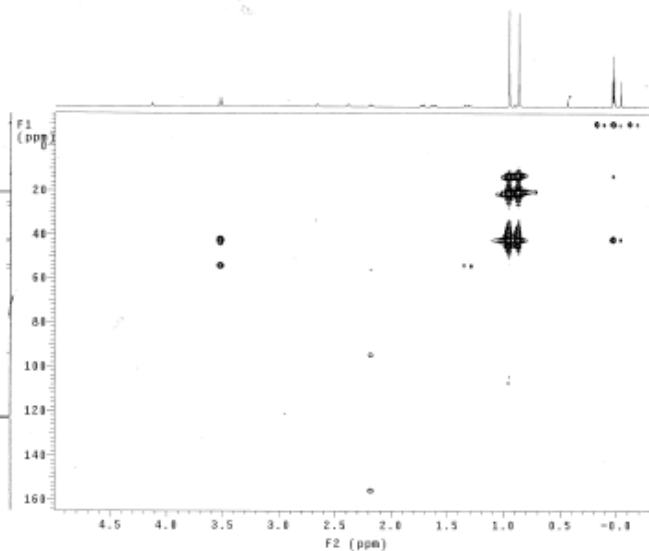
Data Collected on:
m60-mrcaisy00
Archive directory:
...expert/home/jfrabon/mrcaisy/data
Sample directory:
File: gHMQC
Pulse Sequence: gHMQC
Solvent: Benzene
Temp: 26.0 C / 299.2 K
Water: delay 1.000 sec
AQ: 1.186 s 15.00 sec
Width: 2355.2 Hz
2D Width: 1833.4 Hz
0 repetitions
2 x 128 increments
OSCILL: 49.1218031 MHz
RECOUPLE C13: 150.6187882 MHz
Power: 52 dB
on during acquisition
off during delay
GMP-1 modulation
DATA PROCESSING:
Sfr: sine bell 8.350 sec
Shifted by -0.250 sec
F1 (DATA PROCESSING)
Sfr: sine bell 8.828 sec
Shifted by -0.828 sec
FT size 512 x 2048
Total time 45 min

```



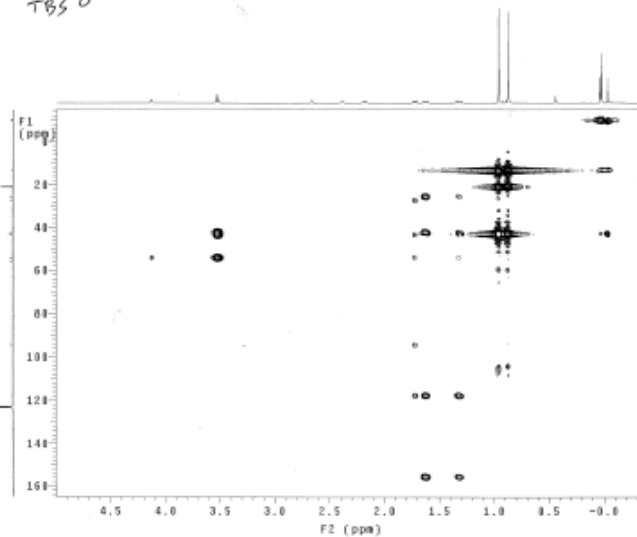
Spectrum NN 2D HMQC NMR of 2.25 exo

24-832-C2-Fr42-46-4662
 Data Collected on:
 m88-mercury400
 Archive directory:
 /report/home/1/haase/vmwr01/data
 Sample directory:
 File: g886C
 Pulse Sequence: gHMBC
 Solvent: Me2SO-d
 Temp. 29.8 C / 283.1 K
 Relax. delay 1.000 sec
 Acq. time 8.150 sec
 Width 2155.2 Hz
 2D Width 2815.8 Hz
 8 repetitions
 128 increments
 OBSERVE H1 400.121833 MHz
 DATA PROCESSING
 Size 8x11 0.276 sec
 F1 DATA PROCESSING
 Size 8x11 0.004 sec
 F1 Size 812 x 1048
 Total time 22 min



Spectrum OO 2D HMBC NMR of 2.25 endo

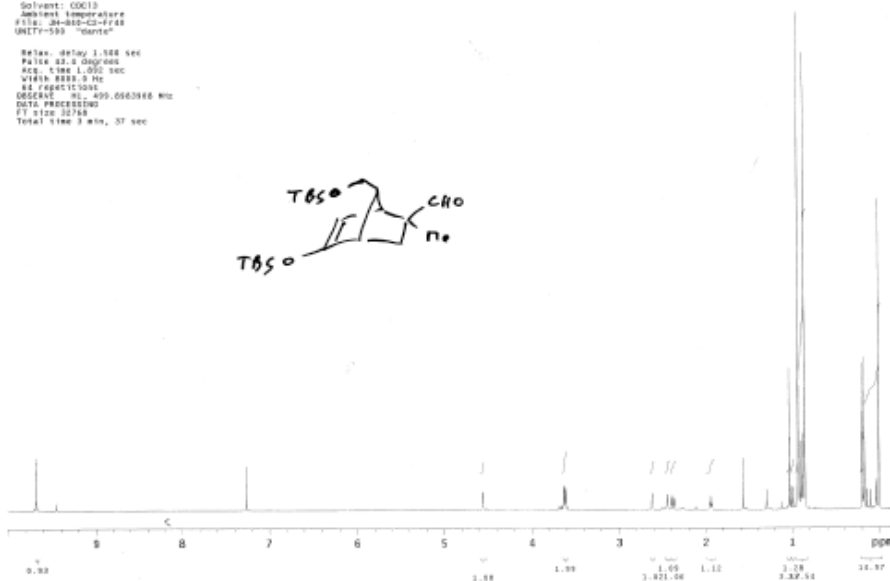
24-832-C2-Fr42-46-4662-longcoupling - {
 Data Collected on:
 m88-mercury400
 Archive directory:
 /report/home/1/haase/vmwr01/data
 Sample directory:
 File: g886C
 Pulse Sequence: gHMBC
 Solvent: Me2SO-d
 Temp. 29.8 C / 283.1 K
 Relax. delay 1.000 sec
 Acq. time 9.150 sec
 Width 2155.2 Hz
 2D Width 2815.8 Hz
 8 repetitions
 128 increments
 OBSERVE H1 400.121833 MHz
 DATA PROCESSING
 Size 8x11 0.276 sec
 F1 DATA PROCESSING
 Size 8x11 0.004 sec
 F1 Size 812 x 1048
 Total time 25 min



Spectrum PP 2D HMBC long range (3-5 bonds coupling) of 2.25 exo

JH-049-C2-Fr48
 Pulse Sequence: szpa1
 Solvent: CDCl3
 Ambient Temperature
 File: JH-049-C2-Fr48
 UNITS: 100 "hz"

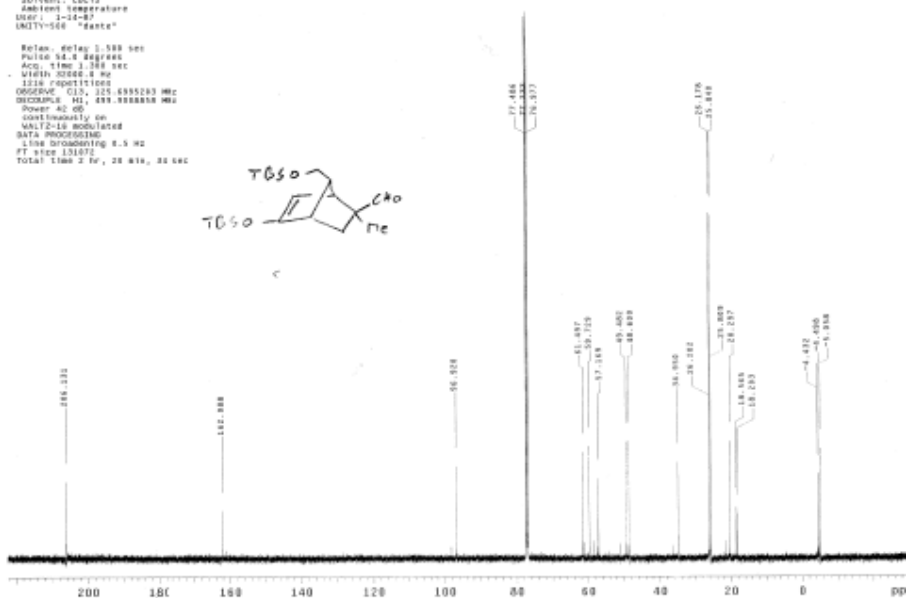
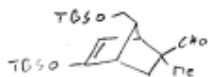
Relax. delay 1.000 sec
 Pulse 22.5 degrees
 Acq. time 1.000 sec
 Width 8000.0 Hz
 #2 REPEATS: 300
 OBSERVE: H1, 499.800360 MHz
 DATA PROCESSING
 FT size 32768
 Total time 3 min, 37 sec



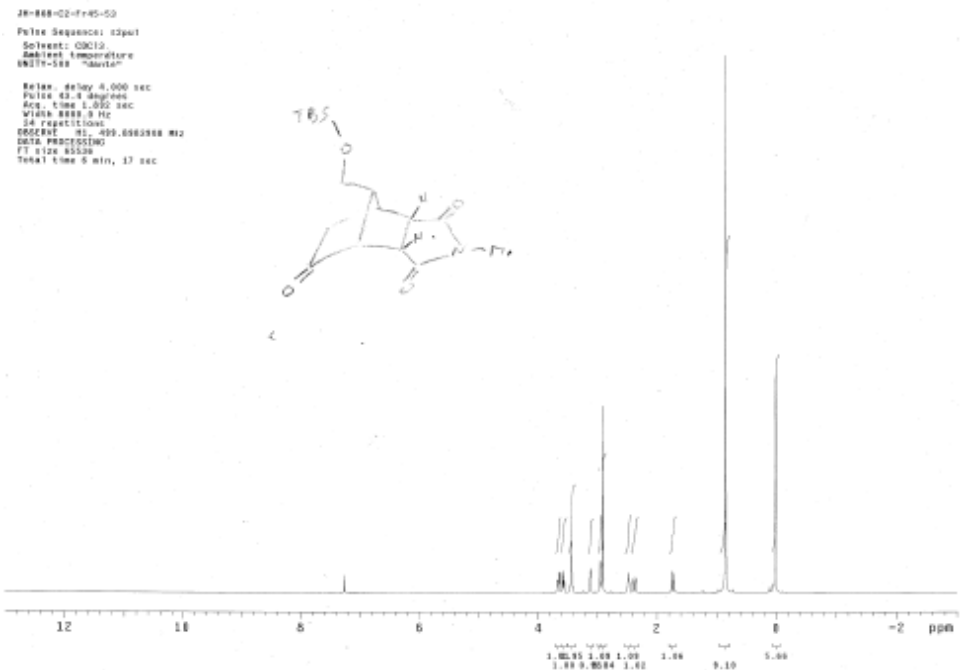
Spectrum QQ ¹H NMR of 2.27 exo

JH-048-C2-Fr8-CL3
 Pulse Sequence: szpa1
 Solvent: CDCl3
 Ambient Temperature
 User: j-14-87
 UNITS: 500 "hz"

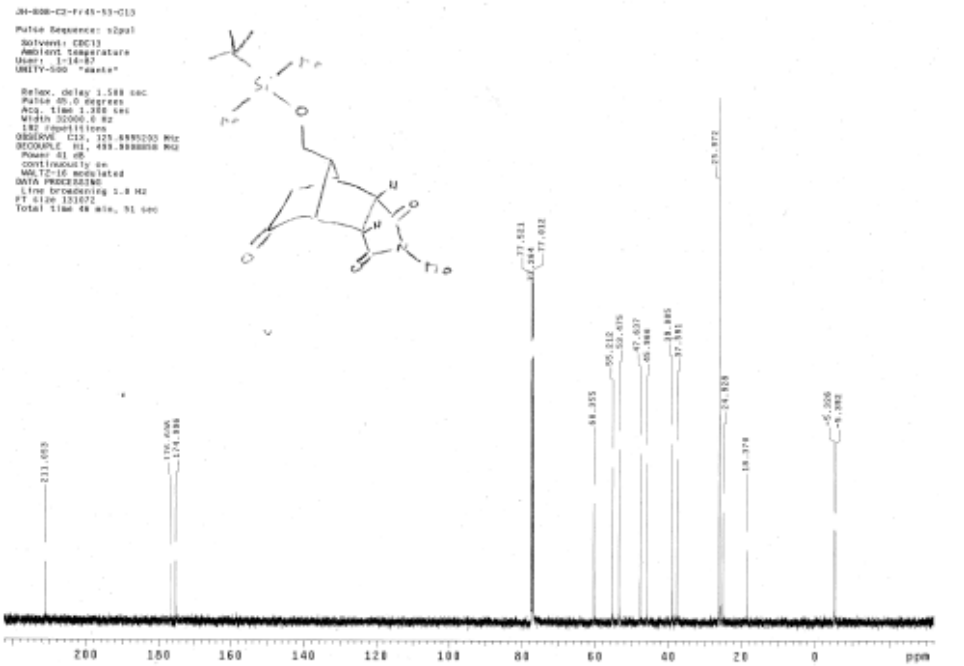
Relax. delay 1.500 sec
 Pulse 22.5 degrees
 Acq. time 2.368 sec
 Width 10000.0 Hz
 #128 REPEATS: 300
 OBSERVE: C13, 125.835133 MHz
 OBSERVE: H1, 499.800360 MHz
 Power: 40.00
 Continuously on
 MALTZ-16 MODULATED
 DATA PROCESSING
 Line broadening 0.5 Hz
 FT size 131072
 Total time 2 hr, 28 min, 30 sec



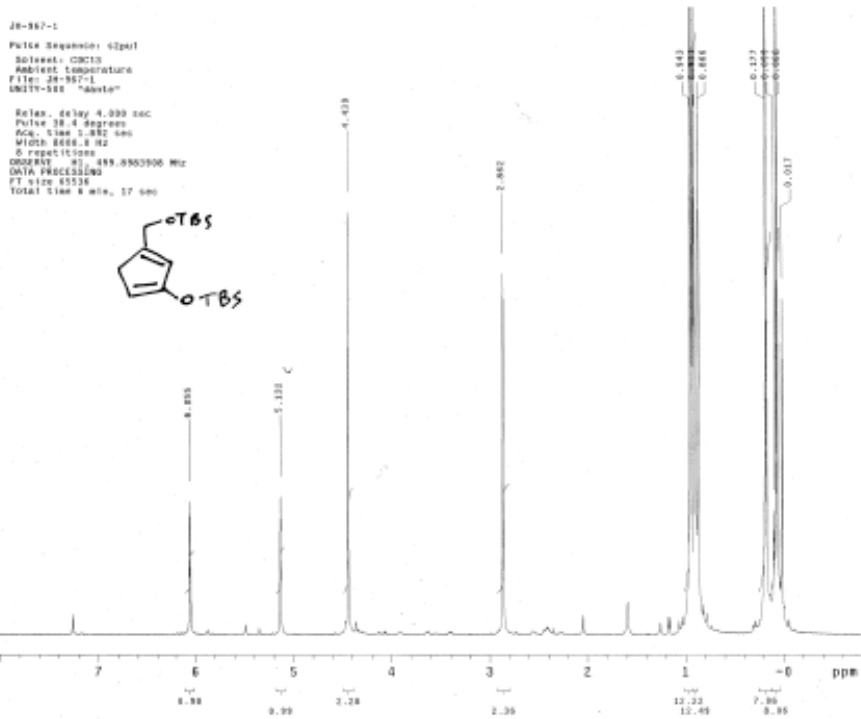
Spectrum RR ¹³C NMR of 2.27 exo



Spectrum SS ¹H NMR of 2.49

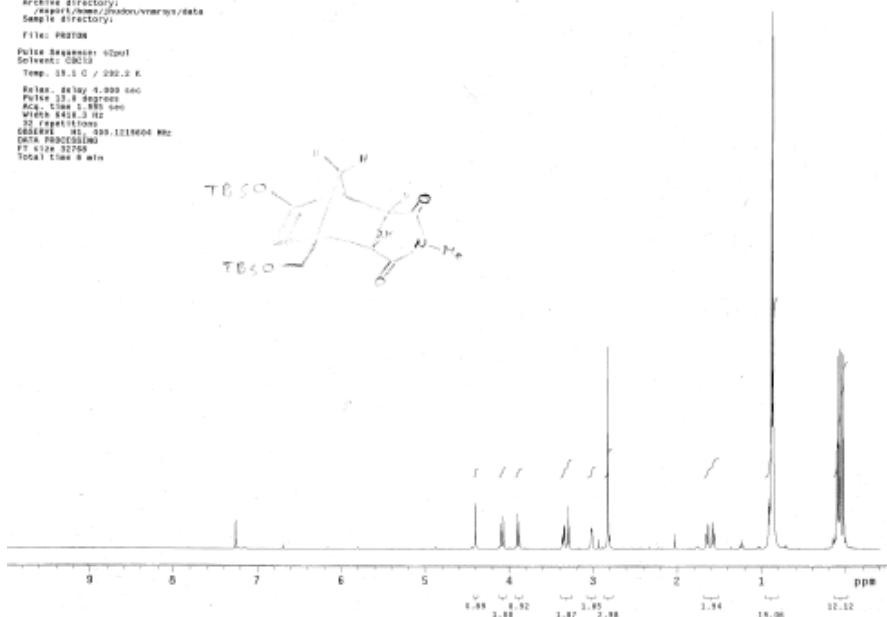


Spectrum TT ¹³C NMR of 2.49



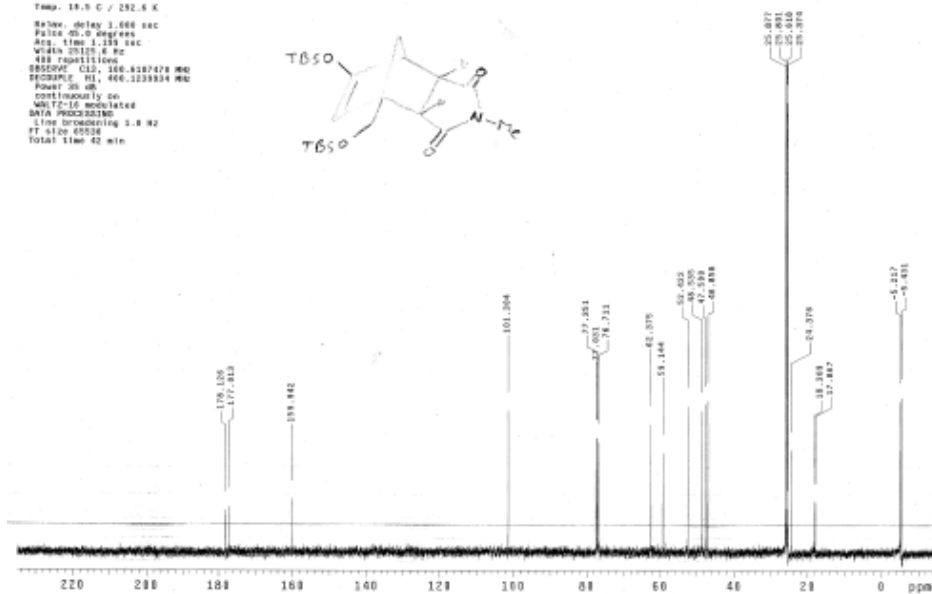
Spectrum UU ¹H NMR of 2.10

20-348-F762-93-120_Exp
 Date Collected: 01/18/93
 Archive directory: /export/home/jjwinn/vnmr/93/data
 Sample directory:
 File: F7620M
 Pulse Sequence: zgpg30
 Solvent: CDCl3
 Temp: 19.5 C / 292.2 K
 Relax. delay: 4.000 sec
 Pulse: 12.0 degrees
 Acq. time: 1.300 sec
 Width: 6402.3 Hz
 32 repetitions
 OBSERVED: 400.101600 MHz
 Data Processing:
 FT size: 32768
 Total time: 9 min

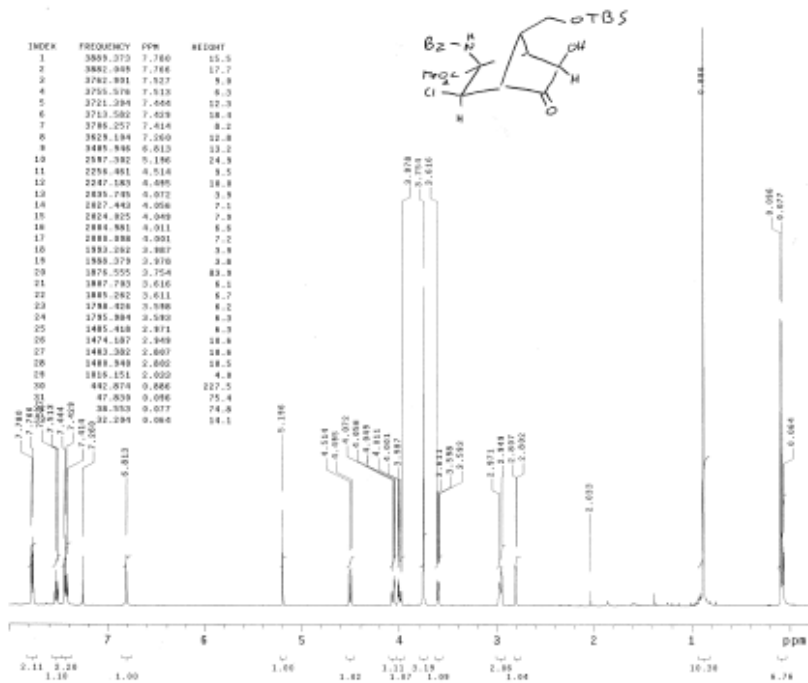


Spectrum VV ¹H NMR of 2.50

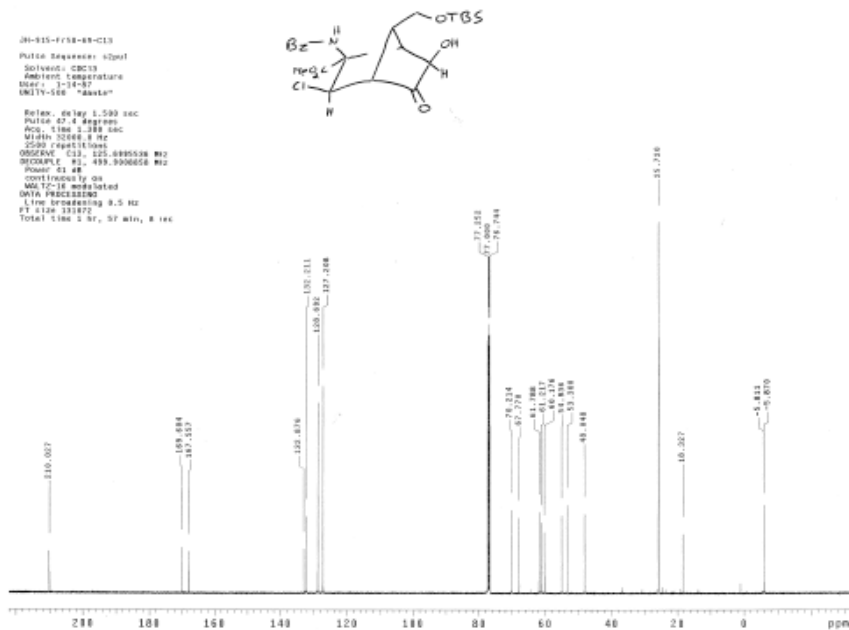
20-348-F762-93-120_Exp
 Date Collected: 01/18/93
 Archive directory: /export/home/jjwinn/vnmr/93/data
 Sample directory:
 File: F7620M
 Pulse Sequence: zgpg30
 Solvent: CDCl3
 Temp: 19.5 C / 292.2 K
 Relax. delay: 3.000 sec
 Pulse: 12.0 degrees
 Acq. time: 1.193 sec
 Width: 6402.3 Hz
 488 repetitions
 OBSERVED: 400.101600 MHz
 Data Processing:
 FT size: 32768
 Total time: 42 min



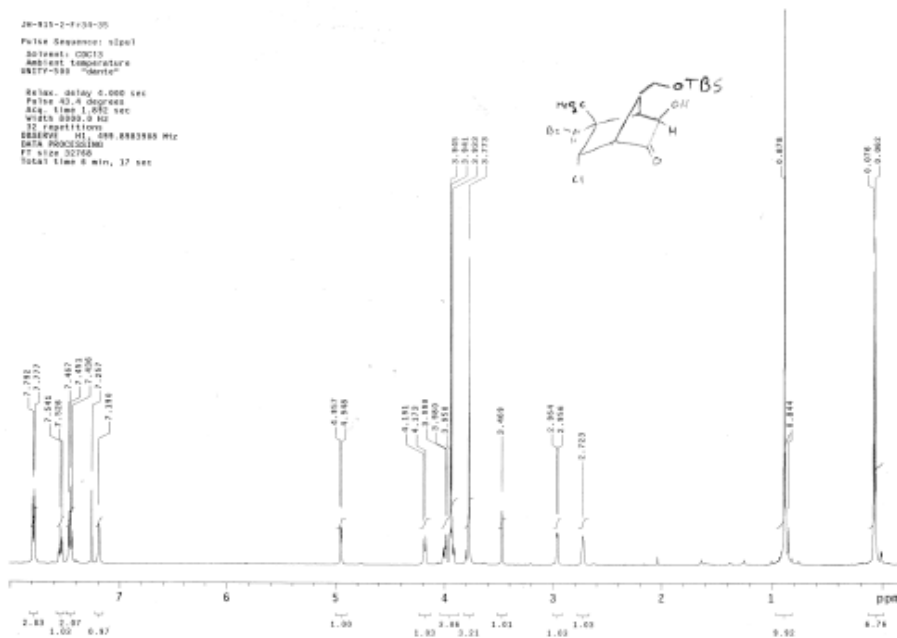
Spectrum WW ¹³C NMR of 2.50



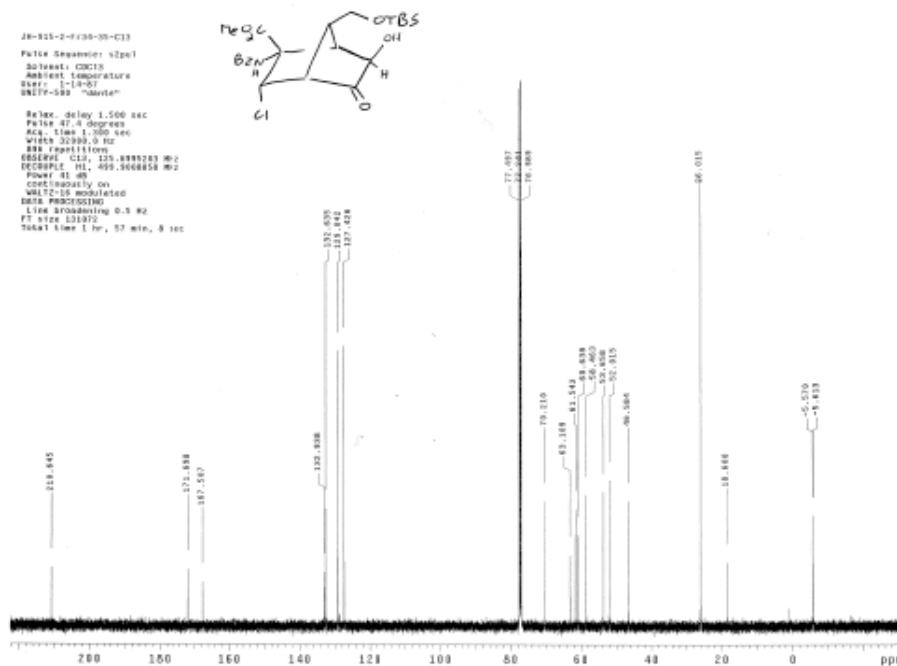
Spectrum XX ¹H NMR of 3.24



Spectrum YY ¹³C NMR of 3.24



Spectrum ZZ ^1H NMR of 3.23

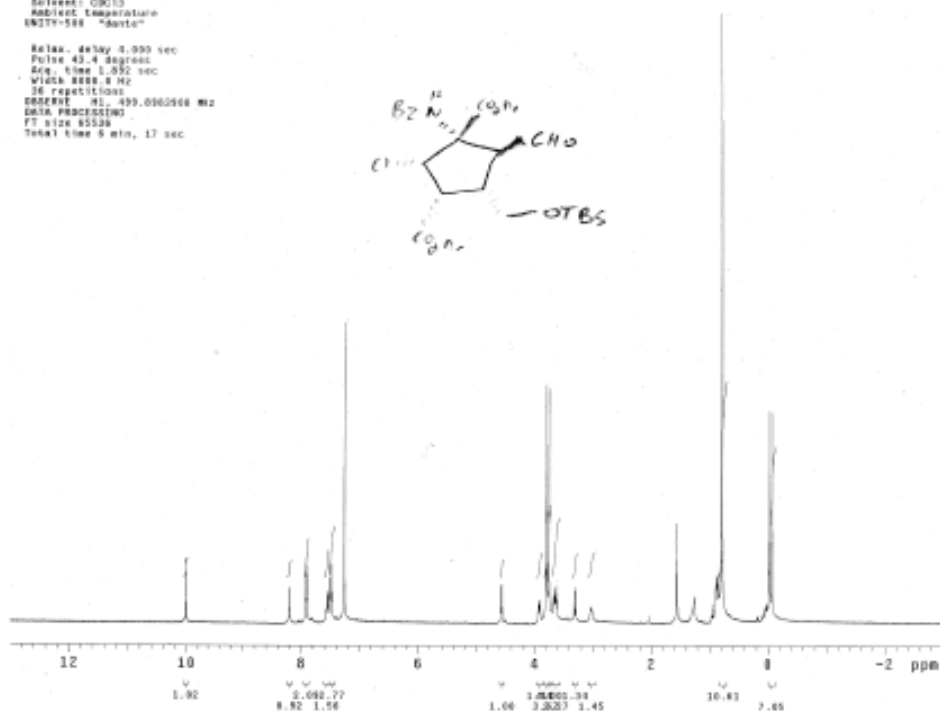


Spectrum AAA ^{13}C NMR of 3.23

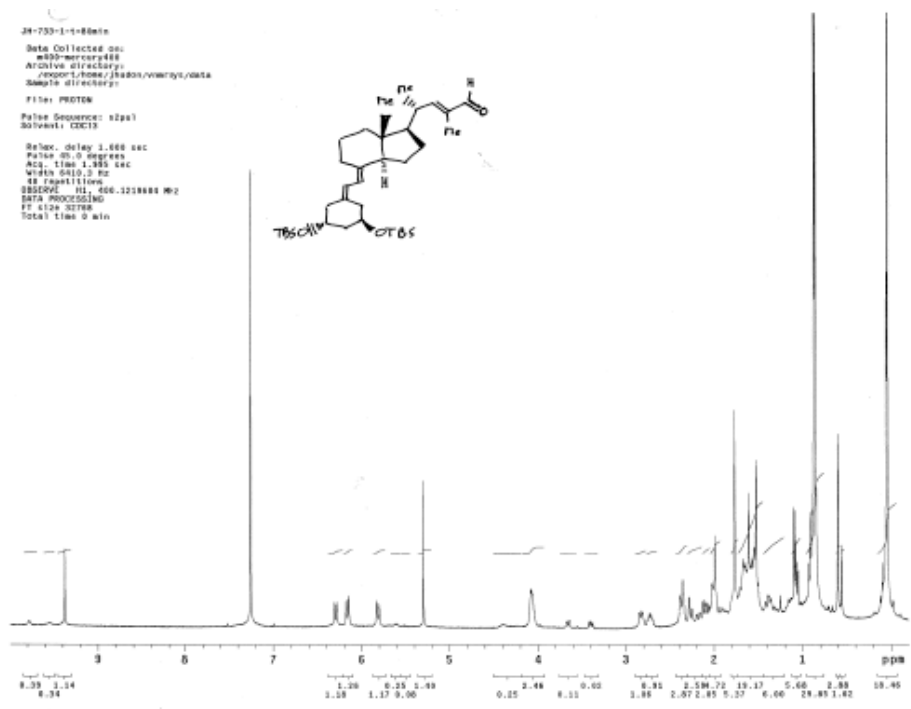
20-048-03-F11-16

Pulse Sequence: zgpg30
Solvent: CDCl3
Acquire Temperature
400MHz-500 "delta"

Relax. delay 0.500 sec
Pulse 42.4 degree
Acq. time 1.050 sec
Width 8888.0 Hz
35 repetitions
CONCENT 41.409.0000000 MHz
DATA PROCESSING
FT size 65536
Total time 9 min, 17 sec

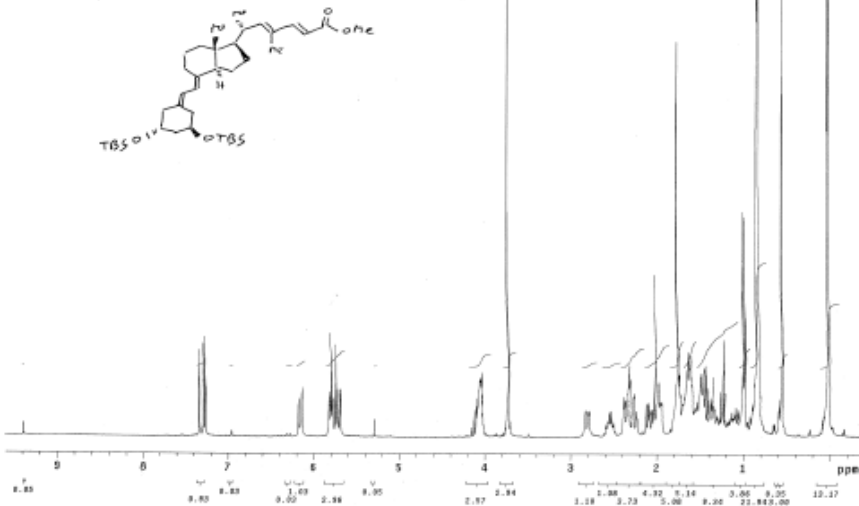


Spectrum DDD ¹H NMR of 3.27



Spectrum EEE ¹H NMR of 4.27

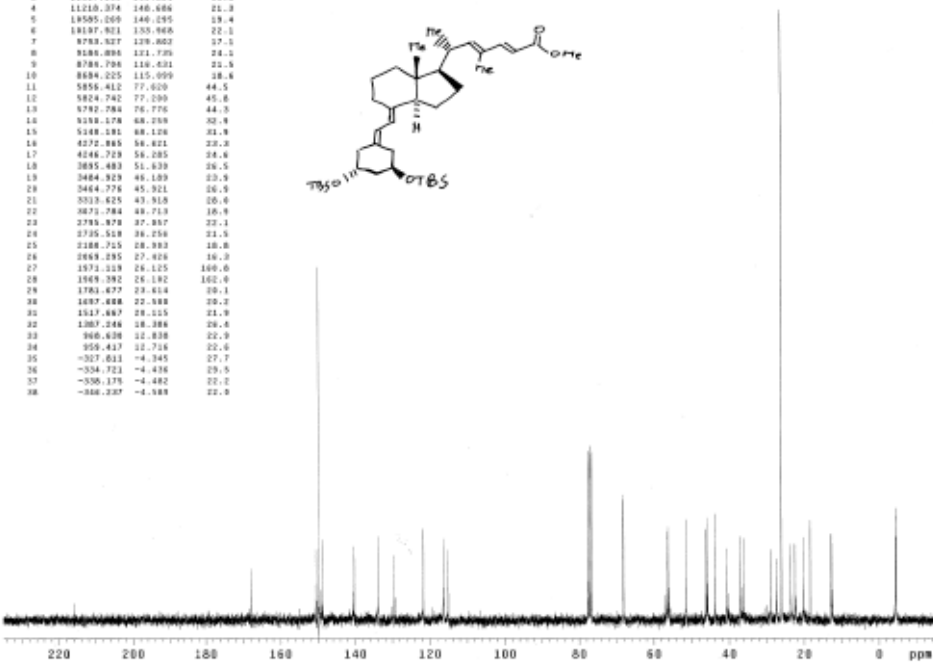
JN-734-G2-F60-06
 Pulse Sequence: zgpg30
 Solvent: CDCl3
 Solvent Temperature: Mercury-200 "None"
 Relax: delay 1.000 sec
 Pulse 1: 9.000 sec
 Acq: time 1.000 sec
 VISTA: 4000.0 Hz
 64 repetitions
 SCHEDULE: 01_300_0548000 Hz
 DATA PROCESSING
 FT: size 32768
 Total Time 8 min, 0 sec



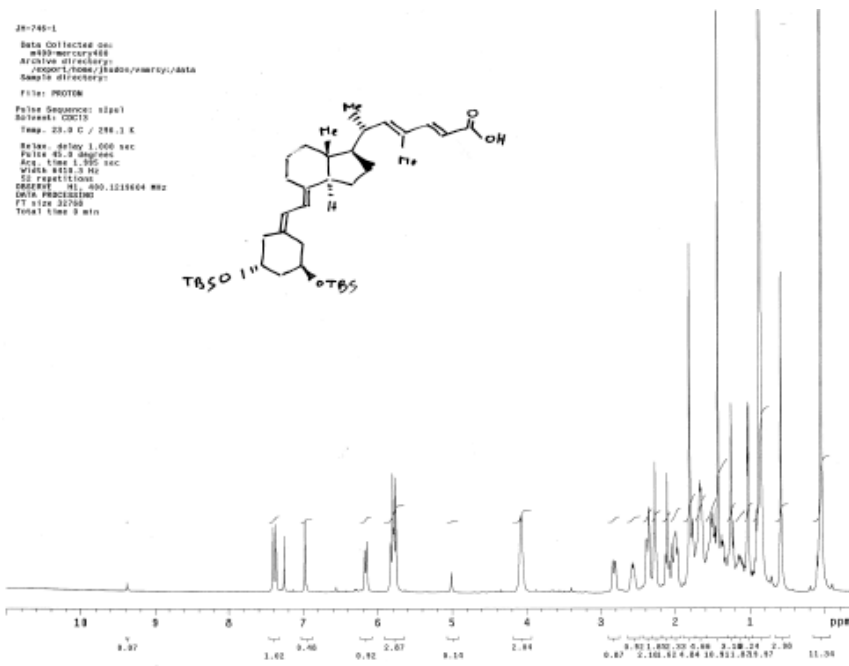
Spectrum FFF ¹H NMR of 4.28

✓

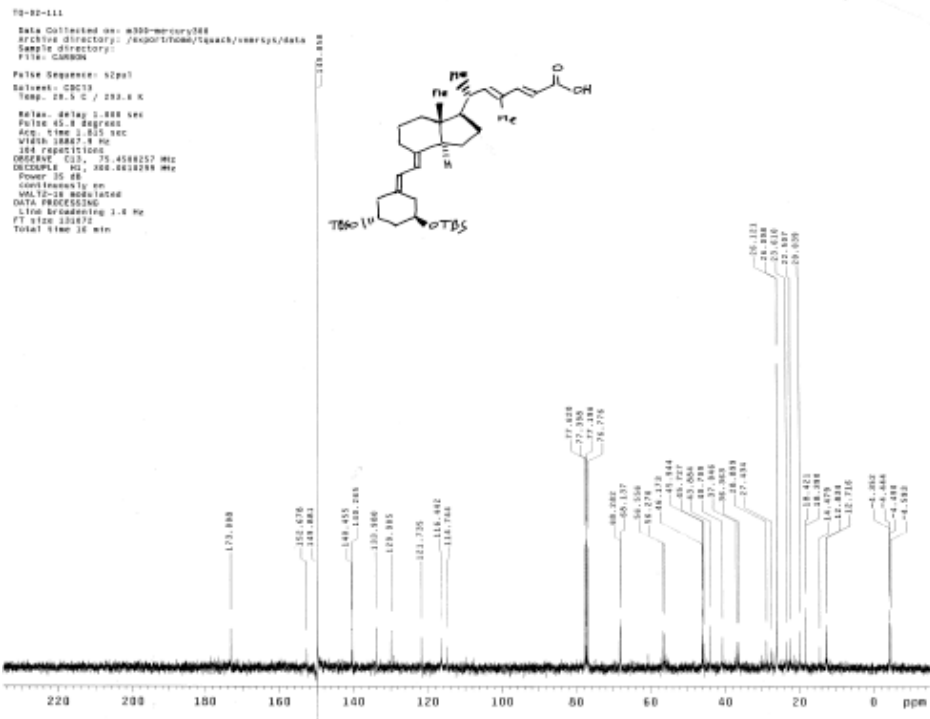
INDEX	FREQUENCY	PPM	HEIGHT
1	12879.634	169.648	19.9
2	11300.024	192.364	18.7
3	11201.009	189.881	82.3
4	11210.374	188.686	21.3
5	10505.009	140.295	19.4
6	10197.921	135.906	22.1
7	9793.527	129.802	17.1
8	9181.896	121.735	24.1
9	8781.798	116.231	21.5
10	8594.225	115.999	18.8
11	5856.412	77.020	44.5
12	5824.742	77.090	45.6
13	6782.784	76.776	44.3
14	5193.178	68.299	32.8
15	5189.181	68.138	31.9
16	4272.866	56.621	22.2
17	4246.729	56.285	24.6
18	3895.483	51.639	26.5
19	3464.329	46.189	23.9
20	3464.276	46.191	26.9
21	3033.625	43.918	20.0
22	3071.784	44.713	16.9
23	2783.874	37.387	22.1
24	2735.518	36.256	21.5
25	2388.715	28.393	18.8
26	2064.295	27.028	16.2
27	1971.119	26.125	166.0
28	1969.292	26.182	162.0
29	1761.677	23.614	20.1
30	1687.688	22.588	20.2
31	1517.687	20.115	21.9
32	1387.266	18.388	20.6
33	966.616	12.338	22.9
34	959.417	12.716	22.0
35	-327.613	-4.345	27.7
36	-334.721	-4.438	29.5
37	-336.176	-4.482	22.2
38	-346.237	-4.589	22.0



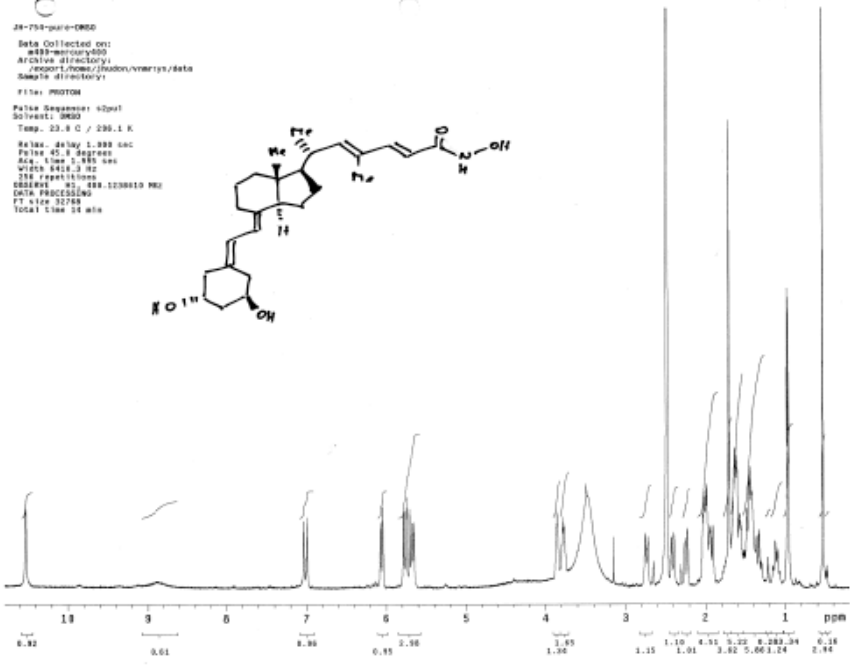
Spectrum GGG ¹³C NMR of 4.28



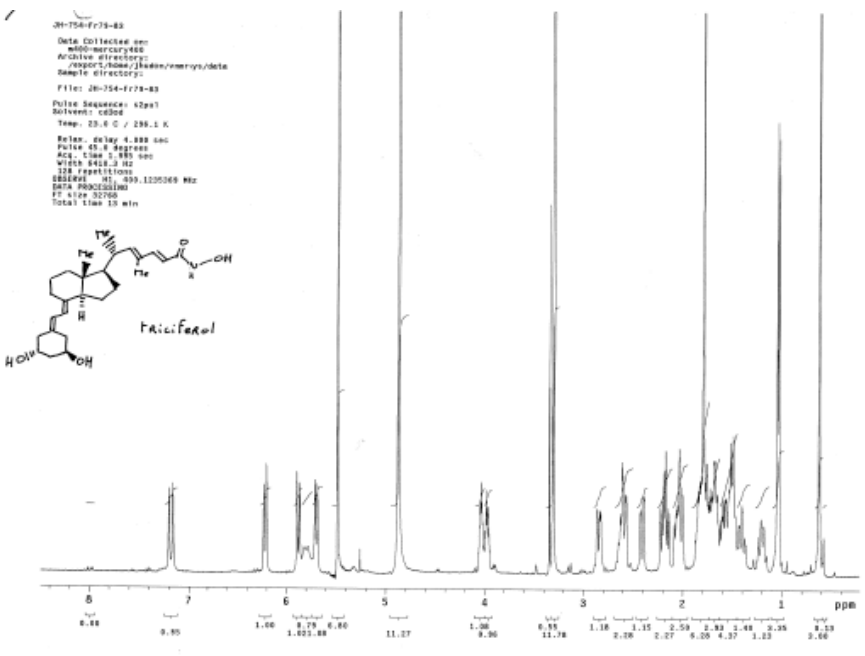
Spectrum HHH ¹H NMR of 4.29



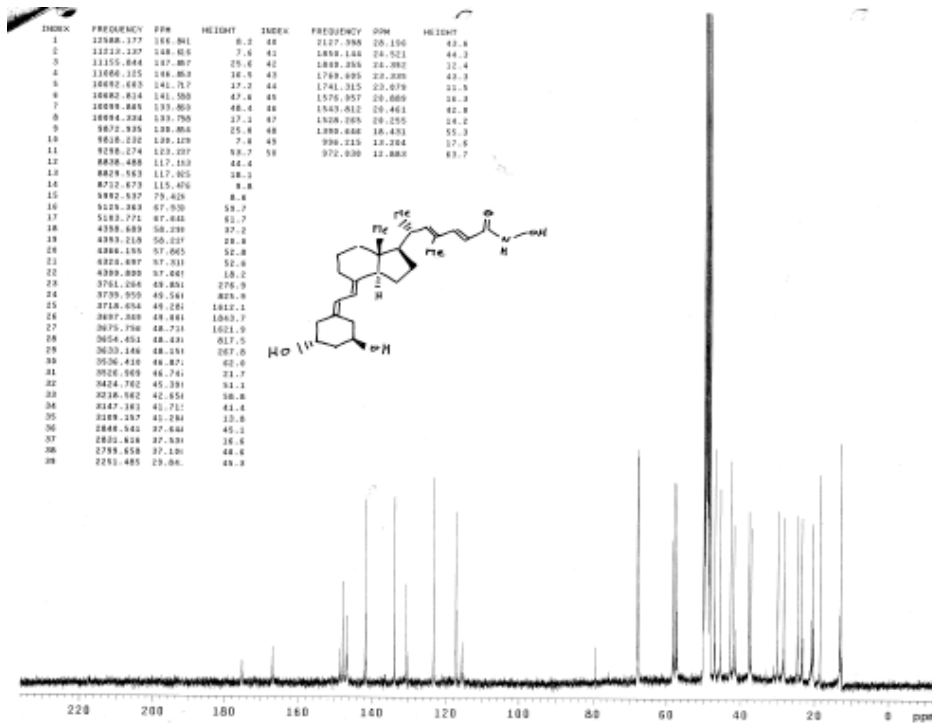
Spectrum III ¹³C NMR of 4.29



Spectrum JJJ ¹H NMR of triciferol 4.8 (in DMSO-d₆)



Spectrum KKK ¹H NMR of triciferol 4.8 (in MeOH-d₄)



Spectrum LLL ¹³C NMR of triciferol 4.8 (in MeOH-d₄)

10 Appendix 4 : Conversion of the calculated Activation Energies (Ea) for the 1,5-H shift of 2-substituted cyclopentadienes into a value suitable to perform a Hammett plot

A Hammett plot consists of a 2D graph where the ordinate = $\log(k_X/k_H)$ and abscissa = σ_{pX} .⁹⁵ The slope of the graph is the reaction constant ρ , which is a measure of how sensitive a reaction is to the effects of electronic perturbation. Since the Hammett sigma constants σ_{pX} are based on the dissociation of *para*-substituted benzoic acids in water at 25 °C, the reaction constant ρ for this benchmark reaction is therefore 1.00. Reactions with a more pronounced slope are therefore more sensitive than benzoic acid to electronic effects. Reactions with a positive slope are similar to benzoic acid in that electron-withdrawing groups accelerate the reaction and electron-donating groups slow down the reaction's rate. A reaction with a negative reaction constant would therefore be accelerated by electron-donating groups.

Starting from the following equations:

Arrhenius equation:

$$k = A e^{-E_a/RT} \quad (10.1)$$

where:

k = rate constant for the reaction

A = pre-exponential factor for the reaction

E_a = Activation energy for the reaction (J mol⁻¹)

R = Gas constant (8.314472 J K⁻¹ mol⁻¹)

T = temperature (K)

Hammett's equation

$$\text{Log} (k_X/k_H) = \rho \sigma_{pX} \quad (10.2)$$

where :

k_X = rate constant for the reaction with substituent X

k_H = rate constant for the reaction with H substituent

σ_{pX} = The Hammett's sigma *para* constant for substituent X

ρ = reaction constant

other variables used:

E_{aH} = Energy of activation for the H-substituted cyclopentadiene

E_{aX} = Energy of activation for the X-substituted cyclopentadiene

To convert the E_a obtained from the DFT calculation into data which is usable for a Hammett plot, the following conversion must be made using the Arrhenius equation

$$\log (k_X/k_H) = \log (A_X e^{-E_{aX}/RT} / A_H e^{-E_{aH}/RT}) \quad (10.3)$$

Assuming that the pre-exponential factors are very similar for each 1,5-H shift reaction no matter with the substituent X is, the following assumption can be made:

$$A_X \cong A_H \quad (10.4)$$

Leading to the following simplification:

$$\log (k_X/k_H) = \log (e^{-E_{aX}/RT} / e^{-E_{aH}/RT}) \quad (10.5)$$

Which can be re-written as:

$$\log (k_X/k_H) = [\ln (e^{-E_{aX}/RT} / e^{-E_{aH}/RT})] / 2.303 \quad (10.6)$$

expanding the logarithm, we obtain:

$$\log (k_X/k_H) = [\ln (e^{-E_{aX}/RT}) - \ln (e^{-E_{aH}/RT})] / 2.303 \quad (10.7)$$

canceling the logarithm with the exponential, we obtain :

$$\log (k_X/k_H) = [(-E_{aX} / RT) - (-E_{aH} / RT)] / 2.303 \quad (10.8)$$

or:

$$\log(k_X/k_H) = [(E_{aH} / RT) - (E_{aX} / RT)] / 2.303 \quad (10.9)$$

or :

$$\log(k_X/k_H) = [(E_{aH} - E_{aX}) / RT] / 2.303 \quad (10.10)$$

which leads to:

$$\log(k_X/k_H) = (E_{aH} - E_{aX}) / (RT * 2.303) \quad (10.11)$$

Therefore, using E_{aX} in J mol^{-1} , the value of R in $\text{J K}^{-1} \text{mol}^{-1}$

($8.314472 \text{ J K}^{-1} \text{mol}^{-1}$) and $T = 297.15 \text{ K}$ (or $25 \text{ }^\circ\text{C}$), we can obtain the following

graph as a Hammett plot :

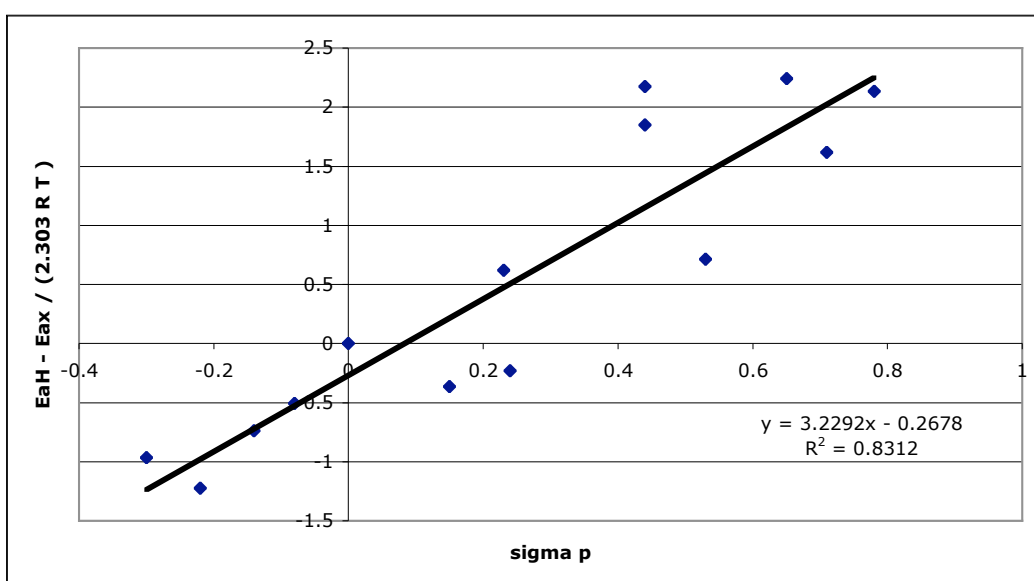


Figure 10-1 Hammett plot for the 1,5-H shift of 2-substituted cyclopentadiene at 297 K correlating the predicted reaction rate versus the substituent's Hammett sigma constant

The calculated reaction's constant $\rho_{\text{diene 1,5-shift}}$ (with the assumption that the pre-exponential factors for all reactions are the same) is therefore 3.2292 at $25 \text{ }^\circ\text{C}$, meaning that the 1,5-H shift of 2-substituted cyclopentadienes is more than two orders of magnitude more sensitive to electronic perturbation than the standard dissociation of benzoic acid in water ($\rho_{\text{benzoic acid dissociation}} = 1.00$). Another way of giving meaning to this number is to say that a variation in $\sigma_{\text{p X}}$ of 1 will lead to a change in reaction rate of $10^{3.23}$. For example, going from an OH substituent ($\sigma_{\text{p OH}} = -0.22$) to a NO_2 substituent ($\sigma_{\text{p NO}_2} = 0.81$) would lead to an increase in reaction rate of about three orders of magnitude.

10.1 References:

⁹⁵ Isaacs, N.S., *Physical Organic Chemistry*. Harlow; Essex, England, 1987; 828

pp.

and references cited therein